PD
539.7
G 326
V 6, No 4

POWER REACTOR TECHNOLOGY

A Quarterly Technical Progress Review

Prepared for DIVISION OF TECHNICAL INFORMATION, USAEC, by
W. H. ZINN and J. R. DIETRICH, GENERAL NUCLEAR ENGINEERING CORPORATION

TELLURIDE STATE LIBRARY
DEC 2 - 1963

Fall 1963

● VOLUME 6

● NUMBER 4

FEATURE ARTICLE:

Efficient Utilization of Nuclear Fuels

TECHNICAL PROGRESS REVIEWS

To meet the needs of industry for concise summaries of current atomic developments, the Atomic Energy Commission is publishing this series, Technical Progress Reviews. Issued quarterly, each of the reviews digests and evaluates the latest findings in a specific area of nuclear technology and science.

The five journals published in this series are:

Isotopes and Radiation Technology, P. S. Baker, A. F. Rupp, and associates, Oak Ridge National Laboratory

Nuclear Safety, Wm. B. Cottrell, W. H. Jordan, and associates, Oak Ridge National Laboratory

Power Reactor Technology, W. H. Zinn and J. R. Dietrich, General Nuclear Engineering Corporation

Reactor Fuel Processing, Stephen Lawroski and associates, Chemical Engineering Division, Argonne National Laboratory

Reactor Materials, R. W. Dayton, E. M. Simons, and associates, Battelle Memorial Institute

Each journal may be purchased ($2.00 per year for subscription and individual issues $0.55) from the Superintendent of Documents, U. S. Government Printing Office, Washington 25, D. C. See back cover for remittance instructions and foreign postage requirements.

The views expressed in this publication do not necessarily represent those of the United States Atomic Energy Commission, its divisions or offices, or of any Commission advisory committee or contractor.

Availability of Reports Cited in This Review

Unclassified AEC reports are available for inspection at AEC depository libraries and are sold by the Office of Technical Services, Department of Commerce, Washington 25, D. C. Some of the reports cited are not available owing to their preliminary nature; however, the information contained in them will eventually be made available in formal progress or topical reports.

Unclassified reports issued by other Government agencies or private organizations should be requested from the originator.

Unclassified British and Canadian reports may be inspected at AEC depository libraries. British reports are sold by the British Information Service, 45 Rockefeller Plaza, New York, N. Y.; Canadian reports (AECL series) are sold by the Scientific Document Distribution Office, Atomic Energy of Canada, Ltd., Chalk River, Ontario, Canada.

Classified U. S. and foreign reports identified in this journal as Classified may be purchased by properly cleared Access Permit Holders from the Division of Technical Information Extension, U. S. Atomic Energy Commission, P. O. Box 1001, Oak Ridge, Tenn. Such reports may be inspected at classified AEC depository libraries.

POWER REACTOR TECHNOLOGY

A REVIEW OF RECENT DEVELOPMENTS

Prepared for DIVISION OF TECHNICAL INFORMATION, USAEC,
by W. H. ZINN and J. R. DIETRICH,
GENERAL NUCLEAR ENGINEERING CORPORATION

● FALL 1963

● VOLUME 6

● NUMBER 4

Foreword

This quarterly review of reactor development has been prepared at the request of the Office of Technical Information of the U. S. Atomic Energy Commission. Its purpose is to assist interested organizations in the task of keeping abreast of new results in reactor technology for civilian application.

Power Reactor Technology contains reviews of selected recently published reports that are judged noteworthy in the fields of power-reactor research and development, power-reactor applications, design practice, and operating experience. It is not meant to be a comprehensive abstract of all material published during the quarter, nor is it meant to be a treatise on any part of the subject. However, related articles are often treated together to yield reviews having some breadth of scope, and from time to time background material is added to place recent developments in perspective.

The intention is to cover the various areas of reactor development from the general viewpoint of the reactor designer rather than from the more detailed points of view of specialists in the individual areas. To whatever extent the coverage of *Power Reactor Technology* may occasionally overlap the fields of the other Technical Progress Reviews, the overlaps will be motivated by this objective of viewing current progress through the eyes of the reactor designer.

A degree of critical appraisal and some interpretation of results are often necessary to define the significance of reported work. Any such appraisals or interpretations represent only the opinions of the reviewers and the editor of *Power Reactor Technology*, who are General Nuclear Engineering Corporation personnel. Readers are urged to consult the original references in order to obtain all the background of the work reported and to obtain the interpretation of the results given by the original authors.

W. H. Zinn, President
J. R. Dietrich, Vice-President and Editor
General Nuclear Engineering Corporation

Contents

FEATURE ARTICLE

Efficient Utilization of Nuclear Fuels 1

by J. R. Dietrich, General Nuclear Engineering Corporation

Foreword

I REACTOR PHYSICS: THERMAL-NEUTRON SPECTRA 39
Transport Equation 39
Generalized Heavy Free Gas Approximation 41
Spectrum Hardening by Absorption . . . 46
Scattering-Law Formulation 46
Theoretical Scattering Kernels 49
References 52

II FLUID AND THERMAL TECHNOLOGY . 54
Liquid-Metal Heat Transfer 54
Boiling-Water Heat-Transfer and Fluid Dynamics 55
Short Notes 60
References 61

III DESIGN PRACTICE: THE CAROLINAS-VIRGINIA TUBE REACTOR . 63
Fuel Elements 63
Fuel Assemblies 65
Control Rods 66
Pressure Tubes 67
Moderator Tank 69
Core Support Structure 70
Header and Jumper Assembly 71
Fuel and Control Program 71
Thermal and Hydraulic Data (Initial Core of 36 Pressure Tubes) 73
Reactor Instrumentation and Control . . . 73
Primary Coolant Circuit 75
Emergency Injection System 78
Fuel Handling 78
Plant Details 79
Containment (Fig. III-9) 79
Shielding 81
Plant Control 81
References 81

IV OPERATING EXPERIENCE: YANKEE 82
In-Core Power Instrumentation 83
Reactivity Characteristics 86
References 91

V BOILING-WATER REACTORS: WATER CHEMISTRY 92
Water Decomposition 92
Corrosion and Activation 94
References 96

VI NUCLEAR SUPERHEAT 97

VII SPECIFIC APPLICATIONS: SHIP PROPULSION 106
Gas-Cooled Plant 106
Pressurized-Water Plants 111
References 117

INDEX, VOLUMES 4–6 119

Issued quarterly by the U. S. Atomic Energy Commission. Use of funds for printing this publication approved by the Director of the Bureau of the Budget on November 1, 1960.

FEATURE ARTICLE

Efficient Utilization of Nuclear Fuels

By J. R. Dietrich

(Editor's Note: In the preparation of Power Reactor Technology, *the most difficult problem has always been to chart an editorial course that will give adequate and timely coverage to the incremental progress in specific areas while maintaining some breadth and perspective in the view of the technology as a whole. Lately the difficulty has increased, as more and more specialized information has been published. We believe the problem will be simplified by separating, to some extent, the functions of current reporting and synthesis of information. Hereafter the latter function will be performed mainly by feature articles that will appear from time to time, whereas the remainder of* Power Reactor Technology *will concentrate more heavily on review of specific current publications. The feature articles may be prepared either by members of the editorial staff or by guest authors.*

We expect that most feature articles will be shorter than this initial one. The subject of efficient utilization of nuclear fuels is one of considerable complexity, and we believe its importance and timeliness justify a treatment at some length.)

A previous issue of *Power Reactor Technology*, 6(2): 1-4, contained a brief review of the AEC Report to the President.[1] Subsequently that Report has been entered into the record of the "202 hearings" before the Joint Congressional Committee on Atomic Energy, along with a background statement[2] that gives further information. In the Report to the President, both the finite magnitude of the nuclear fuel resources and the need for policies to promote the efficient and nonwasteful use of those resources are for the first time formally recognized as timely problems. The Report makes a strong point for the development of breeder reactors, and, further, recommends that the greatest emphasis in converter reactor development be placed on those types which can show improved nuclear fuel utilization. The purposes of this article are to consider the problem of efficient nuclear fuel utilization, to attempt to define that problem, and to determine what is meant by a better converter reactor in terms of the efficient utilization of nuclear fuel.

The Problem

It is common knowledge that the potential content of energy in the fertile nuclear materials, U^{238} and thorium, is very large. This large energy resource can be utilized only if the fertile materials can be converted to fissile materials by means of breeder reactors or converter reactors with very high conversion ratios. If this can be done economically, the specific energy content of the fertile materials is so large that even the fertile materials contained in very low-grade ores will qualify as cheap fuels, and the usable energy content of the available nuclear fuels will be very great indeed—much greater than that in the estimated reserves of fossil fuels. If breeders are not available and if nuclear energy is derived principally from the fissioning of the natural fissile material, U^{235}, then the specific energy content of the basic nuclear fuel is very much

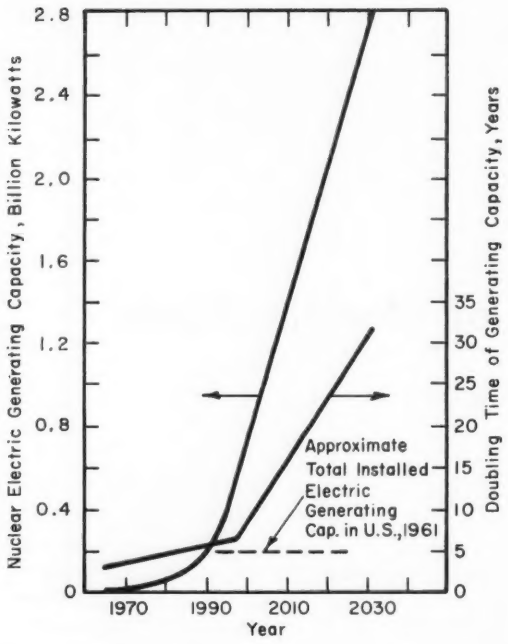

Fig. 1 Postulated growth of nuclear electric generating capacity in the United States (from the AEC Report to the President).[1,2]

smaller and the economically usable fuels are restricted to the high-quality low-cost ores, with the result that the total energy economically available in the nuclear fuels becomes rather insignificant. It could not, for example, support the nuclear power industry postulated in the Report to the President (Fig. 1) for more than a few decades. Table 1, which is from that report, indicates that even by the year 2000 the postulated industry would have consumed or committed some 2.1 million tons of U_3O_8 if the reactors used were H_2O-moderated converters, typical of current practice, and employing plutonium recycle. This quantity of U_3O_8 is 2.6 times the total estimated U. S. resource of "cheap" U_3O_8 (recoverable at \$5 to \$10 per pound) and 40% greater than the total estimated resource recoverable at costs up to \$30 per pound (Table 2).

In recognition of the rapid depletion of cheap nuclear fuel resources by any large-scale nuclear power-generating system based on converter reactors, there has been general agreement that breeder reactors must be used if nuclear fuels are to be important sources of energy. Most differences of opinion on the development of breeder reactors have had to do with the urgency of the development rather than with the ultimate need for it.

If it is assumed that breeder reactors will be developed and that these reactors can utilize the fertile materials U^{238} and thorium, which are available in abundance, a resource problem may still be recognized, which arises because breeder reactors require substantial inventories of fissile isotope to support criticality. This inventory must be paid for by way of inventory charges that constitute part of the fuel-cycle costs of the breeder reactor. Although the breeder industry could afford to *burn* the expensive uranium or thorium extracted from the low-grade ore deposits, it is by no means clear that it could afford to use for inventory the high-cost U^{235} that may be extractable from such deposits. Indeed, the indications are that the inventory costs would be prohibitively high for those breeder-reactor types which are currently the most highly developed.

To the extent that the breeder reactors yield net breeding gains, they can generate a growing supply of fissile isotope. This may constitute a source of low-cost inventory, provided the demand for new breeders does not outstrip the net rate of generation of new fissile isotope. The concern is that the demand may indeed exceed this rate and that, meanwhile, the wasteful use of U^{235} in converter and "burner" reactors may have depleted the natural resource of cheap

Table 1 NATURAL-URANIUM REQUIREMENTS FOR THERMAL CONVERTERS SUPPLYING THE POSTULATED NUCLEAR POWER GENERATION WITH PLUTONIUM RECYCLE
(As Estimated in Ref. 2, on the Basis of Fig. 1)

	Short tons of U_3O_8, cumulative		
Year ending	Mined*	Committed for remainder of plant lives†	Mined plus committed
1965	3,000	3,000	6,000
1970	10,000	11,000	21,000
1975	30,000	30,000	60,000
1980	70,000	70,000	140,000
1985	140,000	160,000	300,000
1990	300,000	330,000	630,000
1995	560,000	640,000	1,200,000
2000	1,000,000	1,100,000	2,100,000

* Uranium mined to provide initial inventory and makeup requirements through the year stated.

† The additional amount of uranium that would be required to sustain operation of reactors built through the year stated. New plants are all based on a 30-year life.

fissile isotope to the point that it cannot fill the gap between the demand for new inventory and the production of inventory by breeding.

The rate at which a breeder system generates excess fissile isotope is usually expressed in terms of the doubling time.* This is the time that would be required to fuel additional breeder capacity equal to the initial capacity if the excess fissile isotope generated were used to expand the system as it became available. The doubling time is determined by the ratio of the breeding gain (the number of grams of excess fissile isotope produced per gram of fissile isotope destroyed) and the specific inventory requirement (the quantity of fissile isotope required in the system per effective unit of thermal generating capacity).

The growth of inventory demand in an idealized breeder system can be illustrated by assuming that the total nuclear capacity postulated in Fig. 1 is provided by breeder reactors of constant specific inventory requirement and constant doubling time. Figure 2 shows the gross and net inventory requirements for two different breeder systems, each of which supplies the generating capacity of Fig. 1. Both systems are chosen to give a doubling time of 20 years, but one achieves this doubling time by means of reactors with large breeding gains in combination with a high specific inventory requirement, whereas the other system has a moderate breeding gain and a proportionately lower inventory requirement. The figure shows, for each system, the gross inventory, the inventory bred by the system itself, and the difference, which must be supplied from the uranium resources. To facilitate comparison with the estimates of uranium resources, all these quantities are given in terms of the equivalent amounts of natural uranium. The bred inventory, for example, is the quantity of natural uranium that would have to be fed to diffusion plants to produce a quantity of U^{235} equivalent to the bred plutonium for fueling new reactors.

Table 2 NATURAL-URANIUM RESOURCES IN THE UNITED STATES[2]

Cost of mining and extraction, dollars per pound of U_3O_8	Reasonably assured resources		Estimated total resources	
	Million short tons of U_3O_8	Million metric tons of U*	Million short tons of U_3O_8	Million metric tons of U*
5 to 10	0.38	0.301	0.8	0.634
10 to 30	0.40	0.317	0.7	0.554
30 to 50	5	3.96	8	6.34
50 to 100	6	4.75	15	11.9
100 to 500	500	396	2000	1585

* Extra significant figures are carried in the conversion to metric tons of uranium to preserve consistency in later calculations.

In both cases (Fig. 2) the net inventory requirement reaches a maximum at a time when the doubling time for breeding corresponds to the doubling time of capacity expansion (see Fig. 1). If enough fissile isotope can be supplied from outside sources to furnish the net requirement up to this time of inventory crisis, there will be no further demand (in this idealized system), and the breeders will in fact begin to "pay back" the fissile isotope previously withdrawn from the stockpile. This excess could presumably be used in converter or burner reactors, or for other purposes.

Unfortunately development has not progressed sufficiently to indicate whether the performances likely to be achieved in practical, economic breeder systems will be much better or much worse than those illustrated in Fig. 2. The development of an economically competitive system that matches the performance of the better of the two would, however, at the present time be ranked as a solid achievement. Since

*The doubling time considered here is for a system composed of many reactors. The breeding gain and the specific inventory requirement are for the system as a whole, and they are intended to include all losses (e.g., reprocessing losses) and all inventory components (e.g., inventory in fuel reprocessing) for the system. The more common usage — the doubling time for a single reactor — is somewhat different. The differences are considered more specifically in a later section.

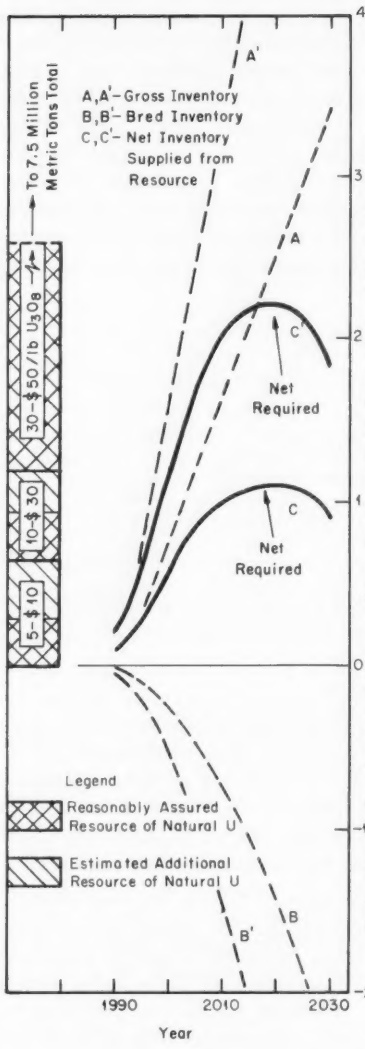

Explanatory note for Fig. 2:

Two different breeder systems are considered, both having doubling times of 20 years. The unprimed letters refer to a system having a breeding gain of about 0.2 which requires 0.488 metric ton of natural uranium to supply the initial U^{235} inventory for each megawatt of thermal capacity. The primed numbers refer to a system in which the breeding gain and the specific inventory are both higher by a factor of 2. There is no intent to imply that high breeding gains and high specific inventories inherently accompany each other. The intent is to demonstrate that systems with the same doubling time can have widely different net inventory requirements.

Fig. 2 Fissile material requirements for inventory in breeder systems.

this performance appears only marginally successful in reconciling the forecast of nuclear power generation with the estimates of low-cost uranium resources—even if all nuclear plants could match the performance now—the threat of a shortage of fissile isotope evidently does exist. Although the threat might be removed by the discovery of very much larger uranium deposits, by the development of very much cheaper methods for extracting uranium from low-grade deposits, or by a drastic scaling down of the nuclear power forecast, it seems only prudent to consider what courses might be taken to minimize the threat and its possible consequences.

Waste and Utilization of Fissile Isotope

In general, nuclear reactors make demands on the natural resource of fissile isotope, both for inventory and for actual net consumption in the reactor, by the processes of fission and neutron capture. The inventory requirement represents a borrowing from the stockpile: for an indefinitely long period in the case of a converter reactor system and for some finite period, probably a number of reactor lifetimes, in the case of a reactor system with a significant breeding gain. However, if the total demand for fissile isotopes is at any time high enough to require the use of higher cost resources, the result can only be a tendency to higher nuclear fuel costs, regardless of whether the isotope is used for inventory or is actually consumed.

Aside from the actual net destruction of fissile isotope in the reactor, there may be other losses of the isotope that are connected with its use either for burnup or for inventory. In the rather qualitative discussion here, a number of these potential losses are either considered negligible relative to the uncertainties in the fissile isotope resource itself or are lumped in with other variables. Thus any losses connected with the mining and extraction of uranium are assumed to be already included in the estimates of the uranium resource, and the effects of losses in the recycle of fissile isotope in breeder reactors are lumped in with those considerations which determine the breeding gain or doubling time for the system as a whole.

There is one loss, however, that must be considered specifically because it is an important one and because it may vary strongly

from one reactor type to another. This is the effective loss of U^{235} by excessive dilution with U^{238}. An example of such diluted U^{235} is that in the tailings from the isotope-separation plants. The U^{235} extracted from any isotopic mixture of less than natural enrichment will cost more for the separative work than U^{235} extracted from natural uranium, and this cost will increase steadily as the enrichment of the feed mixture decreases. When the enrichment of the mixture in the separation plant decreases to such a value that the cost of further separation is not economically justifiable, the mixture is discharged as tailings. A reworking of these tailings may be justifiable in the future if natural-uranium costs rise by a large amount; the U^{235} so obtained, if current separation techniques were used, would be expensive. For most of the present discussion it is assumed that this would not be done: the U^{235} in diffusion-plant tailings and in any uranium mixture discharged from a reactor, when the U^{235} content is less than that in current diffusion-plant tailings, is considered to be lost. For purposes of calculation, this tails assay will be assumed to be 0.25%. This is the approximate tails assay for the minimum unit product cost, as discussed in *Power Reactor Technology*, 5(4): 6. Whenever the fissile isotope requirements of nuclear plants are divided into the categories of inventory and burnup, any effective losses of U^{235} as the result of dilution are included in the category to which they apply. Near the end of the discussion the effects of allowing the tails enrichment of the isotope-separation plants to vary in response to economic pressure, and of reworking previous tailings, are considered briefly.

To treat the net consumption of fissile isotope in converter reactors, it is necessary to define terms that will specify, quantitatively, the wastefulness (or "nonwastefulness") of the process. The term "fuel utilization" has been used in various ways for this purpose in the past: always, in the general sense, as the antithesis of "waste." For this discussion the term *specific utilization* (Υ) will be defined as the energy produced per unit of (net) fissile isotope destroyed. Since the fissile isotopes produced in a converter are, in general, neither identical to those destroyed nor equivalent to those destroyed as nuclear fuel, the specific utilization is not a fixed characteristic of a given reactor but only a fixed characteristic of the reactor plus its fuel cycle. Further, unless the reactor types in question each constitute a closed system in which converted fissile isotope is recycled until it is used up, the relative rankings of the types in terms of their specific utilizations do not necessarily correspond strictly to their relative rankings with respect

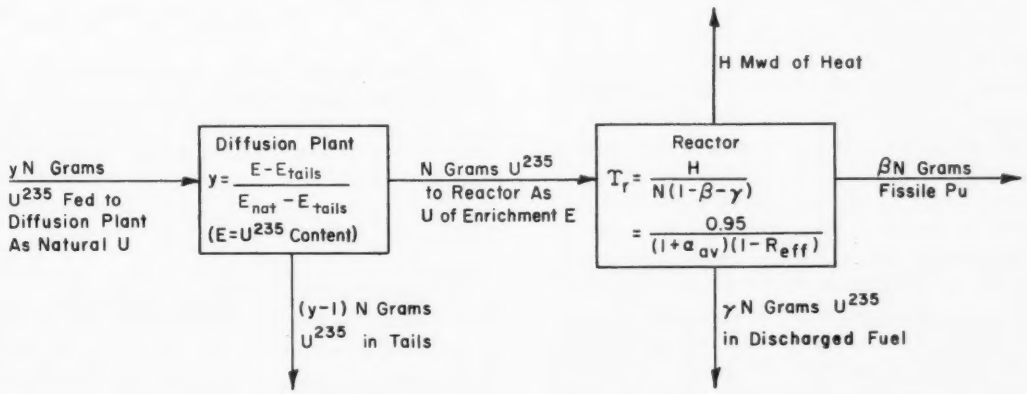
H Mwd of Heat
yN Grams U235 Fed to Diffusion Plant As Natural U
Diffusion Plant
y = (E - Etails) / (Enat - Etails)
(E = U235 Content)
N Grams U235 to Reactor As U of Enrichment E
Reactor
Υr = H / N(1-β-γ) = 0.95 / (1+αav)(1-Reff)
βN Grams Fissile Pu
(y-1) N Grams U235 in Tails
γN Grams U235 in Discharged Fuel
Υ = H / (yN-βN) = Υr [(1-β-γ)/(y-β)] = 0.95/(1+αav)(1-Reff) [(1-β-γ)/(y-β)] Mwd (t)/gram
If y = 1 (Natural-U Reactor)
Υ = Υr [(1-β-γ)/(1-β)] = Υr [1-γ/(1-β)] = 0.95/(1+αav)(1-Reff) [1-γ/(1-β)] Mwd (t)/gram

Fig. 3 Specific utilization of fissile isotope in reactor without recycle of U^{235}.

to fuel conservation within the overall nuclear energy system. Despite these shortcomings, the concept is a useful one.

It is helpful to resolve the specific utilization into components whose values can be attributed separately (at least to a first approximation) to the basic properties of the fissile materials, to the reactor characteristics, and to the characteristics of the fuel cycle. This is done in the following paragraphs with the help of Figs. 3 and 4.

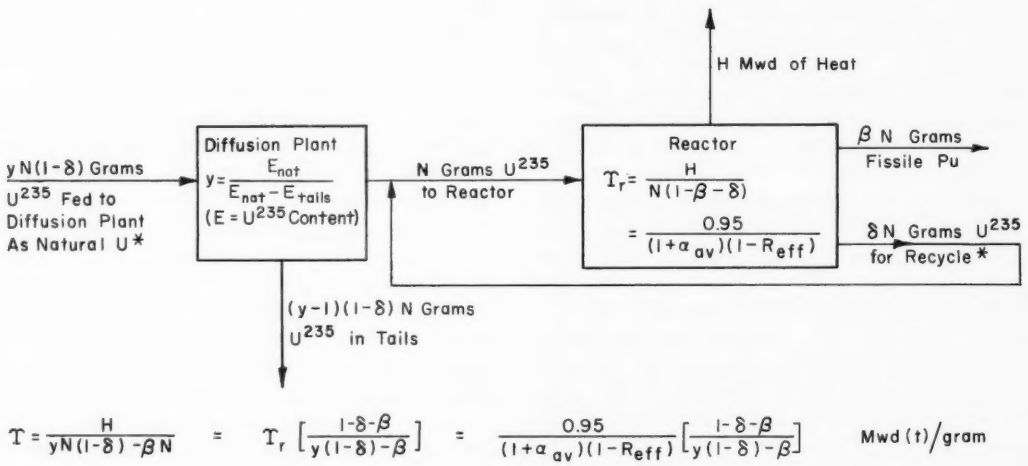

Fig. 4 Specific utilization of fissile isotope when U^{235} is recycled.

* To simplify the accounting, it is assumed that the uranium discharged from the reactor is recycled directly to the reactor after reenrichment by the addition of highly enriched uranium from the diffusion plant. The overall material balance remains the same, whether this is done or whether the discharged uranium is actually recycled through the diffusion plant.

The amount of energy liberated upon fission is nearly the same for all fissile isotopes, and this amounts to approximately 0.95 Mwd/g of material fissioned. The fissile isotope can be destroyed by the radiative capture of neutrons, as well as by fission, and the ratio of the capture to the fission cross section, denoted by α, varies from one isotope to another. The energy produced per gram of fissile isotope destroyed in the reactor consequently amounts to $0.95/(1+\alpha)$ Mwd/g.* To treat a mixture of fissile isotopes in a reactor, an average value of α, α_{av}, is introduced in this discussion. It is to be understood that the average is taken over those fissile atoms which are destroyed in the reactor. The value of α_{av} will therefore be variable from reactor to reactor and from fuel cycle to fuel cycle, but within a reasonably narrow range.

It is customary to specify the production of new fissile isotope within a reactor in terms of a conversion ratio R. In this discussion the effective conversion ratio, which would apply over the entire life of a typical sample of fuel in the reactor, is used. This effective conversion ratio, R_{eff}, is defined as follows:

$$R_{eff} = \frac{\text{atoms of fissile isotope produced}}{\text{atoms of fissile isotope destroyed}} \qquad (1)$$

For a reactor using a mixture of U^{235} and U^{238} as the feed, the ratio would be

$$R_{eff} = \frac{\text{atoms of } Pu^{239} + Pu^{241} \text{ produced}}{\text{atoms of } U^{235} + Pu^{239} + Pu^{241} \text{ destroyed}}$$

With these relations a specific utilization of fissile isotope in the reactor, T_r, is given by the relation

*In some reactors the direct fission of fertile isotope by fast neutrons can make a significant contribution to the energy production. This contribution is neglected here. It may be important in fast reactors and in H_2O-moderated reactors of high fuel-to-moderator ratio.

$$\Upsilon_r = \frac{\text{energy produced}}{\text{net grams of fissile isotope destroyed}}$$

$$= \frac{0.95}{(1+\alpha_{av})(1-R_{eff})}* \qquad (2)$$

The relation expressed by Eq. 1 does not take into account any losses of fissile isotope through isotopic dilution. However, these losses may be taken into account as indicated in Figs. 3 and 4, which apply, respectively, to the case in which U^{235} in the discharged fuel is discarded and to the case in which U^{235} is recycled to the reactor after reenrichment by the diffusion plant.

If the approximation is made that the fissile isotope produced by conversion is equivalent to U^{235}, the specific utilization of fissile isotope can be related to the specific utilization of the basic natural resource (natural uranium) simply by multiplication by the U^{235} content† of natural uranium:

$$\Upsilon_{nat} = \frac{\text{Mwd(t) of energy produced}}{\text{metric ton of } U^{nat} \text{ used}}$$

$$= 7.2 \times 10^3 \Upsilon \qquad (3)$$

where Υ is given by Fig. 3 or Fig. 4.

Specific Utilization in Thermal Converters

In the expression for the specific utilization in the reactor (Eq. 2) the effective conversion ratio, R_{eff}, is the important variable. It is useful to examine the limitations of R_{eff} in thermal-neutron converter reactors.

The instantaneous value of the conversion ratio, R, can be defined either in a manner analogous to Eq. 1:

$$R = \frac{\text{atoms of fissile isotope produced per second}}{\text{atoms of fissile isotope destroyed per second}}$$

or, equivalently,* as a neutron absorption ratio:

$$R = \frac{\text{neutrons absorbed per second in fertile isotope}}{\text{neutrons absorbed per second in fissile isotope}}$$

When the second expression is adopted, it is found that the neutron balance in a reactor can be expressed in terms of production terms, leakage terms, and ratios analogous to R which account for the absorption in the various materials within the reactor. Thus, for example,

$$R_{fp} = \frac{\text{neutrons absorbed per second in fission products}}{\text{neutrons absorbed per second in fissile isotope}}$$

and

$$R_f = \frac{\text{neutrons absorbed per second in fissile isotope}}{\text{neutrons absorbed per second in fissile isotope}} \equiv 1$$

If all productions, leakages, and absorptions in the reactor are taken into account and if the reactor is critical, the neutron balance (net neutron production) should be zero. It is often convenient, however, to evaluate those components of the balance which are associated with the fixed components of the core, and to lump into a single ratio, R_{ex}, any remaining components that have not been accounted for:

$$R_{ex} = \frac{\text{no. of excess neutrons produced per second}}{\text{no. of neutrons absorbed in fissile isotope per second}}$$

$$= \frac{\text{no. of neutrons removed by control system per second}}{\text{no. of neutrons absorbed in fissile isotope per second}}$$

if the reactor is critical.

* The two factors in the denominator are not independent, for R_{eff} depends on $\overline{\eta}$, and hence on α_{av}, as discussed in later sections. The intention here, however, is to show how the conversion ratio, which is the quantity usually quoted to characterize the neutron economy of the reactor, enters the expression for specific utilization.

†Throughout this article a nominal value of 0.72% is used for the U^{235} content of natural uranium, and no numerical distinction is made between the weight content and the atomic content. A recent AEC press release[30] points out that the weight percent of U^{235} in natural uranium varies from about 0.7103 to 0.7113. In the release it also announces that, for regulatory and contractual purposes, the AEC will consider the U^{235} content to be 0.711 wt.% unless a measured value is available for the sample in question.

*This is strictly true only if the reactor power is constant over a time period that is long relative to the half-lives of the precursors of bred fissile isotopes. If significant neutron absorption occurs in such a precursor (e.g., Pa^{233}) it should be considered as part of the absorption rate in the fissile isotope.

With these definitions the neutron balance for a thermal or near-thermal converter reactor is given, to a good approximation, by the relation

$$R_{ex} = \frac{\overline{\eta}\epsilon}{1+\tau B^2} - 1 - R - R_{fp} - R_p - (1+R_{th})L^2B^2 \qquad (4)$$

In this equation the ratios R, R_{fp}, and R_{ex} have already been defined. R_p is the similar ratio for neutrons absorbed in "parasitic" materials; i.e., reactor structure, moderator, and any other materials besides fissile isotopes, fertile isotopes, fission products, or control materials. R_{th} is the similar ratio for neutrons absorbed *thermally* in fertile isotope (R_{th} is thus the thermal component of the conversion ratio). The quantity $\overline{\eta}$ denotes the number of fission neutrons produced per neutron absorbed in fissile isotope; the use of the barred symbol denotes that an appropriate average is to be taken over all fissile isotopes present and over all energies in the thermal-neutron spectrum. The symbol ϵ is the fast-fission factor, and the symbols τ, L^2, and B^2 have their usual reactor physics meanings. The numeral 1 in the equation ($= R_f$) accounts for the neutrons required to maintain the chain reaction.

The symbol R_{ex} in Eq. 4 denotes the number of excess neutrons (per absorption in fissile isotope) which may be produced in the reactor.

If the term $\overline{\eta}\epsilon/(1+\tau B^2)$ in Eq. 4 is approximated by a term $1-\tau B^2$, the neutron balance can be expressed conveniently in terms of the neutrons used productively (either for conversion or for sustaining the chain reaction) and those lost by nonproductive processes:

$$\underset{\text{Neutrons produced}}{\overline{\eta}\epsilon} = \underset{\text{Used productively}}{(1+R)} + \underset{\text{Lost to controls}}{R_{ex}}$$

$$+ \underset{\text{Lost by absorption}}{(R_{fp}+R_p)} + \underset{\text{Lost by leakage}}{[\overline{\eta}\epsilon\tau B^2 + (1+R_{th})L^2B^2]} \qquad (5)$$

This neutron-balance equation may be regarded as defining the maximum value that the conversion ratio, R, may have after every effort has been made to reduce the loss terms to their minimum practical values through appropriate reactor design. Although the various losses entering the equation can be discussed effectively only in terms of specific reactor designs, the crucial quantity, $\overline{\eta}$, is amenable to some general discussion.

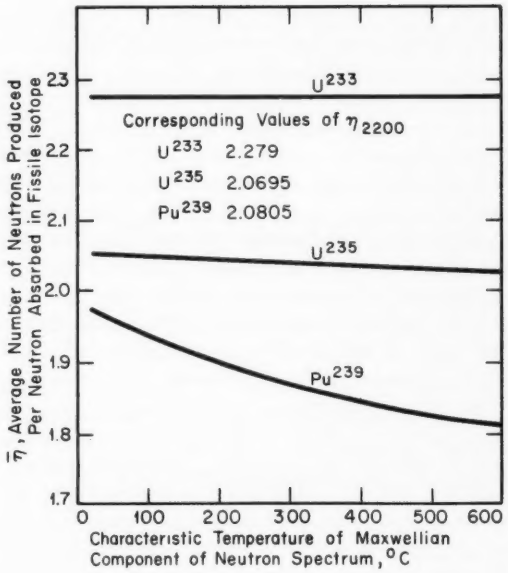

Fig. 5 Effective values of η for fissile isotopes. From Westcott[3] (η_4 values, $r = 0.07$).

At a given neutron energy, η is fixed for a given fissile isotope. However, its value does vary with neutron energy, and so, in general, the value of $\overline{\eta}$ will be characteristic of the reactor and its neutron-energy spectrum, as well as the value of the fissile isotope used. The usual variation is a decrease in $\overline{\eta}$ as the average neutron energy is increased (in the thermal and near-thermal ranges) either by increasing the moderator temperature or by decreasing the moderator-to-absorber ratio.

The effect of moderator temperature, in a well-thermalized system, is illustrated in Fig. 5. These values are from the 1960 compilation of Westcott*[3] and are intended to apply in the fuel of a D_2O-moderated reactor ($r = 0.07$).

The effect of fuel-to-moderator ratio is not so easily defined by data taken from the published literature, for it does not lend itself to generalized presentation, and it strongly involves the fission characteristics in the resonance-energy region where there are still

* Type 4 joining of thermal and epithermal components.

substantial uncertainties. Examples of the effect can, however, be extracted from the literature.

Figure 6 gives computed values[4] for $\overline{\eta}$ of U^{235} in UO_2-H_2O lattices of two different enrichments as a function of the uranium-to-H_2O volume ratio. The moderator is at room temperature. Figure 7 gives calculated values[5] for $\overline{\eta}$ for Pu^{239} in uniform mixture with H_2O at a temperature of 500°K. Two curves are shown, one calculated by the MUFT and SOFOCATE codes and the other arrived at by the Westcott[3] approach. The value of $\overline{\eta}$ for U^{233}, from Ref. 6, is given in Fig. 8 as a function of the moderation ratio $\xi\Sigma_s/N_{23}$ (no absorbers present other than U^{233}). The system is at room temperature. Note that the curves for the three isotopes are not calculated for identical conditions. The curves are intended to be illustrative and not to give comparative values for the isotopes.

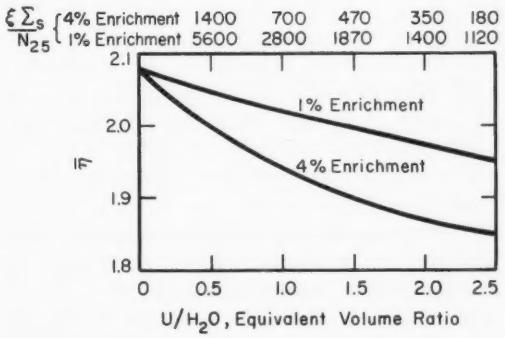

Fig. 6 Calculated values of $\overline{\eta}$ for U^{235} in uranium dioxide–water lattices at room temperature.[4]

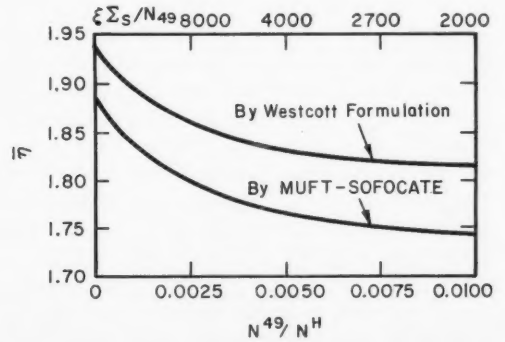

Fig. 7 Calculated values of $\overline{\eta}$ for Pu^{239} as a function of plutonium-to-hydrogen atomic ratio[5] at 500°K.

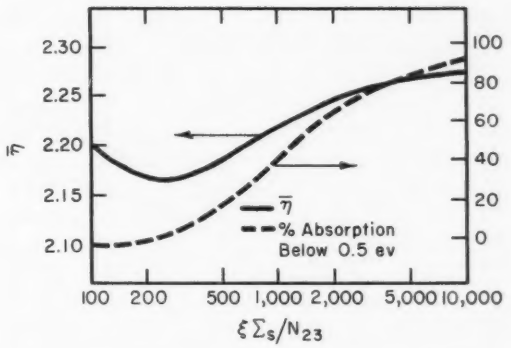

Fig. 8 Calculated values of $\overline{\eta}$ for U^{233} as a function of the moderation ratio[6] at room temperature. This is the curve for the "new data" considered in Ref. 6. See the reference for a discussion.

With the exception of the term $\overline{\eta}\epsilon/(1+\tau B^2)$, all the components of Eq. 4 tend to change, as the fuel-to-moderator ratio (and, necessarily, the enrichment) is increased, in such a way as to increase the number of neutrons available for conversion.* Since $\overline{\eta}$ decreases as fuel-to-moderator ratio is increased, there will, in general, be a fuel-to-moderator ratio that yields the maximum conversion ratio. This ratio may not yield the highest fuel utilization because of the considerations illustrated in Figs. 3 and 4. It may also be impractical for other reasons. To assess the larger question of fuel utilization, it is necessary to consider specific reactor types separately and to take into account the effects of fuel-to-moderator ratio in each.

Details of the Utilization in H_2O-Moderated Converters

The studies reported in Ref. 7 are helpful for analyzing the fuel utilization in H_2O-moderated reactors. In those studies a pressurized-water reactor, fueled with UO_2 in zirconium jackets, was studied at various values of fuel enrichment and fuel-to-moderator ratio. The reactor was

* In fact, in H_2O-moderated lattices using slightly enriched uranium fuel, the increase in ϵ with fuel-to-moderator ratio is usually enough to override the effects of decreasing $\overline{\eta}$ and to yield an increase in the product $\overline{\eta}\epsilon$.[4] This is not necessarily true, however, if plutonium is an important component of the fissile isotope content.

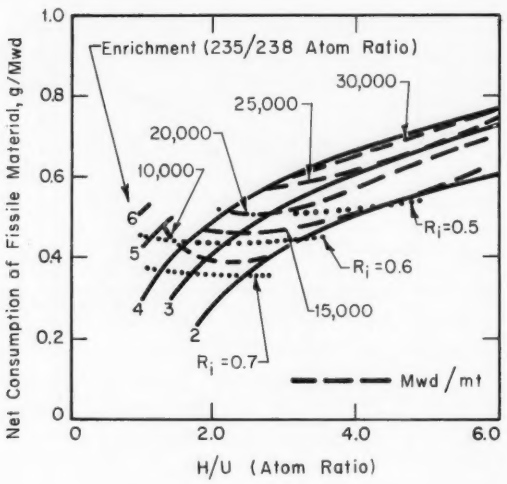

Fig. 9 Net consumption of fissile material (grams per megawatt-day) for 1000-Mw(t) reactors (0.400-in. fuel-rod diameter).[7]

idealized to the extent that the fuel-water lattice was a uniform one (i.e., no water channels were left for control rods, etc.). Conceptually the core was designed for an output of 1000 Mw(t); this resulted in a relatively large core size, the diameter and height being in the range 7 to 9 ft. The reactor was fueled on a single-batch program, and it was assumed that shuffling of the fuel elements would take place during the lifetime of each batch in such a way as to yield a uniform exposure to all elements.

Some of the results of the study are shown in Fig. 9. The net consumption of fissile material is plotted for several fuel enrichments as a function of hydrogen-to-uranium ratio. On this curve any given combination of enrichment and hydrogen-to-uranium ratio provides a characteristic initial excess reactivity, a characteristic initial conversion ratio, and a characteristic exposure lifetime for the fuel batch. Curves of constant exposure lifetime and constant initial conversion ratio are superimposed on the figure. The net consumption of fissile material is just the reciprocal of the specific utilization of fissile material in the reactor (Υ_r).

It is evident in Fig. 9 that the net consumption of fissile material is not very sensitive to the hydrogen-to-uranium ratio, provided the enrichment is adjusted (as the hydrogen-to-uranium ratio is changed) to maintain a constant reactivity lifetime. When the diffusion-plant losses are taken into account, the utilization is somewhat more sensitive to enrichment and is increased as the enrichment is decreased, as demonstrated in Table 3.

The initial conversion ratios indicated in Fig. 9 are not very high, and, if effective conversion ratios are computed from the net consumption of fissile material by Eq. 2, it is found that they are also rather low. A net consumption of 0.4 g/Mwd, for example, corresponds to an effective conversion ratio of 0.73 over the life of the fuel batch on the assumption that $\overline{\alpha} = 0.4$.

It is instructive to examine the neutron balance for a particular case to determine the neutron losses and to rationalize the value of the conversion ratio. For this purpose the point corresponding to a reactivity lifetime of 10,000 Mwd/metric ton on the 2% enrichment curve has been selected for examination. The neutron balance, as specified by Eq. 5, is given in Table 4 in terms of quantities inferred from

Table 3 SPECIFIC UTILIZATION IN H_2O-MODERATED CONVERTER OF FIG. 9

Enrichment, N^{235}/N^{238}	0.02	0.03	0.04
Net U^{235} burned, g/Mwd $\left[=\frac{N(1-\delta)}{H}\right.$, Fig. 4$\left.\right]$	0.83	0.92	0.99
Net fissile plutonium produced, g/Mwd $(=\beta N/H)$	0.44	0.53	0.57
Net fissile isotope destroyed in reactor, g/Mwd $\left[=\frac{N(1-\delta-\beta)}{H}\right]$	0.39	0.39	0.42
Reactor utilization T_r, Mwd/g $\left[=\frac{H}{N(1-\delta-\beta)}\right]$	2.56	2.56	2.38
Net U^{235} fed to diffusion plant as natural U, g/Mwd $\left[=\frac{yN(1-\delta)}{H}\right]$	1.27	1.41	1.52
Net fissile isotope made unavailable, g/Mwd $\left[=\frac{yN(1-\delta)-\beta N}{H}\right]$	0.83	0.88	0.95
Specific utilization, T, Mwd/g $\left[=\frac{H}{yN(1-\delta)-\beta N}\right]$	1.21	1.14	1.05

Table 4 APPROXIMATE NEUTRON BALANCE IN 2% ENRICHMENT BATCH-LOADED H_2O REACTOR* AT BEGINNING OF LIFE: HOT, FULL-POWER EQUILIBRIUM XENON AND SAMARIUM

k_∞ (without xenon and samarium)	1.21
τB^2	0.04
L^2B^2	~0.00
$\overline{\eta}_{25}$	2.05
ϵ	1.04
$\overline{\eta}_{25}\epsilon$	2.13
R	0.66
Inherent losses (= L_i)	
R_{Xe+Sm} (= R_{fp})	0.052
R_{H_2O} (= R_p)	0.087
R_{Zr} (= R_p)	0.013
$\overline{\eta}_{25}\epsilon\tau B^2$	0.085
Total	0.237
$R_{ex} = \overline{\eta}_{25} - 1 - R - L_i$	0.23

* These values were derived from Ref. 7, in some cases by estimate, for illustrative purposes. See Ref. 7 for original data.

Ref. 7. The balance is set up in such a way as to determine the excess neutron ratio, R_{ex}, which is not specified directly in Ref. 2. It is clear that the greatest neutron loss in the fresh reactor is the absorption in the control rods necessary to absorb the neutrons represented by R_{ex}, and thereby to control the excess reactivity of 10 to 11% k_{eff}. If the reactor were designed with negligible excess reactivity for operation, the neutrons represented by R_{ex} (Table 4) could be diverted to conversion and the conversion ratio could be as high as about 0.90. The reactivity lifetime would, of course, be nearly zero. If this were done it would be necessary, in order to utilize the extra neutrons for conversion, to increase the absorption of U^{238} relative to that of U^{235}. Such an increase could be accomplished (1) by decreasing the enrichment of the fuel in order to increase the thermal-neutron absorption by U^{238} relative to that by U^{235} or (2) by decreasing the hydrogen-to-uranium ratio in order to increase the relative absorption of resonance neutrons by U^{238}. Either of these procedures would change the parasitic absorption slightly; thus the resulting conversion ratio would not be exactly 0.90, but it would approximate that number. The point here is that the provision of excess reactivity, in order to provide for reactivity lifetime, produces a very substantial reduction in the initial conversion ratio.

To determine the relation of the initial wastage of neutrons in control rods to the utilization of fissile isotope in a practical fuel cycle, it is necessary to examine the approximate neutron balance at the end of core life. To simplify this examination, and because more detailed information is not included in Ref. 7, it will be assumed here that the macroscopic absorption cross section of all the fissile isotopes present at the end of core life (10,000 Mwd/metric ton) is the same as the macroscopic absorption cross section of the U^{235} present at the beginning of life. The significant changes in neutron balance will then result only from the change in $\overline{\eta}$ and the presence of long-lived fission products.

At 10,000 Mwd/metric ton, Ref. 7 indicates that the initial U^{235} content, 19.4 g of U^{235}/kg of uranium, has decreased to 11.1 g/kg of uranium, whereas the plutonium content has built up to 5.0 g/kg of uranium. If it is assumed that 60% of the plutonium is Pu^{239}, then there are about $^3/_{11}$ as many Pu^{239} atoms as U^{235} atoms present. In the neutron spectrum of the reactor, the effective absorption cross section of Pu^{239} is about 3.5 times that of U^{235}. Hence at end of life the absorption rate in Pu^{239} is about equal to that in U^{235}, and $\overline{\eta}$ is just about the average of the U^{235} and the Pu^{239} values. The neutron balance arrived at with this average, and with a reasonable assumption for fission-product absorption, is given in Table 5. In this case the balance has been set up to determine an estimated value for the conversion ratio R at the end of core life. These numbers involve a con-

Table 5 APPROXIMATE NEUTRON BALANCE IN A 2% ENRICHMENT BATCH-LOADED H_2O REACTOR AT END OF 10,000 Mwd/metric ton CORE LIFE: HOT, FULL-POWER EQUILIBRIUM XENON AND SAMARIUM

k_∞ (with xenon and samarium)		1.04
τB^2		0.04
L^2B^2		~0.00
$\overline{\eta} = \frac{\overline{\eta}(25) + \overline{\eta}(49)}{2} = \frac{2.05 + 1.75^*}{2}$		1.90
ϵ		1.04
$\overline{\eta}\epsilon$		1.98
Losses		
R_{Xe+Sm}	as in new core	0.052
R_{H_2O}	as in new core	0.087
R_{Zr}	as in new core	0.013
R_{fp}		0.067
R_{ex}		0.000
$\overline{\eta}\epsilon\tau B^2$		0.080
Total losses		0.299
$R = \overline{\eta}\epsilon - 1 -$ losses		0.68

*Approximate value is derived from Fig. 6, Ref. 5.

siderable amount of approximation, but they serve to show the relative importance of the several effects.

It is clear that in a case of this kind the end-of-life conversion ratio is low because of the low η of Pu^{239} and because of the neutron absorption by fission products. When the initial excess reactivity is compensated by neutron absorption in control rods or by other neutron-wastage methods, the initial conversion ratio is perforce reduced to something like the end-of-life ratio. The loss in the average conversion ratio is significant but may be somewhat smaller than would be expected. In the case considered above, for example, approximately 59% of the fissile isotope destroyed in the core during its entire lifetime was U^{235}; the remainder, 41%, was Pu, of which nearly all would be Pu^{239}. If $\overline{\eta}$ over the core lifetime is computed as the average for U^{235} and Pu, weighted in proportion to the burnup of each, the result is 1.92. This is only slightly higher than the end-of-life value in Table 5 (1.90). Similarly, the long-lived fission products over the core lifetime would exert an average effect equal to about half their end-of-life effect. This difference amounts to about $0.067/2 \approx 0.03$. If the wastage of neutrons in control rods were avoided by the use of continuous refueling or by a spectral-shift control scheme, the gain in average conversion ratio might for this case be about $0.02 + 0.03 = 0.05$.

Fuel Requirements of H_2O Converter Systems

The reactor utilizations arrived at above are probably slightly high for practical reactors operating on single-batch fuel-loading programs because of the idealization of the system and because practical reactors may sacrifice more neutrons to leakage for the sake of power flattening. On the other hand, schemes that reduce the wastage of neutrons in control rods may produce improvements that will overcompensate, by some small amount, for these effects. Therefore it appears that Ref. 7, from which the above results were derived, gives a reasonable prediction for the maximum utilization that is likely to result from H_2O reactors which are designed according to current technology and which operate without plutonium recycle. The fuel requirement for burnup is just the reciprocal of the specific utilization; it is given in terms of the natural-uranium requirement by Eq. 3.

The fuel utilization attained in the H_2O reactor systems is low for two major reasons: (1) the low value of η for Pu^{239} and (2) the loss of fissile isotope in the diffusion-plant tailings. These two effects work together to restrict the range of possible utilizations to low values. If an attempt is made to minimize the effect of plutonium η by increasing the enrichment of the feed fuel, and thus reducing the burnup of plutonium in the reactor, it is found that the utilization suffers because of the increase in diffusion-plant losses. If, on the other hand, there is an attempt to decrease the effect of the diffusion-plant losses by utilizing high fuel exposures, the effect of the plutonium η increases and again limits the possibility of improving the utilization.

These conclusions appear to be in reasonable agreement with the assumptions of fuel utilization in converter reactors which were made in developing the Report to the President. In Table 6 are listed the specific utilizations computed for the converters postulated in Ref. 2 for the years 1966 through 1980. To derive these quantities from the data of the reference, it has been necessary to assume a value for the fissile isotope content of the plutonium discharged from the reactors. A value of 75% has been assumed for all cases; this is perhaps slightly optimistic. The resulting specific utilizations are slightly higher than those in Table 3.

The specific inventory requirements of any reactor system, i.e., the number of tons of natural uranium required to supply the total fuel inventory associated with 1 Mw(t) of installed capacity, depend on the specific power of the reactor (thermal megawatts per ton of fuel in the reactor), the enrichment of the fuel, and the ratio of the out-of-core inventory to the in-core inventory. For H_2O reactors of current types, there is perhaps more uncertainty in the latter of these three quantities than in the other two.

The reactors now operating achieve specific powers slightly below 20 Mw(t)/metric ton of uranium. Some increases may be expected, but probably not large ones so long as oxide fuels are used. The background analysis[2] for the Report to the President assumes that the specific power may reach 25 Mw(t)/metric ton of uranium in the 1965 to 1980 period, and this is probably a reasonable assumption. The same

analysis, in estimating fuel-cycle costs, assumes an ex-core inventory equivalent to 1.5 years of reactor throughput. For an estimate of resource requirements, it would perhaps be appropriate to increase this value somewhat to allow for holdups that do not show up as inventory costs in fuel-cycle cost calculations.

In Table 7 the inventory requirements for the converter reactors of Ref. 2 are given for two different ex-core inventory values, one corresponding to 1.5 years of reactor throughput and the other to 2.5 years. The requirements for the Dresden and Yankee reactors are also given on the same ex-core inventory bases. The requirements are given in terms of the quantity of natural uranium required to supply the inventory. This quantity is a function of the enrichment of the reactor fuel. The relation may be expressed as*

$$y = \frac{E - E_{nat}}{E_{nat} - E_t} + 1 = \frac{E - E_t}{E_{nat} - E_t}$$

where y is the number of tons of natural uranium fed to the diffusion plant to yield 1 ton of uranium of enrichment E, E_{nat} is the enrichment of natural uranium (0.0072), and E_t is the enrichment of the diffusion-plant tails.

* This equation contained a typographical error when it was previously given in *Power Reactor Technology*, 2(3): 6.

Table 6 SPECIFIC UTILIZATIONS FOR CONVERTER REACTORS POSTULATED IN REF. 2
(Compare Tables 13 and 14 of Ref. 2)

Year	1966	1970	1975	1980
Fuel exposure, Mwd/kg of U	16	18	22	25
Feed enrichment, g of U^{235}/kg of U	23	25	28	30
Discharge enrichment, g of U^{235}/kg of U	11	12	13	14
Burnup of U^{235}, g/kg of U	12	13	15	16
Plutonium discharged, g of Pu/kg of U	6.4	6.9	7.3	7.5
Fissile plutonium discharged,* g/kg of U	4.80	5.17	5.47	5.62
Net fissile isotope burned, g/kg of U	7.20	7.83	9.53	10.38
Reactor utilization, T_r, Mwd/net g of fissile isotope burned	2.22	2.30	2.31	2.41
U^{235} fed to diffusion plant as natural uranium, g/kg of reactor feed	18.4	19.9	23.0	24.5
Net fissile isotope made unavailable, g/kg of reactor feed	13.60	14.73	17.53	18.88
Specific utilization, T, Mwd/g of fissile isotope made unavailable	1.18	1.22	1.26	1.32

* Assumed to be 75% of total plutonium discharged.

Fuel Requirements of D_2O Converter Systems

Of the possible D_2O power reactors, the pressure-tube type, which is currently the most highly developed, has a number of features favorable to good fuel utilization. With the on-power reloading feature, it avoids the necessity for control rods to compensate the reactivity changes associated with fuel burnup. Although the pressure tubes introduce some parasitic neutron absorption, they make possible the construction of very large reactors from which the loss of neutrons by leakage is small. They also make possible the use of cold D_2O as moderator with substantial benefits to the effective value of η for Pu^{239}.

Systematic studies of the effects of fuel-to-moderator ratio on fuel utilization in pressure-tube D_2O-moderated reactors have not been found in the literature. However, in the typical Canadian reactors, as exemplified by CANDU,[8,9] the fuel-D_2O lattices appear to be about as close to the optimum for fuel utilization as is consistent with practical considerations for the specific case of a once-through natural-uranium fuel cycle. These reactors are considered here as examples of what can be accomplished with D_2O moderation without any implication that higher utilizations are impossible with the system.

Table 7 INVENTORY REQUIREMENTS OF H_2O-MODERATED CONVERTERS

	Dresden[7]	Yankee[8]	From Ref. 2			
			1966	1970	1975	1980
Reactor specific power (S), Mw(t)/metric ton of U	11.5	18.8	16	18	22	25
Reactor specific inventory (= 1/S), metric ton of U/Mw(t)	0.087	0.053	0.063	0.056	0.045	0.040
Initial enrichment, % U^{235}	1.5	3.4	2.5	2.8	3.0	3.0
Tons of natural uranium/ton of enriched inventory	2.66	6.70	4.79	5.43	5.65	5.65
Reactor specific inventory, metric ton of U^{nat}/Mw(t)	0.231	0.356	0.302	0.304	0.254	0.226
Fuel residence time in reactor, years	2.98	1.43	3.9	4.2	3.9	3.4
Ratio, $\frac{\text{total inventory}}{\text{reactor inventory}}$, for						
Ex-core holdup of 1.5-year throughput	1.50	2.05	1.38	1.36	1.38	1.44
Ex-core holdup of 2.5-year throughput	1.84	2.75	1.64	1.60	1.64	1.74
Specific inventory of system, metric ton of U^{nat}/Mw(t) installed, for						
Ex-core holdup of 1.5-year throughput	0.35	0.73	0.42	0.41	0.35	0.33
Ex-core holdup of 2.5-year throughput	0.43	0.98	0.50	0.49	0.42	0.39

Table 8 COMPARISON OF INITIAL NEUTRON BALANCE IN A BATCH-LOADED H_2O-MODERATED REACTOR WITH THE NEUTRON BALANCE IN A FUEL SAMPLE THAT HAS JUST BEEN LOADED INTO A CONTINUOUSLY REFUELED D_2O-MODERATED REACTOR

Reactor type	D_2O*	H_2O*
Feed enrichment, E, % U^{235}	Natural	2.0
Target fuel exposure, Mwd(t)/metric ton of U	9000 to 10,000	10,000
τB^2	0.016	0.04
L^2B^2	0.02	~0.0
$\overline{\eta}_{25}$	2.05†	2.05†
ϵ	1.017	1.04
$\overline{\eta}_{25}$	2.09	2.13
R (initial conversion ratio)	0.77	0.66
Inherent losses (= L_i)		
R_{Xe+Sm}	0.057	0.052
R_p	0.085	0.100
$\overline{\eta}_{25}\epsilon\tau B^2$	0.033	0.085
$\left(1+\frac{0.57E}{0.72}\right)L^2B^2$	0.03	~0.0
Total L_i	0.21	0.24
$R_{ex}=\overline{\eta}_{25}\epsilon-1-R-L_i$	0.11	0.23

* The characteristics listed are based on Refs. 7 and 10 for H_2O and D_2O, respectively. However, several characteristics were necessarily derived by inference by the author.

† The values of $\overline{\eta}_{25}$ do not show the effect of the softer neutron spectrum in the D_2O reactor because of differences in calculation methods and differences in basic cross-section data used for the two reactors. The value of $\overline{\eta}_{25}$ for the D_2O reactor has been selected to be in agreement with Fig. 5.

It is instructive to examine the neutron balance in fresh fuel loaded into CANDU in the form specified by Eq. 5, and to compare it with the neutron balance for the H_2O reactor previously considered in Table 4. The comparison is made in Table 8. It is to be noted that the neutron losses, except for those represented by R_{ex}, are not greatly different for the two reactors, although the effect of the lower average parasitic-absorption cross section in the D_2O reactor is evident inasmuch as fuel enrichment is not required to attain a low value of R_p.

The big difference between the two reactors is the difference in R_{ex}, which amounts to 0.12, and is responsible for most of the difference between the initial conversion ratio of 0.77 for the D_2O reactor and 0.66 for the H_2O. More important, however, the two neutron balances do not mean the same thing in the two reactors. In the batch-loaded H_2O reactor, the balance applies to the entire initial core, whereas in the D_2O reactor, which is reloaded essentially continuously, the balance applies only to the fuel that has just been loaded. In this case the neutrons represented by R_{ex} are not wasted but are absorbed usefully elsewhere in the reactor. They serve to maintain the chain reaction in old segments of the fuel whose neutron balances would show a negative value for R_{ex}. It follows also that the initial conversion ratio listed is not the conversion ratio for the D_2O reactor but only for the sample of freshly loaded fuel. It is quite evident that initial conversion ratios are at best only qualitative indicators of the fuel utilization to be attained in the reactor.

Reference 10 reports a study of various once-through fuel cycles, covering a range of enrichments, in a reactor having CANDU characteristics. Although the study was directed at short-term economic evaluations and hence does not treat the precise situations that would be most informative here, some of the ap-

propriate results are summarized in Table 9. The third and fourth columns (cases 1 and 2), which refer to natural-uranium and 1.5% enriched fuel, respectively, apply to a reactor that has the size and lattice characteristics of CANDU and utilizes the bidirectional push-through scheme of fuel reloading with variable push-through rates in different core regions to yield power flattening. The fifth column (case 3) has been synthesized from data in Ref. 10, and it is intended to represent a larger reactor that should be able to attain an exposure of at least 10,000 Mwd/metric ton of uranium with natural-uranium fuel.

The reactor in the third column (Table 9) produces 3.4 Mwd(t) for each net gram of fissile isotope destroyed (Υ_r), but, for each gram of U^{235} fed to the reactor, approximately 0.20 g is discharged at an enrichment too low to justify recovery. The energy production per net gram of fissile isotope made unavailable (Υ) consequently drops to 2.20 Mwd(t). When the fuel burnup is extended to 10,000 Mwd/metric ton of uranium by reducing the leakage from the reactor (column 5), the reactor utilization (Υ_r) drops to 3.23, probably because the greater fractional-energy production from plutonium results in a lower effective value of η for the fuel cycle. However, the specific utilization for the system (Υ) increases to 2.36 because less U^{235} is discarded with the spent fuel.

It is quite evident that one of the problems of fuel utilization in low-enrichment reactors that operate with the once-through fuel cycle is the avoidance of large U^{235} losses in the spent fuel. These losses can be reduced in graded irradiation systems by an increase in the feed enrichment to make possible a greater burndown of the U^{235}. This, however, introduces the diffusion-plant losses, and the net gain in utilization is apt to be small, although the longer exposure may be attractive for economic reasons. The fourth column (case 2) of Table 9 shows an extreme case in which the enrichment has been increased to 1.5%. In this case the utilization has suffered not only from diffusion-plant losses but from a substantial decrease in the reactor utilization as well; the latter may be attributed to the slightly increased fractional contribution of plutonium to the energy production, the hardening of the neutron-energy spectrum as the enrichment is increased, and the

Table 9 FUEL THROUGHPUTS AND UTILIZATIONS IN A HEAVY-WATER REACTOR OF THE CANDU TYPE

Line	Item	Case 1*	Case 2*	Case 3†
A	Feed enrichment, at.% U^{235}	Natural	1.5	Natural
B	Reactor power, Mw(t)	716	716	716
C	Energy production, Mwd(t)/full-power year	2.52×10^5	2.62×10^5	2.62×10^5
D	Fuel exposure at discharge, Mwd(t)/metric ton of U	9080	25,400	10,000
	Feed rates to reactor			
E	Uranium, metric tons of U/full-power year	28.8	10.3	26.1
F	U^{235}, g/full-power year	2.07×10^5	1.54×10^5	1.88×10^5
	Feed rates to system, including diffusion plant			
G	Uranium, metric tons of U^{nat}/full-power year	28.8	27.4	26.1
H	U^{235}, g/full-power year	2.07×10^5	1.97×10^5	1.88×10^5
	Discharge rates from reactor			
J	U^{235}, g/full-power year	0.42×10^5	0.06×10^5	0.30×10^5
K	Pu^{239}, g/full-power year	0.76×10^5	0.24×10^5	0.67×10^5
L	Pu^{241}, g/full-power year	0.12×10^5	0.06×10^5	0.10×10^5
	Contribution of plutonium to total energy production, %	52	55	52
	Utilization ratios			
	Mwd/g of U^{235} fed to reactor (= C/F)	1.27	1.70	1.39
	Mwd/g of U^{235} fed to system (= C/H)	1.27	1.33	1.39
	Mwd/net g of fissile isotope destroyed [= reactor utilization = Υ_r = C/(F − J − K − L)]	3.40	2.22	3.24
	Mwd/net g of fissile isotope made unavailable by reactor [= C/(F − K − L)]	2.20	2.12	2.36
	Mwd/net g of fissile isotope made unavailable [= specific utilization of system = Υ = C/(H − K − L)]	2.20	1.57	2.36

*Data from Ref. 10.

†Inferred from curves of isotopic variation with exposure in Ref. 10, on assumption of 10,000 Mwd/metric ton of U discharge exposure.

greater inventory of fission products in the reactor.

With regard to inventory requirements, the D_2O reactors should achieve specific powers at least as high as those of the H_2O reactors and perhaps somewhat higher because of the flatter power distributions achievable in D_2O reactors.

Table 10 ESTIMATED INVENTORY REQUIREMENTS OF LARGE HEAVY-WATER REACTORS

Feed enrichment, % U^{235}	Natural	1.5
Reactor specific power, Mw(t)/metric ton of U	25	25
Reactor specific inventory (= 1/S), metric tons of U/Mw(t)	0.04	0.04
Tons of natural uranium/ton of enriched inventory	1.00	2.66
Reactor specific inventory, metric tons of U^{nat}/Mw(t)	0.04	0.106
Discharge exposure of fuel, Mwd(t)/metric ton of U	10,000	25,000
Fuel-residence time in reactor, years (80% P.F.)	1.37	3.42
Ratio, $\frac{\text{total inventory}}{\text{reactor inventory}}$, for		
Ex-core holdup of 1.5-year throughput	2.10	1.44
Ex-core holdup of 2.5-year throughput	2.82	1.73
Specific inventory of system, metric tons of U^{nat}/Mw(t) installed, for		
Ex-core holdup of 1.5-year throughput	0.084	0.153
Ex-core holdup of 2.5-year throughput	0.113	0.183

These result partly from the more complex fuel-management schemes that are favored for the D_2O reactors and partly from the relative mildness of water-channel peaking effects in D_2O. The generally lower enrichment of the D_2O reactors reduces the inventory demand on the natural-uranium resource very substantially, even though the ratio of ex-core to in-core inventory may be higher for the D_2O reactors using natural or near-natural enrichment because of the relatively low fuel exposures. In Table 10 the inventory requirements for D_2O reactors that employ fuel of natural enrichment and 1.5% enrichment are given for two different ratios of ex-core to in-core inventory, corresponding to ex-core holdups of 1.5 and 2.5 years of reactor throughput. It seems reasonable that, in practice, the 1.5-year holdup might apply for the natural-uranium case and the 2.5-year holdup might apply for the enriched case.

Plutonium Recycle

Clearly, if the fuel utilization is to be extended in the uranium-plutonium fuel cycle through the energy contributions of plutonium, plutonium must be recycled until it is used up. If the reactor system is composed entirely of thermal converters, the extension of utilization achievable in this way will suffer from the low value of η of Pu^{239} in the thermal spectrum. On the other hand, plutonium is a considerably better fuel than U^{235} for fast-breeder reactors, and, in a nuclear power system made up of fast breeders and thermal converters, there is a substantial fuel-utilization advantage in using the plutonium output of the converters for fast-breeder inventory rather than recycling it to the converters. This advantage persists even if the plutonium must be stored for some years before it is needed for the fast breeders, although a fraction of the advantage may be lost through the decay of Pu^{241} to Am^{241} (see Fig. 10).

Since the eventual large-scale use of fast breeders appears almost inevitable if the nuclear power industry is to grow to large size, one may wonder why there is an emphasis upon the development of plutonium recycle for thermal converters. The incentives appear to lie in shorter-term considerations, most of which are of an economic nature. It is, of course, true that the development of recycle technology in thermal reactors may advance the technology for the fast breeders at the same time. A more compelling argument, however, is that there is a need to establish an immediate value for plutonium to preserve a favorable economic environment for the development of the nuclear industry. If the plutonium value should drop to or near zero in a free nuclear fuel market, the fuel-cycle costs for most enriched reactors would suffer significantly. In an indirect way, a low value for plutonium might also react upon the utilization of U^{235} itself, for Staebler[12] has pointed out that, if there is no financial return from the recovery of plutonium, the reprocessing of uranium fuels with U^{235} contents less than about 0.95% is not economically attractive in the current technology. Whether the (temporary) discarding of exposed uranium with a significant plutonium content, and with a U^{235} content equal to or somewhat higher than that of natural uranium, would aggravate the long-term resource problem is not, however, obvious.

If the nuclear power industry does develop to anything like the size indicated in Fig. 1, the total economic consideration involving plutonium will be quite large. If, for example, the power generation implied by Fig. 1 were supplied by converter reactors of the type indicated in Table 6, the total plutonium produced by the year 2000 would be about 800 metric tons. If its potential value were on the order of $10 per gram, the total would be some $8 billion.

It appears that plutonium will be recycled in thermal converters unless the development of fast breeders proceeds very rapidly. Although there are many problems in plutonium recycle, a large development effort is under way. The most recent summaries of progress were given at the symposium on plutonium as a power-reactor fuel which was held at Hanford in September 1962.[13]

Analyses of plutonium recycle which have been made to date have been directed primarily toward economic considerations for the purpose of defining a reasonable value for plutonium as a recycle fuel. Therefore these analyses do not include an exploration of the limits of utilization that may be achieved with recycle, but they are informative. Data on utilization derived from a recent economic study are shown in Table 11. The H_2O-moderated reactor to which the analysis applies did not have extremely high neutron economy because it used steel-jacketed fuel elements, although the jackets were rather thin (12 mils). The table shows the fuel compositions and the corresponding values of fuel

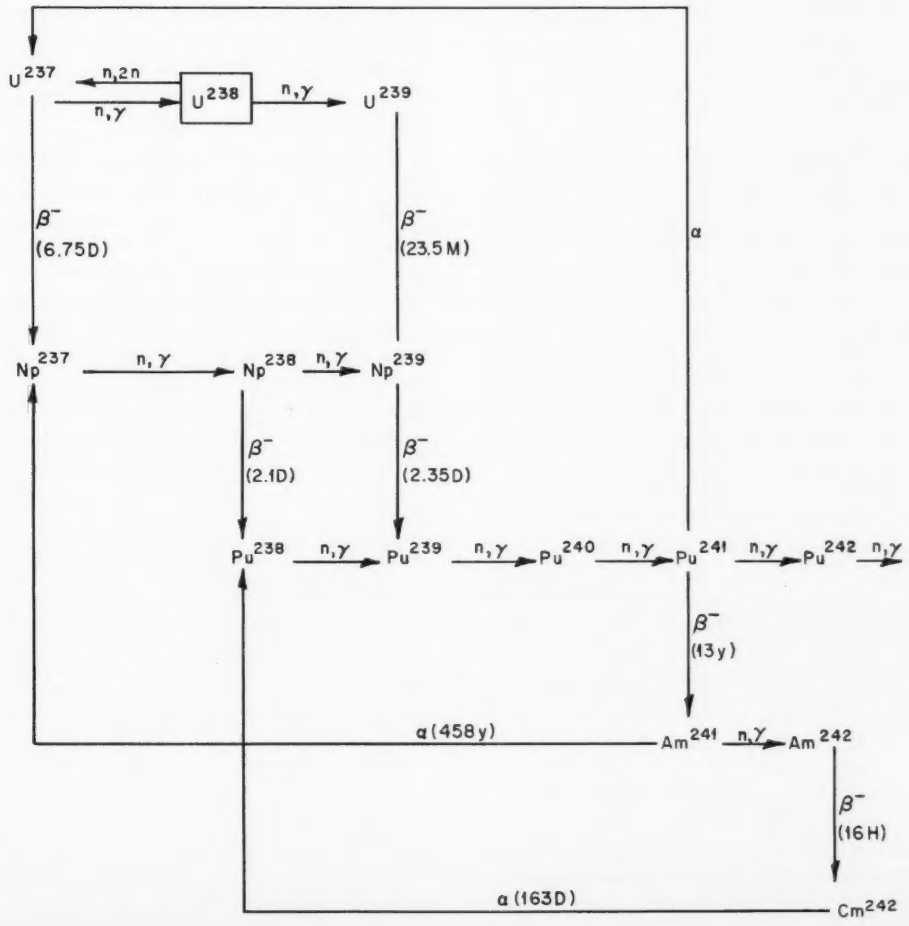

Fig. 10 Formation of plutonium radionuclides and daughters.[11]

Table 11 CALCULATED FUEL UTILIZATION WITH PLUTONIUM RECYCLE IN AN H_2O-MODERATED REACTOR WITH 12-MIL STAINLESS-STEEL FUEL JACKETS[14]

	First cycle	Equilibrium recycle
U^{235} in feed, g/kg of fuel*	24.4	21.1
U^{235} discharged, g/kg of fuel	10.4	11.1
$Pu^{239} + Pu^{241}$ discharged, g/kg of fuel	4.4	6.2
U^{235} burned, g/kg of fuel	14.0	10.0
Net fissile isotope burned, g/kg of fuel	10.0	10.0
Net U^{235} fed to system,† g/kg of fuel	21.4	15.3
Energy produced, Mwd/kg of fuel	16.5	16.5
Utilization		
Mwd/g of U^{235} burned	1.18	1.65
Υ_r, Mwd/g of net fissile isotope burned	1.65	1.65
Mwd/g of U^{235} made unavailable	0.77	1.08
Υ, Mwd/g of net fissile isotope made unavailable	0.97	1.08
Υ_{nat}, Mwd/metric ton of U^{nat}		7800
Fraction of energy from plutonium	0.31	0.51

* "Fuel" is used here to include all elemental uranium and plutonium in the reactor core.

† Including discard in diffusion-plant tails.

utilization for the first cycle and for a typical cycle after the attainment of equilibrium when the plutonium is recycled. The first cycle is equivalent to once-through operation without plutonium recycle. The utilizations are not high in either case, and the improvement due to recycle is not spectacular: it corresponds to an increase from 31 to 51% in the fraction of the total energy provided by plutonium fission.

A somewhat more favorable result is reflected in Table 12, which considers H_2O reactors with zirconium-jacketed fuel [the boiling-water reactor (BWR)], as well as those with steel-jacketed fuel [the advanced pressurized-water reactor (APWR)]. This table has been reprinted from *Power Reactor Technology*, 5(4): 12, and that issue, or the original article,[15] may be consulted for more details on the reactors. The table refers to reactors in whose initial loadings (step 1) U^{235} is the only fissile isotope. In the succeeding steps, the plutonium produced in the previous step is recycled, and the U^{235} feed enrichment is reduced to maintain the most economically favorable fuel exposure. In the later steps, which approach equilibrium recycle, the U^{235} enrichment of the feed is about 1.4% for the BWR case, and the reactor utilization is about 2.4 Mwd/g of U^{235} burned. When the diffusion-plant losses are applied to the latter value, the system utilization for the BWR with graded fuel exposure is about 1.6 Mwd/g of U^{235} made unavailable. For the batch-loaded BWR case, the corresponding value is 1.4 Mwd/g of U^{235}. These values correspond to 11,300 and 10,000 Mwd/metric ton of virgin natural uranium, respectively.

The D_2O reactor considered in Table 12 appears to be somewhat less favorable for fuel utilization than that considered in Table 9, for in step 1 it requires a U^{235} enrichment of 1.33% to attain an exposure of 16,800 Mwd/metric ton. The reactor of Table 9 would attain the same exposure with an enrichment of slightly more than 1%.[10] In the later steps (Table 12) the enrichment for the D_2O reactor in the graded case approaches 0.99%. This is not a favorable enrichment for high utilization at the exposure level of 16,000 to 17,000 Mwd/metric ton be-

Table 12* CALCULATED UTILIZATION OF U^{235} IN REACTORS WITH PLUTONIUM RECYCLE

	Megawatt days per gram of U^{235} destroyed†										
	APWR simulation‡				D_2O simulation‡			BWR simulation		OMR simulation	GCR simulation
Step No.	I (batch)	II (batch)	III (batch)	IV (batch)	I (batch)	II (batch)	III (graded)	Batch	Graded	(batch)	(batch)
1	1.07	1.06	1.05	1.06	1.28	1.30	1.65	1.25	1.39	1.05	1.21
2	1.31	1.31	1.30	1.31	1.80	1.78	2.39	1.76	2.04	1.33	1.45
3	1.40	1.41	1.41	1.41	1.99	1.95	2.45	1.98	2.29	1.47	1.50
4	1.44	1.44	1.47	1.45	2.02	2.00	2.48	2.07	2.39	1.55	1.51
5	1.47	1.46	1.49	1.45	2.02	1.98	2.43	2.14	2.42	1.53	1.50
6		1.46	1.49	1.46	2.07	1.97	2.44	2.15	2.44		1.52

* The material in this table is from the analyses reported in Ref. 15, but some of the material does not appear in the reference. The table was furnished by E. A. Eschbach for *Power Reactor Technology*, 5(4).

† Note that this refers to destruction of U^{235}, including the formation of U^{236}. This is approximately 20% less than the formulation per gram of U^{235} fissioned.

‡ The Roman numerals refer to various cases, for which the reader is referred to Ref. 15.

cause it not only leaves a significant fraction of U^{235} in the spent fuel but introduces a diffusion-plant loss as well. It is expected that higher utilizations should be possible with natural-uranium feed, perhaps with a reactor having a higher D_2O-to-fuel ratio. If it is assumed that the reactor of Table 9, with plutonium recycle and natural-uranium feed, could attain a reactor utilization at least as high as that shown for the D_2O reactor in Table 12 (2.44), the system utilization would lie between 15,000 and 16,000 Mwd/metric ton of virgin natural uranium, whereas the system utilization would exceed 20,000 Mwd/metric ton if the reactor utilization of 3.24 (Table 9, last column) could be approached.

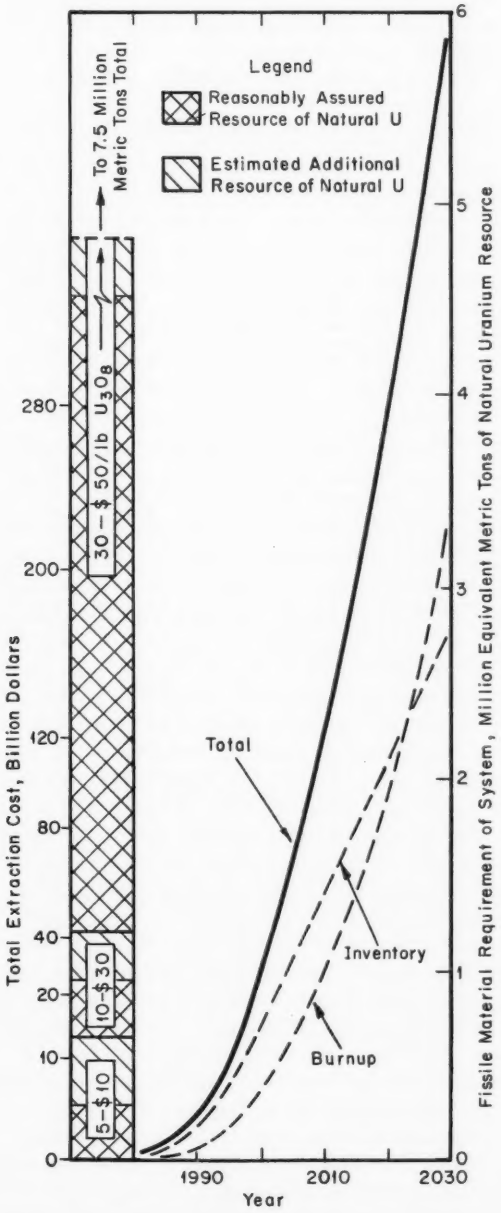

Fig. 11 Fissile material requirements of H_2O-moderated converters with plutonium recycle.
See Table 17 for reactor characteristics.

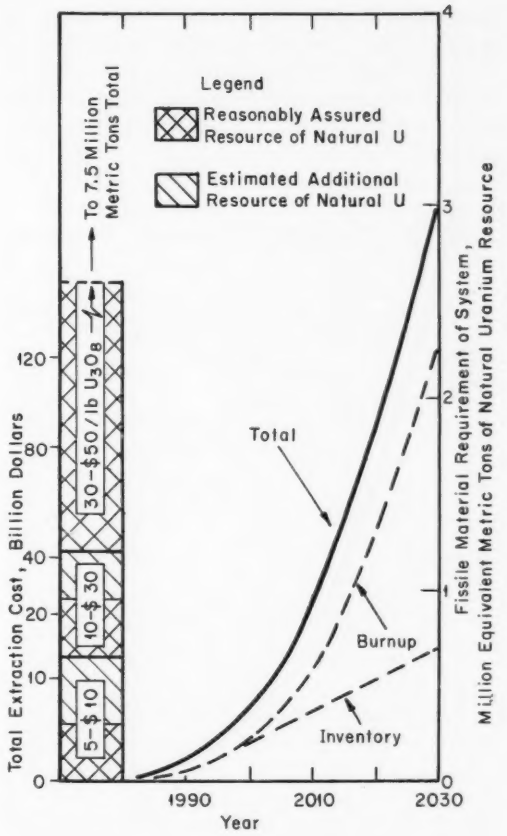

Fig. 12 Fissile material requirements of D_2O-moderated converters with natural-uranium feed and plutonium recycle.
See Table 17 for reactor characteristics.

In the absence of more pertinent calculations, it is perhaps reasonable and conservative to guess that H_2O-moderated reactor systems with plutonium recycle might achieve utilizations of about 11,000 Mwd/metric ton of virgin natural uranium, whereas D_2O-moderated systems with natural-uranium feed might achieve utilizations

of about 16,000 Mwd/metric ton. Practically all of this difference is attributable to the loss of U^{235} in diffusion-plant tailings in the H_2O case. These estimates are lower than some which have been made on the basis of earlier information.[16]

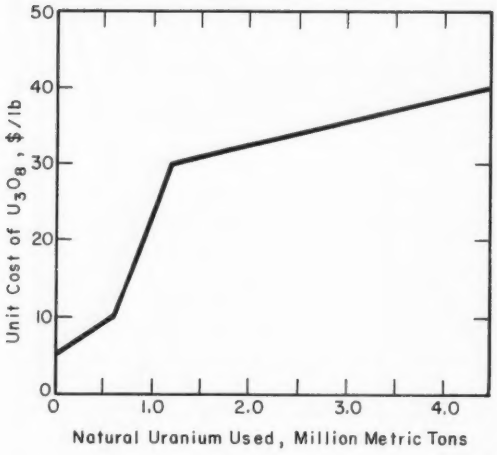

Fig. 13 Assumed variation of cost of mining and extracting U_3O_8 with quantity of natural uranium used.

In Figs. 11 and 12 the fissile isotope requirements are shown for the nuclear power industry described by Fig. 1 on the assumptions that the nuclear power is provided by the H_2O converters and D_2O converters, respectively, with the utilization of plutonium recycle. The fuel utilizations and inventory requirements assumed are consistent with the preceding discussion (i.e., they are representative of near-future technology) and with Tables 7 and 10. On the right-hand scales of the graphs the requirements may be read as equivalent tons of natural uranium, i.e., as the number of tons of natural uranium required to furnish the fissile isotope requirement. Diffusion-plant enrichment was utilized where appropriate. The curves may also be compared directly with the bar chart on the left which shows the estimated U. S. resources of natural uranium in accordance with Table 2. To give an approximate picture of the cost of mining and extracting the uranium as U_3O_8, the assumption has been made that within each category of total estimated resource listed in Table 2 the unit extraction cost varies linearly with the amount of uranium extracted. The resulting variation is shown in Fig. 13. This curve has been integrated, and the total cost of extracting the U_3O_8 has been marked off on the left-hand sides of the bar charts.

The difference in total requirements shown in Figs. 11 and 12, which amounts to about a factor of 2 over most of the range, is due mainly to the lower inventory requirement of the D_2O reactor.

Other Thermal Converters

The foregoing discussion has shown that, for thermal reactors operating either with or without plutonium recycle, the characteristics that favor high fuel utilization are a low effective temperature for the thermal-neutron spectrum and the ability to achieve high neutron economy with low fuel enrichment. Basically the latter characteristic is synonymous with a high value of moderating ratio, $\xi\Sigma_s/\Sigma_a$. Although reactors employing other moderators probably cannot approach the values of the moderating ratio which can be achieved in D_2O-moderated reactors, some of them may be capable of some improvements over the H_2O performance if they use low-absorption materials for coolants and fuel jackets. It is hardly to be expected, for example, that the utilization in a thermal-neutron sodium-graphite reactor, employing steel-jacketed fuel elements, would equal that of a good H_2O reactor, but the gas-cooled or water-cooled graphite-moderated types might show some improvements. The extent of this possible improvement is probably quite limited because the graphite moderator usually operates at a high temperature; thus the gains in η which may be hoped for because of a more highly thermalized spectrum are likely to be eliminated by the higher temperature of that spectrum. The gas-cooled graphite reactors of the British type do operate on natural uranium and consequently avoid the loss of U^{235} in diffusion plants; however, unless the fuel exposures of these reactors can be extended very substantially, a comparable U^{235} loss will occur in the fuel discharged from the reactor.

The organic-moderated reactors may be expected to exhibit utilization capabilities comparable to those of the H_2O reactors since the important constituent of the organic is hydrogen, as it is in H_2O. Organic-cooled reactors moderated by graphite or D_2O would be expected to approach the utilization values that characterize

those moderators, except insofar as the organic coolant may change the parasitic-absorption ratio indirectly through its influence on the choice of the fuel-jacket material and the chemical composition of the fuel body.

The spectral shift reactor, employing a variable mixture of H_2O and D_2O, will tend to exhibit reactor utilizations intermediate between those of H_2O- and D_2O-moderated reactors but does not appear to offer the possibility of very low enrichment, which is the principal advantage of the D_2O type. Some improvement in reactor utilization may also be expected because the spectral shift control scheme avoids the parasitic loss of neutrons in control rods. However, this improvement will be relative to batch-loaded reactors but will not be relative to those reactors employing graded-irradiation fuel cycles. Since graded irradiation is not easily had in H_2O-moderated reactors, the spectral shift approach may well give utilization improvements over the "practical" reactors, which are actually built without improving on the best of the idealized H_2O-moderated types that have been considered here. Utilization results that have been computed from the fuel-mass balance for a recent[17] "reference design" of a 330-Mw(e) spectral shift reactor employing Zircaloy-jacketed fuel elements are given in Table 13.

The "homogeneous" or "semihomogeneous" gas-cooled reactors, which employ unjacketed fuel dispersed in a moderator (usually graphite) represent approaches that are intended to minimize the parasitic absorption of neutrons through the elimination of "parasitic" structural material. In some cases the continuous removal of volatile fission products is also undertaken, as in the Peach Bottom reactor in the United States and the Dragon reactor in Great Britain.

The "homogeneous" approach has not, however, been considered seriously for the uranium-plutonium cycle, because such reactors, when they contain a substantial quantity of Pu^{239}, tend to be characterized by a prompt positive power coefficient of reactivity. Whether this is an insurmountable difficulty has apparently not received extensive investigation. Instead, the development of the reactor type has been directed toward operation on the thorium-U^{233} cycle. This cycle is discussed briefly in a later section.

With regard to inventory, most of the nonaqueous reactor types currently under development appear to have requirements at least as high as those which characterize the H_2O reactors. Although the excellent heat-transfer properties of sodium will support very high heat fluxes, it appears that, in the sodium graphite reactors, economic considerations and heat-transport considerations result in designs having only moderate values of specific power. The use of more dense fuel material (uranium metal, or possibly uranium carbide, rather than uranium oxide) also tends to result in lower specific powers. The specific power of the Hallam sodium graphite reactor, for example, is about 9 Mw(t)/metric ton of uranium. Current designs of sodium graphite reactors reflect, of course, current economic pressures, which do not place great emphasis on specific power per se. The reactor type might be capable of large increases in specific power if such increases were justified economically by a scarcity of fuel for inventory.

Table 13 FUEL UTILIZATION IN THE REFERENCE-DESIGN SPECTRAL SHIFT CONTROL REACTOR*

Power output, Mw(e)	330
Fuel	UO_2 in Zircaloy
Average feed enrichment, % U^{235}	3.33
Average discharge enrichment, % U^{235}	1.92
Average discharge exposure, Mwd/metric ton of U	16,780
Mass balance, kg	
U^{235}	1343† and 752‡
U^{238}	38,982† and 38,329‡
Pu^{239}	319.1‡
Pu^{240}	34.1‡
Pu^{241}	41.1‡
Pu^{242}	10.2‡
Thermal energy produced, Mwd	6.75×10^5
Net fissile isotope destroyed in reactor, g	2.31×10^5
Υ_r, Mwd/net g of fissile isotope destroyed	2.92
Net U^{235} fed to system, g	9.05×10^5
Net fissile isotope fed to system, g	5.45×10^5
Υ, Mwd/net g of fissile isotope made unavailable	1.24

* Basic data from Ref. 17.
† Beginning of life.
‡ End of life.

The low-enrichment reactors of the gas-cooled type are limited in specific power by the well-known heat-transfer and heat-transport limitations of gases. Those which use natural or near-natural enrichment may make no greater

demands on the uranium supply, for inventory, than do the H_2O-moderated reactors, but the demands are not likely to be much less than those of the H_2O reactors unless the moderator employed for the gas-cooled case is heavy water. The reactor-inventory requirement of the later British (natural uranium) gas-cooled reactors is about 0.4 metric ton of uranium/Mw(t) installed, which may be compared to a typical value of 0.3 metric ton of U^{nat}/Mw(t) for the H_2O reactors.

The heat-transfer properties of the organic coolants are, in general, poorer than those of water, and the specific powers of organic-cooled reactors tend to be lower — and inventory requirements higher — than for comparable water-cooled types, except in those cases where central fuel temperatures limit the specific powers of both types to comparable values.

The Thorium Cycle

The characteristics of the thorium-uranium fuel cycle are the inverse of those of the uranium-plutonium cycle in that the bred material has a higher effective η than the U^{235} feed. The conversion-ratio gains from the higher η of U^{233} are to some extent offset by a lower fast-fission effect in thorium than in U^{238} and by the loss of some potential U^{233} through neutron absorption in Pa^{233}, its radioactive precursor. This loss depends on the thermal-neutron flux level and on the neutron-energy spectrum, but it probably will not amount to more than 0.01 or 0.02 in terms of conversion ratio in the reactors that might be contemplated. The combined effects of the reduction in fast-fission effect and the Pa^{233} loss might amount to a reduction in potential conversion ratio somewhere in the range 0.03 to 0.10 if thorium were substituted for U^{238} in a reasonably well-moderated reactor using U^{235} as the fissile isotope.

It is clear from Fig. 5 that the value of $\bar{\eta}$ of U^{233} is higher than that of U^{235} by at least 0.23. This difference actually becomes greater in more epithermal spectra, as may be seen by comparing Figs. 6 and 8. The preceding discussion has shown that both H_2O- and D_2O-moderated reactors, when using a U^{235}-U^{238} mixture as fuel, could achieve initial conversion ratios of about 0.90 if there were no wastage of neutrons in control rods. If a round number of 0.07 is taken for the loss in initial conversion ratio when thorium is substituted for U^{238}, then it might be expected that similar reactors would be capable of initial conversion ratios of about 0.83 when thorium is used as the fertile isotope. If U^{233} were used as fissile isotope, the initial conversion ratio might be increased to about $0.83 + 0.23 = 1.06$. A system which is fueled initially with U^{235} and thorium and which utilizes some method of preserving the optimum neutron balance as fuel exposure proceeds (e.g., an incremental fuel-reloading system) should, except for fission-product losses, yield average conversion ratios somewhere within the approximate range of 0.83 to 1.06, depending upon the fraction of the total energy derived from U^{233}. The losses to long-lived fission products may amount to about 0.06 or more for very long fuel exposures. Hence, with H_2O and D_2O reactors designed for high-neutron economy and operating on the thorium cycle with U^{235} as the initial fissile isotope, but employing more or less conventional solid-fuel technology, average conversion ratios might be hoped for in the range from about 0.77 to nearly 1.0. The values at the higher end of the range would, however, be achieved only if most of the energy were generated by the fission of U^{233}, i.e., after many recycles of the bred U^{233}. These possibilities are illustrated by Table 14, which applies to a "potential" plant design utilizing a spectral shift reactor with U^{233} recycle. The table shows the isotopic mass balance for the first cycle and the third cycle (second U^{233} recycle). In this case both the reactor utilization and the overall utilization have become quite high by the third cycle.

Although the potentialities for high fuel utilization exist when the thorium-uranium cycle is used, it is important to recognize that the possible improvement is an improvement in the basic nuclear performance (with low-energy neutrons) of the bred material. The difference shows up more strongly as the basic neutron economy of the reactor is improved. If the thorium-uranium cycle is compared with the uranium-plutonium cycle in a reactor which has a conversion ratio too low to yield a substantial fraction of the total energy output from the bred material, then little or no improvement in reactor utilization may result from a change to the thorium-uranium cycle. If the decision has been made to adopt the thorium-uranium cycle for the purpose of improving fuel utilization, and the price has been accepted that must be paid for this approach, i.e., the necessity of

Table 14 FUEL UTILIZATION IN A "POTENTIAL" SPECTRAL SHIFT CONTROL PLANT[17] OPERATING ON THE THORIUM CYCLE, FED WITH U^{235} AND RECYCLING U^{233}

Net power output, Mw(e)	333
Fuel	ThO_2-UO_2 in Zircaloy-4 (collapsed cladding)
Energy production per cycle, Mwd(t)	7.25×10^5

	First cycle		Third cycle	
	Beginning	End	Beginning	End
Mass balances				
U^{235}, kg	1320	643	343	206
U^{233}, kg		439	686	753
U^{234}, kg		35	84	130
U^{236}, kg		137	185	203
U^{238}, kg	70	69	69	68
Pa^{233}, kg		39		41
Th^{232}, kg	39,197	38,458	39,190	38,419
D_2O, mole %	50	2	63.5	2
Net grams of fissile isotope destroyed in reactor*	1.95×10^5		0.29×10^5	
Υ_r, Mwd/net g of fissile isotope destroyed	3.72		25	
Net U^{235} fed to system, g	10.37×10^5		2.10×10^5	
Net fissile isotope fed to system,* g	5.59×10^5		1.02×10^5	
Υ, Mwd/net g of fissile isotope made unavailable	1.30		7.11	

* Pa^{233} counted as U^{233}.

using fully enriched U^{235} as the feed material, then it is important to minimize all parasitic losses of neutrons in the reactor, including losses to parasitic control elements. The spectral shift control scheme is one method of avoiding losses of the latter type. Another method is the use of incremental fuel replacement, as is afforded in the pressure-tube D_2O reactors employing on-power reloading.

The other novel approach to obtaining high fuel utilization with the thorium cycle is the "homogeneous" gas-cooled reactor type mentioned previously. The Dragon and Peach Bottom projects are directed toward the development of this concept, but high utilization can be expected only from reactors that are large enough to reduce the neutron leakage to a small fraction. If the conversion ratio can be made high enough, through the reduction of neutron leakage and the partial removal of fission products, the loss of reactivity with fuel exposure may be slow, and serious neutron losses to control rods can be avoided. Although this reactor type, in principle, has the potentialities of high fuel utilization, a better assessment of its prospects will be possible after more practical experience has been attained with it.

With regard to inventory requirements, it has been indicated that the British, in their development of the Dragon type reactor, have a target of at least 1 Mw/kg of fissile isotope for the reactor specific power. This is about the specific power, relative to fissile isotope, which is characteristic of the reactors cooled and moderated by H_2O. The design of the Peach Bottom[18] reactor gives a specific power of 0.77 Mw/kg of U^{235}, at a core power density of about 9 Mw/m^3. The power density in the Dragon[19] reactor is about 14 Mw/m^3. It therefore appears reasonable to assume, at this time, that the inventory demands of the gas-cooled, H_2O-cooled, and spectral shift reactors operating on the thorium cycle will be comparable to those of the H_2O reactors operating on the uranium-plutonium cycle. It is to be noted, however, that the long-range development effort being carried out at the Lawrence Radiation Laboratory[20] toward the development of homogeneous or semihomogeneous gas-cooled reactors has a target power density of 3 Mw/cu ft. This is almost an order of magnitude higher than the power densities in the Peach Bottom and Dragon reactors and, if it could be achieved, would presumably correspond to a major reduction in inventory requirement.

Heavy-water reactors designed for operation on the thorium cycle could presumably achieve specific powers, relative to fissile isotope, comparable to those which they currently attain on the uranium-plutonium cycle. There is some

uncertainty in this estimate since the thermal-neutron absorption cross section of thorium is considerably higher than that of U^{238}, and the dilution of fissile isotope by fertile isotope would therefore necessarily be less in the thorium case than in the U^{238} case. Relative to the resource of natural uranium, the inventory requirement of the D_2O reactor on the thorium cycle would necessarily increase by about 50% above that of D_2O reactors fed by natural uranium because of the diffusion-plant losses connected with the use of pure U^{235} in the thorium case.

It seems highly probable that one or more types of thermal-converter reactors can be developed which, on the thorium-uranium cycle, can achieve rather high overall fuel utilization, although there is no indication that they can reduce the problem of inventory supply. If there were little confidence in the development of fast breeders for several decades, these types would represent an important possibility for achieving some extension of the effective nuclear fuel supply. If a nuclear power industry is visualized, in which, after a few years, fast breeders play an important part, the role of the thorium-cycle reactors is not so clear. They do not contribute to the important operation of supplying fissile isotope for fast-breeder inventory. This is true not only because the U^{233} produced by the thorium-cycle reactors is not as attractive as plutonium for fast breeders but, more fundamentally, because the thorium-cycle reactors achieve their superiority in fuel utilization only by burning the bred U^{233} themselves.

Fast Breeders

There is now no doubt that breeding, even with a reasonably high breeding gain, can be achieved in fast-neutron reactors. The development of the reactor type has not, however, progressed far enough to support predictions of the performance that will actually be achieved in practical, economically competitive fast-breeder systems.

The performance characteristics most directly applicable to the question of uranium resources are the inventory requirement and the doubling time of the fast-breeder system. These two are not independent; a large share of the uncertainty in predicting either lies in the magnitude of the out-of-pile inventory.

A fast breeder operating with a breeding gain of G would, in operating one year at a power

Table 15 CALCULATED CORE LOADINGS AND BREEDING RATIOS FOR IDEALIZED SPHERICAL FAST BREEDERS

Core composition, vol. %	Core volume,* liters	Feed fuel	Breeding ratio	Core load, kg of fissile isotope
23 metallic fuel 66 sodium 11 stainless steel	500	Pu^{239}	2.07	281
		U^{235}	1.41	453
	1000	Low-quality Pu†	2.27	234
		Pu^{239}	2.07	456
		U^{235}	1.40	711
	2000	Low-quality Pu†	2.15	408
		Pu^{239}	2.05	770
		U^{235}	1.39	1162
32 oxide fuel 52 sodium 16 stainless steel	875	Pu^{239}	1.67	378
		U^{235}	1.16	553
	1750	Low-quality Pu†	1.78	323
		Pu^{239}	1.65	639
		U^{235}	1.14	899
	3500	Low-quality Pu†	1.69	582
		Pu^{239}	1.62	1126
		U^{235}	1.12	1536

* The core-volume choices are intended to correspond to equal electric-power levels from the core generation rates in the metal-fueled and oxide-fueled reactors. The core power densities are assumed to be 1.0 Mw(t)/liter and 0.5 Mw(t)/liter, and the thermal efficiencies are assumed to be 35% and 40%, respectively, for metal and oxide cores.

† Low-quality plutonium: 40% Pu^{239}, 25% Pu^{240}, 15% Pu^{241}, and 20% Pu^{242}. Only Pu^{239} and Pu^{241} are counted as fissile isotopes.

factor F, produce excess fissile isotope, e, given by[21]

$$e = 365F \frac{1 + \alpha_{av}}{0.95} \frac{SG}{10^6 H} \quad (6)$$

where e is the excess as a fraction of the reactor inventory (i.e., it is the "interest rate" of the breeding process), S is the reactor specific power in kilowatts (thermal) per kilogram of fissile isotope, and H is the ratio of total inventory associated with the reactor to the in-pile inventory.

The two fast reactors under construction in the United States, EBR-II[22] and the Enrico Fermi Fast Breeder,[23] are designed for specific powers in the range 160 to 170 kw/kg of fuel. If this performance could be maintained in much larger reactors of the type, for which the fissile isotope content of the fuel might be on the order of 10%, the value of S in Eq. 6 might be something like 1600 kw/kg of fissile isotope. At this value of specific power and with a breeding gain even as low as 0.30, Eq. 6 would give an interest rate of about 17% per year at a plant factor of 0.80 if the ex-pile inventory were ignored ($H = 1$). Thus the reactor itself might be said to have a doubling time of 1/0.17 or about six years.

When a system of breeders is considered in which bred plutonium is used to fuel new breeders in the expanding system as rapidly as it becomes available, e becomes a rate of "compound interest," and the doubling time (in years) is given by t in the equation

$$2 = (1 + ce)^{t/c} \quad (7)$$

where c is the conversion period, or the average interval (in years) during which plutonium is allowed to build up in the blanket of the "mother" reactor before it is extracted and finally used as inventory for a "daughter" reactor. For the system of breeders, the ex-pile inventory must, of course, be taken into account.

It may be noted that the specific powers relative to *fuel* which are quoted above are far above the specific powers (~20 kw/kg) which characterize the thermal reactors. Yet, because of the higher enrichment, the specific power relative to *fissile isotope* does not differ greatly from that of the thermal reactors. The fast-reactor designer must strive for high specific power relative to fuel in order to keep the inventory of fissile isotope within reason. However, the high specific power will be of little benefit if it results only in a high rate of fuel throughput for the reactor, with a pileup of ex-reactor inventory in the cooling, reprocessing, and fuel-fabrication stages. Further, for enrichments above about 3%, the cost of chemical reprocessing by conventional methods tends to be proportional to the quantity of fissile isotope processed rather than to the quantity of fuel processed. To keep the total inventory of fissile isotope at an economically low level and to avoid large reprocessing contributions to the fuel-cycle cost, the developers of fast breeders either must find alternate reprocessing and refabrication methods that are quicker and cheaper than the conventional ones or must develop fuels that will operate to very high exposure levels.

Table 16 CHARACTERISTICS OF A SELECTED OXIDE-FUELED FAST BREEDER FROM PARAMETRIC STUDY[28]

Power	
Thermal, Mw(t)	812
Electric, Mw(e)	300
Plant factor, %	70
Fuel density, % of theoretical	90
Fuel-rod diameter, in.	0.20
Thermal conductivity of fuel, Btu/(hr)(ft)(°F)	1.0
Peak/average specific power	2.5
Peak fuel temperature rise (surface to center), °F	3500
Thickness of stainless-steel fuel jacket, in.	0.02
Volume of stainless steel for structure, % of fuel-cladding volume	10
Isotopic composition of UO_2-PuO_2 feed fuel, %	
Uranium	All U^{238}
Pu^{239}	60
Pu^{240}	25
Pu^{241}	12
Pu^{242}	3
Fuel exposure, Mwd/metric ton	100,000
Sodium temperatures, °F	
Inlet	750
Outlet	1000
Sodium flow velocity, ft/sec	23
Core diameter (= core height), ft	4.94
Loading of fissile isotope, kg	940
Specific powers	
kw/kg (U + Pu)	96
kw/kg (Pu^{239} + Pu^{241})	867
Breeding ratios	
Core	0.76
Blanket	0.60
Total	1.36
Fuel residence time in reactor, years	4.67
Ratio, (total inventory)/(in-pile inventory)	1.14
Doubling time, years	17.5
Specific inventory, kg of fissile Pu/Mw(t) installed	1.32

Table 17 CHARACTERISTICS OF REACTOR TYPES USED FOR ESTIMATES OF RESOURCE DEPLETION

Characteristics common to all types	Year								After 2000	Remarks
	1965	1970	1975	1980	1985	1990	1995	2000		
Plant factor	0.80	0.80	0.80	0.80	0.775	0.750	0.725	0.70	0.70	Derived from Ref. 2
Average thermal efficiencies of all plants in operation	0.32	0.33	0.335	0.385	0.40	0.40	0.40	0.40	0.40	Derived from Ref. 2

Characteristics of Specific Types

Type	Inventory requirements	Utilization characteristics	Used in figure	Remarks
Fast breeder	1.525 kg of fissile Pu/Mw(t) installed or 2.29 kg of U^{235}/Mw(t) installed or 0.488 metric ton of U^{nat}/Mw(t) installed	20-year doubling time for system	2,15,16,17,18	
Fast breeder (high inventory)	0.976 metric ton of U^{nat}/Mw(t) installed	20-year doubling time for system		
H_2O converter with plutonium recycle	0.406 metric ton of U^{nat}/Mw(t) installed	T_{nat} = 11,000 Mwd(t)/metric ton of U^{nat}	11	Compare Table 7 for inventory
H_2O converter without plutonium recycle	0.406 metric ton of U^{nat}/Mw(t) installed	Utilization of U^{235} equivalent to 7350 Mwd(t)/metric ton of U^{nat}; production of fissile Pu = 0.225 g/Mwd(t)	15,18	Utilization and production approximately as in Table 6, on assumption that plutonium is 75% fissile isotope
D_2O converter with plutonium recycle (natural-uranium feed)	0.105 metric ton of U^{nat}/Mw(t) installed	T_{nat} = 16,000 Mwd(t)/metric ton of U^{nat}	12	Compare Table 10 for inventory
D_2O converter without plutonium recycle (natural uranium)	0.105 metric ton of U^{nat}/Mw(t) installed	Utilization of natural uranium = 10,000 Mwd(t)/metric ton of U^{nat}; production of fissile Pu = 0.299 g/Mwd(t)	16,18	Utilization and production as in last column of Table 9
Thorium-cycle converter	0.406 metric ton of U^{nat}/Mw(t) installed	Net burnup assumed negligible	17,18	Inventory assumed same as for H_2O converters

Both of the above approaches are being followed in the fast-reactor program. In general, the development effort on metallic fuels encompasses also the development of rapid reprocessing and refabrication by systems involving pyrometallurgical techniques,[24] whereas the ceramic-fuel effort, centered principally about oxide fuels, is directed toward the achievement of very long exposure lifetime.[25] The development of the metallic-fuel complex is centered about the EBR-II, which includes a facility for pyrometallurgical reprocessing and remote refabrication as an integral part of the plant.[26] The two approaches do overlap, however, for the Argonne program is considering also the use of refractory compounds, such as the carbides, with pyrometallurgical reprocessing methods, whereas the proponents of the ceramic approach include also the possibilities of carbide fuels and do not rule out the possibility of developing unconventional reprocessing methods.

At the present time it appears difficult to attain sufficiently high exposure levels with the metallic fuels, even within the range that would be economically acceptable with the integral pyrometallurgical reprocessing and refabrication systems. The development of metallic fuels containing plutonium, in particular, appears to be very difficult.[24] On the other hand, although sample irradiations of oxide fuels for fast reactors have been encouraging,[25] the general experience with fast-breeder development to date has shown that the characteristics and difficulties of a particular concept cannot be considered as known until a prototype of reasonable size has been built and operated. Consequently large uncertainties remain as to the doubling times that may be expected in practical economic fast breeders and as to the total inventory requirements.

A recent economic study[27] has visualized the possibility of total inventories ranging from 1.5 to 10 times the in-pile inventory, although a range from 1.5 to 5 was considered more nearly consistent with the concepts treated. The study was aimed at the evaluation of appropriate price ranges for plutonium as a fast-reactor fuel, and consequently the various reactors studied were treated in an idealized way, and the results cannot be considered as predictions of practical fast-breeder characteristics. Nevertheless, the calculated reactor characteristics for oxide and metal fuel cores are reproduced in Table 15 to illustrate characteristics that result from reactor physics considerations. In particular, the differences between the plutonium-fueled cases and the U^{235}-fueled cases with respect to inventory requirements are useful in connection with uranium resource considerations.

A recent parametric study[28] of oxide-fueled fast breeders has considered the reactor characteristics in more detail. A range of specific powers was considered, the range being covered by variations in the diameter of the oxide fuel pins. The characteristics of one of the reactors, from the region of the study considered most favorable on an overall basis, are listed in Table 16. The inventory and doubling time include considerations of out-of-pile inventory based on the use of aqueous reprocessing.

Because of the very large uncertainty in fast-breeder performance, the discussions of resource utilization by fast breeders in this review have been based on performance characteristics (Table 17) that should be considered as minimum targets for the industry postulated in Fig. 1 rather than as predicted values. They are, however, reasonably close to the values estimated in Table 16.

Thermal Breeders

Although it appears reasonable that certain fixed-fuel thermal reactors operating on the uranium-thorium cycle might achieve conversion ratios of unity or slightly larger, particularly if some means of reducing the losses of neutrons to fission products are used, it is not obvious that practical designs can yield ratios high enough to achieve breeding in the sense of producing excess fuel at an important rate. This question has not been discussed recently in the literature.*

*Some analysis of the possibilities with pressure-tube D_2O-moderated reactors has recently been carried out by D. S. St. John at Savannah River. The substitution of thorium-U^{233} for uranium in previous design studies (DP-830, with some modifications) indicates the possibility of breeding ratios as high as 1.04 to 1.06. It is pointed out that a breeder system of this kind could be brought into being without recourse to enriched uranium: natural uranium could be used to produce plutonium that would then be used as the initial fissile isotope for thorium operation.[31]

It is well known that the circulating fuel systems, at least the aqueous homogeneous systems, offer breeding possibilities. Although these systems would appear to have difficulty in competing with the fast breeder on the basis of doubling time, they may offer possibilities of very substantial reductions in inventory requirement. The specific powers quoted for the aqueous homogeneous concepts listed in Ref. 29 range from about 1.3 to 3.2 Mw/kg of fissile isotope in the reactor system. If integral continuous reprocessing is used, as visualized, the ex-reactor inventory might be quite small, and the total inventory requirement might be less than that of the fast breeder by a substantial factor. In addition to the advantages of low inventory illustrated by Fig. 2, there is the additional advantage that the low-inventory reactor can utilize a higher cost supply of fissile isotope for initial inventory without exceeding the economic limits of fuel-cycle costs.

The difficulties of the aqueous homogeneous breeder are, of course, well known, and, until the problems of this reactor type are solved, there must be large uncertainties in the level of performance that could actually be achieved. There are similar uncertainties in the other thermal fluid-fuel breeder concepts, and therefore it appears at the present time that the fast breeder is the only reasonably assured approach to breeding, even though the thermal concepts appear to have some promise of superior performance in some respects.

Combination Systems

Since economic breeders do not now exist, the growing nuclear power system will necessarily contain some converters, at least during the early stages. Three different idealized systems have been considered, and these utilize fast breeders with a doubling time of 20 years in combination with three different converter types, in a mixture described by Fig. 14. This combination is arrived at by assuming that the development of fast breeders lags behind that of converters by 10 years up to the year 2000. That is to say, up to the year 2000 the installed capacity in breeders follows a curve which is identical to the total nuclear capacity curve (the same curve as that of Fig. 1) but which is displaced 10 years to the right. The remainder of the total capacity is assumed to be provided by converters. It is further assumed that the construction of converters will be stopped in the year 2000 and that all new capacity will thereafter consist of breeders. The converter capacity in existence dies off according to a curve which corresponds approximately to a 30-year plant life but which has been approximated by two straight-line segments to facilitate computation. For computational convenience Fig. 14 specifies thermal rather than electrical capacity. The curve of total capacity agrees with Fig. 1 when the efficiencies specified in Table 17 are applied.

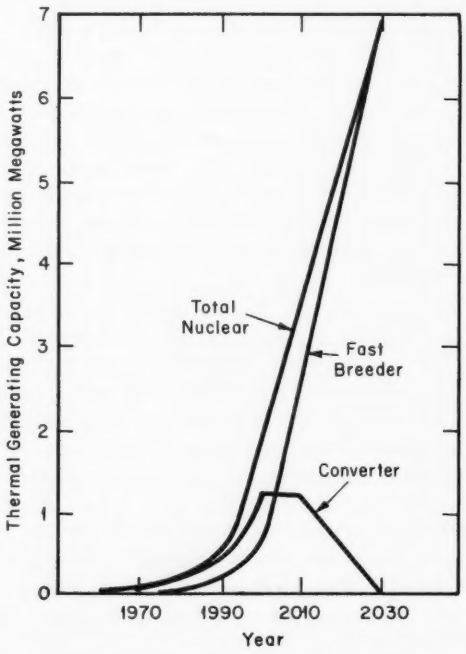

Fig. 14 Assumed mixture of fast-breeder and thermal-converter reactors up to the year 2030. The curve of total capacity is consistent with the electrical capacity shown in Fig. 1.

The characteristics of the reactors assumed to make up the converter-breeder complex are listed in Table 17 along with the characteristics of the reactors used for other estimates of resource utilization in this review. Reference to preceding sections will show that they are consistent with the discussions of the fuel-utilization capabilities of the several reactor types. Those discussions do not assume any developments beyond those which are the objects of rather spe-

cific programs currently under way. Consequently the technology assumed can probably be described most reasonably as "near future," but with the reservation that the "nearness" of the future is more definitely established for the aqueous reactors than for the others. When the nuclear fuel requirements of the reactor types are estimated to the year 2030, the objective, therefore, is not to forecast the fuel demand by extrapolating to that date on the basis of "near-future" technology, but simply to evaluate that technology in terms of the problem of fuel supply.

The three converter types considered in combination with the fast breeder are an H_2O converter, a D_2O converter, and a converter of unspecified type which operates on the uranium-thorium cycle with an effective conversion ratio of 1.00. The inventory requirement of the latter, per unit of installed capacity, is assumed to be the same as that of the H_2O converters. This converter could be considered to be representative of the ultimate in fuel utilization that might be obtained with fixed fuel reactors operating on the uranium-thorium cycle, whether these reactors be H_2O- or D_2O-cooled reactors, spectral shift reactors, or reactors of the high-temperature gas-cooled type.

In the combination cases involving the H_2O and D_2O converters, the converters operate on a once-through cycle with respect to plutonium. The plutonium produced is not recycled to the converters but is used as inventory for the expanding fast-breeder capacity. The remainder of the fissile isotope needed for fast-breeder inventory, beyond the plutonium supplied by the converters and that bred by the breeders, is assumed to be supplied as U^{235} from the natural-uranium resource. An allowance is made for the difference between U^{235} and plutonium with regard to inventory requirement, as indicated in Table 17, but all the fast breeders are assumed to have an effective doubling time of 20 years regardless of whether they are fueled initially with U^{235} or plutonium.

The thermal efficiencies (Table 17) are assumed to be the same for all types of plants, and they are assumed to vary as postulated in Ref. 2 up to the year 2000; thereafter they are held constant at 40%. This is not to imply that all the types will give equal efficiencies, but the expected range of variation, when expressed in terms of fuel requirement, could hardly amount to more than ±15%. This uncertainty is small relative to other uncertainties, and the correction is one which the reader can easily apply if he wishes.*

The fissile isotope requirements of the three combination systems are shown in Figs. 15 to 17 in units of effective metric tons of natural uranium. The components of the requirement are shown in terms of the inventories, burnups, and productions for the breeders and the converters, with productions of fissile isotope indicated as negative requirements. The net requirement is the algebraic sum of the components and specifies the actual amount of natural uranium which must be withdrawn from the resources to supply the system in question. In most cases the net requirement passes through a maximum value. After the requirement begins to drop off, it may be considered that some fissile isotope becomes available in the system for other purposes such as the fueling of burner reactors. The requirement of each system may be compared with the estimated natural-uranium resources in the United States by means of the bar graph on the left of the figure. The left-hand scale shows the total cost of mining and extracting the natural uranium in the form of U_3O_8 according to the schedule indicated by Fig. 13.

In the combination systems it is assumed that, as the converter capacity decreases (after the year 2000), the fissile inventory released is applied to the breeder component of the system. Thus by the year 2030, when the converter capacity reaches zero, the high-conversion-ratio converters of Fig. 17 have not, in themselves, used up any of the resource of fissile isotope because the net burnup for this type is assumed to be zero. The same can be said for the D_2O converter in combination with the breeder, since an examination of Fig. 16 (curves *C* and *D*) will show that the production of fissile isotope by the converter (in terms of its worth for fast-breeder inventory) is just about equal to the consumption. Yet in both cases the net requirement of the combination system is con-

*The development of high-temperature reactors that use topping devices, such as thermionic converters, in conjunction with the Rankine cycle systems, represents one possibility for very substantial efficiency increases. The speculation as to whether this represents a method of alleviating fuel shortages, which is easier of accomplishment than the development of the fast breeder, is left to the reader.

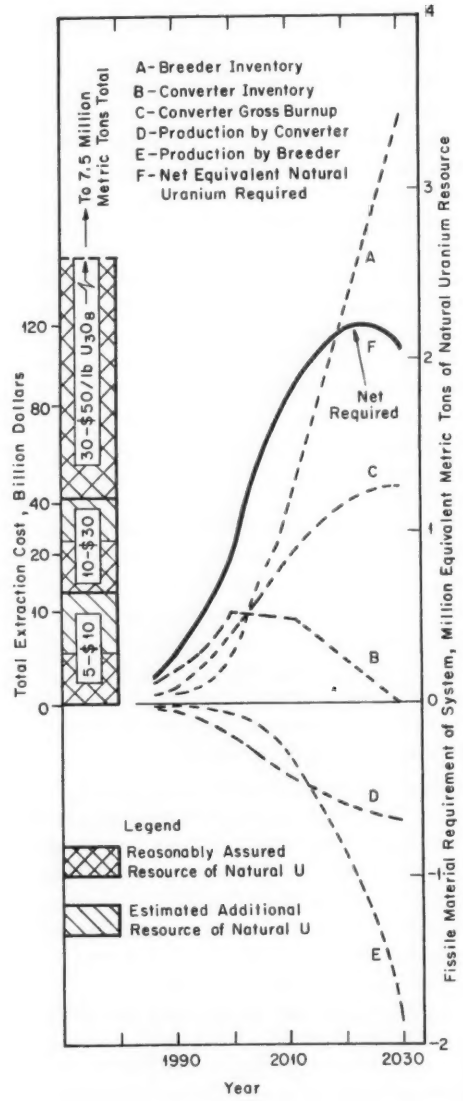

Fig. 15 Fissile material requirements of a system of fast breeders and H_2O-moderated converters, with all converted and bred plutonium used for breeder inventory.

Breeder-converter mixture as shown in Fig. 14.

Reactor characteristics as in Table 17.

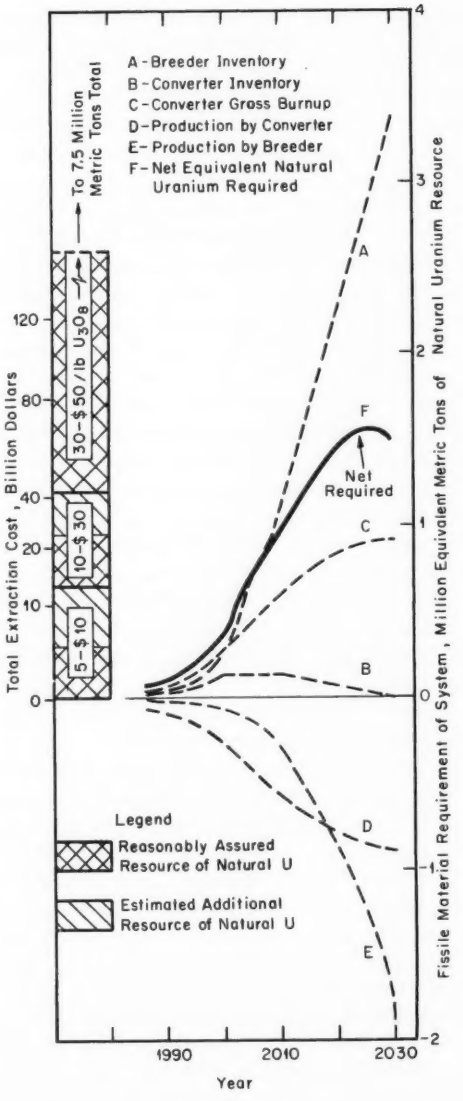

Fig. 16 Fissile material requirements of a system of fast breeders and D_2O-moderated, natural-uranium converters with all converted and bred plutonium used for breeder inventory.

Breeder-converter mixture as shown in Fig. 14.

Reactor characteristics as in Table 17.

siderably greater than that for the system which produces the same total energy by fast breeders alone (Fig. 2, curve *C*). The increase occurs because the generation of part of the energy by converters reduces the amount of net fissile isotope produced by the breeders. This may be further demonstrated by a plot of the fissile requirement of a system that is in all respects identical with the breeder-converter systems except that the converter capacity is replaced by a nonnuclear source of power. Such a curve is shown in Fig. 18 (curve *D*) along with the net-

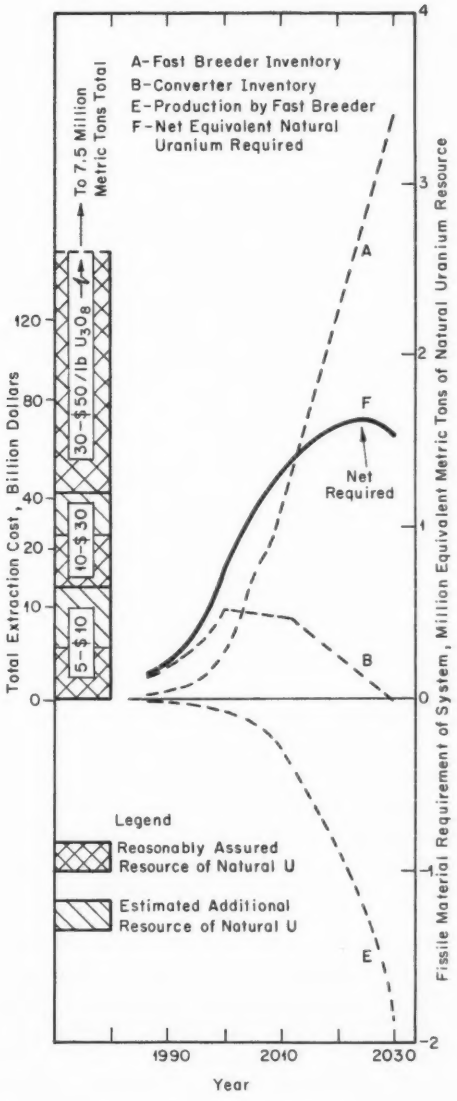

Fig. 17 Fissile material requirements of a system of fast breeders and thorium-cycle converters that recycle U^{233}. The net burnup of the converters is neglected.

Breeder-converter mixture as shown in Fig. 14.

Reactor characteristics as in Table 17.

requirement curves of the other combination systems and the pure-breeder system.

The foregoing results emphasize the importance of the early development of breeders. They also demonstrate that the estimated net fissile requirement for a given system is determined by the shape as well as the end point of the assumed curve of nuclear power growth, in a way which at first glance may seem surprising.

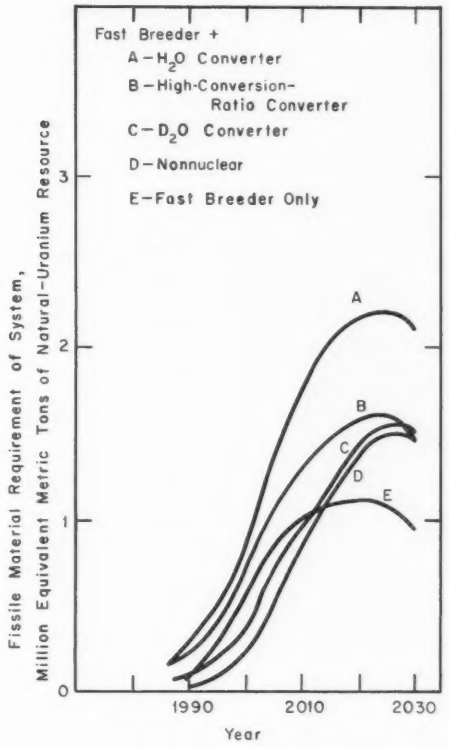

Fig. 18 Net fissile material requirements of several nuclear power systems involving fast breeders. Curve *D* applies to a system in which the "converter" component of the generation (Fig. 14) is supplied by a nonnuclear source.

Table 18 is a summary of the maximum points in the curves of uranium requirement, up to the year 2030, for the various reactor systems that have been considered here. For the pure converter systems the curves are, of course, still rising at the end of this period, but all the assumed systems, which include breeders, have passed through a maximum at an earlier date.

Variation for Tails Assay

As the price of natural uranium increases because of resource depletion, the economic optimum for the U^{235} content of the diffusion-plant tails will decrease, and, if adjustments are made in the plants to keep in step with this economic

Table 18 MAXIMUM REQUIREMENTS OF NATURAL URANIUM TO THE YEAR 2030 FOR VARIOUS REACTOR SYSTEMS

System	Year of maximum requirement	Maximum requirement, million metric tons of U^{nat}	(Maximum requirement)/(estimated total resource of U^{nat} at \$5 to \$10/lb of U_3O_8)	Total mining and extraction cost at maximum, billion dollars
Fast breeders only	2018	1.1	1.7	34
H_2O converters with plutonium recycle				
Tails enrichment 0.25%	2030	6.1	9.6	450
Optimum tails enrichment*	2030	4.8	7.6	337
D_2O converters with plutonium recycle	2030	3.0	4.7	190
Fast breeders and H_2O-moderated converters				
Tails enrichment 0.25%	2025	2.2	3.5	120
Optimum tails enrichment*	~2025	1.7	2.7	83
Fast breeders and D_2O-moderated converters	2026	1.6	2.5	72
Fast breeders and thorium-cycle converters	2024	1.6	2.5	72

*Including rework of tailings as optimum tails enrichment decreases.

optimum, the amount of U^{235} extracted from each unit of natural uranium will increase. According to ideal diffusion-cascade theory, it will also be economically attractive to reprocess previously discharged tailings whenever the tails assay is reduced, provided there is no expense connected with reintroducing those tailings into the plant. This would also lead to a reduction of the amount of resource used for a given consumption of U^{235}. In a situation where the unit cost of uranium was increasing with the quantity used, a net reduction in the cost of obtaining U^{235} would also result. This reduction would be the difference between the cost saving in mining and extraction and the extra cost of isotope separation.

In the analyses of uranium requirement, the effect of variations in tails assay has up to this point been ignored. The intent of the consumption estimates has been to relate current practice and near-future reactor technology to the bench marks that are afforded by the estimates of uranium resources. It is possible to examine the effect of changing tails assay, if it is assumed that diffusion-plant characteristics remain essentially unchanged and that the unit cost of separative work remains constant. Figure 19 shows the computed optimum tails assay as a function of the cost of natural-uranium feed for a constant separative work cost of \$30 per kilogram of uranium. By means of this curve, the consumption of natural uranium has been recomputed for the two H_2O converter cases previously considered (Figs. 11 and 15). This was done on the assumption that the tails enrichment is always adjusted to the economic optimum, and that previously discharged tailings are continuously reworked as the optimum tails assay changes. The results are shown in Fig. 20, where they are compared to the previously calculated results of a fixed tails assay of 0.25% U^{235}, and in Table 18.

No doubt the tails enrichment of the diffusion plants will vary in response to economic pressures, and an increasing uranium price will promote the more effective extraction of U^{235} from natural uranium, just as it will promote the search for further uranium deposits, the development of cheaper methods of extracting uranium from low-grade deposits, and the efforts to obtain higher fuel utilization and higher specific powers in the reactor types that are in existence. Just what the net economic pressure on isotope separation will be is not entirely clear, for the "separative work" used in the

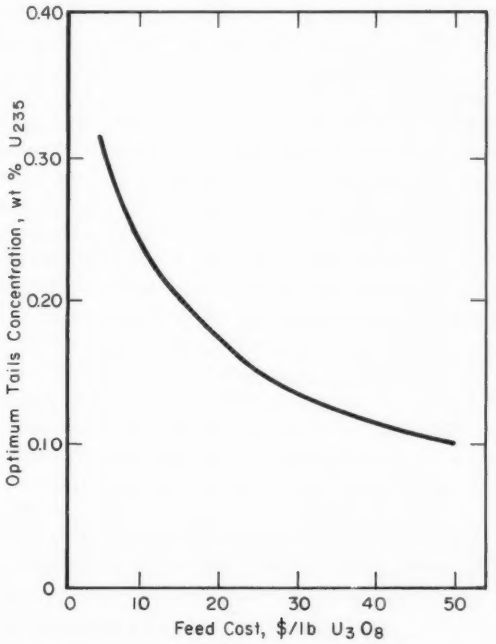

Fig. 19 Variation of theoretical optimum tails assay with cost of natural-uranium feed. This curve shows how the U^{235} content of the diffusion-plant tailings would vary, to give the lowest total cost for enriched uranium, as the cost of the natural-uranium feed increases. The curve is calculated on the basis of Ref. 32. The cost of correcting U_3O_8 to UF_6 has been neglected, and the cost of separative work has been held constant at $30 per kilogram of uranium.

ideal diffusion-cascade analyses includes the capital costs of the diffusion plants. Any serious depletion of the low-cost uranium reserves by enriched fuel reactors implies a large rate of consumption and a large diffusion plant throughput. Any reworking of old tailings would increase the throughput markedly. It is difficult to guess what the cost of separative work would be after the throughput became high enough to require the construction of additional diffusion plants.

The essential consideration, however, is probably that the curves of estimated uranium requirement have only academic interest after the resource depletion has caused the uranium price to increase by a substantial factor. Those reactor types which deplete the resource most rapidly are also those which will suffer most from increasing uranium prices, and it seems doubtful that they could avoid serious economic troubles if they were forced to use expensive

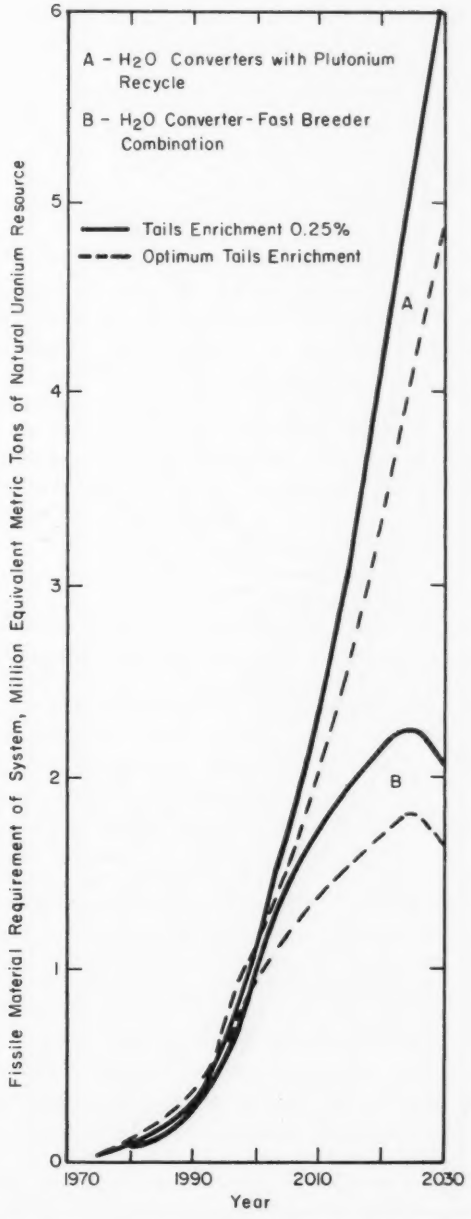

Fig. 20 Effect of variable U^{235} content in diffusion-plant tailings on uranium requirements of systems using H_2O-moderated reactors. The solid curve shows the requirements when the U^{235} content of the tailings is held constant at 0.25%. These curves are identical to the solid curves of Figs. 11 and 15. The dashed curves show the requirement if the U^{235} content of the tailings is reduced, in accord with Fig. 19, as the price of natural uranium increases, and if the tailings from previous separations are reworked to the same U^{235} content.

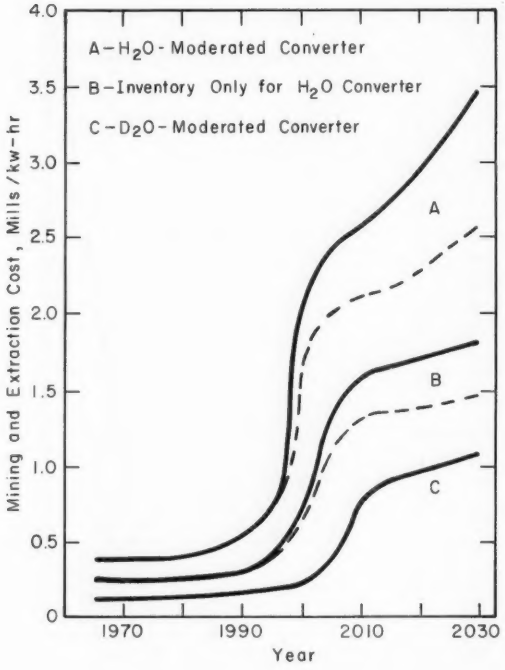

Fig. 21 Contributions of mining and extraction costs to fuel-cycle costs for H_2O and D_2O converters with plutonium recycle. The curves show the effects of increasing U_3O_8 costs as the uranium resource is depleted, as in Figs. 11 and 12, respectively. Curve *B*, which would apply to H_2O reactors if there were no net burnup of fissile isotope, can be considered to represent a thorium-cycle reactor with very high conversion ratio. The solid curves apply if the U^{235} content of the diffusion-plant tails is held constant at 0.25%. The dashed curves apply if the U^{235} content of the tailings is varied with the cost of natural-uranium feed (Fig. 19) and old tailings are reworked. None of the curves includes any enrichment costs.

uranium. This point is illustrated by Fig. 21, which shows the contribution of mining and extraction costs to the fuel costs of the H_2O-moderated and D_2O-moderated converter systems which have been considered here. The much lower cost for the D_2O reactor is due not so much to its better conservation of the uranium resources as to the lesser impact of uranium cost increases upon its fuel cost.

Conclusions

As stated at the beginning, one of the purposes of this article has been to determine what is meant by a "better" converter reactor. The thesis has been that the answer to this complex question cannot be given in terms of a single nuclear characteristic such as the conversion ratio. In order to explore the effects of a number of the characteristics that were considered important, the point of view has been taken that the "best" converter (from the point of view of fuel conservation), over a given period of time, is that which makes the lowest demand on the nuclear fuel resource in that period of time. Even this straightforward approach does not yield a definitive result unless the rate of growth of nuclear power consumption is specified and unless the time interval considered is sufficiently long to define the long-term trend of nuclear fuel consumption. For the purposes of the discussion, the curve of nuclear power demand from the Report to the President[1] was adopted, and the analysis indicated that the fuel consumption must be followed to about the year 2030 on this curve to indicate the ultimate trend.

To illustrate how various reactor characteristics affect fuel consumption, the fuel requirements of several current reactor types have been estimated, on the basis of the assumed power-demand curve, to the year 2030. In doing so the estimated "near-future" characteristics have been assumed for the reactor types. Hence it is important to recognize that the resulting curves are not predictions of how much fuel *will be* used by the various reactor types to the "distant-future" year 2030, but predictions of how much *would be* used if the nuclear demand were filled by these reactor types with the characteristics set by near-future technology. Thus the function of the curves is not to forecast the future but to provide the means for evaluating that technology which is currently in evidence and those reactor characteristics which can now be predicted. Nevertheless, the analysis has shown that the characteristics of the reactors built in the early part of the time interval have a disproportionately large effect on the ultimate uranium requirement. To this extent current and near-future technology have real and direct effects on the resource problem.

With these considerations in mind, it is possible to draw the following conclusions from the discussion that has gone before.

1. There is a problem of nuclear fuel resources. Its magnitude depends both on the rate of growth of the nuclear power industry and on

the ultimate magnitude of that industry. If the rate of growth is slow, the problem may be solved by the leisurely development of breeder reactors. If the rate of growth is fast and if current estimates of uranium resources are correct in order of magnitude, the solution requires both the rapid development of breeder reactors and improvement in the fuel utilization by converter reactors. In this context the rate of growth postulated in the AEC Report to the President (Fig. 1) is a rapid one.

2. The resource problem is purely a problem of shortages of fissile isotope. Any remedy that solves this problem will automatically guarantee that the supply of fertile isotope is adequate for many years to come.

3. Since thorium contains no fissile material, it cannot contribute to the solution of the resource problem in the United States as a resource per se. Its only significance in relation to the problem is as a parent of the fissile isotope U^{233}, which is superior to plutonium as a fuel for thermal reactors.

4. If the postulated growth of the nuclear power industry does occur, a delay in the development of breeder reactors will cause a substantial increase in the total uranium requirement even if "perfect" converters (effective conversion ratio of 1.0, zero net burnup) are used to supply that portion of energy which is not supplied by breeders.

5. The recycle of plutonium in thermal converters will not solve the resource problem and, in fact, is less favorable than the use of converter-produced plutonium for fast-breeder inventory even if the latter approach requires the storage of plutonium until fast breeders are developed. Plutonium recycle in thermal converters will, however, probably come about for other reasons.

6. Converters of the current H_2O-moderated type, even with plutonium recycle, would use up the estimated supplies of low-cost fissile isotope rather quickly if they were the basis of a large-scale nuclear power industry. It is not evident that other enriched-fuel thermal converters, of types currently under development, will show large improvements over the H_2O converters when operating on the uranium-plutonium cycle. Some of these types, operating on the uranium-thorium cycle with recycle of U^{233}, may give substantial improvements with respect to the burnup of fissile isotope; but there is no present indication that they will reduce the inventory requirements. The natural-uranium D_2O-moderated reactor with plutonium recycle has the advantages of low inventory and the avoidance of waste of U^{235} in diffusion-plant tailings. From the standpoint of resource conservation, it has an advantage over the higher enrichment thorium-cycle reactors in a rapidly expanding industry because of its low inventory requirement.

7. The practical consequences of resource depletion will be an increase in fuel-cycle costs as the lower cost resources are used up. Low-inventory requirement and high specific fuel utilization not only lower the rate of resource depletion but also reduce the impact of a given natural-uranium price increase on the reactor fuel cost. In these respects the D_2O converter reactor shows very definite advantages over the H_2O converter (Fig. 21).

8. The resource requirements for the enriched fuel reactors are reduced somewhat if the tails enrichment of the isotope-separation plant is reduced to the economic optimum as the price of natural uranium increases. A further reduction in resource requirement results if old tailings are reworked as the uranium price increases. The plausible reduction of requirement by these two expedients increases as the cost of natural uranium increases and reaches about 23% for the highest cost uranium considered here ($40 to $50 per pound of U_3O_8). This causes some reduction in the cost of mining and extraction, which is partly compensated for by the extra cost of isotope separation. The effect on the mining and extraction costs (extra separation cost neglected) is illustrated by the dashed curves of Fig. 21.

9. In a nuclear power system that does not expand indefinitely at an exponential rate, the inclusion of breeder reactors in the system will cause the net fissile material requirement eventually to decrease. At this maximum point the net burnup of the system must be zero or negative unless the power-generating capacity of the system is actually decreasing, and any current requirement for fissile isotope will be for inventory. The point of maximum requirement can therefore be regarded as an inventory crisis. If such a system involves converters as well as breeders, the "best" converter type might be defined as that which results in the lowest fissile isotope requirement at the time of inventory crisis. This best type cannot be specified simply in terms of conversion ratio. Inventory re-

quirement and enrichment may be equally or more important.

10. The various reactors and combinations of reactors that have been considered here as hypothetical bases for the postulated nuclear power industry cover a wide range of total demands on the uranium resource. These differences are accentuated when they are considered in terms of the total costs of mining and extracting the required uranium. The total demands and total costs are summarized in Table 18. As pointed out before, this tabulation is not intended as a forecast of demands or costs, but is intended to illustrate that the differences which now exist among current reactor types take on very significant proportions when considered in terms of a large nuclear power industry.

11. In a nuclear power system that consists of converters and breeders, the impact of the converters on the resource requirement may be far out of proportion to the fraction of energy generated by the converters. Thus, for the breeder-converter systems considered here (Fig. 14), the converter has generated only 25% of the total energy by the year 2030; but in the case of the particular system involving the H_2O converter, the converter has caused approximately a doubling of the resource requirement over that for a pure breeder system and has increased the cost of mining and extraction by a factor of approximately 3 (see Table 18).

None of the above conclusions defines just how important the resource problem is or demonstrates the certain need for any remedy beyond the development of a breeder reactor at some time in the future. The impossibility of clear-cut answers to these questions is due mainly to the uncertainties in the future rate of growth of the nuclear power industry, the magnitude of the uranium resources, and the actual costs of extracting uranium from low-quality ore deposits at some time in the future. Nevertheless, there are considerations that argue strongly against ignoring the resource problem even momentarily. Clearly the converter reactor types currently in use in the United States cannot support a nuclear power industry comparable to the present electric utility industry for very long unless much larger resources of uranium are found, and some attention to the problem is therefore necessary even if the estimates of growth are much lower than those of Fig. 1. If there is even a small probability of achieving growth rates comparable to those of Fig. 1, the order of magnitude of the possible saving in the cost of supplying uranium for the industry (Table 18) is so great as to justify a considerable effort now toward finding and developing the lowest cost system.

The one conclusion that does seem obvious is that free economic pressures alone can have no important effect in directing reactor development toward the conservation of resource in the rapidly expanding industry. It is significant that the resource depletion considered in this review takes place over a period covering only 60 years—two plant lifetimes—after nuclear plants are assumed to become economically competitive. At the moment neither we nor the uranium suppliers have any way of knowing whether we are indeed at the 1963 point on the curve of Fig. 1. Yet, if we are, we should be feeling economic pressure toward the development of breeder reactors. Just the opposite is true: the uranium market is glutted. Since it takes 10 years or more to develop a new reactor type, and since the construction of a particular nuclear plant preempts a fuel supply for that plant for something like 30 years, the economic feedback simply has too long a time constant to be effective in controlling a resource depletion that can assume serious proportions over a period of a few decades.

In short, if very pessimistic assumptions are made about the rate of growth of nuclear power or if very optimistic assumptions are made about the discovery of new uranium resources or the development of cheap extraction methods for low-grade deposits, an argument may be supported that neglect of the resource problem for the time being is a reasonable gamble. However, without such assumptions, to argue that developments spurred by free economic pressures will automatically forestall serious depletion problems requires a faith in the law of supply and demand strong enough to ignore the laws of cause and effect.

References

1. Civilian Nuclear Power, a Report to the President—1962, Nov. 20, 1962.
2. Appendix 16, Background Statement Relating to Civilian Nuclear Power—A Report to the President, 1962, in *Hearings before the Joint Committee on Atomic Energy, Congress of the United States, February 20 and 21, 1963,* Part 1, p. 428, U. S.

Government Printing Office, Washington, 1963. This material, along with Recommendations on Central-Station Power Reactors by the General Advisory Committee, has also been issued as a separate AEC document: Civilian Nuclear Power, Appendixes to A Report to the President — 1962.

3. C. H. Westcott, Effective Cross Section Values for Well-Moderated Thermal Reactor Spectra, Canadian Report CRRP-960 (AECL-1101), Oct. 1, 1960.
4. J. Bengston and R. L. Hellens, A Survey of the Beginning of Life Characteristics of Uranium-Fueled, Water-Moderated Lattices, USAEC Report CEND-137, Combustion Engineering, Inc., July 1961.
5. E. Fein and L. C. Noderer, An Evaluation of Effective Plutonium Cross Sections in Reactivity Calculations, USAEC Report CEND-146, Combustion Engineering, Inc., Sept. 30, 1961.
6. J. Chernick and S. Oleksa Moore, Breeding Potential of Thermal Reactors, *Nucl. Sci. Eng.*, 6(6): 537 (December 1959).
7. J. Bengston, J. M. Ravets, and R. J. Rickert, Lifetime Characteristics and Economics of Slightly Enriched Uranium Dioxide in Water Lattices, USAEC Report CEND-145, Combustion Engineering, Inc., Sept. 30, 1961.
8. *Nucleonics*, 18(10): (October 1960).
9. Atomic Energy of Canada Limited, The Eighth AECL Symposium on Atomic Power held at Chalk River, Ontario, September 24, 1962, Canadian Report AECL-1599, September 1962.
10. N. B. McLeod, M. Benedict, K. Uematsu, H. L. Witting, and K. S. Ram, The Effect of Fuel and Poison Management on Nuclear Power Systems, June 1959–September 1961, USAEC Report NYO-9715, Massachusetts Institute of Technology, Sept. 15, 1961.
11. C. M. Unruh, The Radiological Physics of Plutonium, in Proceedings Plutonium as a Power Reactor Fuel, American Nuclear Society Topical Meeting, Richland, Washington, September 13 and 14, 1962, pp. 2.1-2.10, USAEC Report HW-75007, December 1962.
12. U. M. Staebler, Plutonium as a Power Reactor Fuel, in Proceedings Plutonium as a Reactor Fuel, American Nuclear Society Topical Meeting, Richland, Washington, September 13 and 14, 1962, USAEC Report HW-75007, pp. 1.1-1.6, December 1962.
13. F. G. Dawson (Comp.), Proceedings Plutonium as a Reactor Fuel, American Nuclear Society Topical Meeting, Richland, Washington, September 13 and 14, 1962, USAEC Report HW-75007, December 1962.
14. E. L. Zebroski, B. Wolfe, P. Greebler, and J. Sueoka, Plutonium Recycle Values in Thermal and Fast Reactors and Expected Patterns of Use of Plutonium, in Proceedings Plutonium as a Reactor Fuel, American Nuclear Society Topical Meeting, Richland, Washington, September 13 and 14, 1962, USAEC Report HW-75007, pp. 23.1-23.49, December 1962.
15. E. A. Eschbach, D. E. Deonigi, M. F. Kanninen, D. P. Granquist, G. J. Busselman, and B. B. Lane, Fuel Cycle Analysis for Successive Plutonium Recycle. I. Results for Five Reactor Concepts, USAEC Report HW-72217, Hanford Atomic Products Operation, February 1962.
16. W. H. Zinn and J. R. Dietrich, Nuclear Fuel Resources and Reactor Fuel Costs, paper presented at World Power Conference Sectional Meeting, Madrid, June 9, 1960.
17. D. Mars and D. Gans, Jr., Spectral Shift Control Reactor Design and Economic Study, USAEC Report BAW-1241, The Babcock & Wilcox Co. and Stone & Webster Engineering Corp., December 1961.
18. Philadelphia Electric Co., Application to U. S. Atomic Energy Commission for Construction Permit and Class 104 License. Part B, Preliminary Hazards Summary Report, Peach Bottom Atomic Power Station, Vol. I, Plant Description and Safeguards Analysis, Report NP-9115, July 1960.
19. L. R. Shepherd and P. J. Marien, Research and Development Aspects on the Dragon Reactor Experiment; G. E. Lockett, Engineering Aspects of the Dragon Reactor Experiment, Proceedings Series, in *Symposium on Power Reactor Experiments, Vol. I, Vienna, October 23-27, 1961*, International Atomic Energy Agency, Vienna, 1962.
20. R. Fox, The LRL Advanced Reactors Studies Program — A Review, USAEC Report UCRL-6863, University of California, Lawrence Radiation Laboratory, Apr. 3, 1962.
21. W. H. Zinn, Review of Fast Power Reactors, *Proceedings of the International Conference on the Peaceful Uses of Atomic Energy, Geneva, 1955*, Vol. 3, pp. 198-204, United Nations, New York, 1955.
22. L. J. Koch, H. O. Monson, W. R. Simmons, M. Levenson, F. Verber, E. Hutter, R. A. Jaross, T. R. Spalding, J. R. Simanton, and A. Lovoff, Construction Design of EBR-II: an Integrated Unmoderated Nuclear Power Plant, *Proceedings of the Second United Nations International Conference on the Peaceful Uses of Atomic Energy, Geneva, 1958*, Vol. 9, pp. 323-347, United Nations, New York, 1958.
23. Power Reactor Development Co., Enrico Fermi Atomic Power Plant Technical Information and Hazards Summary Report, Report NP-10458(Vol. 7), 1961.
24. Frank G. Foote, Plutonium Fuel Programs at Argonne National Laboratory, in Proceedings Plutonium as a Reactor Fuel, American Nuclear Society Topical Meeting, Richland, Washington, September 13 and 14, 1962, USAEC Report HW-75007, pp. 7.1-7.21, December 1962.
25. F. J. Leitz, Plutonium as a Fuel for the Fast Ceramic Reactor, in Proceedings Plutonium as

a Reactor Fuel, American Nuclear Society Topical Meeting, Richland, Washington, September 13 and 14, 1962, USAEC Report HW-75007, December 1962.

26. L. J. Koch, Plutonium as a Fuel for the Experimental Breeder Reactor II (EBR-II), in Proceedings Plutonium as a Reactor Fuel, American Nuclear Society Topical Meeting, Richland, Washington, September 13 and 14, 1962, USAEC Report HW-75007, pp. 16.1-16.23, December 1962.
27. L. E. Link, The Value of Plutonium in Fast Reactors, in Proceedings Plutonium as a Reactor Fuel, American Nuclear Society Topical Meeting, Richland, Washington, September 13 and 14, 1962, USAEC Report HW-75007, pp. 20.1-20.16, December 1962.
28. P. Greebler, P. Aline, and J. Sueoka, Fast Oxide Breeder-Reactor Physics. Part I. Parametric Study of 300(e)MW Reactor Core, USAEC Report GEAP-3287, General Electric Co., Atomic Power Equipment Dept., Nov. 15, 1959.
29. J. A. Lane, H. G. MacPherson, and Frank Maslan (Eds.), Fluid Fuel Reactors, Addison-Wesley Publishing Co., Inc., Reading, Mass., 1958.
30. AEC Announces Reduction in Official Amount of U-235 Isotope in Natural Uranium, USAEC Press Release No. F-103, May 27, 1963.
31. D. S. St. John, Savannah River Laboratory, personal communication.
32. A. J. Snyder, Methods of Calculating U^{235} Outputs and Charges by Use of Ideal Cascade Theory, USAEC Report TID-8522, February 1960.

Section

I

Power Reactor Technology

Reactor Physics: Thermal-Neutron Spectra

The calculation of the energy spectrum of the neutron population in the range of thermalization is of increasing importance to the reactor designer, and it is an area of reactor physics in which rapid progress is being made. The methods of attacking the problem cover a wide range of complexity. At one end of the scale, high-speed computers can be used together with the best available cross sections to obtain direct numerical solutions; at the other end of the scale, simple approaches can be used in which diffusion theory is combined with elements of transport theory. At an intermediate level simplified models for the thermalization process can be used with semianalytical solutions to the transport equation. The latter approach is typified by the modified heavy-gas model.

In the early sections of this review, the approximations made to the transport equation in the calculation of neutron spectra, in both the more sophisticated and the simpler approaches, are discussed. This is followed by a description of the modified heavy-gas model, and comparisons of the predictions of this model with experiment, using the Nelkin water kernel and the Egelstaff graphite kernel. The calculation of multigroup cross sections and neutron spectra from experimental data reduced into the form of the Egelstaff scattering law is then discussed, the extension by Brugger of the Egelstaff scattering law is considered, and the advantages of the new formulation are indicated. Finally, some of the current scattering kernels for graphite, water, and polyethylene are discussed, and comparisons of the predictions of these models with experiment are given.

Much of the material reviewed appears in the papers presented at the neutron thermalization conference held at the Brookhaven National Laboratory in the spring of 1962.

Transport Equation

The starting point for the calculation of neutron spectra is the time-independent transport equation that describes the steady-state balance of the neutron flux. Since the transport equation is too complicated to solve exactly for this problem, various simplifying assumptions have been made to obtain a tractable equation. Some of these approximations will be discussed in the following paragraphs, with particular attention focused on the scattering operator, which determines the details of the neutron spectrum.

Angular Variation of the Flux*

The angular variation of the flux, $\phi(r, E, \Omega)$, and the variation with angle of the scattering process are represented by nth order polynominals in the P_n, double P_n, and the discrete ordinate approximations to the transport equation. The P_1 approximation ($n = 1$, in the time-independent transport equation) yields the ordinary diffusion theory. In general, the double P_n method is more accurate than the P_n method near boundaries. The SLOP-1 and the EXCEL P-3 codes use this procedure.

Another method of approximating the angular variation of the flux and scattering is to represent the flux and scattering by n linear segments, using the S_n formulation of Carlson. Computer programs that use this approximation, such as the Carlson SNG and DSN codes, can accommodate large numbers of space points and energy groups and have no restrictions on the group-transfer matrix. These programs, however, require considerable computing time, since they simultaneously treat space, energy, and the direction of neutrons.

*Much of this discussion is taken from Ref. 1.

Both the P_n and S_n methods result in coupled first-order differential equations. For these methods the computer storage requirement depends linearly on the size of the region being studied and on the number of angular intervals or polynomials.

If the integral form rather than the differential form of the transport equation is used and if the scattering process can be assumed to be nearly isotropic, then the angular variation of the flux can be treated exactly. In fact, Dalton[2] has found that the zeroth-spherical harmonic approximation in an integral form of the neutron transport equation gives results that are obtainable only with much higher order spherical harmonic approximations to the differential form of the transport equation. In the integral-equation approach, the computer storage requirements vary as the square of the size of the spatial region being studied and as the number of angular moments used in the scattering kernel. The THERMOS code solves the integral transport equation with isotropic scattering.

Although variation of the scattering with angle can be included in the P_n and S_n methods, it is difficult to include in integral transport methods. Scattering kernels that contain sufficient detail to predict anisotropic scattering using the P_n method have only recently come into use. Gelbard[3] and Honeck[4] have made calculations using anisotropic scattering kernels. Their calculations indicated that reasonably good results can be obtained for water when only the P_1 scattering contribution is specified.

In large, weakly absorbing media, low-order P_n or S_n methods are satisfactory. In media which are highly absorbing or small in extent and which have sharp discontinuities, integral transport theory is most applicable. If a variety of conditions must be handled, the S_n method ($\sim S_8$) is expected to give the best accuracy for the least computation effort.

Scattering Operator

The scattering operator L is defined by

$$L\phi(E) = \int_0^\infty dE' \sum_s (E' \rightarrow E)\ \phi(E') - \sum_s(E)\ \phi(E) \qquad (1)$$

where
- L = the integral scattering operator
- $\phi(E)$ = the flux per unit energy about the energy E
- $dE'\ \Sigma_s\ (E' \rightarrow E)\ \phi(E')$ = the number of neutrons gained per second about the energy E by scattering from the energy interval dE' about the energy E'; integration over all E' accounts for the total scattering in source
- $\Sigma_s(E)\ \phi(E)$ = the number of neutrons per unit energy removed by scattering about the energy E

The methods that have been used to represent it are the multigroup formulation, representation by a second-order differential equation, and factorization of the kernel. In the multigroup procedure the flux is expanded in step type functions so that

$$S\phi_i = \sum_j \Delta E_j \sum_{ij} \phi_j - \sum_i \phi_i \qquad (2)$$

where
- S = the multigroup scattering operator
- ϕ_i = the average flux per unit energy in the ith group
- ΔE = the energy width of the ith group
- $\Delta E_j\ \Sigma_{ij}\ \phi_j$ = the number of neutrons gained per second in the ith energy group; summation of overall j groups accounts for the total scattering in source
- $\Sigma_i\ \phi_i$ = the number of neutrons per unit energy removed by scattering from the ith group

This procedure is used in the EXCEL code in which 6 energy groups are used, the SNG code in which 42 energy groups are used, and the THERMOS code in which 30 energy groups are used. The multigroup method seems to be the best method, since the full scattering information is contained in the kernel.

The flux can also be expanded in orthogonal functions, or in functions which are not orthogonal but which represent much of the known behavior of the flux. An example of the latter representation is the SWAKRAUM code, which calculates the approximate Wigner-Wilkins flux spectrum as a linear combination of a number of infinite-medium base spectra. All the above procedures result in coupled linear equations that are solved numerically.

In addition, the scattering operator can be represented as a differential equation.* A number of investigators have explored various differential representations of L, but none have been successful in finding an operator which allows for chemical binding and which is accurate over a wide range of energy. The Wigner-Wilkins equation for hydrogen gas and the heavy free-gas Wilkins equation (valid for small values of μ, where μ is the ratio of the neutron mass to the atomic mass of the gas) are second-order differential equations that are applicable over a wide range of energy; but these equations apply to a free gas. The proposed differential operators that include binding are generally suitable for high energies $E \gg kT$ but fail for energies less than kT.

However, a differential operator that obeys detailed balance, conserves neutrons, and includes chemical binding can be chosen ad hoc. The lowest order differential operator that satisfies these conditions is the modified heavy free-gas operator

$$L\phi(X) = \frac{\partial}{\partial X} P(X) \left(X \frac{\partial}{\partial X} + X - 1 \right) \phi(X) \qquad (3)$$

where $X = E/kT$.

The heavy free-gas equation is a special case obtained by setting the moderating power $P(X)$ equal to a constant $\xi\Sigma_s(\infty)$, where $\xi = 2\mu$ is the average logarithmic energy decrement per collision, $\Sigma_s(\infty)$ is the free-atom epithermal scattering cross section for neutrons, and μ is the ratio of the neutron mass to that of the gas molecule. Equation 3 is also the form of the Wilkins operator when absorption and leakage are small compared to scattering.

Any solution of the transport equation can be written by a suitable choice of $P(E)$, but the differential operator (Eq. 3) will prove to be useful only when $P(E)$ is solely a function of the moderator scattering law and is independent of absorption and leakage. This is the case when the spectrum deviates only slightly from a Maxwellian distribution, as in the diffusion approximation in which absorption and leakage are assumed small relative to scattering. Some of the theoretical models and experimentally derived values for $P(E)$ will be discussed in later paragraphs.

*Much of this discussion is taken from Ref. 5.

In the third method of representing the scattering operator, the scattering kernel is given by a sum of degenerate scattering kernels. This method is relatively new and unexplored.

Generalized Heavy Free-Gas Approximation

It has been mentioned that the scattering operator L can be replaced by a second-order differential operator: the modified heavy free-gas operator, in which the moderating power $\xi\Sigma_s(\infty)$ becomes an arbitrary function of energy $P(E)$, determined by the moderating properties of the medium and the particular problem. However, for a large class of reactor problems, $P(E)$ is insensitive to the problem; i.e., it is independent of leakage and absorption and so can be obtained from the neutron scattering relations at high and low energies.

Form of the Moderating Power P(E) at High Energies

Analytical solutions for neutrons slowing down in an infinite absorbing medium, for energies greater than $10kT$, have been developed by Corngold[6] for $1/v$ absorption and by Parks[7] for general, small absorption. Schaeffer[5] has used Corngold's asymptotic expansion solution to determine $P(E)$, since it contains the chemical binding exactly and since it is easier to handle. If a new variable $f(E)$ is introduced, the resulting $P(E) = f(E)\ \xi\Sigma_s(\infty)$ that is obtained is that of the heavy free-gas solution—$f(E) = 1$, and $\mu = 0$—plus correction terms for free gases of finite μ, for absorption, and for chemical binding. For a nonabsorbing free gas, the correction for μ increases $f(E)$ from unity to $1 + \mu/X$. Although for graphite this increase in $f(E)$ is only 1% at $10kT$, it is 10% for hydrogen. Since a decrease in $f(E)$ is similar to increased binding, the heavy free-gas theory, $f(E) = 1$, effectively adds some binding relative to the exact free-gas theory; it therefore increases the flux at higher energies for the heavy free-gas theory over the exact free-gas theory. The greater success in calculating spectra in water at these energies by Wilkins theory (relative to Wigner-Wilkins theory) is partly attributable to this fact.[8]

The correction for absorption in the gas adds $\sim\sigma_a(X)/\sigma_f$ to $f(E)$, where $\sigma_a(X)$ is the micro-

scopic absorption cross section at X and σ_f is the free-atom microscopic scattering cross section. If $X \gtrsim 10$, $f(E)$ is taken to be independent of absorption when this term is less than a few percent. This correction effectively adds binding when the heavy free-gas model is used.

The chemical binding term is of the form $-(2-\mu)[(\overline{T}/T)-1]$ and decreases $f(E)$ in the proportion that the mean kinetic energy of the moderator nuclei $k\overline{T}$ exceeds the mean kinetic energy of the free gas kT at the same temperature. The $\overline{T}$ and T are simple averages of the phonon frequency spectrum of the moderator. These terms are illustrated as $f_0(X)$ and $f_\Delta(X)$ in Figs. I-1 and I-2 for the heavy free-gas model and a bound model for graphite and for water at room temperature. A phonon spectrum obtained by Egelstaff was used for the graphite, whereas the Nelkin model[9] was used for water.

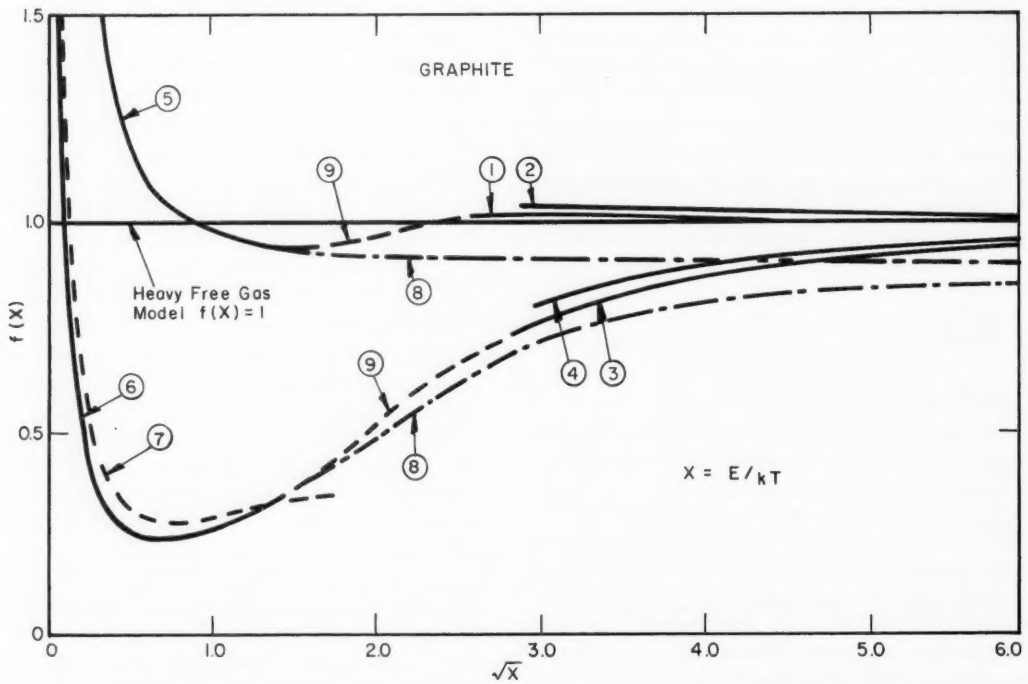

Modified Heavy Gas Model (A = 12)

High Energy

1 f_0 - Corrected for Finite μ

2 f_Δ - Corrected for Finite μ and Absorption $\frac{\sigma_a(kT)}{\mu\sigma_f} = 1$

3 f_0 - Corrected for Finite μ and Binding (Egelstaff Phonon Distribution)

4 f_Δ - Corrected for Finite μ Binding (Egelstaff Phonon Distribution) and Absorption: $\frac{\sigma_a(kT)}{\mu\sigma_f} = 1$

Low Energy

5 f_1 - Corrected for Finite μ

6 f_1 - Corrected for Finite μ and Binding (Egelstaff Phonon Distribution)

7 $f_{1\Delta}$ - Corrected for Finite μ Binding (Egelstaff Phonon Distribution) and Absorption $\frac{\sigma_a(kT)}{\mu\sigma_f} = 0.38$

8 - Extension of f_1 to High Energy

Intermediate Energy

9 - Approximate Joining of f_0 and f_1

Fig. I-1 The moderating power $f(X)$ as a function of energy.[5]

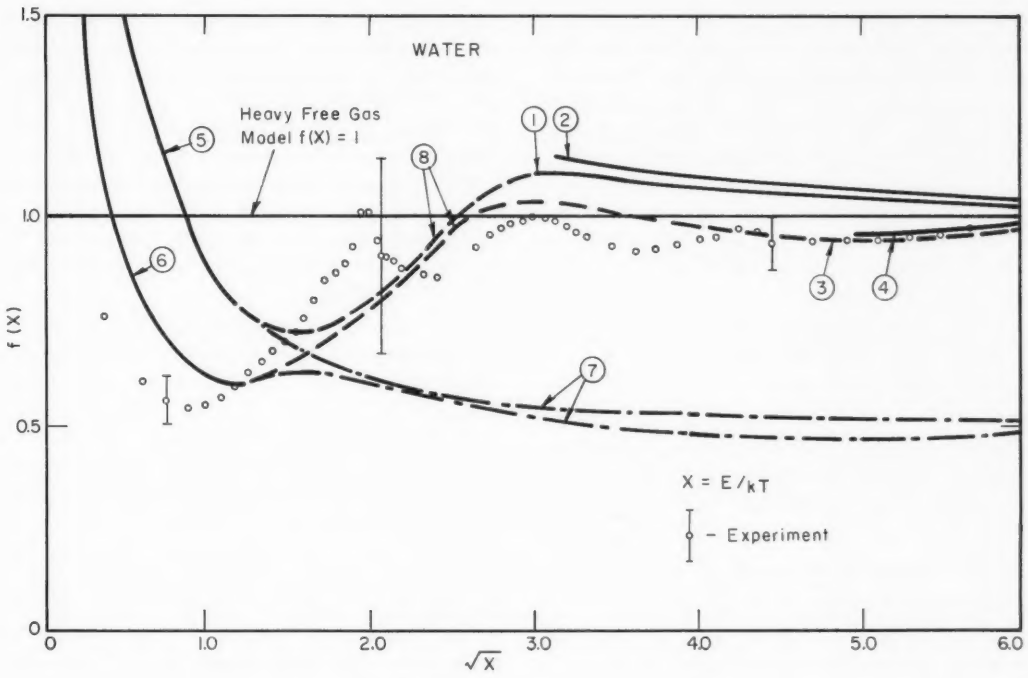

Modified Heavy Gas Model (A = 1)

High Energy

1 f_0 - Corrected for Finite μ

2 f_Δ - Corrected for Finite μ and Absorption: $\frac{\sigma_a(kT)}{\mu\,\sigma_f} = 0.1$

3 f_0 - Corrected for Finite μ and Binding (Nelkin Water Model)

4 f_Δ - Corrected for Finite μ Binding (Nelkin Water Model) and Absorption: $\frac{\sigma_a(kT)}{\mu\,\sigma_f}$

Low Energy

5 f_1 - Corrected for Finite μ

6 f_1 - Corrected for Finite μ and Binding (Nelkin Water Model)

7 – Extension of f_1 to High Energy

Intermediate Energy

8 – Approximate Joining of f_0 and f_1

Fig. I-2 The moderating power $f(X)$ as a function of energy.[5]

Form of the Moderating Power P(E) at Low Energies

For energies less than or equal to $3kT$, there are several methods for determining $P(X)$. The most useful method involves reduction of the scattering operator L to a differential operator by a moments expansion. Unfortunately the convergence of the resulting series must be assessed for each particular problem, and it must be determined whether the $P(X)$ is independent of the particular problem. In general, it is expected that a rapidly convergent series is obtained and that $P(X)$ is independent of the problem when leakage and absorption are small compared to scattering. Although this restriction is more limiting than that at higher energies, many practical problems can be solved with sufficient accuracy in the range $E \leq 3kT$ using only the first term $P_1(X)$ in a series expansion of $P(X)$,

$$P(X) \approx P(X,T) = X^{-2}\, e^X \int_0^X y e^{-y}\, M_1(y,T)\, dy \qquad (4)$$

where M_1 is the first moment

$$M(X,T) = \int_0^\infty \Sigma_s (X \rightarrow y, T)(y - X)\, dy \qquad (5)$$

The scattering law $S(\alpha,\beta)$ enters the problem through the first moment.[10] For a free gas, M_1 and P_1 are both analytic functions and P_i can be evaluated directly. However, the calculation of M_1 for a bound gas is laborious. Generally, the "incoherent Gaussian" approximation is sufficiently accurate for the bound calculations so that $M_1(X)$ and $P_1(X)$ are given a single integration over a rational function $\omega(t)$ that is related to the phonon spectrum $\rho(\beta)$ by

$$\omega(t) = \int_0^\infty \frac{\rho(\beta)\ (\cosh \beta/2 - \cos \beta t)}{\beta \sinh \beta/2}\, d\beta \qquad (6)$$

Here $\rho(\beta)$ is the phonon frequency distribution which for solids is closely related to Fourier transform of the autocorrelation function $P(\beta)$ in *Power Reactor Technology*, 6(1): 9, by

$$\rho(\beta) = \frac{2}{\beta} P(\beta) \sinh \frac{\beta}{2} \qquad (7)$$

Figures I-1 and I-2 show $f_1(X)$ for graphite and water using a free-gas model and a bound model in which a combination of "phonon expansion" and "short collision" time methods were used rather than the width function. The bound models used were the Egelstaff model for graphite and the Nelkin model for water. In the Egelstaff model the phonon distribution $\rho(\beta)$ was obtained by fitting the Chalk River scattering-law results such that $\rho(\beta)$ is proportional to β for $0 < \beta kT < 0.0253$ (293°K) ev, and such that $\rho(\beta)$ is a constant for 0.0253 ev $< \beta kT <$ 0.1771 ev (2050°K).

The approximations of the heavy free-gas model are seen by the deviations of $f(X)$ from unity in the range $X \leq 3$. Hurwitz et al.[11] have shown that the heavy free-gas model is incorrect for $X \leq \mu$ with errors in the order of μ for other X. This is readily seen in Figs. I-1 and I-2. The heavy free-gas theory gives more binding at very low X and less at higher values of X, thus exhibiting a tendency to harden the thermal spectrum relative to a free gas. This has been observed by DeSobrino and Clark[8] in comparing the Wigner-Wilkins and the Wilkins equations for hydrogen.

Moderating Power P(X) at Intermediate Energies

Expansion of $f_1(X)$ to high energies reveals that the first two terms of the expansion are identical with the expansion of $f_0(X)$, except for a leading constant multiplicative factor $2\mu/(1+\mu)^2\ \xi$, whereas the third term differs but little in value. Therefore, for a heavy moderator where the above leading term is approximately unity, $f_1(X)$ is a good approximation for $f(X)$ at high and low energies and so can be used as an extension of general heavy free-gas theory to include chemical binding at all energies. The extension of $f_1(X)$ to high energies is shown in Figs. I-1 and I-2.

No analytical method for determining $f(X)$ at intermediate energies has been found, and the joining of the high- and low-energy branches of $f_1(X)$ can be a poor approximation for many practical moderators. Although the flux in slowing-down problems is generally insensitive to $f(X)$ in this range, this is not true for many eigenvalue problems.

If $f(X)$ can be determined for a free gas, then one method of joining between f_1 and f_0 solutions for bound moderators would be to calculate, from the infinite-medium transport equation with small absorption, those ratios of the bound $f_1(X)$ to the free $f_1(X)$ which are correct at high and low energies and to use the result for interpolating between f_0 and f_1 for bound moderators. A rough estimate of this interpolation is shown in Figs. I-1 and I-2.

Another method of modifying the heavy-gas thermalization model is that proposed by C. W. Lindenmeier.[12] In this approach the cross-section weighted average energy loss is considered to be the important quantity in the slowing-down process, and the required variation in the slowing-down power is determined from either the scattering kernel or from rethermalization experiments. Spectrum calculations for graphite at room temperature were found to agree with experiment to within a few percent when this procedure was used.

Experimental Determination of the Moderating Power P(X)

Time-of-flight techniques have been used to measure the neutron spectrum in the graphite-moderated (Calder Hall) lattice[13] and in a homogeneous "poisoned" water assembly,[14] and the derived values of $f(X)$ have been compared with theory.

The experimentally determined values of $f(X)$ at 293°K and 594°K are shown in Fig. I-3 for graphite. Little significance can be given the ex-

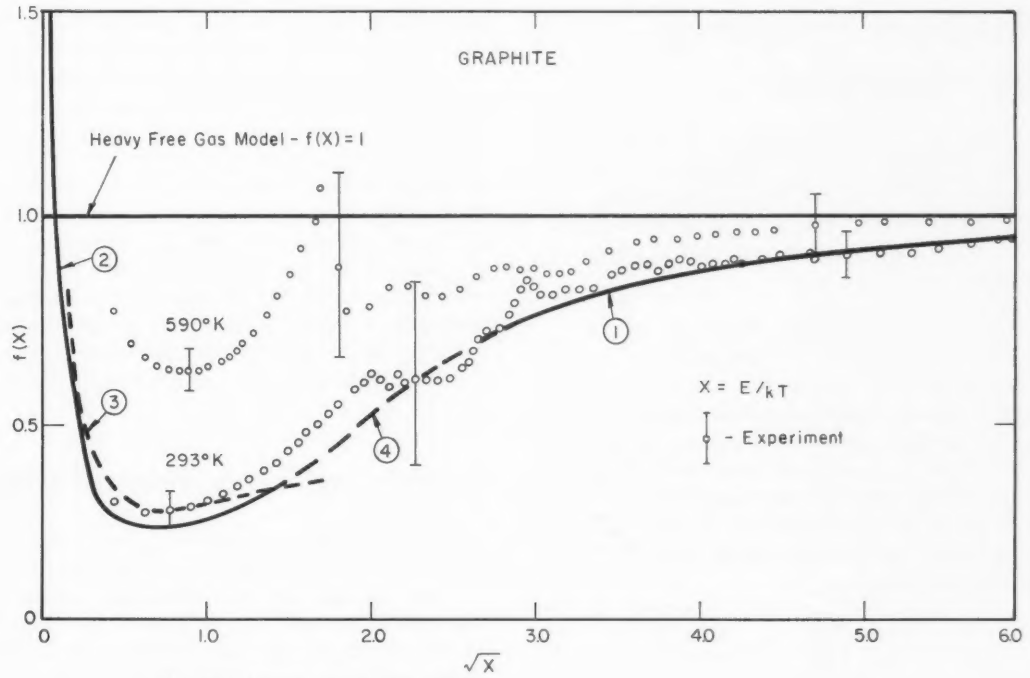

Modified Heavy Gas Model (A = 12)

High Energy

1 f_0 - Corrected for Finite μ and Binding (Egelstaff Phonon Spectrum) (300°K)

Low Energy

2 f_1 - Corrected for Finite μ and Binding (Egelstaff Phonon Spectrum) (300°K)

3 f_1 - Corrected for Finite μ Binding (Egelstaff Phonon Spectrum) and Absorption $\frac{\sigma_0(kT)}{\mu\sigma_f} = 0.38$ (300°K)

Intermediate Energy

4 - Approximate Joining of f_0 and f_1

Fig. I-3 The moderating power $f(X)$ as a function of energy.[5]

perimental values at intermediate energies because of the insensitivity of the flux in this range. The theoretical results at 300°K of the Egelstaff model reproduced from Fig. I-1 are also shown. At high energies $20 < X < 200$, a least-squares fit to the experimental data indicates $\overline{T}/T = 2.07$ at 293°K and 1.24 at 594°K. The Egelstaff phonon spectrum gives good agreement with values of 2.06 and 1.29, respectively. If a Debye model phonon spectrum were used, the corresponding effective temperatures $\overline{T}$ would be $\theta = 5.18T = 1518$°K and $\theta = 2.24T = 1330$°K. The Krumhansel-Brooks model[7] gives 2.36 and 1.43, thus predicting too much binding.

In the thermal range for graphite, the Egelstaff model gives good agreement at room temperature when absorption corrections are made to $P(X)$. The Debye model would fit the results with $\theta = 4T = 1172$°K at room temperature and with $\theta = 2.2T = 1307$°K at 594°K. It is thus indicated that a single Debye temperature will not fit all the experimental results. The Krumhansel-Brooks model predicts nearly twice too much binding.

For water the experimental spectrum with 3.15 barns of $1/v$ absorber per hydrogen atom was used to calculate $f(X)$, as shown in Fig. I-2. The Nelkin theory[9] is in agreement within experimental error for $X > 1$, but at smaller X, $M_1(X)$ is overestimated by this model. This is thought to be due to neglect of molecular translational impedance in the model.

Spectrum Hardening by Absorption

Often the thermal spectrum can be fitted to a good approximation by a displaced Maxwellian distribution having the effective temperature T_n. A simple relation can be found between T_n, absorption, and the scattering law at small absorption as

$$T_n \simeq T\left[1 + \frac{\Sigma_a(kT)}{M_1(kT)}\right] \tag{8}$$

This approximation has been confirmed for many spectra in the range $\frac{1}{4} < X < 3$. The shift in effective temperature is sensitive to chemical binding, being two and a half times as large for the Debye model ($\theta = 4T$) at room temperature as for the free-gas model. The heavy free-gas model gives

$$T_n \simeq T\left[1 + 0.50\,\frac{\Sigma_a(kT)}{\mu\Sigma_s}\right] \tag{9}$$

Cohen,[15] using an approximate analytical model, has obtained 0.60 for the coefficient, whereas Coveyou et al.,[16] using Monte Carlo techniques, obtained 0.91 over a wide range of μ.

Weiss[17] has developed a method for calculating the distribution of the effective neutron temperature as a function of position in an arbitrary heterogeneous moderator assembly of finite or infinite dimensions, with constant absorption and with external and internal sources of epithermal neutrons. This method, however, requires knowledge of a new constant L_t, called the temperature diffusion constant, which is related to a temperature relaxation length λ^{-1} and which apparently must be measured for each moderator if heterogeneous calculations are made. The effective temperature obtained by Weiss for an infinite homogeneous medium, for $\Sigma_a/\mu\Sigma_s \leq 0.15$, equals the small absorption limit established by Cohen:[18] i.e., $T_{\text{eff}} = T[1 + (2/\sqrt{\pi})(\Sigma_a/\mu\Sigma_s)]$. It approaches $T_{\text{eff}} = T[1 + 0.6\,(\Sigma_a/\mu\Sigma_s)]$ for $\Sigma_a/\mu\Sigma_s \sim 0.75$, which was found by Cohen to be the approximate result for $\Sigma_a/\mu\Sigma_s < 0.5$.

The neutron spectrum in heterogeneous lattices has also been studied by the Karlsruhe group.[19] A method was established for calculating the spectrum in a two-dimensional reactor that consisted of fuel plates and moderator. The fuel plates were treated as delta functions, and the Meetz[20] model of heterogeneity was used. This technique made possible a computation of the spectrum across the heterogeneous reactor. The thermal utilization was calculated by this method, and by one-group diffusion theory, for 12 reactors that contained natural or enriched fuel in the form of plates at various spacings in D_2O and graphite. The difference between the proposed method and the diffusion-theory method was negligible for D_2O-moderated reactors with natural fuel elements. However, in the enriched lattices, especially those moderated by graphite, significant differences (as great as 3%) were noted.

Scattering-Law Formulation

In *Power Reactor Technology*, 6(1), the reduction of measured differential scattering data to a "scattering law" was discussed. The use of the scattering law, $S(\alpha,\beta)$, allows the relation among the three variables involved in a scattering collision—the initial energy of the scattered neutrons, its final energy, and the scattering angle—to be expressed in terms of two variables: α, the relative momentum transfer, and β, the relative energy transfer. Experimental evaluations of $S(\alpha,\beta)$, over ranges of α and β, have been made for several moderators. The application of the scattering law to the calculation of reactor spectra and multigroup cross sections was discussed at the Brookhaven Conference, principally in a paper by J. D. Macdougall,[21] which summarized work at Harwell, Winfrith, and Chalk River.

Generalized Frequency Distribution

Since measurements do not cover the complete range of energy and momentum transfer required for spectrum calculations, the experimental data must be extrapolated and interpolated. Egelstaff and Schofield[22] have developed a theoretical method by which a generalized frequency distribution is deduced from the measured results, and the complete scattering law is calculated using this distribution. This method involves finding the generalized frequency distribution $p(\beta)$ from the experimental scattering law as

$$p(\beta)/\beta^2 = \lim_{\alpha\to 0} S_s(\alpha,\beta)/\alpha \tag{10}$$

where $S_s(\alpha,\beta)$ is the self part of the scattering law. The scattering law $S(\alpha,\beta)$ is composed of a self term S_s, which arises from neutron scattering from a single nucleus, and an interference term S_d, which represents interference wavelets scattered from several atoms. The S_d modulates S_s and is significant only for small α's that are unimportant in reactor calculations. In determining $p(\beta)$, the experimental S/α is extrapolated to $\alpha = 0$, ignoring the distinguishable region near $\alpha + 0$ where S_d becomes important.

The term $S_s(\alpha,\beta)$ can then be calculated (neglecting anharmonic effects)[22] using the relation

$$S_s(\alpha,\beta) = \frac{1}{2\pi}\int_{-\infty}^{+\infty} e^{-\alpha\omega(t)+i\beta t}\, dt \qquad (11)$$

where

$$\omega(t) = \int_0^{\infty}\left[\frac{p(\beta)}{\beta^2}\right](\cosh \beta/2 - \cos \beta t)\, d\beta \qquad (12)$$

Because of experimental errors, interference effects, etc., the $p(\beta)$ obtained, using the scheme in Eq. 4 above, is used as a first guess in an iterative procedure that results in a more accurate value of $p(\beta)$. In this procedure $S(\alpha,\beta)$ is calculated with the initial $p(\beta)$, and the discrepancies between the calculated $S(\alpha,\beta)$ and the measured $S(\alpha,\beta)$ are noted. The discrepancies are then used to obtain a corrected $p(\beta)$, and $S(\alpha,\beta)$ is again calculated and compared with experiment. This procedure is repeated until $p(\beta)$ provides a satisfactory fit between the experimental and calculated scattering laws.

Computation of $S(\alpha,\beta)$, Multigroup Cross Sections, and Spectra

The FORTRAN program LEAP written by McLatchie will evaluate $S(\alpha,\beta)$ using Eqs. 5 and 6. The averaging necessary to produce group-averaged cross sections is accomplished using the FORTRAN program PIXSE. The input to PIXSE can be the scattering laws evaluated by LEAP or the scattering laws for a monatomic gas. Although the output of PIXSE is designed for use with the Winfrith DSN code point cross sections, a number of other integrals useful in spectrum calculations can be obtained. In addition, PIXSE can be used in conjunction with the PIXMIX program to calculate scattering matrices for Carlson's SNG code.

The Winfrith DSN program is a one-dimensional discrete-ordinates program written in FORTRAN for cylindrical geometry. This version is an improvement over Carlson's DSN program in the treatment of the reflected boundary conditions and in the iteration technique. The output of the DSN program consists in the eigenvalue and the energy-space-dependent flux solution to the problem plus other useful quantities such as total leakage and absorption.

Comparison of Spectrum Calculations with Experiment

Calculations of thermal-neutron spectra measured in a graphite-moderated Calder Hall lattice cell[13] have been made with the LEAP-PIXSE–Winfrith DSN procedure, using the monatomic gas model and a graphite scattering law. The scattering law $S(\alpha,\beta)$ was calculated by LEAP using a frequency spectrum chosen such that: $2p(\beta)\sinh(\beta/2)/\beta$ was constant for 300°K < βkT < 2100°K; $2p(\beta)\sinh(\beta/2)/\beta$ was proportional to β for βkT < 300°K, except near zero; and $p(\beta)$ was parabolic near $\beta = 0$.

The calculated $S(\alpha,\beta)$ and the monatomic gas-law scattering relations were used in PIXSE to obtain 40-group cross sections from 0 to 1.5 ev with 20 groups in the 0- to 0.2-ev range. These cross sections were entered into cylindrical-cell DSN calculations. The cell consisted of a 1.15-in.-diameter Magnox-canned natural-uranium rod in a 3.75-in. channel, the channels being set on an 8-in. pitch in the graphite moderator. The comparison between theory and experiment was made by comparing the calculated scalar flux at the outside edge of the cell with the experimentally measured directed flux. This comparison was considered valid since the DSN calculations showed that the directed flux differed from the mean flux at this point by less than 1% in all groups. Figure I-4 compares the calculated gas and graphite frequency-distribution spectra with the spectrum measured by Coates and Gayther[13] at 293°K. It is to be noted that the graphite frequency-distribution spectrum is in better agreement than the gas spectrum, especially below $2kT$. At 594°K all the spectra are in better agreement; however, the closest agreement with experiment is still given by the graphite spectrum.

The effects of the scattering model on ηf and the temperature coefficient of reactivity were also calculated. The effect on ηf was small: one-sixth of 1% difference between the gas model and the graphite frequency-distribution model was noted at 293°K, and less than half

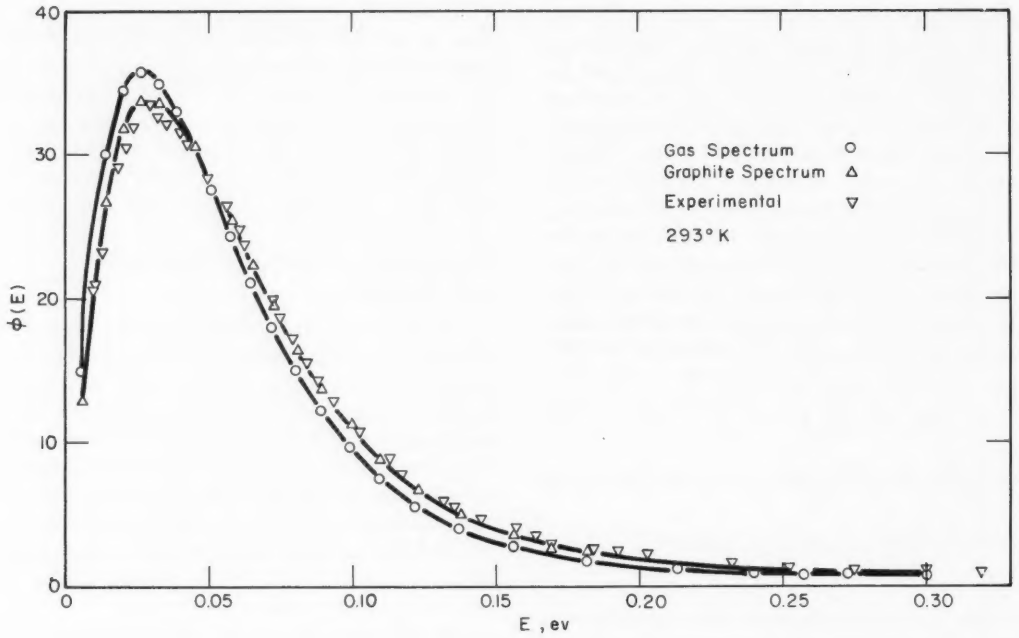

Fig. I-4 Calculated and experimental neutron spectra in graphite.[21]

that amount was noted at 594°K. The calculated temperature coefficients differed by 10% between the gas and the frequency-distribution model.

Reduced Partial Differential Cross-Section Formulation of Scattering Law

One of the drawbacks of the scattering-law formulation is that experimental data in this form are not as easily compared with other data or with theory as they are when given in the form of the conventional differential scattering cross section. Moreover, the cross section σ_b and the mass M must sometimes be arbitrarily selected to transform the partial differential cross section $\partial^2\sigma/(\partial E\ \partial\Omega)$ to $S(\alpha,\beta)$. To eliminate these difficulties while preserving the advantages of the scattering-law formulation, Brugger[23] has presented the law in a different form, which he calls the reduced partial differential cross section.

The Egelstaff-Schofield scattering law $S(\alpha,\beta)$ is related to the differential cross section $\partial^2\sigma/(\partial E\ \partial\Omega)$ as follows:

$$S(\alpha,\beta) = \frac{4\pi}{\sigma_b} kT \sqrt{\frac{E_0}{E}}\, e^{\beta/2} \frac{\partial^2\sigma}{\partial E\ \partial\Omega} \qquad (13)$$

where σ_b = bound-atom scattering cross section
k = Boltzmann constant
T = absolute temperature of the sample
E_0 = incident energy of the neutron (ev)
E = neutron energy after scattering (ev)
$\partial^2\sigma/(\partial E\ \partial\Omega)$ = conventional differential cross section
α = relative momentum transfer = $\dfrac{m[E_0 + E - 2\,(E_0E)^{1/2}\ \cos\,\Omega]}{MkT}$
β = relative energy transfer = $(E - E_0)/kT$
Ω = scattering angle
m = mass of the principal scatterer, amu
M = neutron mass

Brugger's reduced partial differential cross section $S(K,\hbar\omega)$ is related to the scattering law by

$$S(K,\hbar\omega) = \frac{\sigma_b}{4\pi} \frac{1}{kT} S(\alpha,\beta) \qquad (14)$$

which from Eq. 7 is related to $\partial^2\sigma/(\partial E\ \partial\Omega)$ by

$$S(K,\hbar\omega) = \frac{\kappa_0}{\kappa} e^{-\hbar\omega/2kT} \frac{\partial^2\sigma}{\partial E\ \partial\Omega} \qquad (15)$$

where K is the magnitude of the momentum transfer in reciprocal angstroms:

$$K = \frac{1}{\hbar}\sqrt{2Mk_B T\alpha} = \left\{\frac{2m}{\hbar^2}[E_0 + E - 2(E_0E)^{1/2}\ \cos\Omega]\right\}^{1/2}$$

$$= \left\{\frac{2m}{\hbar^2}[2E_0 + \hbar\omega - 2E_0^{1/2}(E_0 + \hbar\omega)^{1/2}\cos\Omega]\right\}^{1/2}$$

$\hbar\omega$ is the relative energy transfer in electron volts: $\hbar\omega = E - E_0$; κ_0 and κ are the wave numbers before and after scattering, respectively: $\kappa_0 = \sqrt{2mE_0/\hbar^2}$ and $\kappa = \sqrt{2mE/\hbar^2}$; $S(K,\hbar\omega)$ is in units of barns per electron volt steradian molecule; $\hbar$ is $\frac{1}{2}\pi$ times Planck's constant, h. The reduced partial differential cross-section formulation permits an unambiguous presentation of the scattering data, since it eliminates the necessity of specifying the bound scattering cross section σ_b and the mass M of the principal scattering atom.

A compilation of experimental reduced partial differential cross-section data for a number of materials at various temperatures is given in Ref. 23. The cross sections $S(K,\hbar\omega)$ are presented as a set of smoothed curves for a series of values of $\hbar\omega$ as a function of K. Data are given for beryllium (20°C), BeO (20°C), carbon (21°C, 300 to 400°C, 600°C), H_2O (20°C, 150°C), D_2O (20°C, 150°C), methane (21°C), propane (21°C), orthoterphenyl (21°C), metaterphenyl (21°C), paraterphenyl (21°C), Santowax R (21°C, 207°C, 267°C), and the ideal gas.

Theoretical Scattering Kernels

Comparison of Nelkin's Theoretical Scattering Law for Water with Experiment

A detailed comparison of Nelkin's theoretical water kernel[9] with recent scattering-law measurements from Hanford[24] and Chalk River[25] has been made by Lindenmeier.[26] The Nelkin model assumes that the H_2O molecule is the basic dynamical unit and that a classification of the atomic motions into translations, hindered rotations, and vibrations can be used to describe the proton motions in the liquid. For an incoming neutron with sufficiently high energy to excite more than one mode, all but the motion requiring the largest energy transfer is treated in the high-energy transfer limit. Consequently the parameters appearing in the total scattering cross-section formula are different depending on which oscillatory motion is being treated exactly, i.e., depending on the amount of energy being transferred in the scattering process.

Since this picture is not compatible with the Egelstaff scattering-law formulation, Nelkin's model was evaluated for various values of α and β using a selection of parameters suggested by Goldman. The calculated results are compared with the combined Hanford and Chalk River data in Fig. I-5. The large discrepancies at small α are intrinsic to the Nelkin model since the experimentally observed continuous broad-peaked phonon distributions $\rho(\beta)$ near the rotational and vibrational resonances are represented by delta functions. Since

$$\rho(\beta) = 2\beta \sinh\frac{\beta}{2} \lim_{\alpha\to 0}\frac{S(\alpha,\beta)}{\alpha}$$

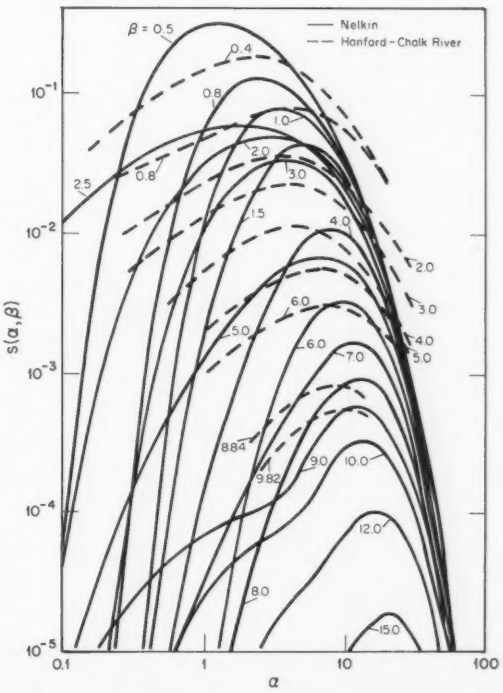

Fig. I-5 Comparison of theoretical and experimental scattering laws for water.[26]

$S(\alpha,\beta)/\alpha$ will tend to infinity for small α, so that for the values of β near the positions of the delta functions in Nelkin's model, $S(\alpha,\beta)$ will fall off too slowly. Moreover, for values of β far from the resonances, $S(\alpha,\beta)$ falls off too rapidly.

At large values of α, the envelope of the bounding experimental curves lies to the right of the bounding envelope of the theoretical curves. This discrepancy can be corrected by a modification of the relative weighting of the vibrational and rotational levels.

Finally, the theoretical curves are narrower than the experimental curves. It is felt that the inclusion in the modified Nelkin model of an unexplained experimentally indicated level at 0.015 ev would broaden the theoretical curves.

The above changes are being incorporated into the Nelkin model, although there is no obvious way of correcting the discrepancy at small α and at the same time preserving the simplicity of the model. However, it is felt that the logarithmic presentation has exaggerated the difficulty and that the model is adequate for certain practical purposes.

Comparison of the Radkowsky and Nelkin Kernels

Gelbard et al.[3] have compared the results of applying the Nelkin and Radkowsky thermal scattering kernels in water, using multigroup P_1 and P_3 calculations (SLOP-1 and the EXCEL-1) in a TRX lattice. Their results show that the 36-group P_1 calculations tend to underestimate the measured variation in the flux shape by about 3% in the fuel rod and by about 6% in the surrounding water region. The 6-group P_3 calculations overestimate the flux variation by about the same amount. Little difference was found between the results with the Radkowsky and Nelkin kernels; slightly better agreement was obtained using the Nelkin kernel in the 6-group P_3 equations, but an overestimation of 4% remained.

Calculation of Thermal-Flux Spectra in Polyethylene

Polyethylene is sometimes used as a substitute for water in critical assemblies because it offers experimental flexibility and is convenient

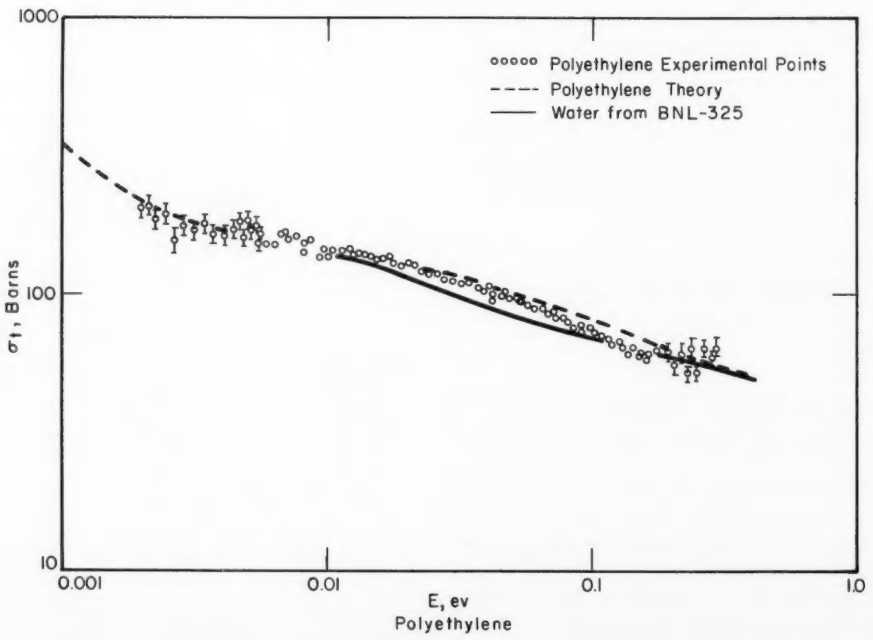

Fig. I-6 Total cross section for the scattering of neutrons by polyethylene.[27]

to use. Generally, it has been assumed in neutron-spectrum calculations that the moderating characteristics of the polyethylene are described by a gas of free protons, the chemical binding of these protons within the molecule being neglected. Although the thermalization process in polyethylene is similar to that in water, it is found that modifications must be made in the bound proton water models in order to produce agreement with the details of the experimental polyethylene data.

Goldman and Federighi[27,28] have extended to polyethylene Nelkin's description of the chemically bound system as a system of harmonic oscillators. The energies of phonon excitation were inferred from the measured infrared absorption spectrum of solid polyethylene. The KERNEL code was utilized to calculate the differential scattering cross section for various scattering angles, using four sets of calculational parameters, the selection of which was based on the range of energy transfer in the scattering process. The total cross section was then computed by integrating the differential cross section over angle and final neutron energy. Figure I-6 compares the calculated total cross section for the scattering of neutrons by polyethylene with the experimental data of Bach. The total cross section for water, also shown, indicates the experimental and theoretical difference between water and polyethylene. The calculated total cross sections obtained, using the polyethylene kernel and the Nelkin water kernel, were then used in conjunction with the SWAK code to calculate the infinite-medium spectra. These are compared in Fig. I-7 with the infinite-medium spectrum measured in borated polyethylene by Beyster. It is to be noted that the infinite-media spectra are very sensitive to the scattering kernel and that, although the Nelkin water kernel is not satisfactory in the calculation of polyethylene spectra, excellent results are obtained when this model is modified to characterize polyethylene.

Although the calculated flux spectrum is sensitive to the choice of scattering kernel, the eigenvalues for arrays calculated using different scattering kernels show only minor differences, primarily because the spectrum-averaged cross sections appear as ratios in the thermal utilization. Thus, in practical applications, the differences in spectrum may only be manifest in the calculation of lifetime and power peaking in reactor cores.

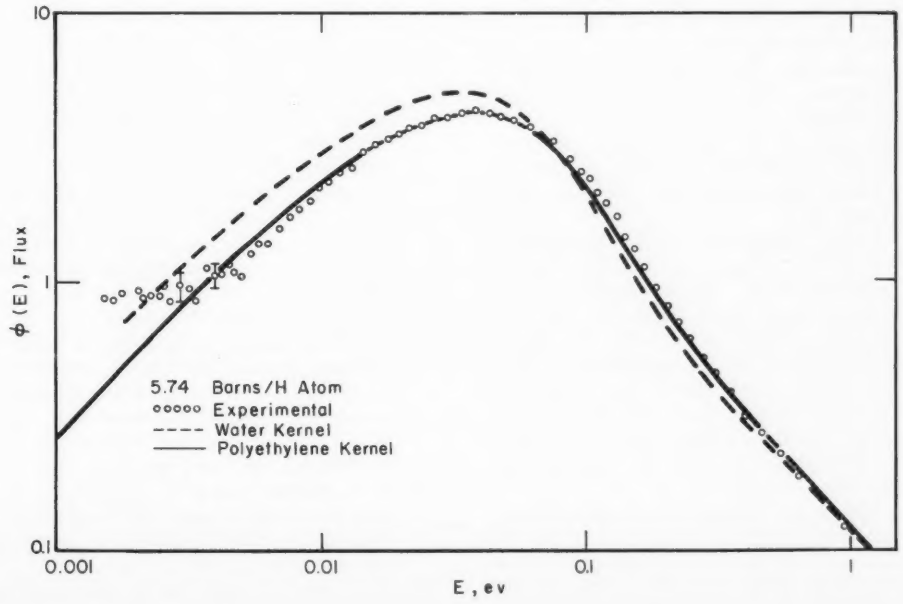

Fig. I-7 Calculated and experimental neutron spectra in borated polyethylene (5.74 barns/H atom.)[27]

References

1. H. C. Honeck, Thermal Neutron Spectra in Heterogeneous Assemblies, in Proceedings of the Brookhaven Conference on Neutron Thermalization, April 30 to May 2, 1962, p. RD-1, USAEC Report BNL-719(Vol. II), Brookhaven National Laboratory.
2. G. R. Dalton, Integral and Numerical Treatments of the Neutron Transport Problem, in Proceedings of the Brookhaven Conference on Neutron Thermalization, April 30 to May 2, 1962, p. 465, USAEC Report BNL-719(Vol. II), Brookhaven National Laboratory.
3. E. M. Gelbard, J. A. Davis, and E. Schmidt, A Comparison of the Properties of the Nelkin and Radkowsky Thermal Neutron Scattering Kernels for Water, USAEC Report WAPD-T-1481, Westinghouse Electric Corp., Bettis Atomic Power Laboratory, March 1962.
4. H. C. Honeck, Calculation of Thermal Utilization and the Disadvantage Factor in Uranium Water Lattices, in Light Water Lattices: Report of a Panel on Light Water Lattices Held in Vienna, 28 May–1 June 1962, pp. 233-265, Report STI/DOC/10/12, International Atomic Energy Agency, Vienna, 1962.
5. G. W. Schaeffer and K. Allsopp, Chemical Binding Effects in the Generalized Heavy Free Gas Approximation, in Proceedings of the Brookhaven Conference on Neutron Thermalization, April 30 to May 2, 1962, p. 614, USAEC Report BNL-719 (Vol. II), Brookhaven National Laboratory.
6. N. Corngold, Chemical Binding Effects in the Thermalization of Neutrons, *Ann. Phys. (N. Y.)*, 11(3): 338 (November 1960).
7. D. E. Parks, The Effects of Atomic Motions on the Moderation of Neutrons, *Nucl. Sci. Eng.*, 9(4): 430 (April 1961).
8. L. DeSobrino and M. Clark, Comparison of the Wilkins Equation and Higher Order Approximations for Solid Moderators, *Nucl. Sci. Eng.*, 10(4): 384 (August 1961).
9. M. S. Nelkin, Scattering of Slow Neutrons by Water, *Phys. Rev.*, 119(2): 741 (July 15, 1960).
10. G. W. Schaeffer and K. Allsopp, Chemical Binding Effects in the Generalized Heavy Free Gas Approximation, in Proceedings of the Brookhaven Conference on Neutron Thermalization, April 30 to May 2, 1962, p. 647, USAEC Report BNL-719 (Vol. II), Brookhaven National Laboratory.
11. H. Hurwitz, Jr., M. S. Nelkin, and G. J. Habetler, Neutron Thermalization, *Nucl. Sci. Eng.*, 1(4): 280 (August 1956).
12. C. W. Lindenmeier, The Modified Heavy Gas Model and Two Group Rethermalization Theory, in Proceedings of the Brookhaven Conference on Neutron Thermalization, April 30 to May 2, 1962, p. 1272, USAEC Report BNL-719(Vol. IV), Brookhaven National Laboratory.
13. M. S. Coates and D. B. Gayther, Time of Flight Measurements of Neutron Spectra in a Graphite Uranium Lattice at Different Temperatures, British Report AERE-R-3829, September 1961.
14. J. R. Beyster, J. L. Wood, W. M. Lopez, and R. B. Walton, Measurements of Neutron Spectra in Water, Polyethylene, and Zirconium Hydride, *Nucl. Sci. Eng.*, 9(2): 168 (February 1961).
15. E. R. Cohen, The Neutron Velocity Spectrum in a Heavy Moderator, *Nucl. Sci. Eng.*, 2(3): 227 (May 1957).
16. R. R. Coveyou, R. R. Bate, and R. K. Osborn, Effect of Moderator Temperature upon Neutron Flux in Infinite, Capturing Medium, *J. Nucl. Energy: Pt. A*, 2(3): 153 (March 1956).
17. Z. Weiss, Neutron Spectrum Temperature Distribution in Heterogeneous Systems with Constant Absorption, Report No. 233/IX submitted for publication in *Nukleonika* by Polish Academy of Sciences, Warsaw, May 1961.
18. E. R. Cohen, A Survey of Neutron Thermalization Theory, in *Proceedings of the International Conference on the Peaceful Uses of Atomic Energy, Geneva, 1955*, Vol. 5, p. 405, United Nations, New York, 1956.
19. W. Häfele, Neutron Spectra in Heterogeneous Assemblies, in Proceedings of the Brookhaven Conference on Neutron Thermalization, April 30 to May 2, 1962, p. 485, USAEC Report BNL-719 (Vol. II), Brookhaven National Laboratory.
20. K. Meetz, Exact Treatment of Heterogeneous Core Structures, in *Proceedings of the Second United Nations International Conference on the Peaceful Uses of Atomic Energy, Geneva, 1958*, Vol. 16, pp. 611-626, United Nations, New York, 1958.
21. J. D. Macdougall, Application of Scattering Law Data to the Calculation of Thermal Neutron Spectra, in Proceedings of the Brookhaven Conference on Neutron Thermalization, April 30 to May 2, 1962, p. 121, USAEC Report BNL-719(Vol. I), Brookhaven National Laboratory, June 1962.
22. P. A. Egelstaff and P. Schofield, On the Evaluation of the Thermal Neutron Scattering Law, British Report AERE-R-3803, as referenced in Ref. 21. Reprinted from *Nucl. Sci. Eng.*, 12(2): 260-270 (February 1962).
23. R. M. Brugger, Compilation of Reduced Slow Neutron Partial Differential Scattering Cross Sections, in Proceedings of the Brookhaven Conference on Neutron Thermalization, April 30 to May 2, 1962, p. 3, USAEC Report BNL-719(Vol. I), Brookhaven National Laboratory, June 1962.
24. D. A. Kottwitz and B. R. Leonard, Jr., Scattering Law for Room Temperature Light Water, USAEC Report HW-75526, Hanford Atomic Products Operation, Nov. 7, 1962.
25. B. C. Haywood and I. M. Thorson, The Scattering Law for Light and Heavy Water at 20°C and 150°C, in Proceedings of the Brookhaven Conference on

Neutron Thermalization, April 30 to May 2, 1962, p. 26, USAEC Report BNL-719(Vol. I), Brookhaven National Laboratory, June 1962.

26. C. W. Lindenmeier, Comparison of Nelkin's Water Kernel with Experiment, in Physics Research Quarterly Report, July–September 1962, pp. 4-9, USAEC Report HW-75228, Hanford Atomic Products Operation, Oct. 15, 1962.
27. D. T. Goldman and F. D. Federighi, Calculation of Thermal Neutron Flux Spectra in an Infinite Polyethylene Moderated Medium with Varying Amounts of Absorption, in Proceedings of the Brookhaven Conference on Neutron Thermalization, April 30 to May 2, 1962, p. 100, USAEC Report BNL-719(Vol. I), Brookhaven National Laboratory, June 1962.
28. D. T. Goldman and F. D. Federighi, Calculation of Thermal Neutron Flux Spectra in a Polyethylene Moderated Medium, *Nucl. Sci. Eng.*, 16(2): 165 (June 1963).

Section

II

Power Reactor Technology

Fluid and Thermal Technology

Liquid-Metal Heat Transfer

The subject of liquid-metal heat transfer has lately received considerable emphasis in connection with the space program, and the literature available on the technology has been surveyed and abstracted in several publications. Reference 1 is a literature survey on liquid-metal boiling. It covers some 1191 documents that were issued from about 1930 to 1961. The survey considers nucleate-boiling correlations, film-boiling correlations, quality, interface and zero-gravity effects in boiling heat transfer, and two-phase flow regimes and two-phase pressure drop. A summary of current experimental liquid-metal boiling programs is also included; these are listed in Table II-1. The MSA Research Corporation periodically publishes a liquid-metals technology abstract bulletin, of which the current issue[2] is available. In addition, there is a new bimonthly publication entitled "High-Temperature Liquid-Metal Technology Review," prepared by the Brookhaven National Laboratory.[3] It summarizes current progress on unclassified projects supported by the AEC, NASA, and the Air Force.

The report on "Proceedings of the 1962 High-Temperature Liquid-Metal Heat-Transfer Technology Meeting" has recently been published.[4] The 1962 meeting, held at Brookhaven National Laboratory, was the second of its kind. The proceedings report contains 24 papers concerned with the physical properties of liquid metals, heat and mass transfer, burnout heat flux, construction materials, and the construction and operation of heat-transfer loops. The papers of the previous meeting were published in a classified document; of the 26 papers presented at the second meeting, all but two were unclassified. Most of the programs discussed in Ref. 4 were in their initial stages and will not be reviewed here.

Reference 5 presents a correlation of liquid fraction in two-phase flow with an application to liquid metals. Figure II-1 illustrates the data ranges used in the correlations; the mercury-nitrogen data appear in Ref. 6, the air-water data in Ref. 7, and the Lockhart-Martinelli air-liquid data appear in Ref. 8. The parameter X_{tt} is defined as follows:

$$X_{tt} = \left(\frac{W_l}{W_g}\right)^{0.9} \left(\frac{\rho_g}{\rho_l}\right)^{0.5} \left(\frac{\mu_l}{\mu_g}\right)^{0.1}$$

where $W_{l,g}$ = liquid, gas flow rate, lb/hr
$\rho_{l,g}$ = liquid, gas density, lb/cu ft
$\mu_{l,g}$ = liquid, gas viscosity, lb/(ft)(hr)

The liquid fraction, R_l, is defined as the fraction of the pipe cross section occupied by liquid in cocurrent liquid-vapor or gas flow. The curve for steam-water at critical pressure was determined using the methods of Martinelli-Nelson.[9] It is evident that the mercury-nitrogen data required extrapolation, and this was done by assuming a slip ratio of unity above a liquid-to-gas flow-rate ratio of 100,000 and using the Lockhart-Martinelli curve as a guide in establishing the shape of the mercury-nitrogen curve.

A cross-plot of Fig. II-1 is shown as Fig. II-2; this is the generalized correlation. For comparative purposes the parameter $(\mu_l/\mu_g)^{0.2}/(\rho_l/\rho_g)$ for the several liquids at various saturation temperatures has been evaluated and is shown along the abscissa. Although few liquid-metal void-fraction data were available at the time of the writing of Ref. 5, the authors compare the generalized plot with steam-water and Santowax R void-fraction data, and, in general, the comparison is good. The correlation is then applied to the design of a boiling mercury reactor of the SNAP type.

Reference 10 discusses burnout predictions for liquid-metal heat-transfer systems. In

Table II-1 LIQUID-METAL EXPERIMENTAL PROGRAMS*

Organization	Test fluid	Test objective	Status
Aerojet-General Nucleonics	Rb, Cs	Operating loops	
AiResearch	K	Materials	Fabrication
AiResearch	K	0-g boiling exp.	Fabrication
Argonne National Laboratory	K	Boiling heat transfer	Design
Argonne National Laboratory	Cd	Boiling heat transfer	Operation
Argonne National Laboratory	Hg-N_2	Two-phase studies	
Atomics International	NaK	Heat transfer and hydraulics	
Atomics International	Hg	Boiling heat transfer	
Atomics International	Na	Burnout studies	
Atomics International	Na	Condensing studies	
Brookhaven National Laboratory	K	Boiling heat transfer	
Columbia University	Na	Condensing studies	
Electro-Optical Systems, Inc.	Hg	Condensing 0-g studies	
General Electric Company	K, Na	Materials	Fabrication
General Electric Company	K, Na	Heat transfer	Fabrication
General Electric Company	K	Turbine	Design
Marquandt Corp.	Li		
The Martin Co.	Li	Operating loops	
MSA Research Corporation	Na	Materials	Operating
NASA— Lewis Research Center	Na	Turbine	Design
NASA— Lewis Research Center	Na	Turbine	Fabrication
NASA— Lewis Research Center	Na	Pumps	Fabrication
NASA— Lewis Research Center	Na	Boiling heat transfer	Fabrication
NASA— Lewis Research Center	Na	Condensing studies	Design
NASA— Nuclear Development Associates	K, Na	Materials	Design
Nuclear Development Corp. of America			
Oak Ridge National Laboratory	K	Boiling heat transfer	Operating
Pratt & Whitney Aircraft	Li, NaK	Materials	Operating
Rocketdyne	K	Materials	Operating
Sundstrand Aviation	Rb	Condensing	Fabrication
Sundstrand Aviation	Rb	Boiling	Fabrication
Sundstrand Aviation	Rb	Heat storage	Design

*From Aeronautical Systems Division, Wright-Patterson Air Force Base.

particular, the correlations of Bernath,[11] Gunther,[12] and Griffith[13] are compared with numbers derived from an "additive method" of calculating the burnout heat flux. This latter method has been discussed in other issues of *Power Reactor Technology* [6(1): 18 and 6(3): 10]. Table II-2 illustrates a comparison of the various correlations for forced-convection local-boiling burnout, and Table II-3 compares the correlations for bulk-boiling burnout. Although the discrepancies among the various correlations are substantial even for water, they become so large in the liquid-metal cases that no useful conclusions can be drawn without experimental data. The authors of Ref. 10 recommend experimental studies to clarify the situation, and they describe appropriate apparatus with which to conduct the experiments. In the interval between the appearance of Ref. 10 and the Brookhaven meeting (Ref. 4), however, it appears that few data on liquid-metal burnout have been obtained at any laboratory.

Boiling-Water Heat Transfer and Fluid Dynamics

Some results of an Atomic Energy Research Establishment program on two-phase flow distributions are reported in Ref. 14. The particular system studied was an air-water system

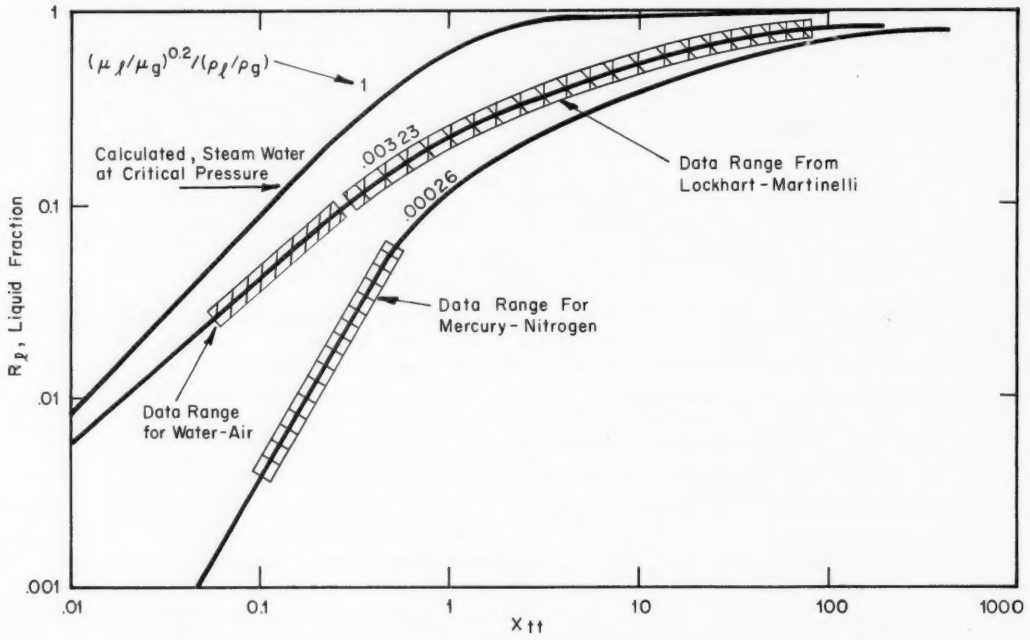

Fig. II-1 Liquid fraction[5] vs. X_{tt} for three values of $(\mu_l/\mu_g)^{0.2}/(\rho_l/\rho_g)$.

wherein the mixture flowed upward in a 1.25-in.-ID vertical tube (with a maximum length of 30 ft) at about 22 psia pressure. The air-water system is not of direct interest to the reactor designer; however, the flow distributions existing in boiling-water-cooled fuel elements are poorly understood, and any information dealing with two-phase flow distributions adds to the general knowledge.

The water was injected into the system through a porous section of the tube wall near the entrance, as indicated in Fig. II-3. The system was instrumented with a precisely located sampling probe to collect air-water samples and with a film-thickness measuring device that operated on the principle of measuring the conductance of the liquid film on the walls and relating this to the film thickness. Pressure taps were also installed.

Figure II-4 shows some oscillograph traces of the film-thickness probe output. It can be seen that near the injector the trace is relatively flat, but disturbance waves form a short distance up the tube with a frequency of about 30 cps. Integration of the droplet mass-velocity profiles, as determined from the sample probe readings, resulted in the data shown in Fig. II-5. Net entrainment was still taking place after about 170 equivalent diameters, and the authors[14] suggest that this is probably being caused by the disturbance waves on the film "throwing" water into the core of flowing air-water mixture. The modification of the velocity profile of single-phase (air) flow by the presence of the water is shown in Fig. II-6. A comparison of the profiles for air and air-water flow at positions near the injector illustrate that the velocity profile is changed from the flat-topped form common for turbulent flow to a sharply peaked form. The reference shows that this behavior is similar to flow in a rough pipe and postulates that the ripples on the surface of the liquid film act as roughness elements.

Reference 15 is itself a review of the state of heat transfer and fluid dynamic research as applied to two-phase gas-liquid systems. The review includes 107 references, most of recent issue, and is of special interest because it covers the literature of most of the countries supporting research in two-phase heat transfer and fluid dynamics. The author discusses in some detail three distinct flow regions in the forced-convection flow of steam-water mixtures:[15]

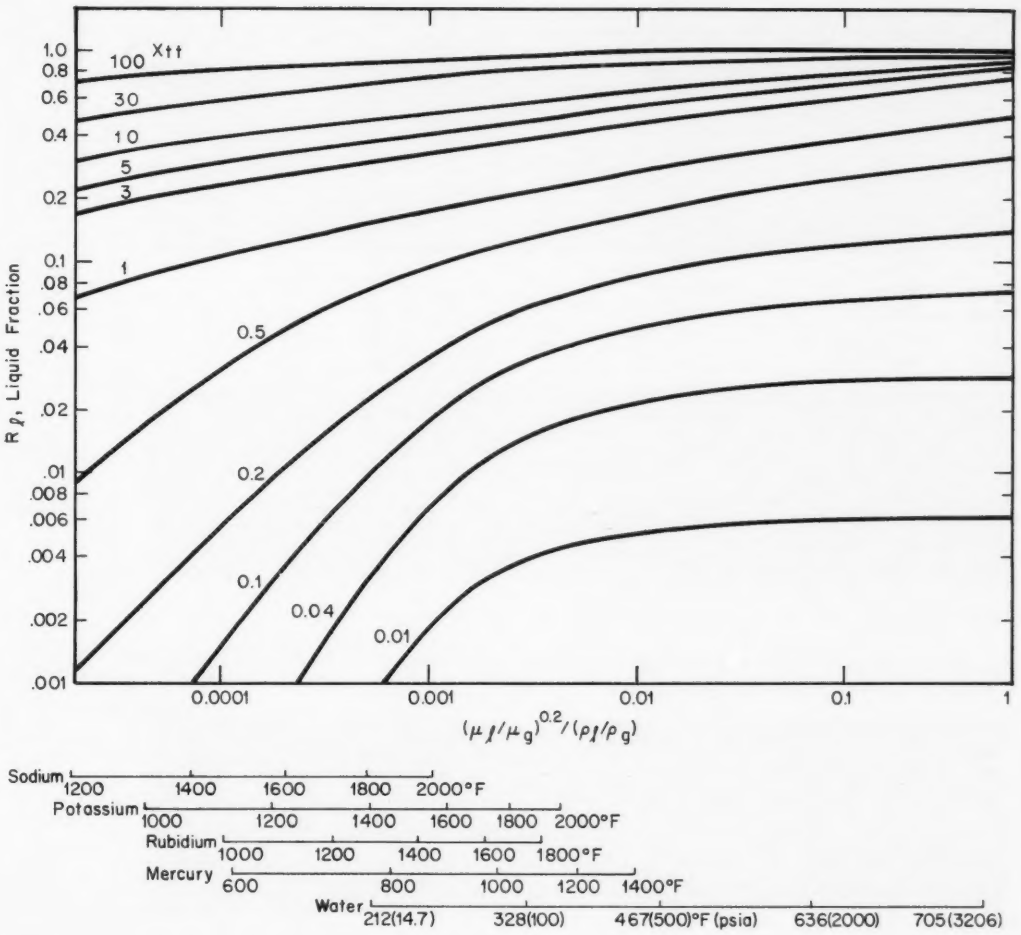

Fig. II-2 Generalized liquid fraction correlation.[5]

(a) Nucleate Boiling Region— This region occurs at low values of steam quality (up to 15–20 wt.% steam) and is characterized by the formation of steam at the heating surface in the form of bubbles which are detached and dispersed in the flowing water. Heat transfer under these conditions is governed by the laws of nucleate boiling.

(b) Forced Convective Region— At higher qualities (20–60 wt.% steam) the increased velocity of the two-phase mixture is sufficient to suppress the boiling mechanism, and the heat transfer process becomes governed by forced convection through the thin liquid films formed on the heating surface. "Fog cooling" takes place in this region.

(c) Liquid Deficient Region— At some critical value of steam quality (the "dry-out point") the heat transfer coefficient is reduced from a very high value in the "forced convective" region to a value near that expected for heat transfer by forced convection to dry steam. This is accompanied by a rise in the heating surface temperature of constant heat flux sources such as reactor fuel elements.

These regions are illustrated schematically in Fig. II-7. An enlightening discussion on the burnout phenomenon in each of the regions is presented in the reference. In the subcooled and low steam-quality regions, departure from nucleate boiling causes film blanketing of the heat-transfer surfaces, with sudden surface temperature increases and, usually, destruction of the heat-transfer surface material. This is termed "fast burnout." At higher steam quantities (greater than 20%), however, the term burnout might better be replaced by "dryout,"

Table II-2 FORCED-CONVECTION LOCAL-BOILING BURNOUT HEAT FLUXES FOR AXIAL FLOW[10]

(P = 1 atm abs, D_i = 3/8 in., V = 10 ft/sec)

	Δt_{sub}, °F	$10^{-6}\ \phi_{bo}$, Btu/(hr)(sq ft)			
		Bernath*	Gunther†	Griffith‡	Additive method¶
H_2O	60	0.96	1.33	2.34	1.64
	120	1.52	2.65	3.54	2.69
	180	2.07	3.98	4.65	3.51
K	60	488		36.2	0.80
	120	834		45.6	1.21
	180	1180		54.1	1.62
Rb	60	340		29.5	0.59
	120	585		37.1	0.87
	180	825		43.5	1.16

*The predictions are point predictions, without consideration of specific values of inlet temperature and tube length which would produce subcoolings at the burnout point equal to those selected for burnout calculation.

†Not applicable to fluids other than water.

‡Mean line through correlation plot used.

¶Tested to date only with axial- and swirl-flow water data.

Table II-3 FORCED-CONVECTION BULK-BOILING BURNOUT HEAT FLUXES FOR AXIAL FLOW[10]

(P = 1 atm abs, D_i = 3/8 in., $t_{in} = t_{sat}$, V_{in} = 2.5 ft/sec)

	x_e	$10^{-6}\ \phi_{bo}$, Btu/(hr)(sq ft)*	
		Griffith†	Additive method
H_2O	0.10	2.52	0.76
	0.30	5.07	0.89
K	0.10	89.1	0.66
	0.30	184	0.85
	0.50	214	0.96
Rb	0.10	78.5	0.47
	0.30	165	0.60
	0.40	185	0.65

*The predictions are point predictions, not simultaneous solutions with the heat balance ($x_e = \phi_{bo} A_h / WL_t$) characteristic of a particular tube length.

†Mean line through the correlation plot is used. Model is based on fog flow (no phase slip).

since the mechanism of film blanketing is not present, and dryout is accompanied by entry into the liquid-deficient region (see Fig. II-7). The film coefficients in the liquid-deficient region are nevertheless much higher than the coefficients for film boiling, with the result that the wall temperature does not ordinarily increase to the melting point but rather increases several hundred degrees Fahrenheit. This may or may not be fatal for material of the heat-transfer surface. This state of affairs

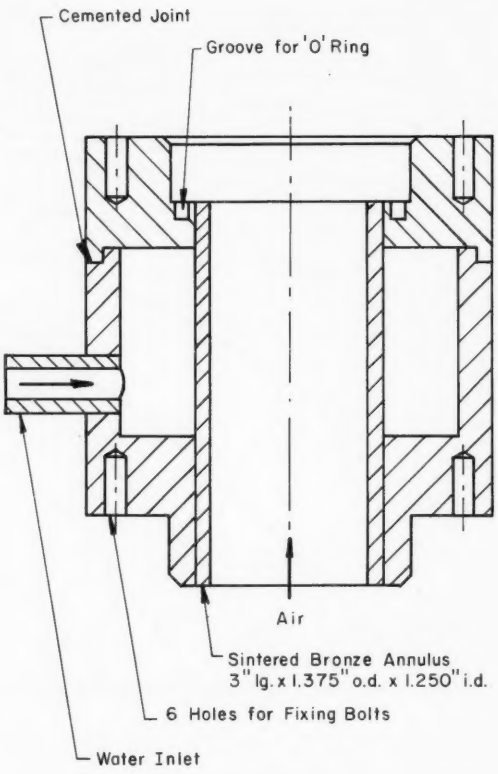

Fig. II-3 Water injector.[14]

is shown in Fig. II-8. Although the dryout heat flux may be exceeded, the wall temperature can still remain within acceptable bounds, especially if the situation should exist only temporarily in a power transient.

Reference 16 is a report on experimental observations of boiling burnout at 1500 psig. The test section consisted of a 0.44-in.-ID Inconel tube with a length of 12 ft and a wall thickness of 0.190 in. Thermocouples were spot welded about every foot along the length of the tube and were used to detect burnout by means of the onset of rapid wall temperature increases. Figure II-9 shows the locations of the thermocouples. What makes the reference of particular interest is that it reports results of experiments wherein burnout occurred upstream of the end of the test section as well as results wherein burnout occurred at the exit end of the test section. The data are shown in Fig. II-10 for mass velocities of 5, 6, and 7 million lb/(hr)(sq ft). The reference states that data were also taken

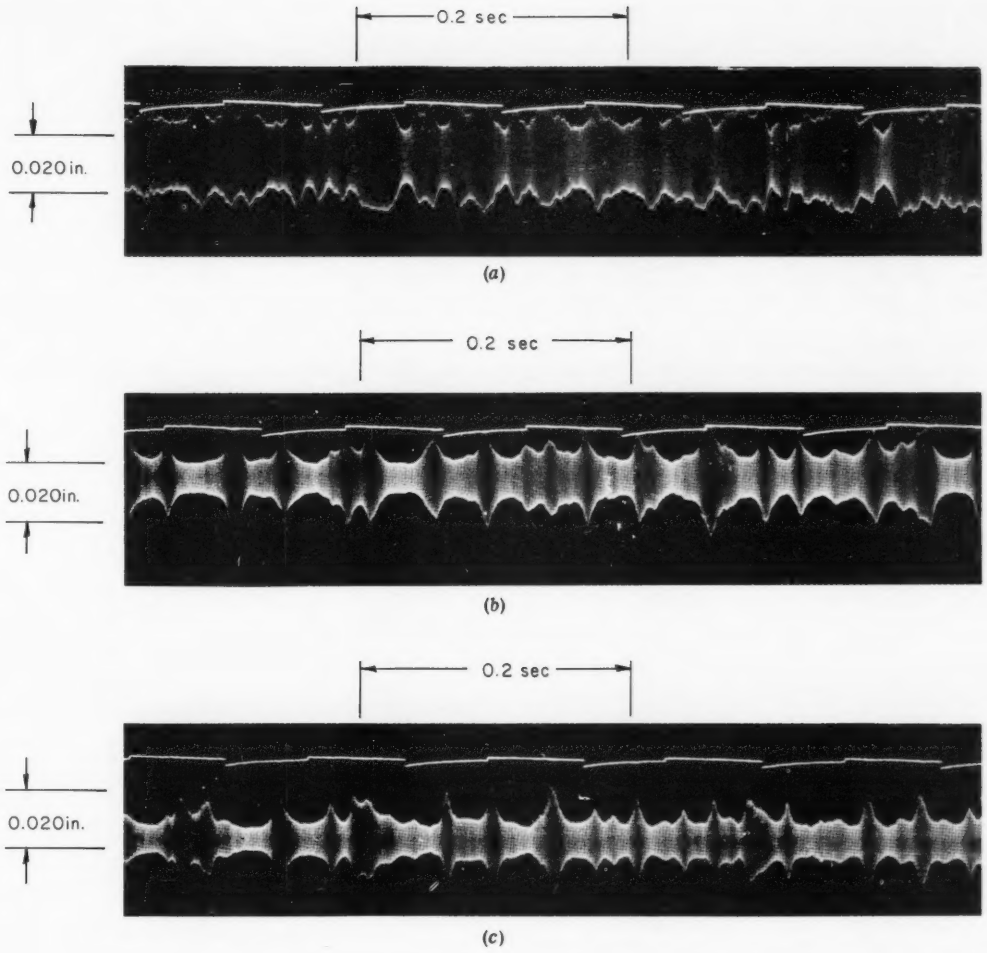

Fig. II-4 Oscilloscope records from conductance probes: (*a*) 3 in. above injector, (*b*) 21 in. above injector, and (*c*) 112 in. above injector.

at mass flow rates of 4 million lb/(hr)(sq ft) and less, although no quantitative information is presented. Figure II-10 presents both upstream and downstream burnout data. The latter is defined as burnout at essentially the exit of the test section. In all cases upstream burnout occurred at higher heat fluxes than downstream burnout, as is evident in Fig. II-10. Conditions were stable during the various upstream burnout detection runs. There were no fluctuations in test-section outlet pressure, pressure drop, and flow rate as measured by fast-response instrumentation. Figures II-11 and II-12 show temperatures during an upstream and a downstream burnout, respectively. It can be seen

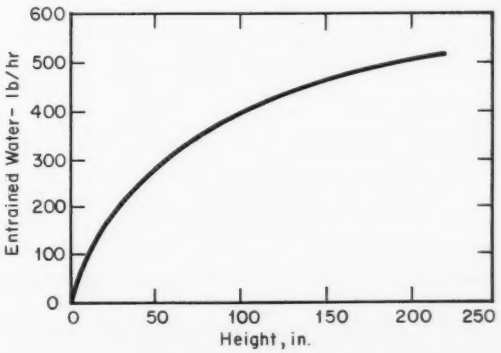

Fig. II-5 Integrated flux of entrained water through center 1.05 in. of tube.[14]

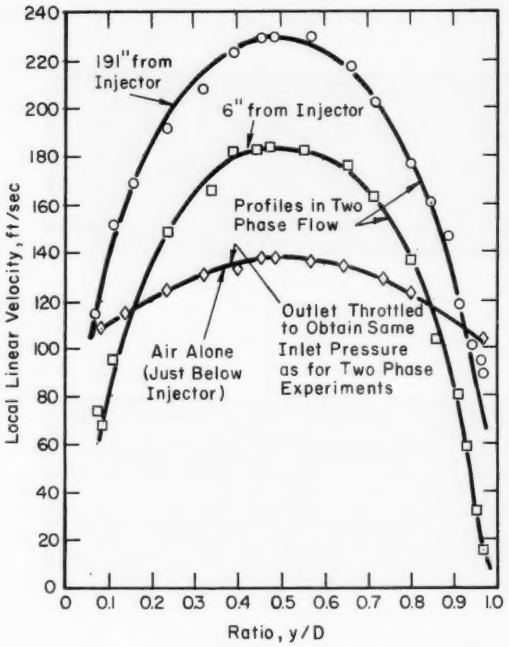
Local Linear Velocity, ft/sec
Ratio, y/D
191" from Injector
6" from Injector
Profiles in Two Phase Flow
Outlet Throttled to Obtain Same Inlet Pressure as for Two Phase Experiments
Air Alone (Just Below Injector)

Fig. II-6 Linear velocity profiles.[14]

that the downstream burnout was first evidenced by a slow increase in temperature, as measured by thermocouple No. 5 (TC 5). This was followed by temperature increases seen by TC 9 and TC 10, respectively. Although the reference suggests that the metal-surface temperature excursions were caused by a transition from nucleate to film boiling, the temperature plots (Figs. II-11 and II-12) fit the description of a slow burnout mentioned in Ref. 15. Since it is difficult to visualize how a uniform tube might dry out in the middle and not at the downstream end, it seems possible that local disruption of the film was involved in the upstream wall temperature excursions.

Short Notes

A review of heat transfer and fluid flow of water in the supercritical region has recently become available.[17] The document, which appears to have been produced as part of a study to design a 1000-Mw(e) supercritical-pressure nuclear reactor plant, contains a critical review of 48 documents. The study is oriented to the design of a once-through reactor. This design was discussed in the last issue of

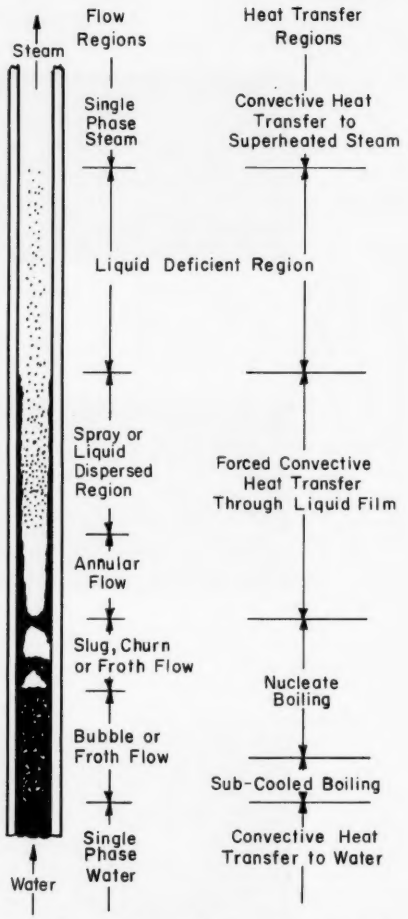

Fig. II-7 Regimes of two-phase flow.[15]

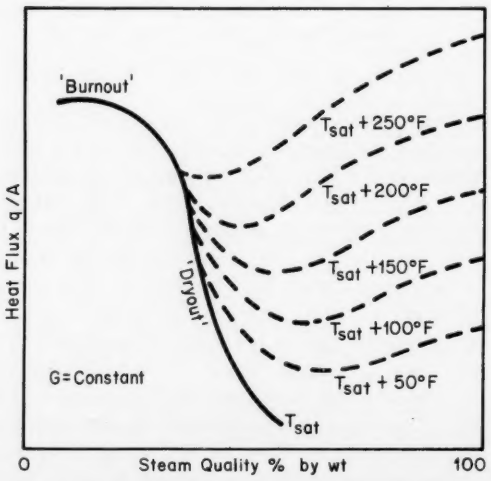

Fig. II-8 Surface temperature isotherms.[15]

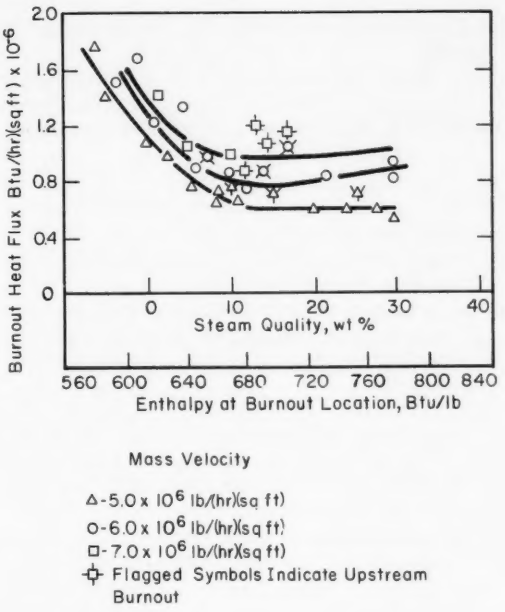
Burnout Heat Flux Btu/(hr)(sq ft) x 10⁻⁶
Steam Quality, wt %
Enthalpy at Burnout Location, Btu/lb
Mass Velocity
△-5.0 x 10⁶ lb/(hr)(sq ft)
○-6.0 x 10⁶ lb/(hr)(sq ft)
□-7.0 x 10⁶ lb/(hr)(sq ft)
Flagged Symbols Indicate Upstream Burnout

Fig. II-9 Test section thermocouple locations.[16]

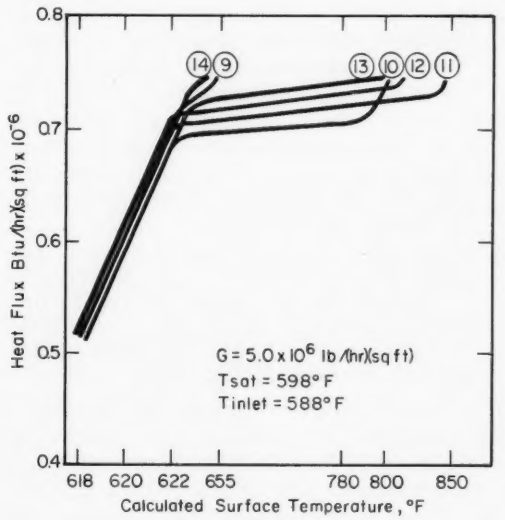

Fig. II-10 Experimental boiling-burnout data.[16]

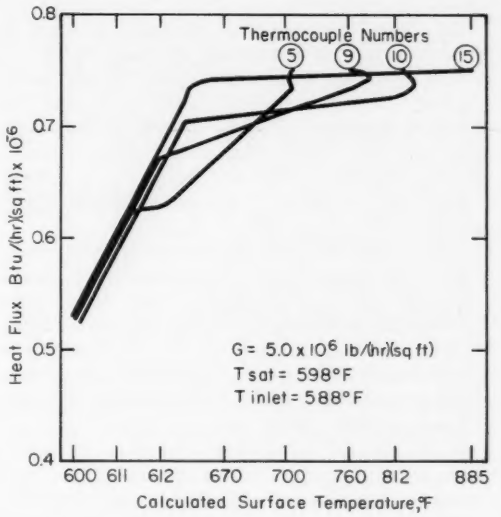
Thermocouple Numbers
Heat Flux Btu/(hr)(sq ft) x 10⁻⁶
G = 5.0 x 10⁶ lb/(hr)(sq ft)
Tsat = 598°F
Tinlet = 588°F
Calculated Surface Temperature, °F

Fig. II-11 Test-section temperatures during a typical upstream burnout run.[16]

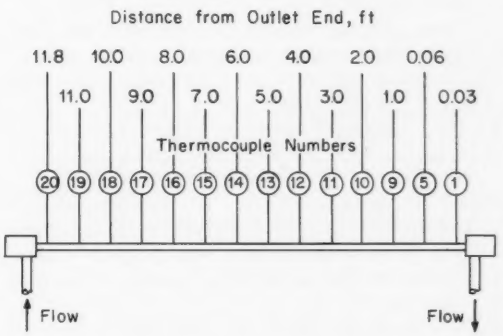

Fig. II-12 Magnitude of temperature excursions during a downstream boiling burnout.[16]

Power Reactor Technology [6(3): 74-78].

Reference 18 reports on the cooling of Plutonium Recycle Test Reactor (PRTR) fuel elements by a transverse flow of air. This would take place during ex-reactor examination of the elements in a hot cell. Electrically heated mockups of the several fuel elements for the PRTR were prepared and cooled by a stream of air. The data are specialized to the PRTR fuel elements studied, but one of the elements was a 19-rod cluster, and this is a fairly standard fuel-element geometry. The remaining reports[19,20] deal with computer solutions to several reactor heat-transfer problems.

References

1. R. E. Balzhiser, J. A. Clark, E. E. Hucke, L. R. Smith, C. P. Colver, H. Merte, Jr., and A. S. Teller, Literature Survey on Liquid Metal Boiling, U. S. Air Force ASD Technical Report 61-

594, The University of Michigan, College of Engineering, December 1961.

2. MSA Research Corporation, Liquid Metals Technology Abstract Bulletin LM/TAB-21 for the period September 1962 to February 1963.
3. O. E. Dyer (Ed.), High-Temperature Liquid-Metal Technology Review, Vol. 1, No. 1, USAEC Report BNL-788(PR-1), Brookhaven National Laboratory, February 1963.
4. Brookhaven National Laboratory, Proceedings of the 1962 High-Temperature Liquid-Metal Heat Transfer Technology Meeting May 17 and 18, 1962, USAEC Report BNL-756(C-35), March 1963.
5. C. J. Baroczy, Correlation of Liquid Fraction in Two-Phase Flow with Application to Liquid Metals, USAEC Report NAA-SR-8171, Atomics International, Apr. 15, 1963.
6. R. Kiraly and A. Koestel, The SNAP II Power Conversion System Topical Report No. 8, Condenser Development and Design Study, Report ER-4104, Thompson Ramo Wooldridge, Inc., June 1960.
7. G. F. Hewitt, I. King, and P. C. Lovegrove, Holdup and Pressure Drop Measurements in the Two-Phase Annular Flow of Air-Water Mixtures, *Brit. Chem. Eng.*, 8(5): 311-318 (May 1963).
8. R. W. Lockhard and R. C. Martinelli, Proposed Correlation of Data for Isothermal Two-Phase, Two-Component Flow in Pipes, *Chem. Eng. Progr.*, 45: 39 (1949).
9. R. C. Martinelli and D. B. Nelson, Prediction of Pressure Drop During Forced-Circulation Boiling of Water, *Trans. ASME*, 70: 696 (1948).
10. W. R. Gambill and H. W. Hoffman, Boiling Liquid-Metal Heat Transfer, Report 1737-61 presented at American Rocket Society Space-Nuclear Conference May 3–5, 1961, Oak Ridge National Laboratory.
11. L. Bernath, A Theory of Local-Boiling Burnout and Its Application to Existing Data, *Chem. Eng. Progr. Symp. Ser.*, 56: 95-116 (1360).
12. F. C. Gunther, Photographic Study of Surface-Boiling Heat Transfer to Water with Forced Convection, *Trans. ASME*, 73: 115-123 (February 1951).
13. P. Griffith, The Correlation of Nucleate Boiling Burnout Data, Technical Report No. 9, Report NP-6446, Massachusetts Institute of Technology, March 1957.
14. L. E. Gill, G. F. Hewitt, and J. W. Hitchon, Sampling Probe Studies of the Gas Core in Annular Two-Phase Flow, Part I. The Effect of Length on Phase and Velocity Distribution, *Chem. Eng. Sci.*, 18: 525-535 (1963).
15. J. G. Collier, Heat Transfer and Fluid Dynamic Research As Applied to Fog Cooled Power Reactors, Canadian Report CRARE-1108 (AECL-1631), June 1962.
16. E. D. Waters, J. K. Anderson, W. L. Thorne, and J. M. Batch, Experimental Observations of Upstream Boiling Burnout, USAEC Report HW-73902(Rev.), Hanford Atomic Products Operation, November 1962.
17. A. A. Bishop, L. E. Efferding, and L. S. Tong, A Review of Heat Transfer and Fluid Flow of Water in the Supercritical Region and During "Once-Thru" Operation, USAEC Report WCAP-2040, Westinghouse Electric Corp., Atomic Power Department, December 1962.
18. E. D. Waters, T. W. Ambrose, and M. E. Shockley, Heat Transfer Experiments for Out-of-Reactor Cooling of PRTR Fuel Elements by Transverse Air Flow, USAEC Report HW-72097(Rev.), Hanford Atomic Products Operation, December 1962.
19. R. P. Anderson, L. T. Bryant, J. C. Carter, and J. F. Marchaterre, Transient Analysis of Two-Phase Natural-Circulation Systems, USAEC Report ANL-6653, Argonne National Laboratory, December 1962.
20. N. Kattchee and W. C. Reynolds, Army Gas-Cooled Reactor Systems Program. HECTIC-II—An IBM 7090 Fortran Computer Program for Heat Transfer Analysis of Gas or Liquid Cooled Reactor Passages, USAEC Report IDO-28595, Aerojet-General Nucleonics, December 1962.

Section

III

Power Reactor Technology

Design Practice: The Carolinas-Virginia Tube Reactor

The Carolinas-Virginia Tube Reactor (CVTR)[1,2] is a power reactor designed to be a prototype of a full-scale plant. This reactor is heavy-water moderated and cooled, is fueled with UO_2, and employs the pressure-tube concept. As the only prototype of a heavy-water power reactor in the United States, the CVTR merits more attention than it might otherwise command on the basis of its rather modest power output. Utilizing a vertical U-tube design, it represents an approach to the pressure-tube concept which is quite different from that of the Canadian designs.[3]

The plant is located adjacent to the Parr Station of the South Carolina Electric & Gas Company and is about 25 miles northwest of Columbia, S. C. The reactor is a joint undertaking of the Carolinas Virginia Nuclear Power Associates, Inc.,* and the U. S. Atomic Energy Commission. The architect-engineer is Stone & Webster Engineering Corporation, and the reactor was designed by the Westinghouse Atomic Power Department. The steam generated is used in existing generating facilities at the Parr Station. The reactor is designed to transfer 56 Mw(t)† to the coolant for a net electrical output of 17 Mw(e). It was scheduled to begin power operation[4] in November 1963.

Basically the reactor consists of a tank of cool heavy water in which are suspended the internally insulated, U-shaped pressure tubes (see Fig. III-1). Each U tube contains two fuel-rod bundles, one in each leg of the U. The heavy-water coolant enters at the top of one leg of the U and leaves from the top of the other leg. The tank hangs in a cavity in the concrete biological shield and supports on its top a heavy base plate on which are mounted the supports for the pressure tubes and the control rods.

*Original members are as follows: The Carolina Power & Light Company, The Duke Power Company, The South Carolina Electric & Gas Company, and The Virginia Electric & Power Company.

†During initial operation the heat to the coolant will be limited to 44.3 Mw(t).

Fuel Elements

The basic fuel element is a full-core-length rod and is composed of pressed and sintered UO_2 pellets in a free-standing Zircaloy-4 jacket. The pellets are dished at both ends to allow for differential thermal expansion. The stack of pellets is restrained longitudinally in the tube by an Inconel spring. This spring is compressed between the upper end plug and an alumina spacer that is in contact with the uppermost fuel pellet. The fuel tube is evacuated during fabrication and back-filled with dry helium gas. One end plug contains a vent hole that is welded shut after the closure plug weld is made. The final fuel-tube inspection involves fully radiographing the welds. Each of the fuel rods (except the center one in the bundle) is wrapped with a Zircaloy-4 wire of 0.1125-in. diameter, to maintain spacing and promote coolant mixing. This wire is welded at each end to the upper and lower end plugs, and it is under tension.

Total number of fuel rods in core	1368
Fuel-rod length, in.	102.4

	Outer zone (see Fig. III-2)	Inner zone
UO_2 pellet enrichment, wt.% U^{235}	2.0	1.5
UO_2 pellet length, in.	0.636	0.530
Approximate number of pellets per rod	150	180
Approximate number of pellets in core	136,800	82,080

UO_2 pellet OD, in.	0.430 ± 0.0005	Outside diameter of fuel cladding, in.	0.4875 ± 0.0020
UO_2 pellet density, % of theoretical	93 ± 1.5	Cladding thickness, minimum, in.	0.0215
Pellet-jacket clearance, nominal, in.	0.007	Cladding material	Zircaloy-4
Length of UO_2 in each fuel rod, in.	95.4	Filling gas	Helium
		Void per rod in gaps between pellets and between rod and cladding, cu in.	0.66

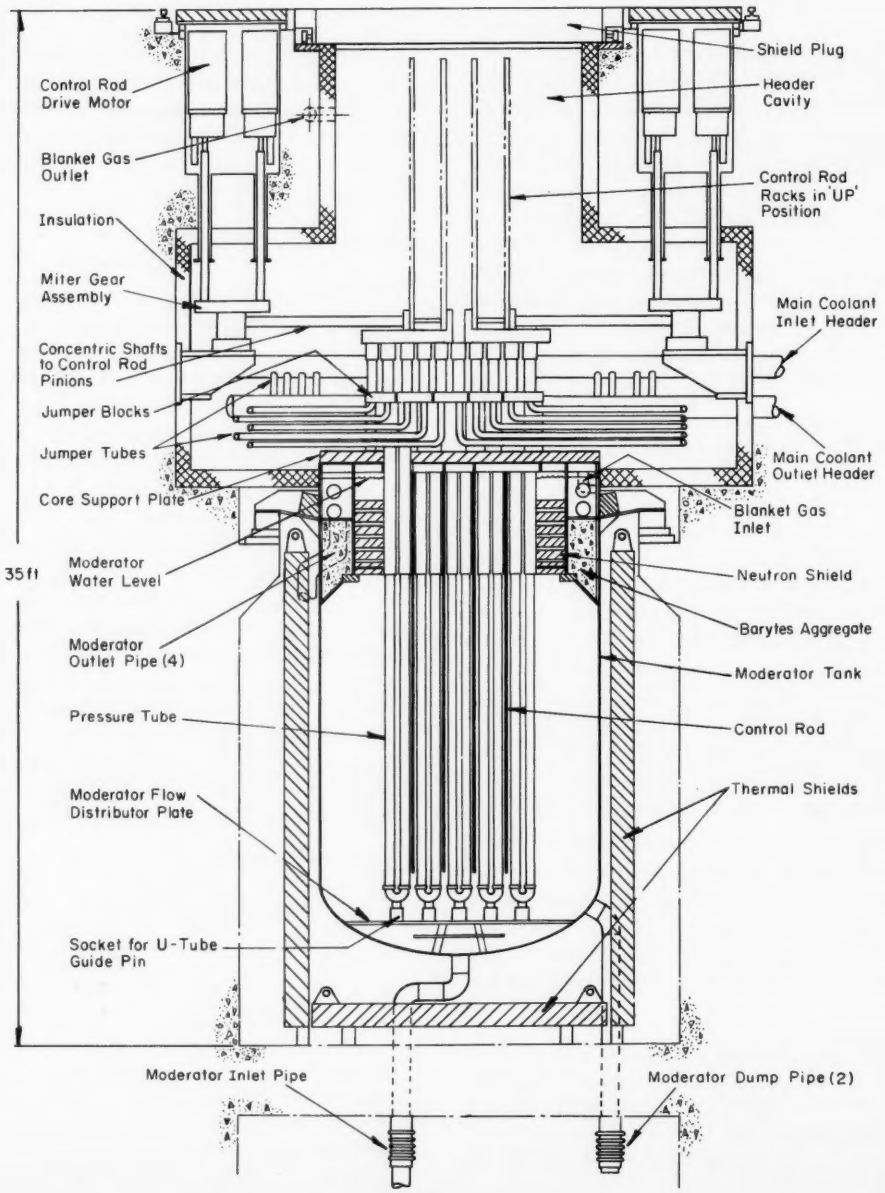

Fig. III-1 Elevation of the CVTR reactor.[2]

Fuel Assemblies

The fuel assembly, defined here as the assembly that is discarded with the spent fuel, consists of a bundle of 19 fuel rods, a hexagonal coolant-flow baffle that surrounds the bundle, a circular thermal baffle (called an inner thermal baffle) that surrounds the hexagonal flow baffle, and a set of six baffle strips that occupy the spaces between the flow baffle and the thermal baffle (Figs. III-3 and III-4). When the assembly is in use, it is surrounded by two additional thermal baffles. These are removed from the pressure tube along with the fuel assembly during refueling; however, they can be slipped off the old assembly and onto a new one in the spent-fuel basin for reuse. The purpose of the thermal baffle system is to prevent convection and to define a series of stagnant heavy-water annuli that serve as thermal insulation between the hot coolant within the pressure tube and the cool moderator outside.

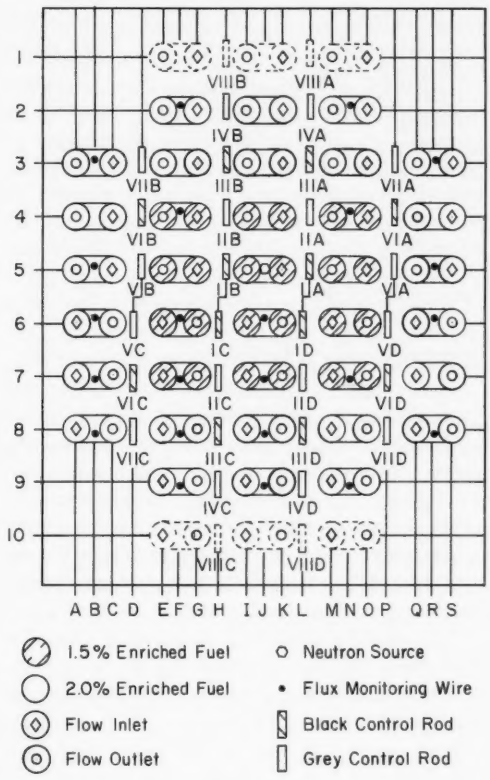

Fig. III-2 Core cross section.

The structure of the fuel assembly is indicated by Fig. III-4. All rods except the center one are wrapped with the Zircaloy-4 wire to ensure spacing and encourage mixing. The rods are positioned by a grid fastened to the flow baffle at the upper end of the bundle. A grid fastened to the lower end of the flow baffle retains the rods in the event one should break loose from the upper grid. The thermal baffles are dimpled to maintain the proper spacings and are filled with stagnant water. The bypassing of flow around the outside of the assembly is prevented by a ball-cone type seal at the point where the assembly is supported on a shoulder in the pressure-tube extension. Heavy water is admitted to the spaces between the thermal baffles through openings near the inlet ends of the assemblies (Fig. III-4), so that the inlet pressure

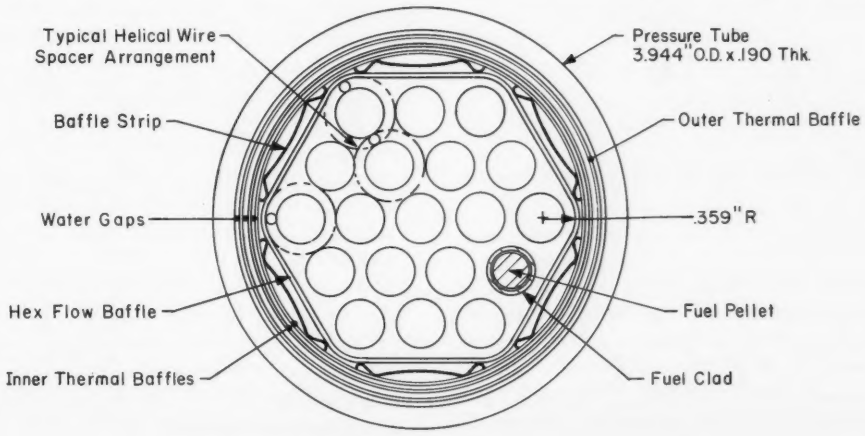

Fig. III-3 Primary-coolant-flow channel.[2]

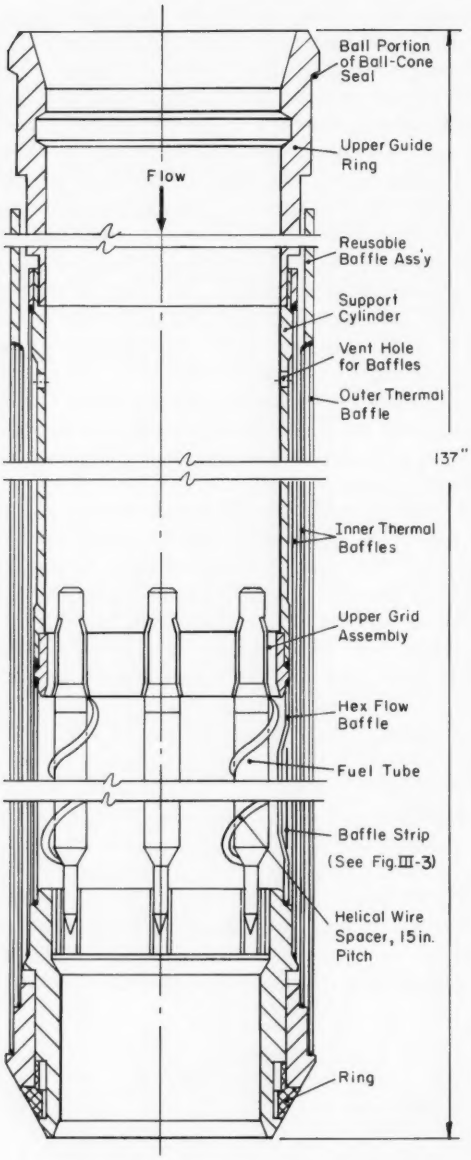

Fig. III-4 CVTR fuel assembly and inlet pressure tube.[2]

is exerted on the outside of the hexagonal flow baffle. This pressure deforms the baffle slightly at points downstream and causes it to bear upon the spacer wires of the fuel rods and to squeeze the fuel bundle tightly together. This feature requires that the stagnant spaces be vented differently in the assemblies that occupy the inlet and outlet legs of a U tube; therefore the inlet and outlet fuel assemblies are distinct and are not interchangeable.

Total number of fuel assemblies	72
Number of fuel rods per fuel assembly	19
Center-to-center distance between rods, in.	0.600
Fuel-rod lattice	Triangular
Structural material	Zircaloy-4
Flow-baffle thickness, in.	0.027
Thermal-convection barrier thicknesses	
Baffle strip, in.	0.009
Inner thermal baffles, in.	0.012
Outer thermal baffle, in.	0.020
Average thickness of stagnant water, in.	0.042
Overall length of fuel assembly (approximate), in.	137

Control Rods

Twenty-eight control rods of two types are provided, black and gray (see Fig. III-2). The rods are driven from the top of the reactor, and they scram by gravity. The black rods are boron stainless steel, whereas the gray rods are stainless steel perforated to obtain the desired reactivity worth. Both types are rectangular in cross section, with dimensions 1 by 4 in. The length, including the active absorber and a rack support member, is 220 in.; to this is attached the drive rack, which has a nominal length of 117 in.

Black absorber rods	
Number	12
Construction	Sandwich of two $^5/_{16}$-in.-thick plates of 1.5 wt.% boron S.S. bolted to a central $^3/_8$-in.-thick supporting member of type 304 S.S.
Weight, lb	260
Gray absorber rods	
Number	16
Construction	Single piece of type 304 S.S. perforated with holes
Weight, lb	224
Snubber	Helical springs backed by a series of rivets and a shear plate; latter to be used in case of failure of springs
Rack material	17-4 PH (1100°F)
Rack-supported-member material	Type 304 S.S.
Rod followers	None

Pressure Tubes

A pressure-tube assembly, shown schematically in Fig. III-5 and conceptually in Fig. III-6, consists principally of a U tube; two short, straight transition tubes; and a connector block. The U tube and the transition tubes penetrate the connector block, which contains internal flow passages between the transition tubes and the legs of the U tube. The transition tubes and connector block serve to connect the U-shaped pressure tube to a header system that distributes the primary coolant. It will be described later. Coolant enters the bottom of one transition tube and flows up the tube to the internal passage within the connector block. The coolant then flows through this horizontal passage and enters the inlet leg of the U tube, in which it flows downward. The flow direction is reversed at the bottom of the U tube, and the coolant then flows upward through the outlet leg of the tube. In the connector block the coolant flows horizontally through another internal passage that carries it to the outlet transition tube. The coolant flows down in the outlet transition tube to complete its passage through the pressure-tube assembly.

The height of the U-shaped pressure tube is 19 ft $3\frac{3}{8}$ in., and the centerline spacing of the legs is $5\frac{1}{2}$ in. The nominal tube diameter and wall thickness in the core region are given in Fig. III-3, and Fig. III-2 shows the relative locations of the tubes in the lattice arrangement. One fuel assembly is installed in each of the two legs of the pressure tube, as indicated in Fig. III-5, and a thermal baffle consisting of a U section and two short, straight, transition sections is located inside the pressure tube and beneath the fuel assemblies. Neutron streaming shields are provided in the pressure-tube legs above the fuel assemblies, and these spiral shields, which are connected by a shaft and heavy spring to the pressure-tube end closures, transmit a hold-down load to the fuel assemblies. Screw type end closures permit access to the pressure tubes for refueling and to the transition tubes for orifice installation or adjustment.

The portion of the pressure tube below the top neutron shield (see Fig. III-1) is made of Zircaloy-4, and the straight sections of the tube are fastened to the U bend by mechanical joints to avoid the problem of hydride embrittlement caused by weld zones. The upper portion of the pressure tube, which is outside the core and reflector regions, is type 403 stainless steel. The dissimilar-metal, upper and lower portions of the pressure tube are connected by a mechanical transition joint that utilizes a Marman Conoseal gasket. The joint, shown in detail on Fig. III-5, is held together by a preloaded Inconel sleeve that is welded to the stainless-steel portion of the pressure tube.

The maximum allowable stress in the Zircaloy-4 portions of the pressure tubes is 18,000 psi, or one-third of the minimum expected ultimate tensile strength of the material. This limiting criterion was determined in accordance with Appendix Q to Sec. VIII of the *ASME Boiler and Pressure Vessel Code*, as modified by the rulings of the ASME Code Committee in Code Case 1205-3. The design pressure of the tubes is based on paragraph UG-125(c) of the Code. The specified nominal wall thickness is the sum of the thickness calculated by the expression given in paragraph UG-27 of the Code plus allowances for corrosion and manufacturing tolerance. The predicted "worst case" of sustained abnormal operation of the tubes results in stresses that do not exceed the limits imposed by the Code, as interpreted under Case 1273-N.

Number of pressure tubes	36
Length of pressure tube, ft-in.	19-$3\frac{3}{8}$
Pressure-tube thermal-convection-barrier details	Inner sleeve of U-bend baffle is type 304 S.S.; inner sleeve of transition baffle is Inconel; outer two sleeves of each baffle assembly are Zircaloy-4; stagnant-water gap thickness = 0.060 in.; upper portion of pressure tube is insulated by an evacuated 304 S.S. shroud
Method of support	Weight of pressure tube is supported on studs located at upper end of pressure tube
Design pressure, psig	1746
Design temperature, °F	250
Maximum allowable hoop stress (design), psi	18,000
Wall thickness (nominal), in.	0.190
Corrosion allowance (hydride), in.	0.0035
Manufacturing tolerance, in.	± 0.006

Pressure-tube materials

Zircaloy-4	All pressure tube parts in the core region except the inner transition baffle, inner U-bend baffle, and U-bend clamp nut and bolt	Type 403 S.S.	All parts of the upper portion of the pressure tube except the transition joint sleeve, shroud tube, shield blocks, and transition joint gasket
Type 304 S.S.	Inner U-bend baffle, shroud tube, and shield blocks	Inconel	Inner transition baffle, U-bend clamp nut and bolt, and transition joint sleeve
Type 321 S.S.	Conoseal transition joint gasket		

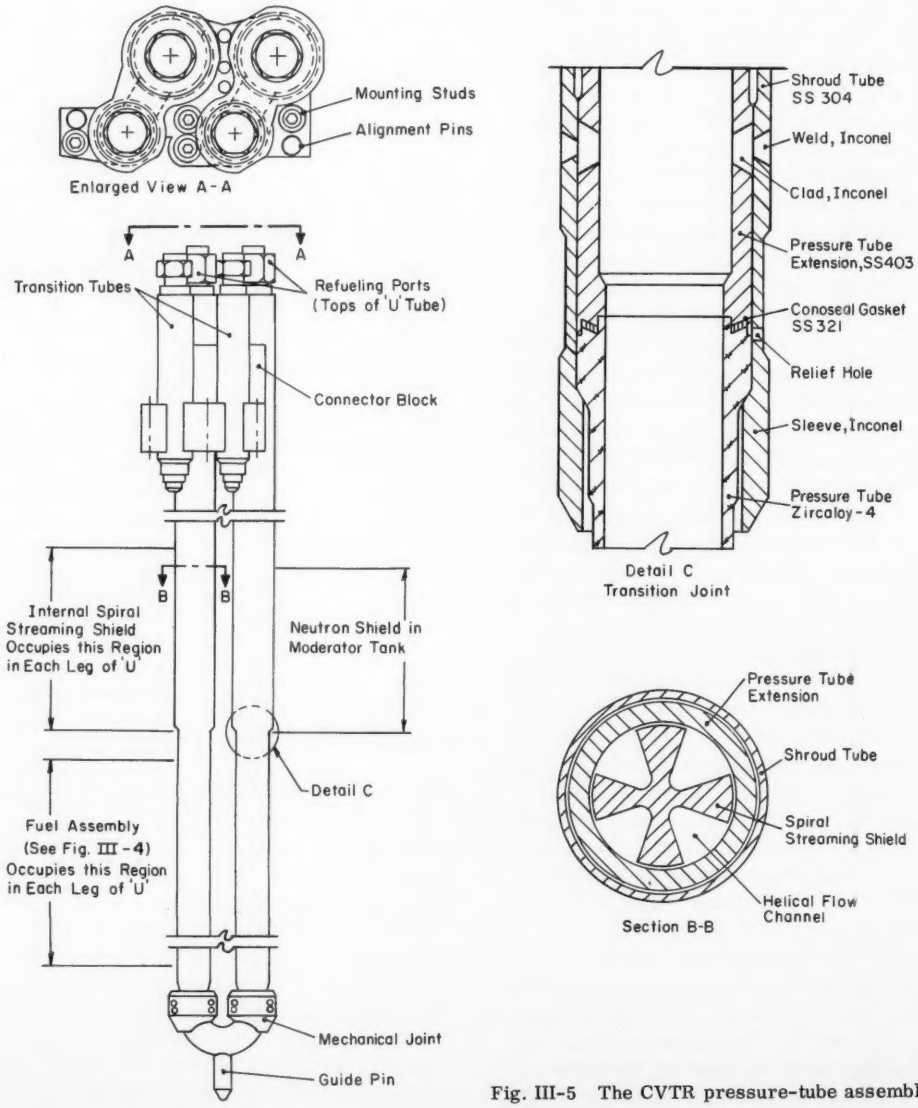

Fig. III-5 The CVTR pressure-tube assembly.

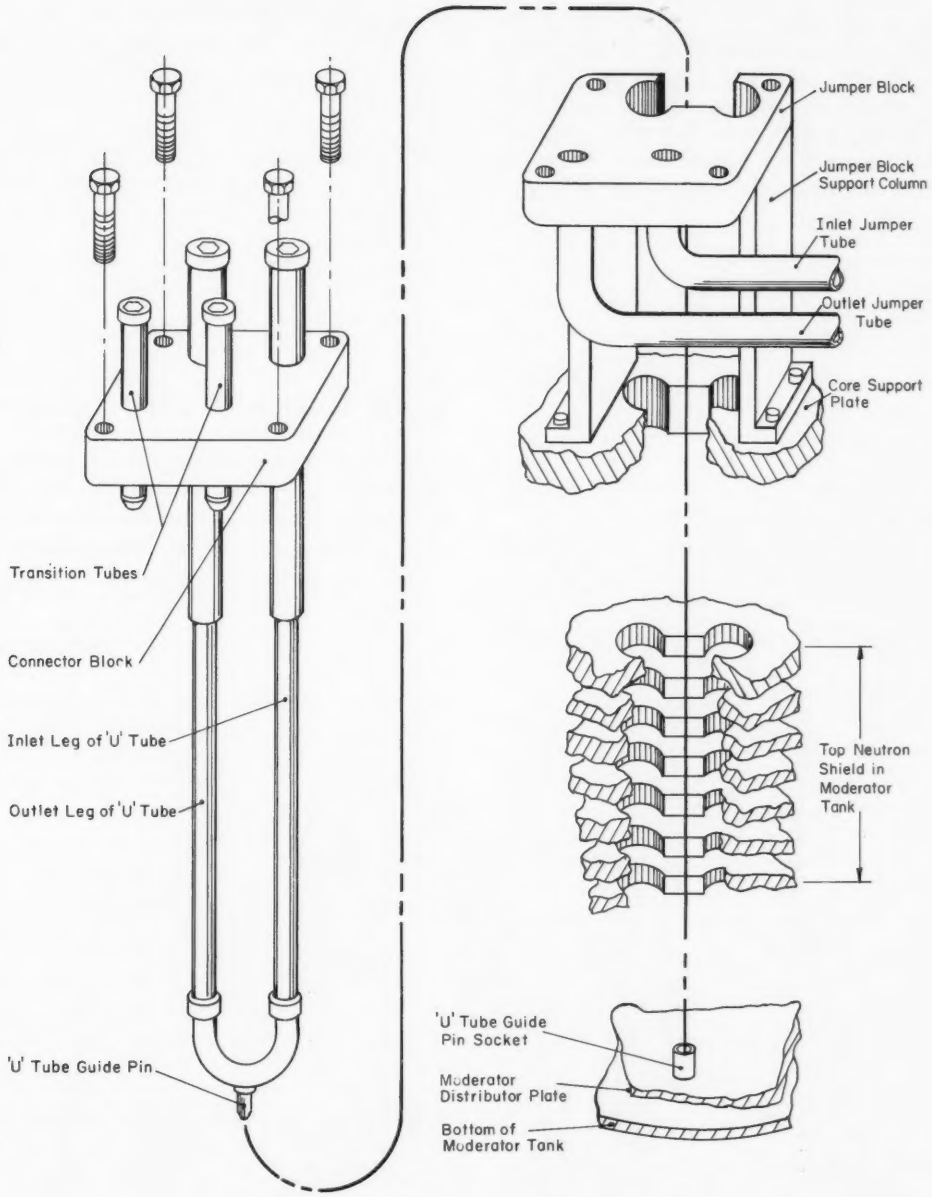

Fig. III-6 The CVTR core structure concept.

Moderator Tank

The moderator tank, shown in Fig. III-1, is an upright cylindrical vessel that contains heavy water. Moderator piping connections to the tank consist of a single supply pipe at the bottom, four peripheral outlet pipes near the top, and two dump lines near the bottom. A neutron shield, formed by alternate layers of steel and heavy water, occupies the top region of the tank, and a moderator distributor plate with sockets for the U-tube guide pins is located near the bottom. A core support plate is attached to the top of the tank, and support pads transfer all loads placed on the tank to the concrete biological shield. Radiolytic gases released from the

surface of the heavy water at the top of the moderator tank are removed by a blanket gas system. Helium enters the moderator tank at its top, sweeps the surface of the heavy water, passes through penetrations in the core support structure to enter the header cavity shown in Fig. III-1, and leaves the cavity through an outlet pipe near its top.

Moderator tank	
Diameter, in.	111
Height, in.	$190\frac{5}{8}$
Geometry and material	Upright cylindrical vessel with ellipsoidal lower head; type 304 S.S.
Wall thickness	
Side, in.	$\frac{3}{16}$
Lower head, in.	$\frac{5}{8}$
Design pressure, psig	12
Design temperature, °F	250
Moderator flow rate, gal/min	1250
Inlet temperature, °F	130
Outlet temperature, °F	180

Tank penetrations

	Number	Size, in.
Pressure relief	4	3
Drain to emergency coolant injection system	2	8
Inlet	1	6
Outlet	4	6

Core Support Structure

The basic member of the core support structure is the core support plate, a disk of type 405 stainless steel with a diameter of 106 in. and a thickness of 5.5 in. The horizontal plate

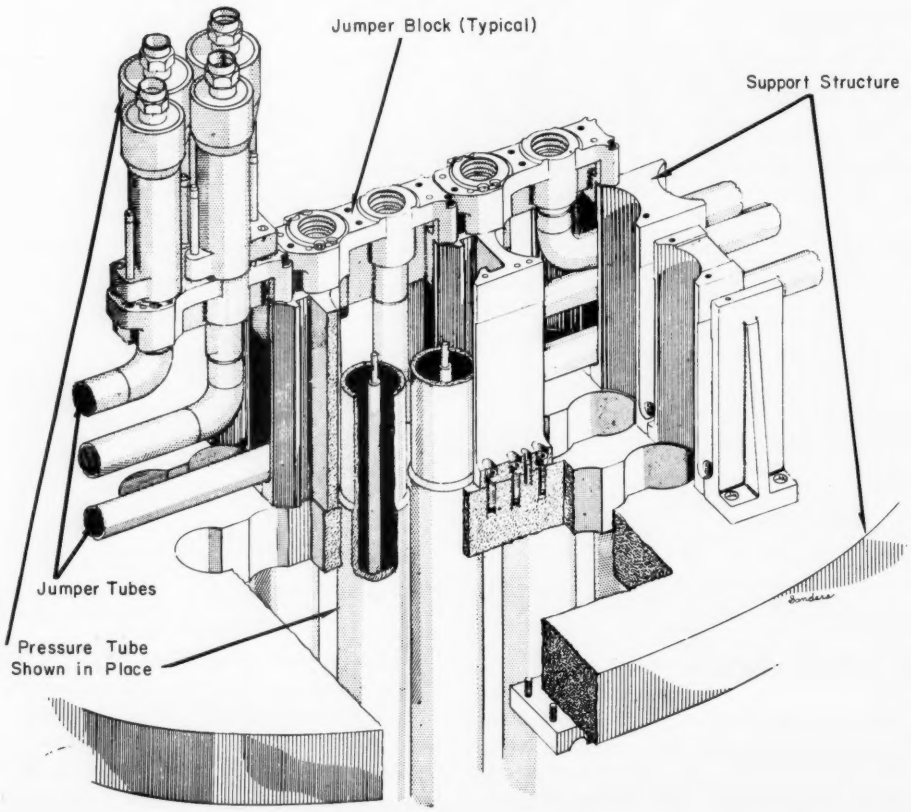

Fig. III-7 Perspective view of the core support.

is provided with vertical holes through which pressure tubes and control rods pass, and vertical support columns (type 405 stainless steel) are bolted to its upper surface. The columns locate and support jumper blocks, which in turn support the pressure-tube assemblies near their tops, as shown conceptually in Fig. III-6. A perspective view of the actual core support structure is given in Fig. III-7. Radial positioning and restraint of the bottoms of the pressure-tube assemblies are accomplished by a pin-and-socket arrangement, with the pin attached to the tube and the socket affixed to the moderator distributor plate. Control-rod pinions are mounted atop the pressure-tube assemblies, and those jumper block support columns situated at control-rod positions are shaped to provide vertical slots for passage and guidance of the rods.

Header and Jumper Assembly

The header and jumper assembly, illustrated by Fig. III-8, provides heavy-water flow channels that connect the primary coolant loop to the individual pressure-tube assemblies. Four headers are arranged in pairs, one inlet and one outlet header being located on each of two opposite sides of the header cavity indicated in Fig. III-1. Jumper tubes, which are welded into the headers, extend to positions over the reactor core and are welded into the bottoms of jumper blocks. Each jumper block is connected to one inlet and one outlet jumper tube, as shown in Figs. III-6 and III-7, and vertical ports in the block form extensions to the inlet and outlet flow channels provided by the jumper tubes. When a pressure-tube assembly is installed, its connector block mates with a jumper block in such a fashion that Conoseal joints are formed between the inlet port of the jumper block and the inlet transition tube of the pressure-tube assembly and between the outlet port and the outlet transition tube. Thus primary coolant is supplied to and taken from each pressure-tube assembly; the route of the coolant through the pressure-tube assembly is described earlier in the subsection on pressure tubes.

Headers	
Number	4 (2 inlet and 2 outlet)
Material	Type 316 S.S.
Diameter, in.	8
Wall thickness (minimum), in.	0.48
Jumper tubes	
Number	21 per header*
Material	Schedule 40S type 316 S.S.
Diameter, in.	2
Jumper blocks	
Material	Type 403 forged S.S. clad with type 316 S.S. at jumper tube end to facilitate welding
Header and jumper design conditions	
Pressure, psia	1730
Temperature, °F	600
Code	ASA Code for Pressure Piping B31.1, 1955
Insulation	None; header-cavity walls are insulated

Fuel and Control Program

The CVTR is a power demonstration prototype reactor, and it is anticipated that it will be operated for a period of five years for an equivalent of 30,000 full-power hours (EFPH) at 17 Mw(e) net. The initial core will operate about 8500 EFPH, and the remaining 21,500 EFPH will involve cyclic addition of fuel.

Initial core burnup (average), Mwd/metric ton of U	8404
Core burnup over five-year life (average), Mwd/metric ton of U	13,400
Maximum fuel burnup, Mwd/metric ton of U	40,000
Gray rods	Used for regulating rods on first core and for regulating rods and shim rods on cycled core
Black rods	Used for shim rods on first core, but not used on cycled core for shim purposes

*This is sufficient for 42 pressure tubes. Although the CVTR as built contains 36 pressure tubes, some of the components have been designed for additional pressure tubes.

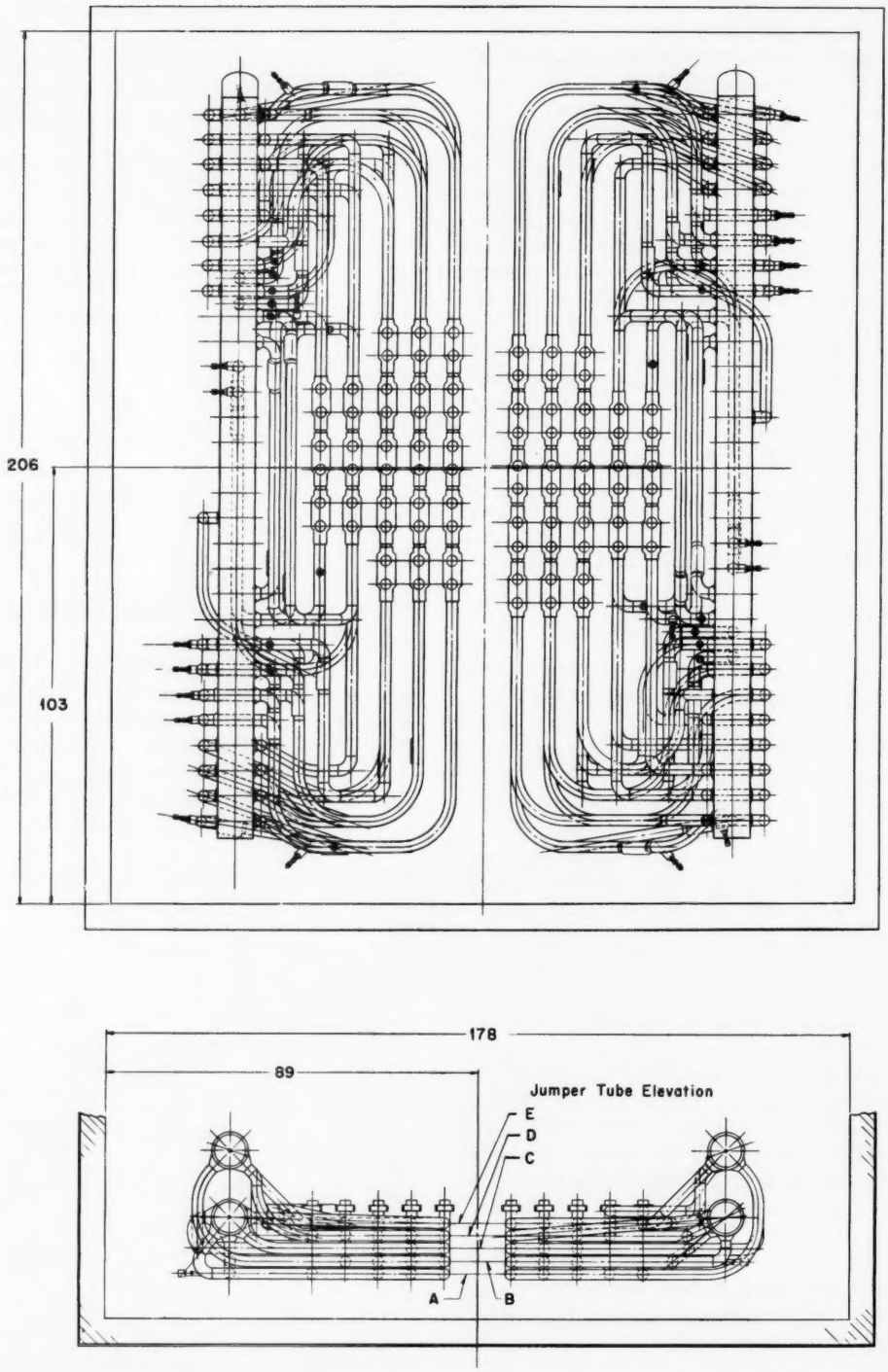

Fig. III-8 Upper header details.[2]

Control-rod programming	Symmetrical withdrawal sequence (Fig. III-2) is: I, IV, VII, II, V; at this point black rod VI or III is exchanged for gray rods IV, VII, II, and V, and the withdrawal sequence II, VII, IV, V is followed

Thermal and Hydraulic Data (Initial Core of 36 Pressure Tubes)

Heat output, Mw(t)	
Heat output from fuel rods	44.3
Heat output to steam generator	41.0
Convective heat loss to moderator	3.0
Heat loss from piping (approximate)	0.3
Heat generated by neutrons and gammas in moderator	2.9
Gross heat release from fission	47.2
Maximum power, %	125
Coolant flow	
Total coolant rate, lb/hr	3.3×10^6
Average flow per tube, lb/hr	9.17×10^4
Maximum flow per hot tube, lb/hr	10.5×10^4
Velocity in hot tube, ft/sec	26.6
Pressure, psia	
System pressure, nominal (outlet of core)	1500
System pressure, maximum (outlet of core)	1550
System pressure, minimum (outlet of core)	1450
System pressure, design	1730
Pressure drop across U tube*	82 ± 3
Pressure drop through fuel assemblies in U tube, psi	47 ± 2
Heat transfer	
Active core surface area, sq ft	1387
Average flux, Btu/(hr)(sq ft)	1.09×10^5
Nominal steady-state maximum flux, Btu/(hr)(sq ft)	3.74×10^5
Average film coefficient in maximum power tube, Btu/(hr)(sq ft)(°F)	10.2×10^3
Maximum flux (125% power), Btu/(hr)(sq ft)	4.69×10^5

*Pressure drop across jumper tubes is not included. Value given is from jumper block inlet fitting to jumper block outlet fitting, inclusive.

Instrument errors, °F	
Reactor inlet temperature	2.5
Outlet pressure-tube temperature	2.5
Burnout (DNB)	
Minimum DNB ratio	
At 100% power	2.44
At 125% power	1.65
Hot-channel factors	
(F_R) heat flux, radial nuclear	1.7
(F_Z) heat flux, axial nuclear	1.5
(G_0) heat flux, maximum to average rod in cluster, nuclear	1.25
(F_q^E) heat flux, engineering	1.08
(F_q^T) heat flux, total	3.44
(F_H^E) enthalpy rise, engineering	1.08
(F_H^N) enthalpy rise, nuclear	1.2
(F_H^T) enthalpy rise, total	1.30
Temperature, °F	
Moderator average	155
Moderator inlet	130
Moderator average rise	50
Coolant average in core	523.1
Coolant inlet to pressure tubes	505
Coolant discharge from pressure tubes (average)	541.2
Coolant average rise in core	36.2
Fuel-rod surface, max.	589
Coolant, outlet of hot channel (at 125% power)	574
Saturation temperature, 1450 psia	589.5
Fuel rod	
Maximum nominal steady-state thermal output, kw/ft	14.0
Average nominal steady-state thermal output, kw/ft	4.07
Maximum transient thermal output at 125% power, kw/ft	17.5
Enthalpies, Btu/lb	
Coolant inlet	479
Coolant discharge from pressure tube (average)	522.6
Coolant average rise in core	42.7
Coolant rise in maximum power tube	63.4
Saturation enthalpy, 1450 psia	586.4
Outlet hot channel (at 125% power)	554.5

Reactor Instrumentation and Control

Figure III-9 is a block diagram of the nuclear instrumentation. Note that it differs from the diagram published in *Power Reactor Technology*, 5(2): 62, which was taken from the preliminary hazards summary report. The neutron detectors (Table III-1) are located in the air space outside the reactor thermal shields (Fig.

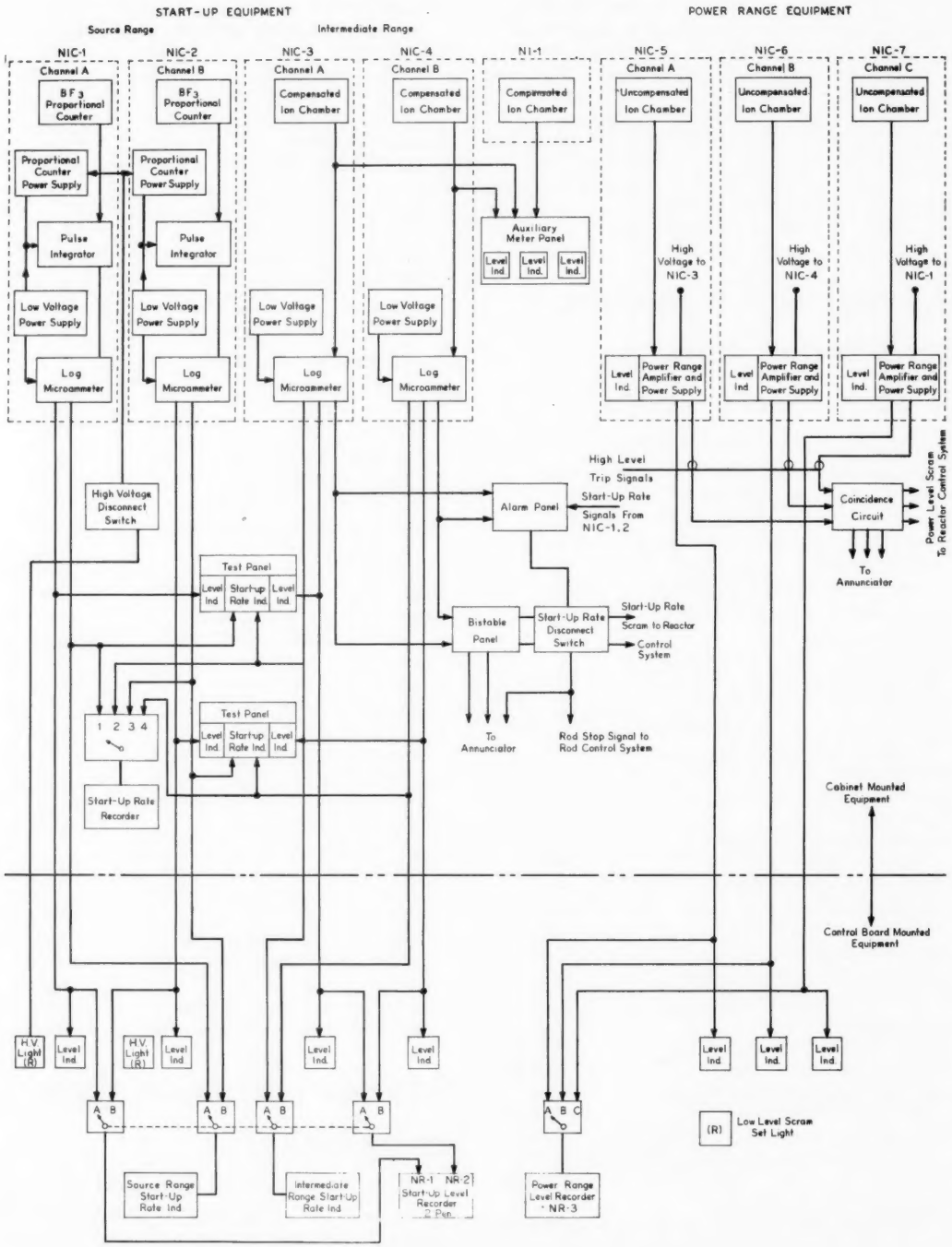

Fig. III-9 CVTR instrumentation block diagram.[2]

Table III-1 NEUTRON DETECTORS

Application	Type	No. of channels	Approx. range, nv	Minimum sensitivity
Startup range	BF_3 proportional	2	8×10^{-2} to 8×10^{3}	13 cps/nv (neutrons)
Intermediate range	Compensated ion chamber	2 protective and readout; 1 readout only; 1 spare	2.5×10^{2} to 2.5×10^{10}	4×10^{-14} amp/nv (neutrons); 3×10^{-13} (amp)(hr)/r (gamma)
Power range	Uncompensated ion chamber	3; 1 spare	2.5×10^{4} to 2.5×10^{10} (100% power shall not exceed 8×10^{9})	4.4×10^{14} amp/nv (neutrons); 5×10^{-11} (amp)(hr)/r (gamma)

III-1) in individual polyethylene containers. These detectors are spaced around the reactor at about 120° intervals and are positioned at different elevations above and below the center of the core. Each position contains one intermediate- and one power-range detector, whereas the source-range detectors are located at only two positions.

A polonium-beryllium neutron source of about 100 curies is located in core position J-5 (Fig. III-2) about 15 ft above the bottom of the fuel.

The reactor is equipped with a failed fuel-element detection and location system. A sample is taken continuously from the primary coolant line at the suction side of the main coolant pumps. It is monitored for fission-product iodine and returned to a low-pressure surge tank. Upon indication of a failed fuel element, the sampling procedure is changed to sample the effluent coolant from each pressure tube.

Control-rod drive

The power unit is a 230-volt d-c servometer with gearing, a magnetic clutch, a potentiometer for transmitting rod-position signal, a tachometer, and a hydraulic dashpot. This power unit is connected to the control-rod-drive rack by horizontal and vertical shafting, a miter-gear unit and a drive pinion (Fig. III-1). Two control rods are driven through concentric horizontal shaft extensions, as shown in Fig. III-1, to conserve space above the core. Scram is accomplished by interrupting current to the magnetic-clutch assembly. Rod-position accuracy is ±0.5% of full travel.

Scram time criterion	Minimum of −3.5% dk/k within 2.0 sec following detection of low flow
Measured drop time to dashpot upper limit, sec	0.82 to 0.92

Control requirements, % dk/k, first core	
Cold to hot	2.7
Fuel Doppler broadening	2.0
Xe and Sm poisoning	4.3
Burnup	18.9
Moderator isotopic degrading reserve (2% H_2O)	1.0
Shutdown margin (k = 0.95)	5.0
Total	33.9

Scram signals

- Low primary coolant flow rate (can be manually bypassed below 15% nuclear power)
- Low primary-coolant-system pressure (can be manually bypassed below 15% nuclear power)
- High primary coolant temperature
- Low pressurizer level
- Low pressurizer pressure
- Trip-out of any primary coolant pump breaker resulting in less than full-speed operation of both pumps (can be manually bypassed below 15% nuclear power to allow continued operation with a minimum of half-speed capability with one pump)
- High nuclear power level
- High startup rate, below 15% nuclear power
- High radioactivity in the condenser air ejector
- Low ratio of nuclear power to steam-generator power
- Manual scram
- High pressure differential between pressurizer and primary system
- Turbine trip

Primary Coolant Circuit

The major components of the primary coolant system, shown in Fig. III-10, are the steam generator, two primary coolant pumps, the pressure tubes, and the associated piping and valves. Pressurization is accomplished by the vapori-

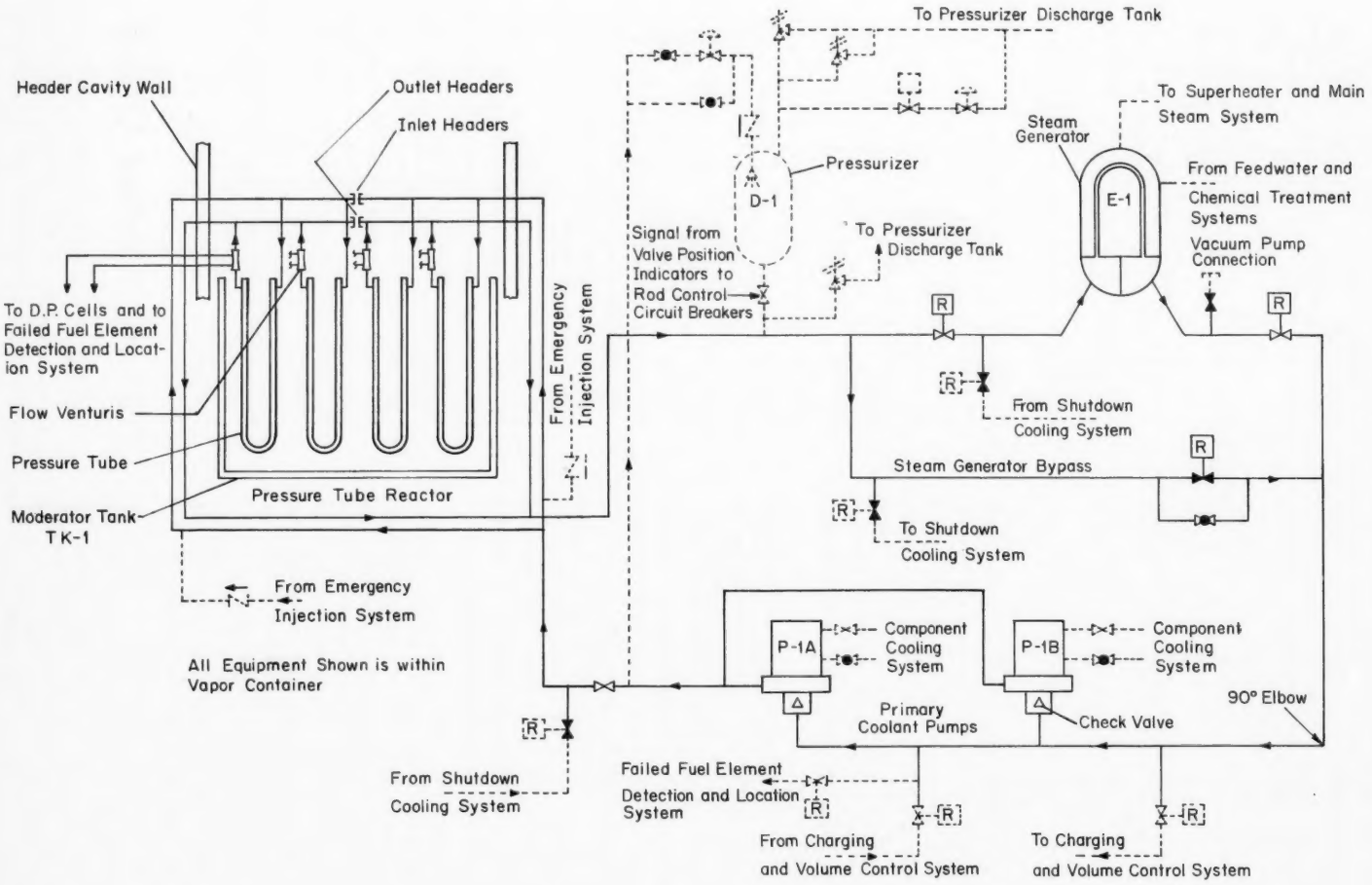

Fig. III-10 Primary coolant system.[2]

zation of heavy water with electric heaters. The system is designed for an internal pressure of 1730 psia and a temperature of 600°F.

Number of independent loops	1
Number of steam generators	1
Number of pumps	2
Circulation rate (total) and head	3.3×10^6 lb/hr (3810 gal/min) at 450 ft

Pumps

Single stage, canned-motor, centrifugal, operated in parallel; vertical mounted with side discharge; two-speed (3520/1760 rpm); one pump operated by motor-generator set, with flywheel, to provide coastdown energy; materials in contact with coolant are austenitic stainless steels except for Hastelloy stator pressure cans, Inconel rotor cans, and graphitar bearings; pump volutes and casings designed for 1865 psig

Piping

Type 316 stainless steel; 10-in.-diameter Schedule 80 pipe used for full flow lines and 8-in.-diameter Schedule 80S used when flow is split adjacent to pumps; steam-generator bypass is 4-in.-diameter Schedule 80S; all fittings are forged type 316 stainless steel

Isolation valves

Number	Size and operation	Purpose
2	10 in., motor	Isolate steam generator
1	4 in., motor	Steam-generator bypass
1	10 in., manual	Closed for maintenance purposes

Steam generator (Fig. III-11)

Geometry	Vertical shell-and tube type; primary coolant inside tubes; light water boiled in shell side
Duty, Btu/hr	191.1×10^6
Materials	Tube sheet is carbon steel clad with stainless steel; tubes are Inconel, ½ in. in outside diameter with 0.042-in. walls; primary head is carbon steel clad with stainless steel; shell-side materials are carbon steel
Shell-side design conditions	985 psig and 600°F; designed in accordance with *ASME Boiler and Pressure Vessel Code*, Sec. VIII, paragraph U-1-e, Case Interpretations 1270N and 1273N
Heatup and cooldown rate, °F/hr	250

Pressurizer

Geometry	Cylindrical vessel with long axis vertical; internal volume = 95 cu ft; normal liquid volume = 40 cu ft
Materials	Carbon steel (ASTM-A-212 grade B) cladding on all surfaces with type 304 S.S.

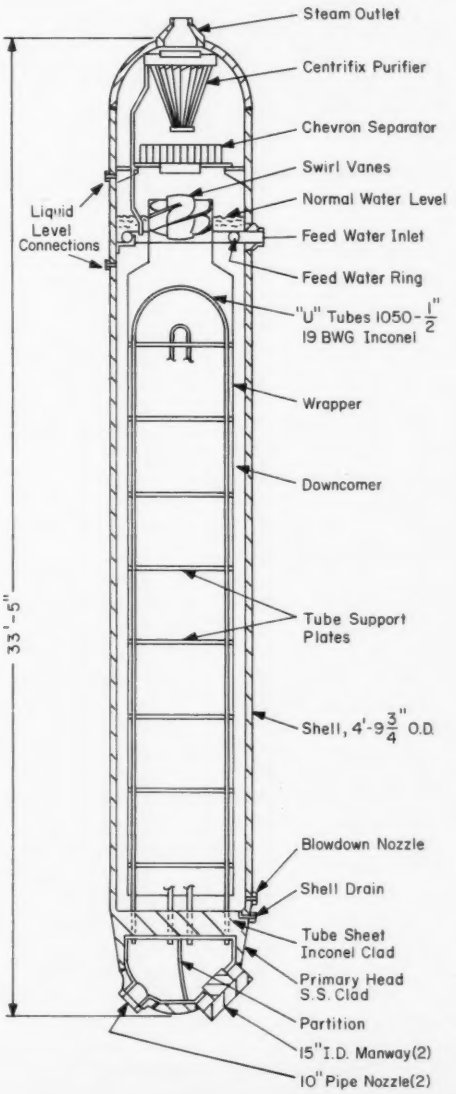

Fig. III-11 Elevation of the steam generator.

Electric heater details	Five banks of heaters of 32 kw each; one bank controlled by pressure and four banks manually controlled ON-OFF; all heaters cut off on low-water level signal

Safety and relief valves

No.	Type	Lift pressure	Capacity
1	Safety, spring loaded	1730 psia	12,000 lb/hr at 1780 psia
1	Safety, spring loaded	1780 psia	12,000 lb/hr at 1780 psia
1	Air-operated relief	1630 psia	9000 lb/hr

Spray system details	Takes water from cold leg of primary coolant circuit; ON-OFF regulation by automatic pressure-control valve sensing pressure in pressurizer
Design basis for pressurizer	1730 psia at 650°F; designed in accordance with *ASME Boiler and Pressure Vessel Code*, 1959 edition, and with Interpretation 1270N and 1273N
Primary coolant purification system	
Water specifications	
Conductivity in absence of Li*	0.5 μmho/cm or less
Dissolved D_2	~25 cm^3 STP/kg
Dissolved O_2	0.1 ppm or less
Chloride	0.1 ppm or less
H_2O	Less than 2 mole %
Total solids	5.0 ppm or less
Nominal flow to ion exchanger, lb/hr	2740
Ion bed composition	Deuterized mixed-bed, organic ion-exchange resin; 5 cu ft
Additives	D_2 gas is added to the primary coolant in the low-pressure surge tank to maintain the dissolved D_2 concentration
Design basis for purification system	Corrosion rates of 5 mg/(dm^2)(month) for type 316 S.S., Zircaloy-4, and Inconel; 10 mg/(dm^2)(month) for type 403 S.S.; 1% failed fuel elements

*The CVTR can be operated with either neutral or alkaline water. If alkaline water is used, LiOD will be added as required and a lithium-based resin will be used in the purification system.

Emergency Injection System

The emergency injection system consists of the following components: an emergency injection pump connecting a moderator overflow tank with the reactor coolant inlet headers by means of a primary injection line; a secondary injection line to the suction side of the primary coolant pumps; a moderator dump line from the moderator tank to the moderator overflow tank; two drain lines from the reactor cavity to a sump and two sump pumps to transfer water to the moderator overflow tank; and associated fill, test, vent, and drain lines. Operation of the emergency system is initiated by any of the following conditions: low level in pressurizer, low pressure in the hot leg of the primary loop, high differential pressure between the pressurizer and the hot-leg piping, and manual initiation. The emergency injection signal scrams the reactor, dumps the moderator to the moderator overflow tank, starts the emergency injection pump, completes the electrical circuits to the sump pumps, and operates various valves to bring the system into operation. The emergency injection pump is a horizontal, multistage centrifugal pump equipped with a special fast-starting motor with high-torque low-inertia characteristics.

Fuel Handling

For replacing or shuffling fuel, the fuel assemblies can either be removed from the pressure tubes or a pressure tube containing fuel can be moved or replaced as a unit. The presently envisaged refueling scheme calls for removal of fuel assemblies from the pressure tubes *in situ*: when empty, the pressure-tube assemblies are removed from the reactor and are replaced with preloaded assemblies.

Method of entrance to core

A portion of the shield over the header cavity consists of a rotating plug designed to provide access to any pressure tube. The pressure-tube refueling

port is closed by a threaded cap that holds down a flange sealed with a Conoseal gasket.

Refueling machine

The refueling machine is designed to remove fuel assemblies from the pressure tubes and transfer these to the spent-fuel basin, remove empty pressure tubes and pressure tubes containing fuel and replace same, and reposition pressure tubes containing fuel within the reactor. The machine is a lead-shielded cask equipped with cooling and hoisting apparatus and mounted on a crane type vehicle. Decay heat is transferred to light water circulating through a heat exchanger. The refueling machine can also handle control rods and neutron streaming plugs from within the pressure tubes.

Fuel transfer mechanism

This mechanism is an underwater conveyor working through a gate valve located between the pools in the containment building and the spent-fuel buildings. The device can handle fuel assemblies, pressure tubes, control rods, and neutron streaming plugs.

Plant Details

The nuclear plant produces 201,000 lb/hr of saturated steam at 605 psia with a maximum moisture of 0.25%. This is superheated in an oil-fired superheater to a temperature of 735°F and is used in an existing turbine with throttle conditions of 400 psig and 725°F. This turbine, installed in 1929, is one of three owned by the South Carolina Electric & Gas Company (SCE&GCO) as part of an existing pulverized-coal-fired steam plant with a nameplate capacity of 72,500 kw. The Parr Hydroelectric Plant, also owned by SCE&GCO, is located adjacent to the CVTR plant site and has a capacity of 15,000 kw. The nuclear plant, which consists of the containment building, the service building, the spent-fuel building, and an auxiliary building, is located southeast of the conventional steam plant and northeast of the hydroelectric plant. The oil-fired superheater is located in the yard of the nuclear plant and is a new piece of equipment.

Containment (Fig. III-12)

The vapor container is a right vertical cylindrical structure with a flat base and a hemispherical dome. It is located about 400 ft from the steam plant and 570 ft from the hydro plant and is a steel-lined reinforced concrete structure.

Inside diameter	58 ft 0 in.
Height, inside, clear	114 ft 3 in.
Excavation depth	59 ft 3 in.
Cylindrical section	
Liner	$\frac{1}{4}$-in.-thick steel plate (ASTM A-285 grade C Fbx)
Concrete	2 ft 0 in. thick
Dome	
Liner	$\frac{1}{2}$-in.-thick steel plate (ASTM A-285 grade C Fbx)
Concrete	$20\frac{1}{2}$ in. thick
Net free volume	243,100 cu ft
Foundation slab thickness	5 ft 9 in.
Design pressure	21 psig
Design leak rate	0.1% of the contained volume in 24 hr

Basis for design pressure

The maximum credible accident postulates the following: a nuclear excursion takes place which releases 10^6 Btu; a zirconium-water reaction goes to 35% completion; preaccident internal temperature of containment building is 120°F; and the primary coolant inventory is 14,605 lb of D_2O.

Pneumatic test pressure (maximum) is 26.25 psig.

Leakage rate at 22.5 psig is less than 0.075% of the contained volume per 24 hr.

Missile protection

The high-pressure primary coolant piping employs seamless pipe with all-welded construction; the pressure tubes and jumper tubes are enclosed in a concrete header cavity; the containment building itself affords missile protection.

D_2O removal

The containment building is the final barrier for any D_2O vapor arising from leakage from the primary coolant and moderator systems. The D_2O removal system is designed to recover 1 lb of heavy water per hour during normal closed vapor-container operation. This is done with silica gel desiccant bed type dryers operating on a batch basis. The average dew point in the vapor container is not more than −1°F. Personnel are excluded from the vapor container during operation and following shutdown until the containment-building atmosphere is purged of D_2O and tritium.

Iodine removal

Iodine in the vapor-container atmosphere can result from operation with defective fuel rods and a leaking primary coolant system. The iodine filters are activated-charcoal filter beds preceded by an absolute filter and a prefilter. The iodine filters are designed to process 1000 cfm of air, removing the gaseous iodine, whereas the absolute filters remove the particulate iodine. Incorporated in this system is the vapor-container atmosphere heating and cooling system. The heating load is 250,000 Btu/hr, and the cooling load is 650,000 Btu/hr.

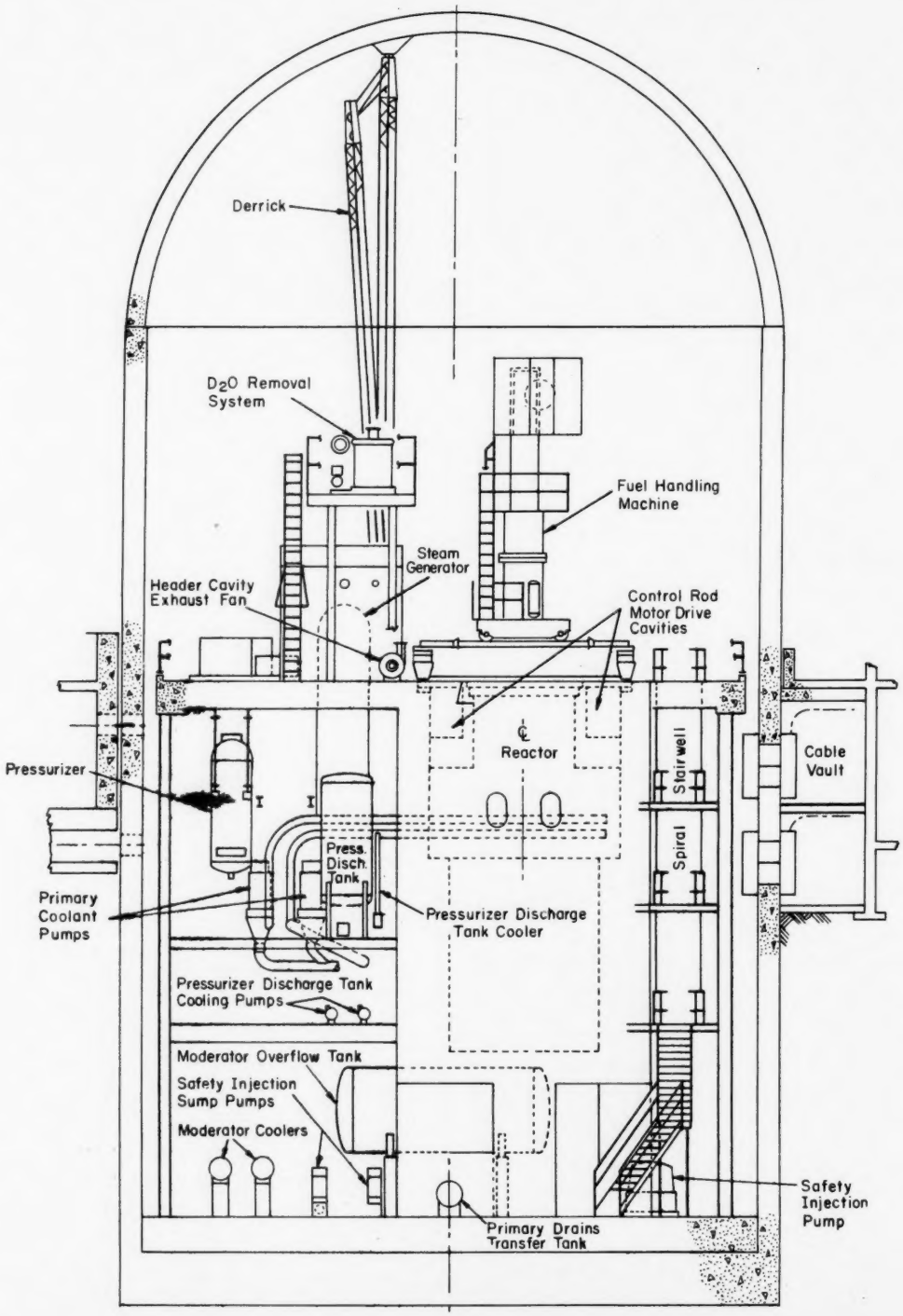

Fig. III-12 Elevation of the CVTR containment building.[2]

Containment penetrations

Number	Size	Use	Seal type
105	Various	Electrical penetrations	Mechanical
73	Various	Piping penetrations	Weld
2	18 in.	Ventilating	Weld
1	18 in.	Spent-fuel chute	Weld
1	13 ft 1 in.	Equipment hatch	Gasket
1	7 ft 1 in.	Personnel hatch	Gasket
1	3 ft 6 in.	Escape hatch	Gasket

Shielding

The CVTR shielding consists of the primary and secondary biological shields. The primary shield is a reinforced-concrete structure surrounding the reactor and thermal shields and is supported by four reinforced-concrete columns. It is designed to reduce the gamma dose rate to 1 r/hr at its outer surface with the reactor at 64.9 Mw(t). The lower half of the shield has a concrete thickness of 4 ft 9 in., whereas the upper half has a radial thickness of at least 4 ft 9 in. and forms a transition section between the cylindrical lower portion and the rectangular header cavity shield. The secondary shield consists of the concrete surrounding the vapor container and the 2.5-ft-thick concrete operating floor. The secondary shield serves to reduce the gamma dose rate to less than 2 mr/hr above ground outside the containment building.

Plant Control

Gray rods are moved to match the reactor power to the power withdrawn from the steam generator and to maintain the core inlet temperature at a given value. Reactor power output is represented for control purposes by the difference between the measured core outlet temperature and a set core inlet temperature. Power delivered by the steam generator is determined by the measured steam flow and feedwater temperature. The two signals are differenced, and they generate a primary signal that controls automatic rod motion. The difference between the measured core inlet temperature and the set point for the core inlet temperature also generates an error signal that modifies the primary signal to reset the core inlet temperature following a transient or other drift. An amplifier converts the primary signal to a d-c voltage to actuate the particular group of gray rods selected for automatic control, with the speed of the gray rod group being proportional to the output of the amplifier. Maximum insertion at 100 in./min and maximum withdrawal of from 10 to 100 in./min are available for the automatically controlled rod group, whereas the rod speed under manual control is nominally 10 in./min for the gray and 22.5 in./min for the black rods. Rod groups not on automatic control can be moved manually.

References

1. Carolinas Virginia Nuclear Power Associates, Inc., Applicant's Proposed Appendix A, Technical Specifications to the Facility Operating License, USAEC Docket No. 50-144, Feb. 21, 1962 (revised July 30, 1962).
2. Carolinas Virginia Nuclear Power Associates, Inc., Part B. License Application, Final Hazards Summary Report, Report CVNA-90 (USAEC Docket No. 50-144), Dec. 14, 1961, issued in four volumes,* as follows: I, Description of Site and Surrounding Area; II, Description of Reactor and Nuclear Power Plant; III, Accidents and Hazards; IV, Plant Operations.
3. *Nucleonics*, Nuclear Canada Issue, 18(10): (October 1960).
4. *The Forum Memo to Members*, Atomic Industrial Forum, Inc., 10(6): 9 (June 1963).

*Final Hazards Summary Report has been amended by Amendments 7 through 16, USAEC Docket No. 50-144.

Section

IV

Power Reactor Technology

Operating Experience: Yankee

The first quarterly report[1] on the core evaluation program of the Yankee reactor was reviewed briefly in the last issue of *Power Reactor Technology* [6(3): 55-56], and the observed failure of the nickel plating on the silver-indium-cadmium control rods was mentioned.

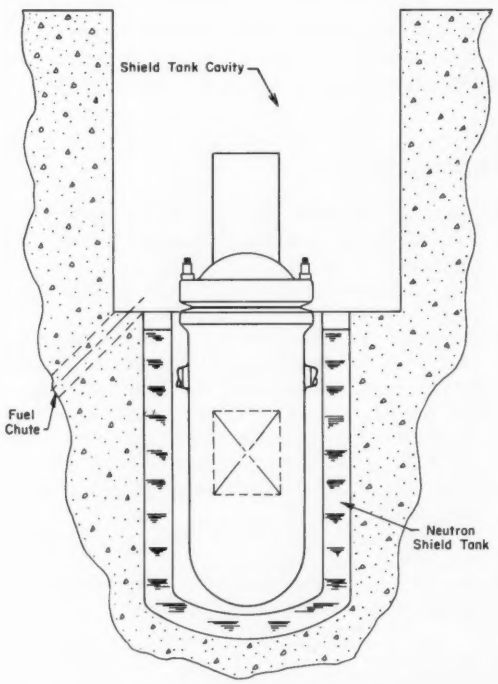

Fig. IV-1 Arrangement of Yankee reactor vessel in shield structure.[8] With the reactor shut down and depressurized, personnel enter the shield tank cavity and prepare the vessel head for removal. The shield tank cavity is then filled with borated water, and removal of the vessel head, refueling, and replacement of the head occur under water. The cavity is drained, and personnel reenter the area to secure the vessel head.

Although this failure caused no malfunction of the rods themselves, it led to a troublesome radioactivity problem that was subsequently reported.[2] At the first refueling a scheduled replacement of the control rods with rods of the same type was carried out. However, the plan is to replace these by 22 solid hafnium and two Inconel-clad silver-indium-cadmium rods at the second refueling.

The radioactivity problem developed during the refueling activity. After the pressure-vessel head had been removed and the shield tank cavity (see Fig. IV-1) had been filled with water for the refueling operation, silver from the exposed control-rod alloy apparently migrated through the water and electroplated on the stainless-steel walls of the cavity. The deposit contained about 100 g of the gamma-emitting isotope Ag^{110m} (253 days), which gave radiation levels as high as 2.5 r/hr in the shield tank cavity after the refueling operation had been completed and the cavity had been drained. Various decontamination attempts succeeded in reducing the level by only about a factor of 5. The radiation level seriously handicapped the rebolting of the reactor vessel head, which normally requires some 600 man-hours of work within the drained shield tank cavity.

The second and third quarterly reports[3,4] on the core evaluation program have now been issued. They cover primarily the planning, design, and procurement of special equipment for transportation and examination of the core components. However,[3] three irradiated* Yankee fuel assemblies were received in March and placed in storage at the Westinghouse Post-

*Presumably these were from the discharged first core, which reached a power production[5] of 10,680 equivalent full-power [392 Mw(t)] hours (EFPH), corresponding to an average core exposure of 8360 Mwd/metric ton.

irradiation Facility pool. These were from core positions H-3, G-4, and J-4 (see Fig. IV-2).

The H-3 fuel assembly was inspected, and no cladding ruptures were found.

There was no evidence of distortion, corrosion, significant wear, cracks, or other defects. Several unusual conditions, similar to those seen at the Yankee site were noted, including:

(1) Copper-brown discoloration on and adjacent to the rubbing straps attributable to the thin film of excess nickel-chromium-phosphorus brazing alloy.

(2) Numerous small scratches of bright, shiny appearance, suggesting that they occurred during the handling of the fuel assembly after core operation.

(3) Thin, gray crud-like deposits on fuel tubes near top and bottom end plates. The appearance of these deposits was similar to that seen in the Yankee Spent Fuel Pit. In one case it was observed that the deposit had been partially removed and "peeled back" as a result of a scratch.[4]

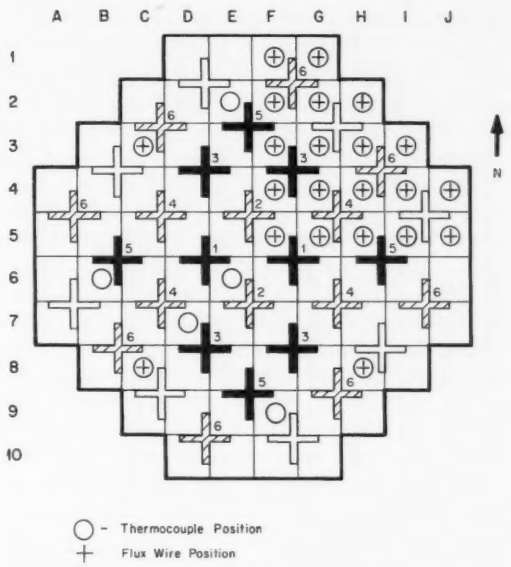

Fig. IV-2 Locations of fuel elements, control rods, and in-core instruments in Yankee core I. The open crosses designate control-rod channels filled with fixed Zircaloy water-displacers. The hatched crosses are the positions of withdrawn control rods. The solid crosses are fully inserted control rods. The pattern of rod withdrawal corresponds to an exposure of approximately 2400 EFPH (see Table IV-1).

In-Core Power Instrumentation

The question of how much, if any, in-core instrumentation for the measurement of power and/or temperature distributions is to be provided in a given reactor is intimately related to the questions of how the progress of fuel burnup and its effects on power distribution are to be followed during the reactor lifetime. Both of these questions are very important ones, and the appropriate answers will, of course, vary from reactor to reactor. If the possibility of spatial oscillations of xenon exists, some kind of in-core instrumentation for the measurement of gross power distribution is almost a necessity. When (as in the Yankee reactor) this is not the case, other considerations remain. If the initial power distribution in the reactor is not the worst that may occur during the reactor lifetime—in the sense of giving the highest hot-spot and hot-channel factors—in-core measurements of power distributions may be desirable. These measurements may also be useful if the reactor is initially rated below its actual expected power capability in anticipation that the power rating will be increased at some later time.

Aside from the specific needs that in-core instrumentation can satisfy, the additional information about the core which it provides will always be useful for increasing the understanding of the core characteristics and will usually increase the accuracy with which core reactivity life can be predicted. Hence, if the cost were negligible, there would be little doubt that a high degree of in-core instrumentation would be generally desirable. The cost is not negligible. The cost of an in-core instrumentation system does not appear only in the initial cost of the plant because the system requires maintenance over the life of the reactor, often adds a great deal of complexity to the internal structure of the reactor, and may add potential sources of leaks from the primary system. Some delays have been reported,[2] for example, in the first reloading of the Yankee core because of damage that was inadvertently done to the in-core instrumentation system. Finally, the incentive for installing in-core instrumentation in water-moderated reactors is reduced because of the limited amount of information that can be gathered by any practical system that has been devised. The flux gradients are usually so steep in water-moderated reactors that it is virtually impossible to install power-measuring devices

in such a way as to measure directly the maximum-to-average power ratios or hot-channel factors. Thus a large amount of calculation is still necessary to arrive at these answers even when a rather large number of measurements are made in the core.

Because the question of in-core instrumentation is such a subtle one, it is of great interest to consider what the benefits of an in-core system have been in a typical operating reactor. Reference 6 describes the programs that were carried out to follow the distributions of power density and fuel burnup in the first Yankee core and makes such an assessment possible.

The location of the in-core instrumentation in the Yankee core is indicated in Fig. IV-2. The instrumentation consists of 27 chromel-alumel thermocouples that measure coolant outlet temperatures at the axes of 27 individual fuel assemblies and 22 thimbles, extending along the central axes of 22 different fuel assemblies, which will accommodate manganese-alloy wires for the measurement of neutron-flux distribution. Eight drive mechanisms are provided for inserting and removing the wires, so that a total of eight wires can be irradiated at one time during normal power operation. The mechanical details of the system have been described in Ref. 7.

It is said[6] that the outlet thermocouples will determine the power output per individual fuel assembly to an estimated accuracy of ±5%, provided the coolant-flow distribution in the core is known. This distribution, however, is poorly known from first principles, since the fuel assemblies in the Yankee core are unshrouded; consequently the thermocouple readings are ordinarily used, in conjunction with the power distributions derived from the flux-wire system, as indications of the actual flow distribution in the core.

The objective of the flux-wire irradiations is to yield information from which the maximum-to-average power-density ratio in the core can be determined. The irradiation of a complete set of wires gives an axial neutron-flux distribution at the center of each fuel assembly in a typical core quadrant and at the centers of enough other assemblies to establish that the quadrant is indeed typical. It can be assumed

Table IV-1 HOT-CHANNEL FACTORS AND DNB RATIOS MEASURED DURING THE YANKEE CONTROL-ROD WITHDRAWAL PROGRAM[6]

Rod group positions (inches withdrawn)						Power,				
6	4	2	3	5	1	Mw(t)	EFPH*	F_Q†	$F_{\Delta T}$†	DNBR
90	70	0	0	0	0	288	359	3.67	2.66	4.26
90	0	0	90	0	54	376	441	3.57	2.85	3.39
90	90	90	19	0	0	376	1241	3.56	2.76	3.67
90	90	90	25.5	0	0	376	1649	3.69	2.71	3.43
90	39.8	0	90	0	90	392	2356	3.83	2.75	3.10
90	90	90	43.9	0	0	392	2548	3.73	2.69	3.22
90	90	90	46.9	0	0	392	2592	3.80	2.78	3.09
90	60	0	90	0	90	392	3216	3.31	2.72	3.45
90	69.8	0	90	0	90	392	3553	3.22	2.79	3.45
90	90	0	90	38.6	90	485	4048	3.08	2.53	3.18
90	90	0	90	46.9	90	485	4540	2.92	2.58	3.27
90	90	90	90	51.4	0	485	4945	2.96	2.61	3.25
90	90	90	90	90	90	380	5408	3.46	2.93	3.27
90	90	90	90	67.5	0	380	5550	2.87	2.61	4.08
90	90	90	90	73.5	0	485	5817	2.85	2.57	3.02
90	90	0	90	90	90	380	6159	2.83	2.52	4.02
90	90	0	90	90	90	380	6511	2.80	2.53	4.10
90	90	42	90	90	90	380	7008	2.96	2.55	4.31
90	90	70.9	90	90	90	470	7470	3.13	2.73	2.84

*Equivalent full-power hours where 392 Mw(t) = full power. Values correspond to date on which measurement was made.

†All listed values of F_Q and $F_{\Delta T}$ include a nuclear factor of 1.045 to account for the nonuniform pitch within fuel assemblies and engineering factors to account for manufacturing uncertainties. The engineering factors are 1.045 on F_Q and 1.28 on $F_{\Delta T}$.

that these flux readings are very nearly proportional to the power densities in the fuel rods immediately adjacent to the wires—i.e., the rods at the centers of the assemblies.

To understand how the maximum-to-average ratio can be derived from the flux readings, it is necessary to consider the Yankee control-rod program. The rods are withdrawn in symmetrical banks and in the sequence 6, 4, 2, 3, 5, 1 (see Fig. IV-2). At any given operating condition, all rod banks except one will be either fully inserted or fully withdrawn. For example (Table IV-1), after operation for 2548 EFPH, rod banks 6, 4, and 2 were in the fully withdrawn position, banks 5 and 1 were fully inserted, and bank 3 was withdrawn 43.9 in. In typical operation there will thus be a lower section of the core that contains some pattern of rods and an upper section that contains the same rods plus one additional bank of rods. In each section the radial power distribution can be calculated by a two-dimensional method (PDQ or TURBO), and from the result two types of calculated ratios can be determined for each individual fuel assembly in each region: (1) the ratio of the centerline power density to the average power density in the assembly and (2) the ratio of the centerline power density to the power density in the corner of the assembly adjacent to a control-rod channel. The latter positions will always include the point of maximum power density (when the control rod is withdrawn). The calculated ratios can be applied to the measured centerline power-density distribution to give for each fuel assembly, as a function of axial position, the average power density and the corner power density. These power densities will be in arbitrary units, but in the same units for all cases. The average power density is simply the integral of the axial distribution for all assemblies divided by the number of assemblies. The maximum-to-average ratio is just the ratio of the maximum power density, which will be found at some axial point on the corner distribution of one of the assemblies, to this average density. The power density hot-channel factor (F_Q, Table IV-1) is the product of this maximum-to-average ratio and any other pertinent factors (e.g., engineering factors such as variations in fuel density) that are not covered by the determination. The nuclear component of the temperature-rise hot-channel factor ($F_{\Delta T}$), which is the ratio of the maximum coolant enthalpy rise (in traversing the core) to the average, can be determined in an analogous manner.

The procedure outlined above is roughly that followed in evaluating the hot-channel factors for the Yankee core I at intervals during its lifetime. The results are given in Table IV-1. The initial two-dimensional power distributions were calculated, for all the planned combinations of rod groups, by the PDQ code.* The results of a typical calculation, for a control-rod configuration that applies near the beginning of core life, are given in Fig. IV-3. The results of

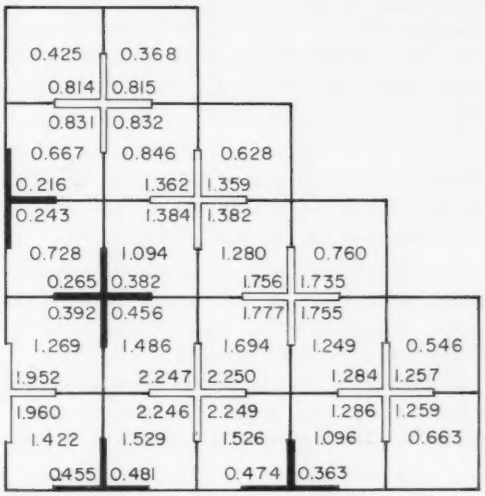

Fig. IV-3 Calculated relative power densities at the centers and corners of fuel assemblies in one quadrant of Yankee core I, early in core life.[6]

these calculations were stored in an IBM-7090 code, which applies them, along with various corrections such as the correction for flux-wire decay, to process the data from the in-core instrumentation. The input to the code consists of flux-wire activation traces, core power level, time elapsed since last measurements were made, and control-rod position. Using these data, the code calculates the following quantities:

1. An integrated power-density distribution in the x-y plane obtained by an axial integration of the measured distributions.

*Later analyses utilized the TURBO code to yield two-dimensional distributions that included the effects of burnup.

2. The axial peak-to-average power density in each fuel assembly.

3. The power density and coolant-enthalpy-rise distribution at each corner point around the control rods and followers (from which the hot-channel factors F_Q and $F_{\Delta T}$ are obtained).

4. The maximum heat flux at the corner points described in 3.

5. The coolant temperature rise in each assembly and a flow distribution. This flow distribution is the ratio* of F_{xy} obtained from flux-wire traces to that obtained from thermocouple readings and is influenced by flow redistribution within the core and mixing near the outlet nozzles.

6. The accumulated burnup, in megawatt-hours, along the length and averaged over given segments of each assembly.

7. The DNB ratio.†

From the descriptions above it is clear that the flux wires perform two functions in the determination of the hot-channel factors:

1. They determine a gross radial power distribution independently of any calculation. This alone, however, gives neither the maximum power density nor the average.

2. They provide the means of synthesizing a three-dimensional power distribution from a set of two-dimensional (radial) distributions.

The latter of these is a great convenience. So far as the accuracy of results is concerned, it is not clear that the measurements give any great improvement over calculation alone. Part *a* of Fig. IV-4 gives a comparison of the calculated and measured centerline power densities in a radial plane at a time near the end of core life (all control rods withdrawn). Part *b* of Fig. IV-4 shows the calculated centerline and corner power densities for the same case. It is evident that the local (corner) peaking factors — which are determined by calculation in any case — are large relative to the differences between calculation and measurement. That the accurate prediction of the local factors requires a sophisticated analytical approach is attested by Fig. IV-5. This figure compares the corner-to-center factors around the group 1 control-rod follower as calculated by PDQ (which makes no allowance for the change in fuel composition with burnup) and by TURBO (which includes the fuel burnup effect). The percentage differences are at least as great as the differences between measurement and calculation in part *a* of Fig. IV-4.

A test of the complete calculational approach is afforded by comparisons of measured and calculated hot-channel factors. The comparison is given in Fig. IV-6. To arrive at the calculated factors, it was necessary to synthesize the three-dimensional power distribution from two-dimensional calculations. This was done by combining the radial-plane results with two-dimensional calculations in the R-Z plane. Figure IV-6 indicates that the technique was successful.

In the Yankee reactor it is apparent that the in-core instrumentation has performed the very valuable service of giving evidence in support of the power and accuracy of the available calculation techniques. It undoubtedly was also a great help in establishing the feasibility of the increase of power rating for the reactor.* As experience such as this accumulates, decisions with regard to in-core power instrumentation will no doubt come to depend more and more on economic considerations. The direction of the trend is not obvious, for, although the instrumentation represents an expense, the cost of a continuing program of detailed calculations is by no means negligible, and the cost and difficulty may well increase with increasing reactor size and increasing fuel burnup. One conclusion appears to be obvious: The case for instrumentation in water reactors might be greatly improved if more convenient methods were developed, particularly methods that could give directly the desired information without requiring complex auxiliary calculations. The difficulties of achieving improvements of the latter type appear, however, to be quite fundamental ones.

Reactivity Characteristics

Reference 5 is a report of the reactivity effects observed and analyzed over the lifetime of

*F_{xy} is the ratio of the enthalpy rise in a given coolant channel to the average coolant enthalpy rise. The maximum value of F_{xy} is denoted as $F_{\Delta T}$.

†DNB denotes departure from nucleate boiling. The DNB ratio is a ratio of the heat flux that would yield this condition to the maximum operating heat flux.

*The increase in core power level from 392 Mw(t) [110 Mw(e)] to 485 Mw(t) [150 Mw(e)] was authorized in June 1961.

Yankee core I. In addition to the reactivity lifetime, the report covers control-rod worths, operating configurations of control rods, reactivity coefficients, and the variations of these characteristics with time. It gives an excellent picture of the subtleties of the problems encountered when the reactor analyst seeks to understand the detailed reactivity behavior of a large power reactor, and it is well worth the reading to any reactor physicist whose interest extends to the realities of the as-built and as-operated reactor. The one deficiency of the report is that it does not specify definitely how the experimental measurements were made.

The operating history of the reactor is summarized as follows:[5]

From January 1961 until June 1961 the first core operated at its design thermal output of 392 MWt or 110 MWe of net electrical power for a total burnup of approximately 3500 EFPH* or 2700 MWD/Tonne. In June 1961 an increase in power level from 392 MWt to 485 MWt (150 MWe) was authorized. End of core lifetime at 392 MWt and rated conditions (514°F, 200 psig) occurred in January 1962 at an average burnup of 8000 EFPH or 6270 MWD/Tonne. At this time all control rods had been removed from the core. This was followed by a core lifetime extension period where power and main coolant temperature were continuously lowered to balance the loss of reactivity due to burnup. Final shutdown occurred on May 18, 1962 at a power level of 270 MWt, main coolant temperature 431°F and a total average burnup of 10,680 EFPH or 8360 MWD/Tonne.

*EFPH = equivalent full power hours referenced at 392 MWt. This definition of EFPH will be used throughout the context of this report.

A summary of design calculations and the later calculations of initial excess reactivity and core lifetime are compared in Table IV-2 with the observed values. The first CANDLE (one-dimensional) and TURBO (two-dimensional

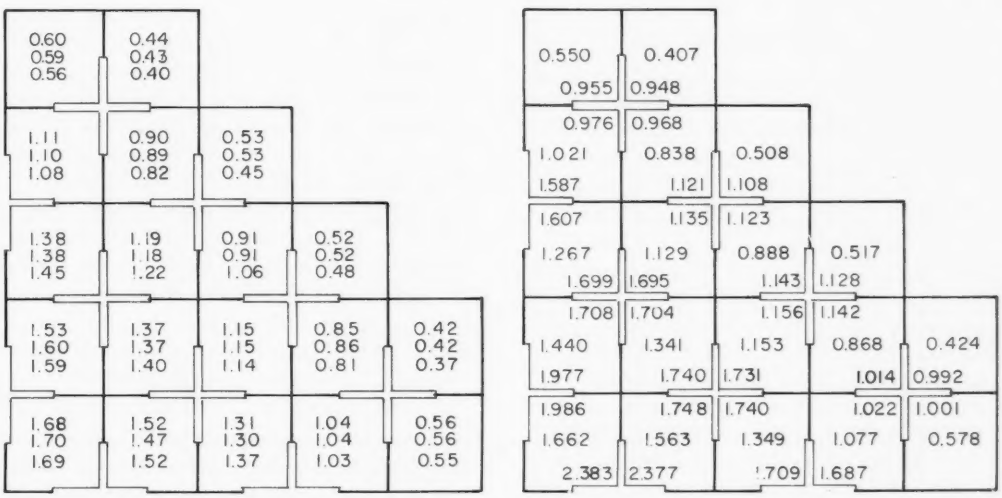

Fig. IV-4 Relative power densities in fuel assemblies of Yankee core I, near end of core life.[6]

In part *a* the top number in each column is the relative power at the center of the assembly, calculated (TURBO) for the nominal program of control-rod withdrawal: 6, 4, 2, 3, 5, 1. The second number is the calculated relative power for the same condition except that control-rod bank 2 was exchanged for bank 1 after an exposure of 3850 EFPH (to promote more uniform burnup). The third number is the measured relative power. In actual operation of the reactor, rod-bank exchanges were employed; consequently the second number in each column gives the more appropriate comparison with experiment.

In part *b* the numbers give the calculated center and corner power densities, for conditions that are nominally the same as those for part *a*. The reason for the slight discrepancy between the central values in part *b* and the calculated values in part *a* is not apparent in Ref. 6, but the discrepancy is unimportant for the discussion in this review.

R-Z geometry) results are from the design calculations. Although the initial excess reactivity is underestimated* by about 1.3%, the core lifetime is overestimated. In the last three CANDLE calculations, revisions of the fission-product cross sections consistent with more recent work, as well as a revised fast cross-section library, were used. The 26.4-barn thermal and 34-barn epithermal cross sections were obtained from calculations performed at Bettis in 1960, the 80.2-barn thermal and 24.2-barn epithermal cross sections were obtained from work by Garrison and Ross, and the 29.0-barn thermal and 23.1-barn epithermal cross sections are from the measurements of Gunst. The use of the Gunst measurements gives good agreement with the core lifetime, but measurements of the reactivity loss rate with fuel exposure, which circumvent the question of initial excess reactivity, were found to be in better agreement with CANDLE calculations using the fission-product cross sections of 26.4 barns thermal and 34 barns epithermal. However, it is pointed out[5] that the choice of a best value for fission-product cross sections to give agreement with measured reactivity loss rate is not entirely justified, since a 5% change in the resonance escape probability of U^{238} will change the reactivity loss rate as much as a factor-of-2 change in the thermal fission-product cross section.

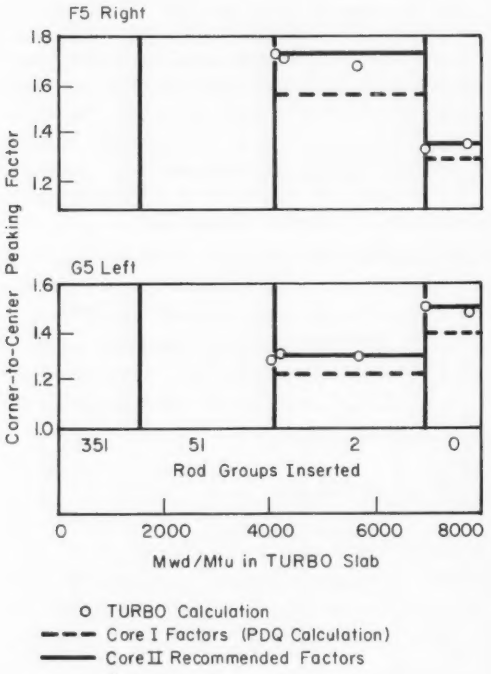

Fig. IV-5 Corner-to-center peaking factors around group 1 follower.[6] O, TURBO calculation. ---, core I factors (PDQ calculation). ——, core II recommended factors.

If some point in the operating history of the reactor is selected as a base and if the reactivity changes that occur from that point on are examined, the changes can be grouped into two classes. One of these includes the changes which result from observable changes in the operating conditions and which can be evaluated, each as the product of the observed change in operating conditions and an experimentally determined reactivity coefficient for that type of change. In the Yankee reactor the reactivity changes of this kind were those due to changes in control-rod insertion, changes in operating temperature, changes in operating pressure, and changes in the boron concentration in the reactor water. The sum of the reactivity changes due to these effects is designated $\Delta\rho^{(\text{measured})}$. Its components, in terms of the reactivity coefficients for temperature, pressure, and boron concentration, are

$$\Delta\rho^{(\text{measured})} = \Delta\rho^{(\text{control rods})} + (T-514)\frac{\partial\rho}{\partial T} + (p-2050)\frac{\partial\rho}{\partial p} + C_B\frac{\partial\rho}{\partial C_B}$$

relative to the base point of operation at 514°F and 2050 psig. The other class of reactivity changes, due to effects that cannot be observed directly, must be calculated and is designated by $\Delta\rho^{(\text{calculated})}$. In the Yankee reactor these consist of the reactivity changes due to xenon, samarium, the Doppler coefficient, and fuel depletion:

$$\Delta\rho^{(\text{calculated})} = \Delta\rho^{(\text{Xe})} + \Delta\rho^{(\text{Sm})} + \Delta\rho^{(\text{Doppler})} + \Delta\rho^{(\text{depletion})}$$

If these are indeed all the reactivity effects and if they can be evaluated with perfect accuracy, their algebraic sum should be zero between any two (critical) operating points in

*It is by no means a straightforward problem to measure an excess reactivity as large as 8 or 9%. Note the range of uncertainty on the measured value in Table IV-2.

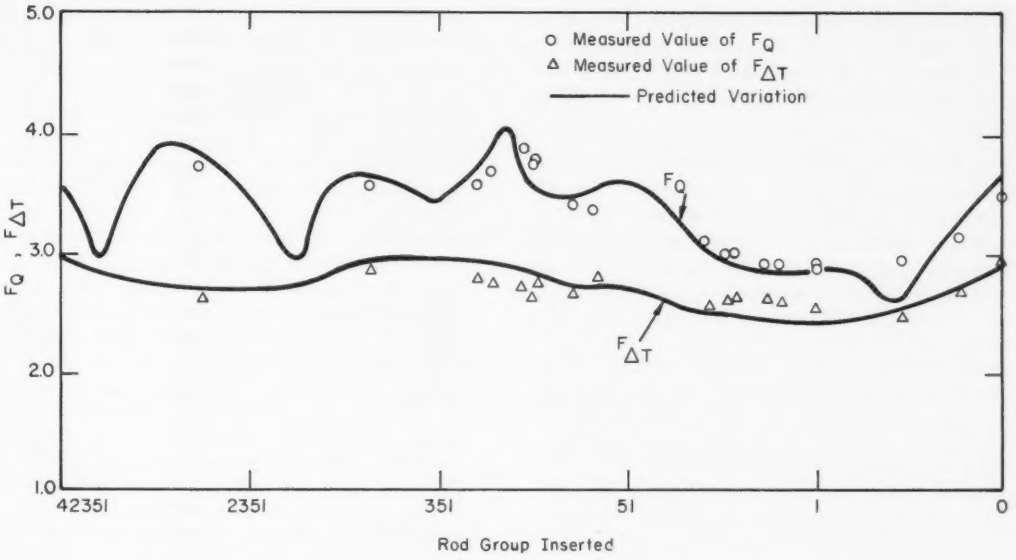

Fig. IV-6 Variation of hot-channel factors during Yankee core I control-rod withdrawal program.[6]

the reactor history. In practice the sum will not be zero because the effects cannot be evaluated with perfect accuracy and possibly because other, unrecognized effects occur. It should be expected that, except for a small scatter of the data, any discrepancies due to imperfect evaluation would enter gradually and would increase slowly with reactor operating time but would not lead to sudden large deviations from the theoretical result. This point of view has been adopted in the Yankee case, and any significant short-term departure from zero in the net reactivity change evaluation has been dubbed an anomalous reactivity variation.

Several anomalous reactivity changes were observed during the life of core I. Most of them have been explained satisfactorily in terms of a number of small effects. Of these effects, the one which has not previously been recognized as being important is the change in the Doppler reactivity effect which is associated with changes in the effective thermal conductivity of the fuel. The conductivity changes are attributed to the cracking and shifting of the fuel pellets under various conditions of power level and power distribution. Such behavior of the pellets may change both the effective conductivity of the UO_2 itself and the thermal resistance of the gap between the fuel and the jacket. These conductivity changes and other effects are applied to explain the observed anomalies, as summarized in the following quotation from Ref. 5:

> 1. The initial rapid loss in reactivity (~.5%) upon returning to power on July 23, 1961 after the 4000

Table IV-2 PREDICTIONS[5] OF REACTIVITY LIFETIME OF YANKEE CORE I

Method	$\rho_{i_3}^{28}$	$\sigma_{a_{th}}^{FP*}$, barns/fission	$\sigma_{a_{epith}}^{FP}$, barns/fission	Initial excess ρ at 392 Mw(t), %	Core life, Mwd/ton
Experiment				9.85 ± 0.73	6270
CANDLE	0.7587	64	0	8.52	6840
TURBO	0.7587	64	0	8.52	6660
CANDLE	0.7575	26.4	34	8.78	5700
CANDLE	0.7575	80.2	24.2	8.78	5120
CANDLE	0.7575	29.0	23.1	8.78	6240

*Hardened cross section.

EFPH shutdown with the subsequent slow gain (~.5%) over a period of about 40 days, is explained in section 3.4.3 [of Ref. 5] as a power coefficient effect resulting from changes in the pellet-clad gap geometry.

2. The gain in reactivity (~.4%) which occurred on September 12, 1961 can be empirically attributed to chemistry effects. On March 13, 1962 and on March 27, 1962, hydrazine was purposely added to the main coolant to raise the ammonia concentration of the coolant to about 4 ppm. These tests were performed in an attempt to duplicate the coolant chemistry conditions of September 12, 1961. Coolant *p*H increased from about 7 to about 9. A reactivity gain of about 0.3% was noticed during both of the tests. The reactivity was lost after the ammonia concentration had been reduced to pretest levels. Although it appears possible that a highly absorbing poison was removed from core surfaces during the test and subsequently redeposited on the core surfaces, no definite conclusion on the processes involved has been reached as of the present time.

3. Approximately 0.8% in reactivity was lost after boration of the core at power on September 13, 1961 which includes the gain of 0.4% that occurred the previous day, as noted below. Although it is not possible to conclude with certainty that boron plate-out on core surfaces is not the cause for the anomalous reactivity loss, it is nevertheless possible to explain the reactivity loss on the basis of mechanisms other than boron plate-out.* Based on the calculations of section 3.0 [of Ref. 5], several possible causes for the reactivity loss during the boron test at power have been combined:

	Reactivity variation
Coolant chemistry — Completion of the transient which was initiated on September 12, 1961	−0.4%
Increase in the statistical weight factor on the power defect (section 3.4.3) [of Ref. 5]	−0.2%
Redistribution of main coolant temperature in the core (section 3.12) [of Ref. 5]	−0.1%
Error in the worth of control rod groups 1 and 5 (section 3.5.2) [of Ref. 5]	−0.1%
Boron depletion during test (section 3.6.3) [of Ref. 5]	+0.1%
	−0.7%

It should also be pointed out that a 10% error in boron worth corresponds to a reactivity of about 0.25%.

4. The anamolous reactivity behavior which followed the 6400 EFPH shutdown from November 7 to November 23, 1961 occurred during an extended period of power coefficient measurements. The power level was raised in small increments over a period of 2 weeks. The anomalous reactivity behavior can be explained on the basis of the use of incorrect control rod worth data during the Xe-135 transients which occurred during the tests. As mentioned previously, the zero power rod worth data measured during the 4000 EFPH were used to calculate ρ^{measured}. In section 3.5.2 [of Ref. 5] it is shown that control rod worth can be significantly different during Xe-135 transients.

5. The slow reactivity variations (~0.3%) which occurred during October, late November and between December 16 and January 12 all showed the same trend: a loss in reactivity followed by a slow gain of reactivity at a rate roughly equivalent to the burnup rate. Two possible explanations can be suggested. First, it is suggested that the anomalous reactivity variations are not real and result from the use of incorrect control rod worth data. The differential worth of groups 1 and 5 have been shown to be significantly affected by burnup and power (section 3.5.2) [of Ref. 5]. However this mechanism does not explain the reactivity gain which followed the complete withdrawal of control rods from the core. Second, it is suggested that the anomalous reactivity variations are real and correspond to variations in the power coefficient. Control rod motion can shift the power distribution into regions of previously low fuel temperature and therefore relatively large pellet-clad gap and high power coefficient. This will lead to a reduction in core reactivity. However, the subsequent expansion, possible cracking of the pellets, and redistribution of UO_2 within the fuel rods will result in a reduction of the power coefficient and a gain in reactivity. This explanation is reinforced by the fact that the reactivity variations mentioned above bear resemblances to the reactivity variation which followed the startup on July 23, 1961, when a variation in the power coefficient was actually measured.

*Examinations of the Yankee spent fuel assemblies after the final shutdown in May 1962 have revealed minimal levels of crud deposited on surfaces. However, it cannot be concluded that the same conditions necessarily existed during power operation.

In any experimental evaluation of reactivity effects, an accurate estimate of the effective delayed-neutron fraction is essential, for all reactivity changes are ultimately evaluated in terms of the inhour equation. Calculations showed the effective delayed fraction for the Yankee core to decrease from 0.00705 to 0.0058 over the life of the core. The importance function for the delayed neutrons varied from about 0.99 to 0.975 over the life of the core. Despite

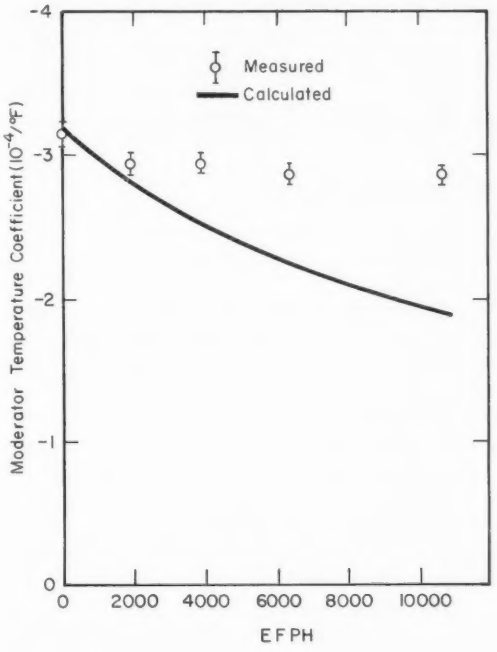

Fig. IV-7 Variation of the zero-power xenon-free moderator temperature coefficient with burnup in Yankee core I.[5]

the lower leakage probability for delayed neutrons, the importance function is less than unity because the delayed neutrons are not effective in producing fast fission of U^{238}.

The calculated moderator temperature coefficient of reactivity (evidently the isothermal coefficient for the core) agreed well with the measured value at the beginning of core life. However, calculation predicted a significant drop in the coefficient with core exposure, primarily as a result of the withdrawal of control rods. Experimentally the coefficient was found to drop off much less rapidly with exposure (Fig. IV-7). This discrepancy is believed to result from the assumption of uniform burnup in the calculations and from the method of treatment of the absorption in plutonium and fission products in the calculation, which did not take into account Doppler broadening and self-shielding effects for these isotopes.

The reference contains a number of curves showing calculated and measured differential worths of control-rod banks as functions of rod withdrawal. In general, the agreement is good. The curves are quite interesting because they show the rather large changes in the rod calibration curves which occur as burnup proceeds. The report notes that these effects must be taken into account in any worthwhile analysis of core reactivity effects.

References

1. Westinghouse Electric Corp., Atomic Power Division, Yankee Core Evaluation Program Quarterly Progress Report for the Period June 20, 1962 to September 30, 1962, USAEC Report WCAP-6052, Oct. 26, 1962.
2. G. A. Reed and R. H. Freyberg, paper presented at Annual Conference of Canadian Nuclear Association, Montreal, as reported in *The Forum Memo to Members*, Atomic Industrial Forum Inc., 10(6): 12 (June 1963).
3. Westinghouse Electric Corp., Atomic Power Division, Yankee Core Evaluation Program Quarterly Progress Report for the Period Ending December 31, 1962, USAEC Report WCAP-6053, Jan. 25, 1963.
4. Westinghouse Electric Corp., Atomic Power Division, Yankee Core Evaluation Program Quarterly Progress Report for the Period Ending Mar. 31, 1963, USAEC Report WCAP-6054, Apr. 26, 1963.
5. C. G. Poncelot, Analysis of the Reactivity Characteristics of Yankee Core I, USAEC Report WCAP-6050, Westinghouse Electric Corp., Atomic Power Division, January 1963.
6. J. D. McGaugh and R. H. Chastain, Power Density and Burnup Distributions in Yankee Core I, USAEC Report WCAP-6051, Westinghouse Electric Corp., Atomic Power Division, January 1963.
7. A. J. Kompanek, Jr., and E. C. Tarnuzzer, Neutron-Activated Wires Plot Fluxes in Yankee Core, *Nucleonics*, 20(2): 44 (February 1962).
8. Yankee Atomic Electric Co., Yankee Nuclear Power Station Technical Information and Final Hazards Summary Report, Part B, License Application, AEC Docket No. 50-29, USAEC Report YAEC-167 (Vols. I and II), April 1960.

Section

V

Power Reactor Technology

Boiling-Water Reactors: Water Chemistry

The Argonne National Laboratory has been preparing a series of three "status of the art" reports on the technology of boiling-water reactors. Two reports have been issued, and the third, covering Engineering Design, is still in preparation. The first of the series, covering Heat Transfer and Hydraulics, was issued some time ago. Since most of the concepts covered have been reviewed before in *Power Reactor Technology*, the report will not be reviewed here. It is, however, a valuable collection of detailed information for the reactor designer.

The second report in the series covers Water Chemistry and Corrosion and has these subheadings: Water Decomposition, Water Chemistry, Corrosion of Materials, Corrosion Product Deposits, and Radioactivity. The information presented was compiled from 217 referenced documents; the literature coverage is stated to be "fairly complete into 1959, but less complete since then."* No adequate summary can be given here, since the report is itself a review of a subject that can still be aptly described as an "art." Nevertheless, some of the more interesting portions will be covered briefly.

Water Decomposition

The radiolytic decomposition of water in the reactor so as to give free hydrogen and oxygen can lead to a number of problems whose severity may vary with the reactor type. These problems include the possibility of explosive hydrogen-oxygen mixtures and, in D_2O reactors, the possible loss of gaseous deuterium. In indirect-cycle boiling reactors, the disposal of the dissociated gases may present a design problem. In all aqueous reactors, moreover, the presence of the dissociation products plays some part in the overall water chemistry and corrosion behavior. In the past there has been concern over the effects of oxygen on turbine corrosion in direct-cycle systems, and the current program for the development of direct nuclear superheat has focused attention on the effects of oxygen on the corrosion of superheat fuel elements. Although the reference[2] does not treat the latter problem, it does summarize the status of knowledge of radiolytic decomposition and recombination processes.

It is believed that the initial effect of ionizing radiation on water is to split the molecule into free radicals:

$$H_2O \rightarrow H + OH \qquad (1)$$

The net effect depends on the relative rates of "forward" reactions that convert the radicals to free gases:

$$H + H \rightarrow H_2 \qquad (2)$$

$$OH + OH \rightarrow H_2O_2 \qquad (3)$$

$$H_2O_2 \rightarrow H_2O + \tfrac{1}{2}O_2 \qquad (4)$$

and "back" reactions that lead to the reconstitution of H_2O molecules:

$$H + OH \rightarrow H_2O \qquad (5)$$

$$H + H_2O_2 \rightarrow H_2O + OH \qquad (6)$$

$$OH + H_2 \rightarrow H_2O + H \qquad (7)$$

In addition, the dissolved gases, H_2 and O_2, may combine directly under the effect of irradiation. At low temperatures the product is H_2O_2, whereas, at temperatures of 200 to 250°C, H_2 and O_2 dissolved in water have been found to

*The Foreword to the series states that subsequent editions in the series will be published periodically as the technology advances.

react stoichiometrically, under the influence of gamma radiation, to form H_2O.

The major factors that affect the equilibrium among the reactions are described in Ref. 2. These include the effects of radiation, temperature, pressure, ionic impurities, decomposition impurities, and undissolved solids.

The essential source of radiolytic decomposition is the energy deposited in the water by the radiation passing through it. Although most of this energy, in a solid-fuel reactor, is initially carried by fast neutrons and gamma rays, it is finally transferred to the water by collisions of fast charged particles. In addition to any fission fragments and beta particles that may result directly from the fissions, these include also (1) the recoil protons and/or other recoil nuclei produced by the slowing-down collisions of fast neutrons and (2) the fast electrons produced in the gamma-ray absorption processes.

The density of energy deposition along the path of one of the charged particles varies greatly with the nature of the particle and to a lesser degree with the energy of the particle. In general, it is higher for the heavier particles; it is also higher for particles of low energy than for particles of high energy, i.e., the density of energy deposition increases near the end of the charged-particle range. The density of energy deposition is expressed in terms of the initial linear energy transfer (LET) parameter. This is defined as the energy transferred to the medium per unit length along the track of the charged particle. Roughly, in water, this ranges from about 5×10^4 kev per micron for fission fragments to about 0.2 kev per micron for fast electrons. This linear energy density plays an important part in determining the degree to which the several possible reactions listed above are favored by the particular type of radiation, and hence it determines the net dissociation product resulting from unit energy deposition by a given radiation. In general, the higher linear energy densities (heavy particles) favor the forward reactions, whereas the lower linear energy densities (light particles) favor, relatively, the back reactions. In a reactor the net decomposition per unit of energy deposited in the water by radiation will therefore depend on the makeup of that radiation and will vary from reactor to reactor.

Ionic impurities in the water can affect the net decomposition by scavenging the free radicals, H and OH, thus inhibiting the back reactions (Eqs. 6 and 7 above) and increasing the net dissociation. Examples are the anions Br^-, Cl^-, and I^-. Cations such as Fe^{2+}, Cu^{2+}, and Ce^{4+}, which can exist in two valent states in solution, can also act as free-radical scavengers but must be present in acid (i.e., low *p*H) solution to prevent hydrolysis. The H^+ ion concentration in a low *p*H solution has little or no effect on the yield of H_2, but it does affect the yield of H_2O_2, which is far less stable (Eq. 4) in basic or alkaline (i.e., high *p*H) solution. The net effect is that H_2O_2 appears as a decomposition product in acid solution, whereas O_2 is the product in a basic or a neutral solution.

Soon after experimental boiling-water reactors went into operation, it was observed that the net water decomposition was very significantly higher than in pressurized-water reactors. Although the net decomposition is ordinarily negligible in the pressurized-water reactors when the water purity is kept high and an excess of H_2 is maintained in the system, these measures do not eliminate net decomposition in the boiling reactor (although they do reduce it). The difference in behavior is attributed directly to the presence of the vapor phase in the boiling-water reactor. At the operating temperature, H_2O_2 is not stable, and the O_2 and H_2 escape into the steam voids where less recombination occurs than in the water phase. Moreover, the flow of steam out of the core produces a scrubbing or sweeping effect that is thought to carry the O_2 and H_2 out of the irradiation zone before recombination can occur.

A summary of the factors affecting water decomposition in pressurized-water reactors is included in Ref. 2. Also included is a review of the investigations that have been made to determine the effects of temperature, pressure, and additives on water decomposition in boiling-water reactors, namely, the Boiling Reactor Experiments III and IV (BORAX-III and BORAX-IV), the Experimental Boiling-Water Reactor (EBWR), the Stationary Low-Power Plant No. 1 (SL-1, formerly ALPR), and the Vallecitos Boiling-Water Reactor (VBWR). Of particular interest is the effect of hydrogen addition on the production of oxygen, the results of which are shown in Figs. V-1*a* and V-1*b*. The data shown suggest that the major factor involved is the stoichiometric recombination between the oxygen formed and the added hydrogen. A quotation from Ref. 2 follows:

The simplest example is the curve for ALPR, where an oxygen production rate of one liter per minute is reduced to essentially zero by a hydrogen addition rate of two liters per minute. Roughly, the same ratios for recombination exist for other reactors at different power levels for the major proportion of oxygen; the last trace of oxygen is difficult to scavenge. In BORAX-III and IV the efficiency of this recombination, as indicated by the variation from the stoichiometric volume ratio between oxygen and hydrogen, is less than in EBWR at 10 and 20 Mw. Two different pressures were involved in these tests: ALPR, BORAX-III and BORAX-IV at 300 psig, and EBWR at 600 psig for both 10 and 20 Mw. The increased efficiency of recombination in EBWR may result from the increased pressure. Unfortunately, no data were taken in EBWR on the effect of hydrogen additions at lower pressures.

Curves ... for BORAX-III and IV, except at *p*H 4.75, show parallel behavior. The efficiency of the recombination increases with decreased rate of oxygen production regardless of whether increased oxygen production is due to increased power (BORAX-III vs BORAX-IV *p*H 6.1) or the presence of undetermined impurity (compare curves *p*H 7.4 and *p*H 6.1 for BORAX-IV). The lack of parallelism between the BORAX-IV curve at *p*H 4.75 and the other curves ... may indicate that a different mechanism is the controlling factor at the low *p*H. Available data do not permit a distinction between the effect of low *p*H per se, and the effect of some specific impurity.

Because of the decreased efficiency of recombination shown by hydrogen addition and the quantity of hydrogen required with increased rates of oxygen production, hydrogen addition does not look attractive as a means of minimizing water decomposition in boiling water reactors.

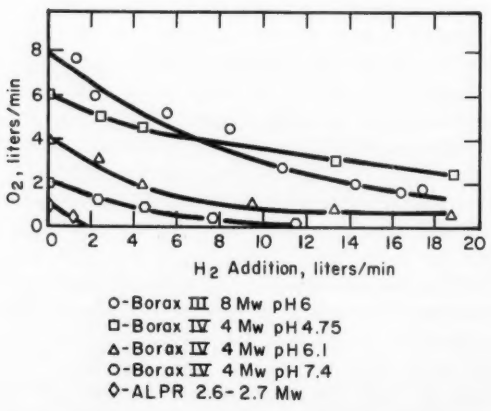

Fig. V-1*a* Effect of hydrogen additions on oxygen production in ALPR, BORAX-III, and BORAX-IV.[2]

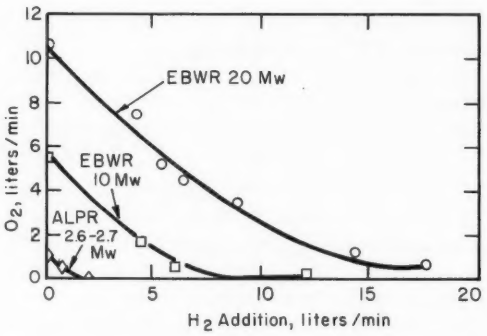

Fig. V-1*b* Effect of hydrogen addition on oxygen production in ALPR and EBWR.[2]

One encouraging conclusion of in-pile and out-of-pile corrosion tests, conducted at the Vallecitos Atomic Laboratory, is that the stoichiometric mixture of hydrogen and oxygen evolved from a boiling-water reactor is less corrosive to carbon steel and stainless steel than the low-oxygen high-hydrogen high-*p*H-water environment of a pressurized-water reactor. This is an aspect of the subject which obviously has great practical importance.

Corrosion and Activation

The materials present in the EBWR system are shown in Table V-1, except for some dummy fuel elements made of aluminum–1% nickel (alloy X8001). The materials listed all appear to have acceptable corrosion rates. The Kanigen nickel appeared to be satisfactory in the low-velocity portions of the steam system but exhibited cracks under EBWR high-velocity

Table V-1 EBWR CONSTRUCTION MATERIALS

Material	Location
Type 304 stainless steel	Pressure vessel lining, core structure, steam dryer, emergency cooler, feedwater, and miscellaneous piping
Zircaloy-2	Fuel cladding and control-rod followers
Boron stainless steel	Four control rods
Hafnium	Five control rods
Aluminum	Main condenser tubing
Carbon and low-alloy steels	Steam system piping
Kanigen nickel	Lining on steam piping, turbine (except rotor), air-ejector heat exchanger shells

steam conditions. The reference concludes that the use of the Kanigen nickel is of questionable value in the EBWR, and notes, in general, that much of the corrosion of the carbon and low-alloy steels (or release of the corrosion products) occurred during the shutdown periods when the plant was not operating. It is noted that " ... deposition of corrosion products on heat transfer surfaces of fuel elements is potentially the most serious problem encountered in EBWR ... ".[2] This scaling problem appears to be peculiar to the EBWR as loaded with the dummy aluminum elements, however, since the scale resulted from the deposition on the Zircaloy-2 cladding of aluminum oxide corrosion products from the dummy elements. The other aluminum parts in the system, i.e., the condenser tubing, seem not to have been affected because no aluminum corrosion products were detected on the feedwater filter.

The other corrosion discussion,[2] which is oriented to a specific reactor, deals with the Dresden plant. It covers the work which was done during the development stage and which was directed toward the possibility—later discarded—of using carbon steel instead of stainless steel in the primary system. It was also directed toward the corrosion problems—primarily those in the turbine—associated with the use of direct-cycle steam that has a typically high oxygen content. Although the subsequent operating experience with EBWR and Dresden gives the more convincing evidence of direct-cycle feasibility, the results of the developmental program remain a contribution to the detailed corrosion technology.

The reference[2] also gives a comprehensive summary of the development of aluminum alloys for use in high-temperature water. This covers work at Westinghouse Atomic Power Division, Hanford, and Chalk River, as well as the Argonne work.

Corrosion-product deposits are discussed[2] in both pressurized-water and boiling-water systems. A fundamental comparison between the two is difficult, however, because all the boiling-water reactors discussed had substantial quantities of in-core aluminum either as fuel jackets or in dummy fuel elements (EBWR). In all these cases the presence of aluminum appeared to be a controlling factor. It is, of course, notable that despite this circumstance no serious deposition problems are encountered other than the scale formation on the EBWR fuel plates.

Radioactivity effects are discussed for the BORAX reactors, EBWR, VBWR, SL-1, and Dresden. These include effects of activated corrosion products, fission products from defective fuel elements, and products of nuclear reactions with water and air initially dissolved in the water. The importance of the decontamination factor afforded by the evaporation in the reactor vessel is emphasized, and experimental values, from reactor operation and laboratory tests, are discussed. The results of operating the BORAX-IV reactor with 22 defective fuel plates are discussed at some length. The conclusions reached from this operation are summarized as follows:

> The first important general conclusion from the results of the BORAX-IV fuel defect test is that it is perfectly feasible to operate a boiling reactor fueled with ceramic fuel with many defects in the fuel cladding, such as were present during this test.
>
> Although radiation levels may be high during operation, it would appear that protracted operation would be feasible without serious contamination to equipment or to the surrounding countryside provided two criteria were met:
>
> (1) The system should be free from leaks.
>
> (2) The delay time from the reactor vessel to the exit from the stack should be longer than one hour.
>
> With such a delay time the amounts of Sr^{89}, Sr^{90}, or Cs^{137} released from the stack would be negligibly small, even for a large number of defected elements. If the delay time were of the order of 24 hours, then the only significant activities released from the stack would be due to Xe^{135} and Xe^{133}.
>
> The second important conclusion is that a means exists for estimating the activity released and the resulting contamination from operating a reactor with defective ceramic fuel. First of all, the only fission products which are released in significant quantities are fission gases. If a release rate for one gaseous nuclide can be measured or estimated, then the release rates of all other fission gases may be calculated. The calculation will lead to conservative results in that estimated release rates for very short-lived fission gases appear to be larger than they actually are. Then, if the reactor, steam, turbine and condenser, and off-gas systems are divided into a number of zones, and an average time that a gas atom will spend therein is assigned to each zone, then the activities throughout the system at steady operation may be estimated and the long-lived contamination resulting from a known period of operation may be calculated both for the reactor system and for the surrounding countryside.

Two proton-induced activities, F^{18} and N^{13}, are reported, which, along with the well-known N^{16} activity, are important activation products

from the water itself. Both of these are positron emitters, and both are formed by knock-on protons resulting from neutron collisions with hydrogen nuclei. The F^{18}, with a 112-min half-life, is reported to dominate the water activity in the VBWR from a few minutes to a few hours after shutdown. The reactions are as follows:

$$O^{18}(p,n)F^{18} - 2.45 \text{ Mev}$$

$$F^{18} \xrightarrow[112 \text{ min}]{\beta^+} O^{18}$$

The N^{13} activity, with a half-life of 10.5 min, is stated to be the principal component of the plant gas activity at Dresden. It is attributed to a (p,α) reaction on O^{16}.

References

1. P. A. Lottes, R. P. Anderson, B. M. Hoglund, J. F. Marchaterre, M. Petrick, G. F. Popper, and R. J. Weatherhead, Boiling Water Reactor Technology Status of the Art Report, Volume I. Heat Transfer and Hydraulics, USAEC Report ANL-6561, Argonne National Laboratory, February 1962.
2. C. R. Breden, Boiling Water Reactor Technology Status of the Art Report, Volume II. Water Chemistry and Corrosion, USAEC Report ANL-6562, Argonne National Laboratory, February 1963.

Section

VI

Power Reactor Technology

Nuclear Superheat

The Nuclear Superheat Program was reviewed in *Power Reactor Technology*, 4(3): 71-85, and subsequent issues have reviewed economic evaluations and fuel-element developments [5(3): 71-84 and 6(2): 75-80]. The following review is a brief summary of two design studies that have been published since the initial review. One of these is an integral boiling-superheating design, whereas the other employs separate reactors for the boiling and superheating functions.

The integral design, which is for a net output of 200 Mw(e), was made by the General Nuclear Engineering Corporation (GNEC) and Combustion Engineering, Inc.[1] A vertical section of the reactor is shown in Fig. VI-1. The core consists of two regions, which are called, for convenience, the boiler region and the superheater region, and these are indicated in Fig. VI-2. Actually, both boiling and superheating occur in the latter region, which is fueled with double-annular elements (part *b* of Fig. VI-3). Steam is superheated on the internal surfaces of the element, whereas boiling occurs on the external surface, which is in contact with the liquid coolant water. The surrounding boiler region is fueled with single-annular elements (part *a* of Fig. VI-3). Boiling occurs on both the inner and outer surfaces of these elements, which is necessary in order to strike the correct balance between steam production and superheat power. The reactor produces a total of 633 Mw of thermal power, giving steam at 1200 psia and 1000°F. A total of 91 bottom-mounted control rods are used. These are made of boron–stainless-steel slugs in stainless-steel jackets, with Zircaloy followers. The control rods in the superheater region are hexagonal in cross section, whereas those in the boiler are rhomboidal.

A diagram of the coolant-flow loop is shown in Fig. VI-4. The liquid coolant flow is two-pass, in that the boiler section and the boiler part of the superheater section are hydraulically in series; the steam formed in the superheater section is separated in the vessel by radial arc-vane mechanical steam separators, whereas that formed in the boiler section is separated in an external steam drum. A heat exchanger is located near the inlet of the saturated steam downcomers to completely dry the saturated steam before superheating.

The reactor power is controlled primarily by control-rod adjustment, and the control system is designed to maintain a constant reactor pressure for power levels down to 100 Mw(e). The water flow to the boiling regions is also controlled as a function of the power to hold the void approximately constant at all power levels. The superheated-steam outlet temperature is controlled by adjusting the relative power of the boiler and superheater regions by the appropriate boiler-region and superheater-region control rods (Fig. VI-2). In addition, small changes in the individual-region power levels are made by varying the feedwater distribution between the boiler zone and the boiling region of the superheater zone and thus changing the relative void fractions in the two zones.

Steam is carried from a manifold at the bottom of the core to the superheating elements via a steam inlet pipe. To prevent water inleakage to the saturated steam, a labyrinth seal is employed which consists of a number of piston rings. A bleed-off connection is provided between two sets of the rings to remove any water that may leak through the first ring set.

The main quantitative characteristics of the design are summarized in Table VI-1.

The separate superheater design, which is for a net output of 600 Mw(e), was developed by the General Electric Company[2] (Atomic Power Equipment Department). It is similar in many respects to an earlier 300-Mw(e) design[3] that

was reviewed previously; however, important changes have been made in the superheater fuel and pressure-tube design, as illustrated in parts *c* and *d* of Fig. VI-3.

A simplified plant flow diagram is shown in Fig. VI-5. The boiling-water reactor (BWR) produces 1203 Mw(t). The superheating reactor (SHR) produces 453 Mw(t) and performs the superheating in a single steam pass. A dual turbine-generator system is required because the steam capacity is stated to be too large for a single system. The gross plant output is 625 Mw(e); the net output is 607 Mw(e). The net thermal efficiency is 36.7%. The plant size was selected to utilize the largest BWR that can be built with current technology, and the SHR was sized to match the steam load from the boiler. The report states that the steam pressure for the plant was selected as the most economical pressure for the BWR.

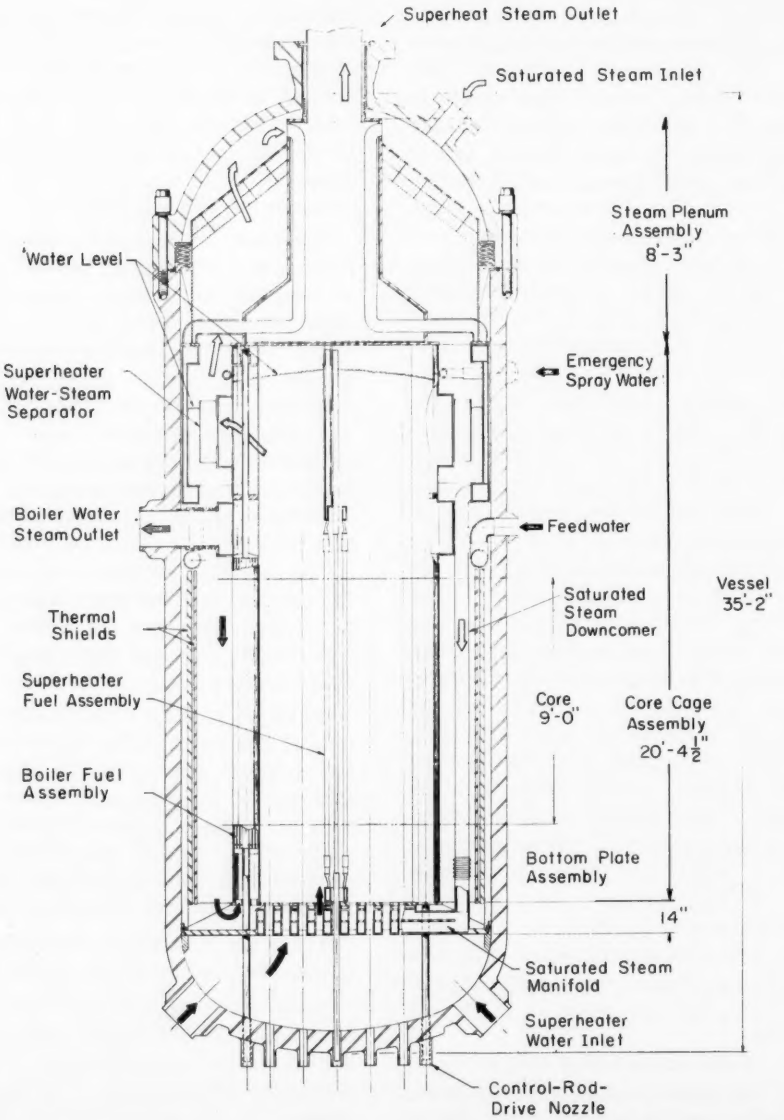

Fig. VI-1 Vertical section of 200-Mw(e) integral boiling-superheating reactor.[1]

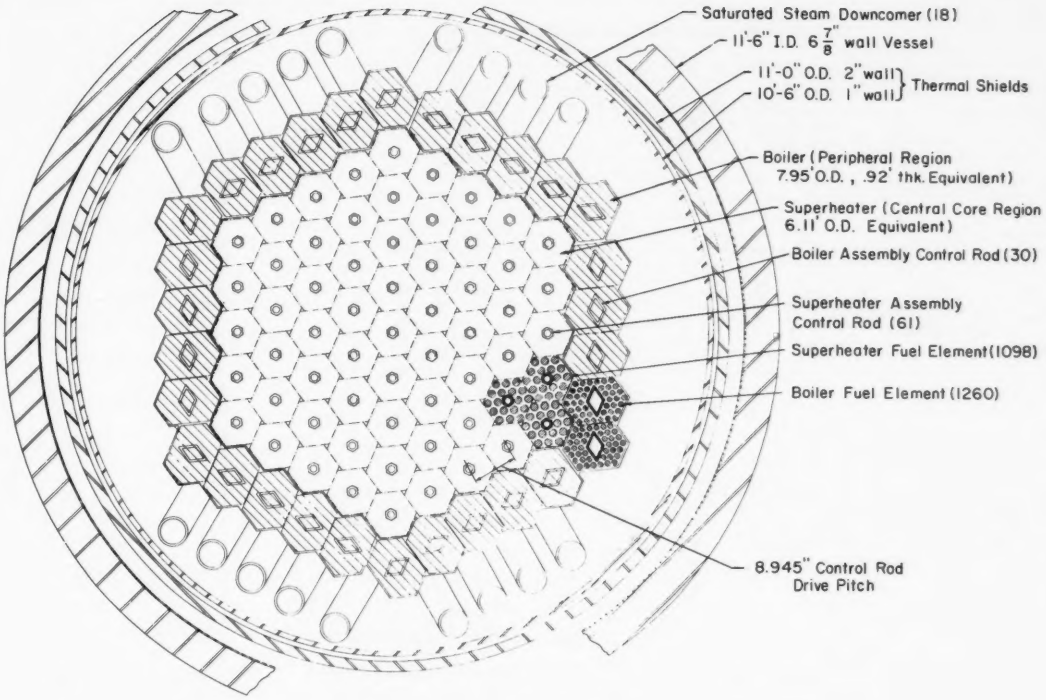
Saturated Steam Downcomer (18)
11'-6" I.D. 6 7/8" wall Vessel
11'-0" O.D. 2" wall
10'-6" O.D. 1" wall
Thermal Shields
Boiler (Peripheral Region 7.95' O.D., .92' thk. Equivalent)
Superheater (Central Core Region 6.11' O.D. Equivalent)
Boiler Assembly Control Rod (30)
Superheater Assembly Control Rod (61)
Superheater Fuel Element (1098)
Boiler Fuel Element (1260)
8.945" Control Rod Drive Pitch

Fig. VI-2 Cross section of 200-Mw(e) boiling-superheating reactor.[1]

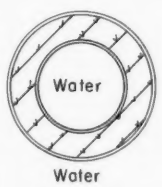

Fuel
UO_2, 1.114" O.D, 0.200" Thk
Outside Clad
304 SS, 1.160" O.D., 0.020" Thk
Inside Clad
304 SS, 0.670" I.D., 0.020" Thk

(a)

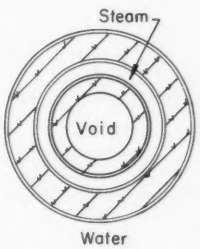

Outer Fuel
UO_2, 1.452" O.D., 0.200 Thk
Inner Fuel
UO_2, 0.761" O.D., 0.115" Thk
Outside Clad
347 SS, 1.500" O.D., 0.020" Thk
Intermediate Clad, Hastelloy X, 0.996" I.D., 0.025" Thk
Inside Clad, Hastelloy X 0.816" O.D., 0.025" Thk
Center, Void or Inert Mat'l. 0.531 D

(b)

Process Tube, Zircaloy-2, 0.932" O.D., 0.025" Thk
Flow Liner
304 SS, 0.836" I.D., 0.008" Thk
Fuel
UO_2, 0.692" O.D., 0.216" Thk
Outside Clad
304 SS, 0.716" O.D., 0.012" Thk
Inside Clad
304 SS, 0.240" I.D., 0.010" Thk
Insulation Gap, 0.015" Thk Stagnant Steam

(c)

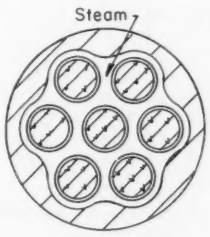

Process Tube-Flow Liner Combination
Outside Wall, SS, 1.817 O.D., 0.008"
Inside Wall, SS, Scalloped, 0.008"
Filled with Al_2O_3 Powder, 0.1" Average Thickness
Fuel
UO_2, 0.450" Dia., 7 Rods
Clad
304 SS or Inconel 0.472" O.D., 0.011" Thk

(d)

Fig. VI-3 Cross sections of fuel elements. (*a*) GNEC boiler fuel. (*b*) GNEC boiler-superheater fuel. (*c*) General Electric 300-Mw(e) superheater fuel design. (*d*) General Electric 600-Mw(e) superheater fuel design.

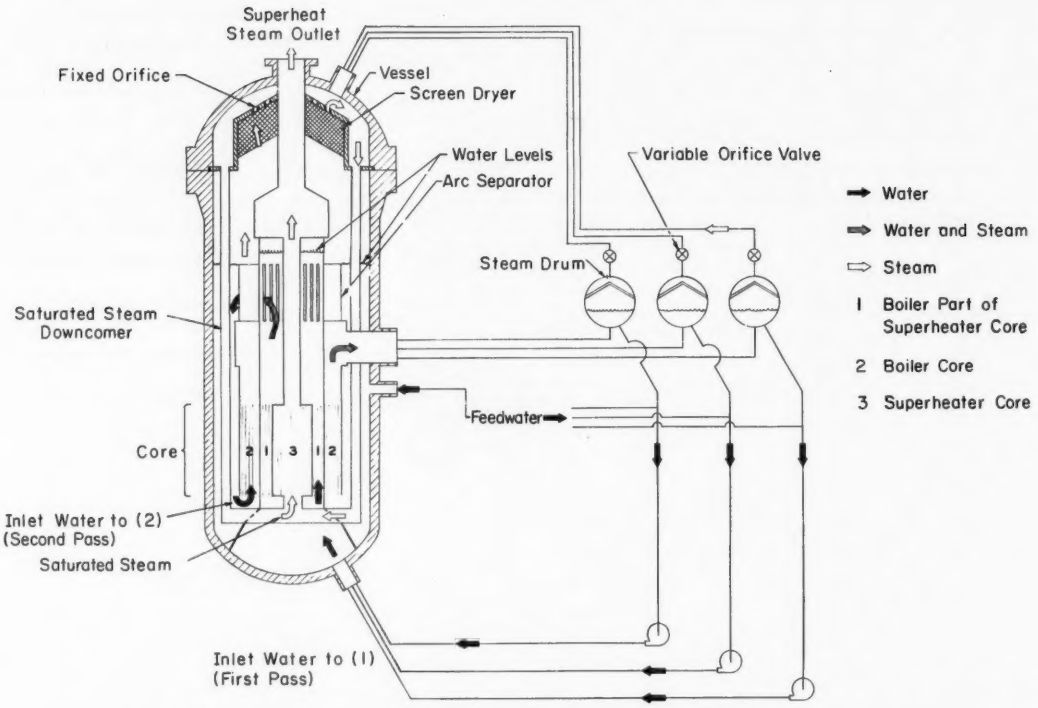

Fig. VI-4 Coolant flow diagram — 200-Mw(e) integral boiling-superheating reactor.[1]

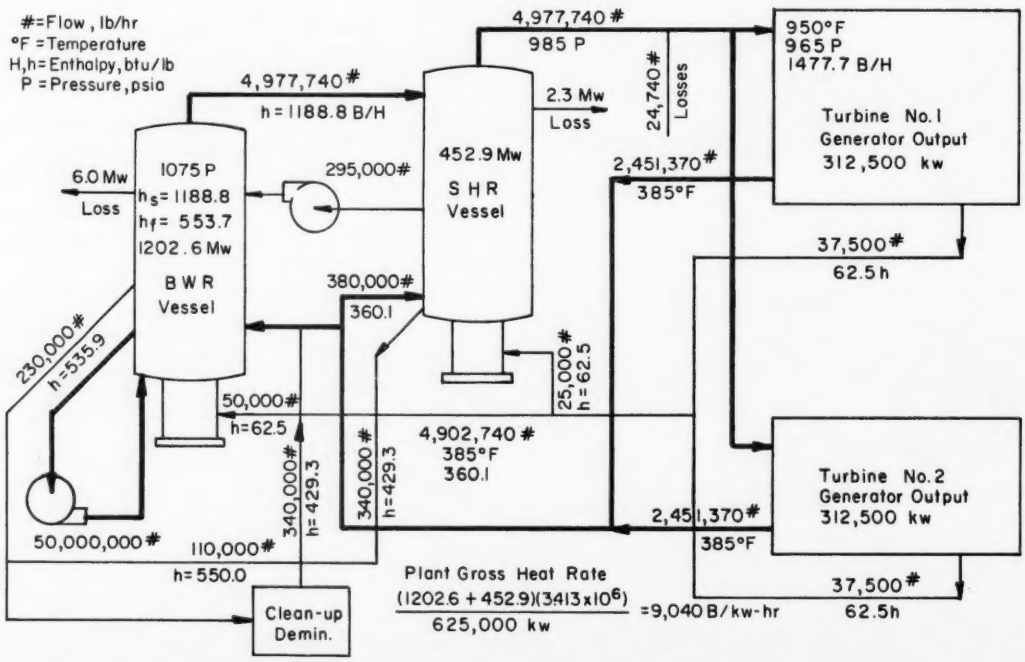

Fig. VI-5 The 600-Mw(e) simplified plant flow diagram.[2]

Table VI-1 SUMMARY OF 200-Mw(e) INTEGRAL BOILING-SUPERHEATING REACTOR DESIGN AND PERFORMANCE DATA[1]

Reactor type	Two region; thermal neutron; heterogeneous; light water moderated; internal superheater region; double-annular, combination boiler-superheater fuel elements in superheater region; single-annular fuel elements in boiler peripheral region; UO_2 fuel pellets
Reactor heat-transfer system	Integral boiling-superheating within pressurized vessel
Reactor coolant	Water coolant: two-pass forced circulation. First pass, water through boiler region of superheater; second pass, water through boiler region Steam coolant: single pass upward through superheater region
Reactor fuel	Uranium dioxide
Fuel-management program	Replace one-third of each region of the core at each refueling

	Mw	Btu/hr	%
Plant heat balance			
Total reactor power	533.2	1.82×10^9	
Gross power at generator terminals	208.7		
Gross plant efficiency			39.1
Plant electric requirement at full load	6.0		
Net plant power	202.7		
Net plant efficiency			38.0

Reactor core	
Active equivalent diameter, ft	7.95
Active height, ft	9
Active core volume, cu ft	446
Average effective power density, kw/liter	42.2
Total uranium loading, short tons of U	32.50
Average effective specific power, Mw/ton of U	16.4

	Boiler	Boiler region of superheater	Superheater
Effective outside diameter, ft	7.95		6.11
Effective thickness of annular boiling region, ft	0.92		
Active height, ft	9	9	9
Active volume, cu ft	181.7		264.3
Average power density, kw/liter	40.1		43.6
Total loading, short tons of U	12.76		19.74
Initial U^{235} content, wt.%	4.5		2.4
Average specific power, Mw/ton of U	16.14		16.58
Structural material	304 S.S.	347 S.S.	Hastelloy X
Number and geometry of fuel assemblies	30, elongated hexagonal	Same assemblies as in superheater	61, hexagonal
Number and geometry of fuel elements	1260, single annular	Same assemblies as in superheater	1098, double annular
Power transferred to water coolant, Btu/hr	0.703×10^9	0.564×10^9	
Power transferred to steam coolant, Btu/hr			0.553×10^9
Saturated steam produced, lb/hr	0.942×10^6	0.758×10^6	

	Boiler region	Superheater region
Fuel assemblies		
Number of fuel elements/assembly	42	18
Fuel element lattice pitch, in.	1.385	2.050
Reactor control		
Method of control	Control rods	Control rods
Control element type	Flux trap	Flux trap
Burnable poison material	B^{10}-S.S.	B^{10}-S.S.
Control-blade configuration	Rhombic	Hexagonal
Absorber material	1% B^{10} in S.S.	1% B^{10} in S.S.
Poison length, ft	8	8
Number of control elements	30	61
Thickness, in.	3/8	3/8
Type of drive	Hydraulic	Hydraulic
Follower material	Zircaloy-2	Zircaloy-2
Length of follower, ft-in.	9-6½	9-6½

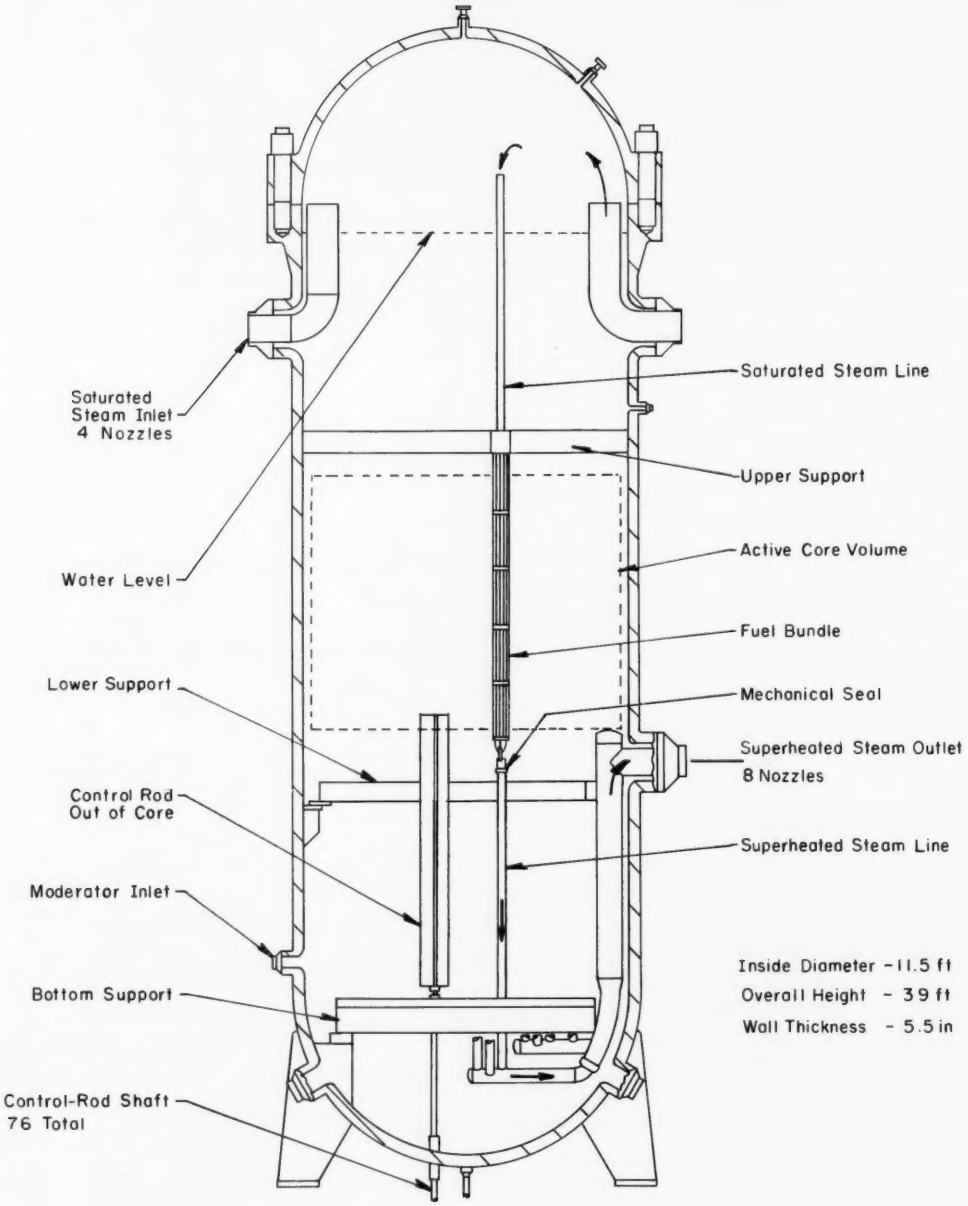

Fig. VI-6 The 600-Mw(e) separate superheating reactor.[2]

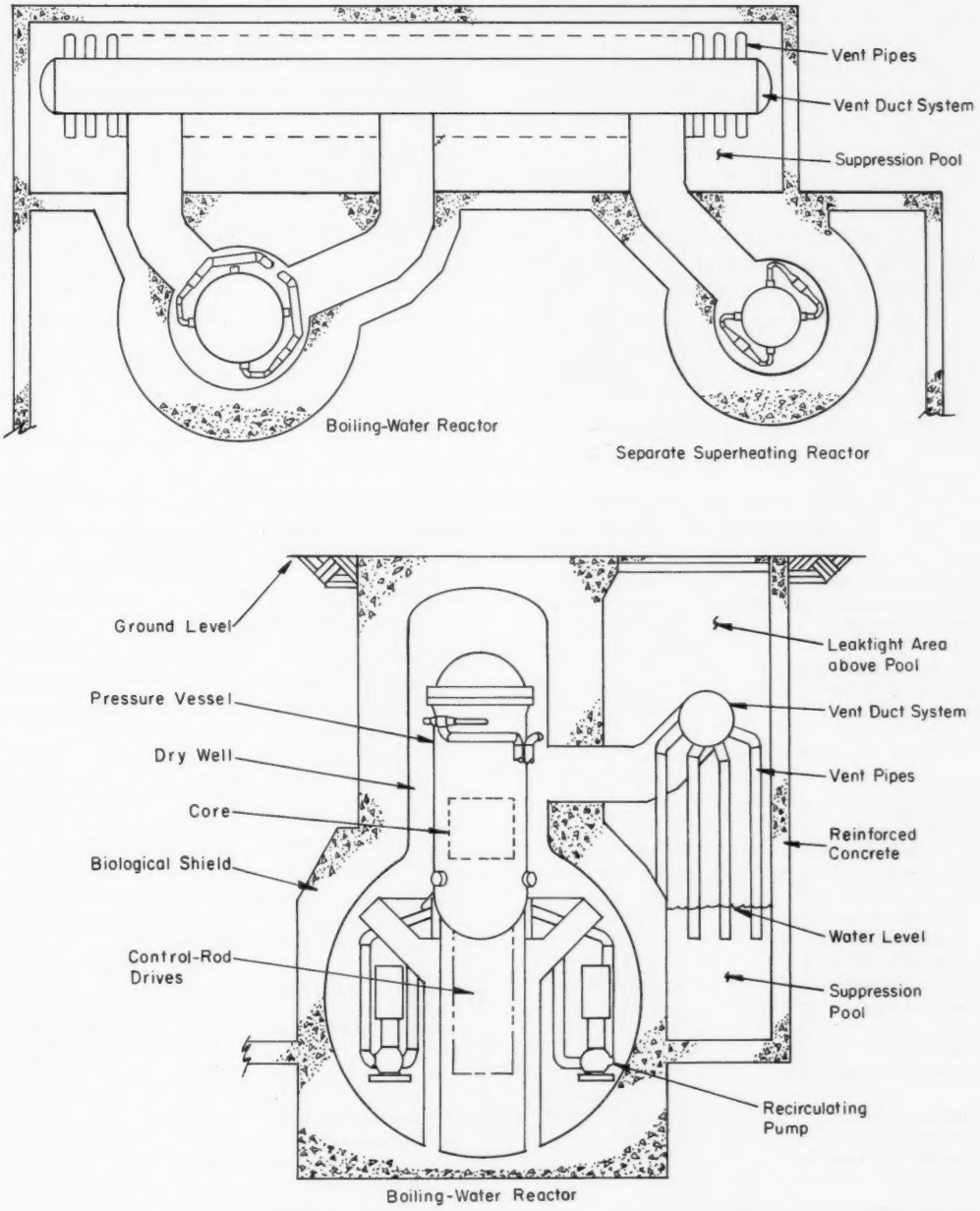

Fig. VI-7 The 600-Mw(e) nuclear steam supply building.

The BWR is stated to represent current technology. It is fueled with stainless-steel-clad UO_2 and employs radial vane steam separators and screen type steam dryers. The fuel rod has a diameter of 0.443 in., and the core operates at a power density of about 37 kw/liter. The reactor is controlled by 145 bottom-driven control rods that contain boron carbide.

The separate superheating reactor is illustrated in Fig. VI-6. It consists of a core that is 8.88 ft high with an equivalent diameter of 8.64 ft. The core is composed of an array of insulating watertight tubes (pressure tubes) which stand in the moderating water and which contain seven-rod clusters of oxide fuel elements (part *d* of Fig. VI-3). The tubes are assembled in groups of nine in square array to form the fuel assemblies. Each assembly is provided with an upper standpipe that rises through the water moderator and terminates in the inlet steam dome at the top of the vessel. It is also provided with a lower standpipe that connects to a radial, insulated, outlet header near the bottom of the vessel. Steam flow is downward through the fuel tubes.

In order that fuel can be loaded and unloaded, there is a seal at the bottom of each fuel assembly where it connects into the lower steam standpipe. The seal proposed for the SHR is (apparently) a bladder type filled with soft solder (50% lead, 50% tin). As the core structure becomes heated during startup, the solder melts and expands and closes the gap between male–female fitting pipes. Reference 2 states that this seal configuration is currently under development.

Table VI-2 SUPERHEAT REACTOR DATA: 600-Mw(e) SEPARATE SUPERHEATER REACTOR[2]

Thermal power, Mw(t)	
Thermal power to steam	421.2
Thermal power to moderator	31.7
Total thermal power	452.9
Steam conditions	
Exit steam temperature, °F	950
Inlet steam conditions, psia	1060
Steam flow, lb/hr	4,978,000
Reactor description	
Reactor core	
Active equivalent diameter, ft	8.64
Active height, ft	8.88
Active core volume, cu ft	523
Total uranium loading, kg	28,200
Fuel enrichment, wt.%	
Initial uranium content	2.80
Final uranium content	1.30
Plutonium at end of life	0.52
Neutron moderator	Light water
Moderator-to-fuel area ratio	2.57
Fuel elements	
Fuel material	UO_2
Fuel-element geometry	Solid rods, 7 per process tube
Cladding material	S.S. or Inconel
Meat diameter, in.	0.450
Cladding thickness, in.	0.011
Process tube	
Rod fuel elements per process tube	7
Process-tube outside diameter, in.	1.81
Process-tube construction	Compacted Al_2O_3 powder between S.S. tubes
Equivalent Al_2O_3 radial thickness, in.	0.100
Stainless-steel tube thickness, in.	0.008
Insulation material	Al_2O_3
Process-tube collapse pressure, psi	250
Fuel assembly	
Total number	172
Process tubes per assembly	9
Assembly cross-section dimensions, in.	6.3 × 6.3
Reactor control	
Method of control	Control-rod movement
Absorber material	Inconel
Number of control elements	76
Cross-section dimensions, in.	11.4 × 11.4 × 5/16 in. cruciform
Active length, ft	8.88
Control-rod pitch, in.	9.91
Type of drive	Hydraulic locking piston
Reactor performance data	
Reactor coolant	Steam
Reactor coolant exit temperature, °F	950
Reactor coolant inlet temperature, °F	553.5
Steam pressure, psia	1060, inlet 980, outlet
Steam velocity, ft/sec	
Average inlet	75
Average exit	147
Maximum exit	225
Maximum cladding temperature at 100% power, °F	1250
Core heat flux, Btu/(hr)(sq ft)	
100% power average heat flux	123,000
Design peaking factor	2.80
Design maximum heat flux 100%	345,000
Average core power density, kw/cu ft	866
Average fuel power density, kw/kg of U	16.0
Fuel management, % batch reloading	20

A cross-sectional view of the SHR fuel arrangement in a pressure tube is shown in part *d* of Fig. VI-3. The fuel elements are composed of UO_2 with a diameter of 0.450 in., and the cladding is type 304 stainless steel or Inconel, probably 0.011 in. thick. A fuel bundle consists of seven rods in a hexagonal pattern. The fuel bundle is surrounded by the scalloped flow liner that also serves as the pressure tube. The fuel rods are spaced with spiral wires and have a centerline pitch-to-diameter ratio of approximately 1.17. The inner and outer walls of the pressure tube are 0.008-in. stainless steel, and the gap is compacted with aluminum oxide powder (Al_2O_3). The average thickness of the insulating aluminum oxide is about $\frac{1}{8}$ in. This construction is expected to be capable of withstanding a differential collapsing pressure greater than 250 psi.

The individual fuel assemblies are provided with downstream fixed orifices for matching the steam-flow distribution approximately to the power-density distribution.

The heat loss to the moderator is estimated to be about 7% of the reactor thermal power and is divided as follows: 3.5% loss due to neutron and gamma heating, 2.5% loss through the pressure tubes, and 1.0% loss through the superheated-steam standpipes and manifolds. The moderator heat is removed by pumping about 400,000 lb of feedwater per hour through the reactor core. No boiling occurs in the moderator. As shown in Fig. VI-5, the SHR moderator is pumped to the BWR, and some of the coolant is processed through the cleanup demineralizer.

The SHR is controlled with 76 cruciform control rods of solid Inconel, and these are individually driven by bottom-entry locking piston drives. One of the reasons for selecting the gray control rods was to decrease the local flux peaking. The system comprising the two reactors and the steam plant is controlled by adjusting the BWR power to maintain a constant saturated-steam pressure and by adjusting the SHR power to maintain a constant superheated-steam temperature.

Both reactors, the reactor auxiliaries, and the fuel-storage facilities are housed in a single building that provides for both shielding and containment. A sketch of the building and equipment arrangement is shown in Fig. VI-7. The containment system utilizes pressure suppression.

The main features of the plant are summarized in Table VI-2.

References

1. General Nuclear Engineering Corporation, A 200-Mw(e) Direct Cycle Boiling Water Reactor with Integral Nuclear Superheat, USAEC Report GNEC-212, January 1962.
2. R. A. Schmidt, S. F. Armour, and W. R. Clancey, Design Study of a 600 MWe Boiling Water—Separate Superheat Reactor Plant, USAEC Report GEAP-4057, General Electric Company, Atomic Power Equipment Department, September 1962.
3. General Electric Company, Atomic Power Equipment Department, Steam-Cooled Power Reactor Evaluation for 300 MW(e) Separate Superheater Reactor, USAEC Report GEAP-3589(Rev. 1), November 1960.

Section

VII

Power Reactor Technology

Specific Applications: Ship Propulsion

A recent evaluation of the economic potential of nuclear propulsion for merchant ships, which was prepared by George G. Sharp, Inc.,[1] for the Maritime Administration, has indicated decidedly favorable prospects. This rather striking departure from the results of most previous studies, which had indicated, at best, marginal benefits from nuclear propulsion in the near future, apparently results from two closely related circumstances. The first of these is the use of advanced nuclear plant designs that exhibit large improvements in weight-to-horsepower ratio over current practice, as exemplified by the N.S. *Savannah;* the second is the exploitation of this higher performance to power ships for speeds in the 30-knot range rather than the 20-knot range that is characteristic of modern conventional freighters. For the higher speeds the required shaft horsepower lies in the range from about 60,000 to 100,000 as contrasted with the range of about 20,000 to 30,000 shp required for 20-knot ships.

The evaluation study has been summarized elsewhere.[2] The intent here is to consider the features of the nuclear plants which were factored into the study in order to indicate the directions of advanced thinking in nuclear marine propulsion and to give some idea of the technological advances required for the realization of the economic potential that has been forecast.

In the study two quite different propulsion-plant concepts were considered: (1) a gas-cooled system that has evolved from the former nuclear aircraft development program and (2) an advanced pressurized-water system. Little net difference was found in the near-term economic performances of the two types, but the conclusion reached was that the gas-cooled plant had the greater future potential. These two concepts are described briefly in the following review: the gas-cooled plant in terms of the General Electric 630A Nuclear Steam Generator and the pressurized-water plant in terms of the Babcock & Wilcox Consolidated Nuclear Steam Generator (CNSG) and the Combustion Engineering Unified Modular (UNIMOD) designs. Of the two pressurized-water designs, only the CNSG was considered specifically in the George G. Sharp[1] study.

The plant descriptions that follow treat primarily the nuclear steam generators. These have been derived from design development reports and therefore do not correspond in power output to the plants postulated in the economic study reported in Ref. 1. The three plants have the common characteristics of close coupling of the primary circuit. They also have the use of once-through steam generators to yield a compact package unit complete with containment provisions. The main characteristics of the three units are summarized in Table VII-1.

Gas-Cooled Plant[3–8]

Subsequent to the cancellation of the Aircraft Nuclear Propulsion (ANP) program, the high-temperature gas-cooled-reactor technology developed under that program was used by the General Electric Company to specify a concept for a nuclear steam generator capable of producing superheated steam as required for modern steam plants. The specific objective of the study was to determine areas in which additional development or engineering would be necessary to modify a reactor of the HTRE-1 (Heat-Transfer Reactor Experiment No. 1, an ANP test reactor) type for use in marine propulsion applications. Reference 3 is a presentation of the results of this scoping study.

A conceptual drawing of the nuclear steam generator, which is designated 630A, is shown

Table VII-1 CHARACTERISTICS OF NUCLEAR STEAM PLANTS FOR SHIP PROPULSION

	CNSG	630A	UNIMOD
Reactor power, Mw(t)	62.4	67.4	80
Normal rating, shp	20,000	27,300*	30,000
Coolant	H_2O (closed cycle)	Air (closed cycle)	H_2O (closed cycle)
Moderator	H_2O	H_2O	H_2O
Fuel inventory	4100 kg of UO_2 (see description)	236 kg of UO_2 93.2 wt.% enriched U^{235}	4460 kg of UO_2 5.9 wt.% enriched U^{235}
Fuel element			
Type	UO_2 mechanically compacted and swaged	Concentric ring (see Fig. VII-2)	UO_2 pellets in tubes
Cladding outside diameter, in.	0.460		0.328
Cladding thickness, in.	0.021		0.015
Cladding material	Zircaloy-2		Stainless steel
Control rods			
Type	Y-shaped rod with Zr follower	Cylindrical rods	Fuel cluster surmounted by a hollow water-filled shutdown rod
Poison material	Boron stainless steel	Boron stainless steel	Boron carbide
Number	7	85 safety; 63 shim; 3 dynamic	12
Active core length, in.	42	27.50	50
Active core equivalent dia., in.	49	48	42
Average heat flux, Btu/(hr)(sq ft)	117,500	61,000	102,000
Reactor coolant flow, lb/hr	6.0×10^6	1.27×10^6	4×10^6
Number of passes through core	1	1	2
Heat transfer area, sq ft	1814	3375	2770†
Core power density, kw/liter (total active core volume)	47	82.5	70
Core inlet temperature, °F	490	580	610
Average core outlet temperature, °F	520	1200	652
Average core operating pressure, psia	816	392	2250
Steam flow, lb/hr	224,605	193,900	300,000
Steam temperature, °F	515	950	606 to 658
Steam pressure, psia	412 to 420	850	655
Superheat, °F	67	425	139
Approximate volume of containment vessel, cu ft	9630	1130 (net)	6800
Design pressure of containment vessel, psia	65	265	315
Total weight of reactor, shielding, and containment, tons (short)	754	410	481
Lb/shp	75	30	32
Core life, Mwd/ton of UO_2	15,000	173,000 (fully enriched)	16,000
Control-rod movement down	Decreases reactivity	Decreases reactivity	Decreases reactivity

*Although the maximum is 30,000 shp, the data here are for a 27,300-shp operating condition.
†Calculated from fuel-pin dimensions.

in Fig. VII-1*a*. The unit consists of a close-coupled combination of a water-moderated pressurized-air-cooled reactor and a once-through steam boiler. The primary air is circulated through a closed loop by a steam-turbine-driven axial-flow blower. The unit is approximately 35 ft high and 18 ft in diameter; its estimated weight, including shielding, is 410 tons, equivalent to 30 lb per shaft horsepower. The normal thermal power of the reactor is 67.4 Mw, and the normal propulsion turbine output is 27,300 shp.

The reactor vessel, 68.8 in. in diameter and 43.0 in. high, is a calandria with 85 steel-walled (0.0625-in.-thick) fuel tubes that penetrate the water moderator and form an active core 48 in. in diameter. The core cross section is shown in Fig. VII-1*b*. A reentrant water-

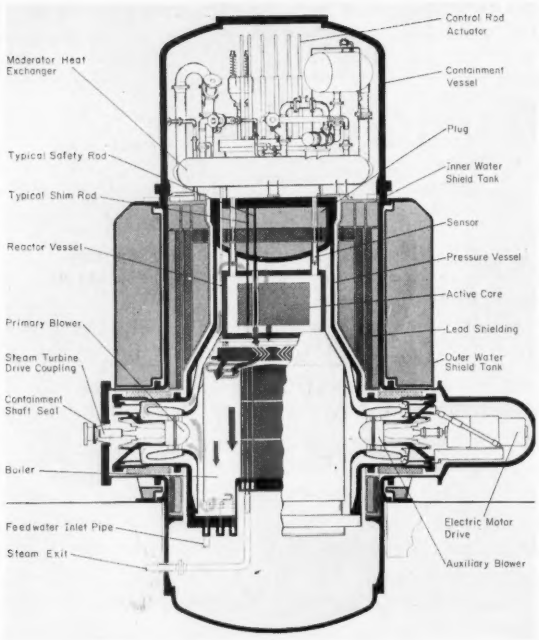

Fig. VII-1*a* **Vertical section of the 630A Nuclear Steam Generator plant. (Courtesy of General Electric Company's Nuclear Materials and Propulsion Operation.)**

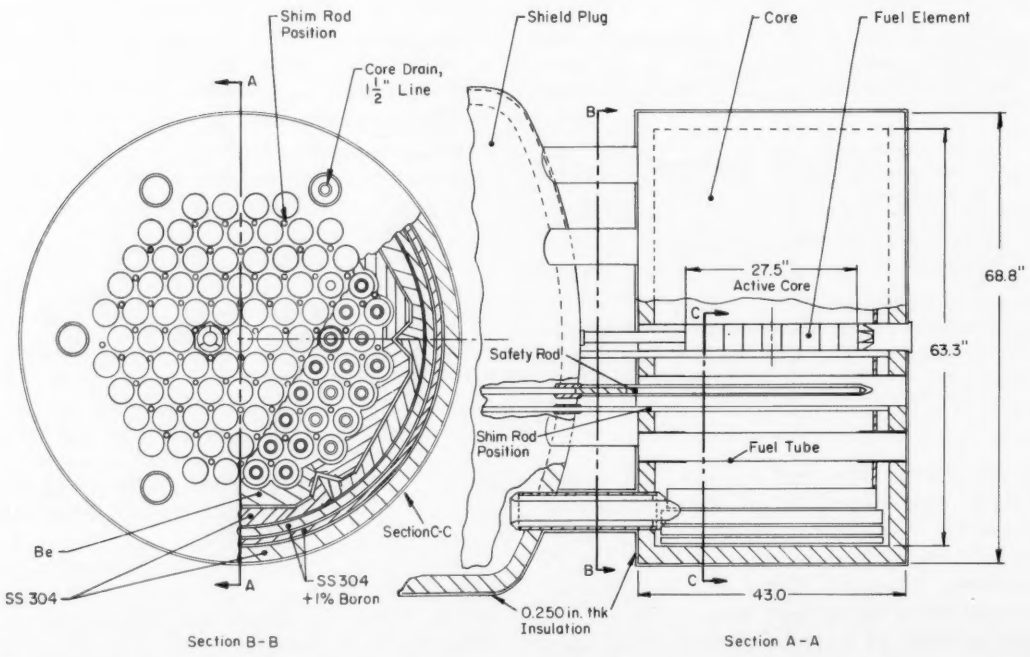

Fig. VII-1*b* **The 630A reactor core assembly.**

filled moderator tube is centered in each of the fuel tubes to provide some neutron thermalization within the fuel assembly and thus reduce the neutron-flux depression through the assembly. These moderator tubes are supported by the shield plug above the reactor. The fuel cartridges are coaxial assemblies of short (3.0 in.) highly enriched fuel rings. The rings consist of a dispersion of 38.2 wt.% uranium oxide in 61.8 wt.% of an 80 nickel–20 chromium alloy and clad with a niobium-stabilized 80 nickel–chromium alloy that is 0.004 in. thick (Fig. VII-2). The rings are assembled into the coaxial assemblies by brazing to support members. Nine fuel cartridges are stacked into each fuel tube, forming an active core 27.50-in. long. A borated stainless-steel foil, 0.005 in. thick, is wrapped around the cartridge to provide burnable poison for partial compensation of fuel burnup. The fuel-element lifetime target is 15,000 hr.

The diameter of the central moderator tube is varied in four radial zones in the reactor for gross radial power flattening (designated types 10, 11, 12, and 13 in Fig. VII-2). The thickness of the coaxial fuel rings within an assembly is varied to compensate for the neutron-flux depression through the assembly and to give approximately equal heat fluxes from all rings in a given assembly. The average thickness of a ring, including cladding, is 0.0255 in.

Surrounding the active core, and within the reactor vessel, is a combination reflector–thermal shield. It consists of 2.8 in. minimum (3.4 average) of beryllium adjacent to the core and is followed by three moderator-cooled stainless-steel annuli inside the reactor vessel. The two outer annuli are borated to reduce secondary gamma production.

The core contains 154 cylindrical control rods, each of which consists of an inner matrix of 50% B_4C and 50% type 304 stainless steel, clad with type 304 stainless steel. These rods operate in the low-pressure water moderator. Of these, 85 are safety rods that operate in the central moderator tubes, whereas the remaining 69 are shim and dynamic rods that are installed between fuel tubes (Fig. VII-2). A very large shutdown margin is considered necessary to take care of the large reactivity increase that would result if the fuel tubes should ever be flooded with water.

The reactor vessel and shield plug constitute an integral unit connected by the control-rod tubes and the moderator-circulation pipes. For refueling, the reactor shield-plug assembly is removed from the ship and is taken to a suitable remote-handling facility where the old fuel cartridges can be removed and replaced by fresh ones.

The once-through boiler produces superheated steam at 850 psig and 950°F. The steam cycle is regenerative, nonreheat, and utilizes four stages of feedwater heating. The first feedwater stage uses the heat from the reactor moderator water. The propulsion turbine is of the cross-compound single-flow type with four extraction openings that provide steam for auxiliary services as well as for feedwater heating.

The progress reports describe the developmental activities that have been carried out since the issuance of the 630A Maritime Nuclear Steam Generator Scoping Study Report. Much of the work has been directed toward the design and construction of a critical experiment, which reached criticality in mid-November 1962, at the National Reactor Testing Station. Fuel development for the 630A reactor is continuing with numerous in-pile and out-of-pile tests.

The shaping of the gross radial power by means of variations in the diameter of the center moderator tubes has been found to be inadequate. In the final design the gross radial power distribution will probably be shaped by fuel-tube pitch variation and by variations in the center moderator tubes.

Early in the period covered by the progress reports, studies were begun on the selection of a containment concept for the plant. Three containment schemes were considered:

1. Individual containment, in which the most critical areas such as blowers, control actuators, the joint between the shield plug and the pressure vessel, and the steam generator and its associated steam lines are contained by separate units

2. Total containment, wherein a pressure shell completely surrounds the reactor assembly

3. Modified individual containment, a system identical to the individual containment concept with the exception that the outer shell of the side shield is designed to contain the pressure resulting from a rupture of the pressure-vessel wall

Work on containment selection continues. The latest efforts are directed toward the investi-

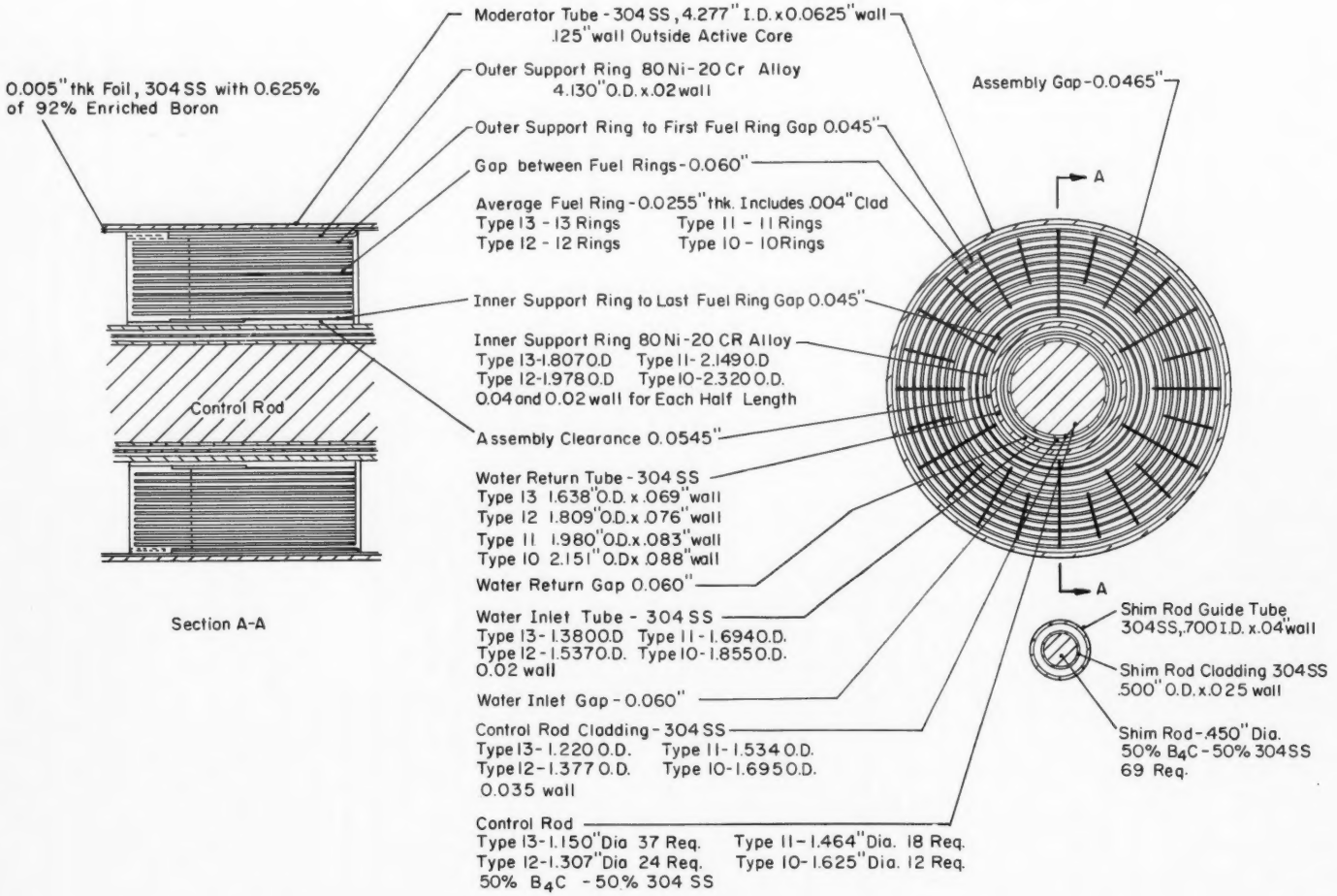
Moderator Tube - 304 SS, 4.277" I.D. x 0.0625" wall
.125" wall Outside Active Core
Outer Support Ring 80 Ni - 20 Cr Alloy
4.130" O.D. x .02 wall
0.005" thk Foil, 304 SS with 0.625%
of 92% Enriched Boron
Outer Support Ring to First Fuel Ring Gap 0.045"
Gap between Fuel Rings - 0.060"
Average Fuel Ring - 0.0255" thk. Includes .004" Clad
Type 13 - 13 Rings
Type 12 - 12 Rings
Type 11 - 11 Rings
Type 10 - 10 Rings
Inner Support Ring to Last Fuel Ring Gap 0.045"
Inner Support Ring 80 Ni - 20 CR Alloy
Type 13 - 1.807 O.D
Type 12 - 1.978 O.D
Type 11 - 2.149 O.D
Type 10 - 2.320 O.D.
0.04 and 0.02 wall for Each Half Length
Control Rod
Assembly Clearance 0.0545"
Water Return Tube - 304 SS
Type 13 1.638" O.D. x .069" wall
Type 12 1.809" O.D. x .076" wall
Type 11 1.980" O.D. x .083" wall
Type 10 2.151" O.D. x .088" wall
Water Return Gap 0.060"
Water Inlet Tube - 304 SS
Type 13 - 1.380 O.D
Type 12 - 1.537 O.D.
Type 11 - 1.694 O.D.
Type 10 - 1.855 O.D.
0.02 wall
Water Inlet Gap - 0.060"
Control Rod Cladding - 304 SS
Type 13 - 1.220 O.D.
Type 12 - 1.377 O.D.
Type 11 - 1.534 O.D.
Type 10 - 1.695 O.D.
0.035 wall
Control Rod
Type 13 - 1.150" Dia 37 Req.
Type 12 - 1.307" Dia 24 Req.
50% B_4C - 50% 304 SS
Type 11 - 1.464" Dia. 18 Req.
Type 10 - 1.625" Dia. 12 Req.
Assembly Gap - 0.0465"
A
A
Shim Rod Guide Tube
304 SS, .700 I.D. x .04" wall
Shim Rod Cladding 304 SS
.500" O.D. x .025 wall
Shim Rod - .450" Dia.
50% B_4C - 50% 304 SS
69 Req.
Section A-A

Fig. VII-2 The 630A fuel element and control rod.

gation of a shielded containment concept that will contain and shield any fission products that might be released as a result of the unlikely simultaneous rupture of the fuel-element cladding and primary pressure vessel. This is the method shown in Fig. VII-1*a*.

Pressurized-Water Plants

The two pressurized-water concepts have the following common characteristics: close coupling of the primary system; once-through steam generators that give some degree of superheat and are installed within the reactor vessel; self-pressurization; and the use of water-filled containment shells. However, the CNSG is a relatively low-pressure plant that utilizes control rods and soluble poison for reactivity control; whereas the UNIMOD plant operates at high pressure, utilizes the temperature coefficient of reactivity to compensate all "hot" reactivity changes, and employs control rods for cold shutdown only.

The CNSG, as described in Ref. 9, is a compact, closed-cycle nuclear steam supply system for a 22,000-shp ship propulsion plant. Operating at 62.4 Mw(t), it produces 224,000 lb of steam per hour at 515°F and 402 psia. The reactor vessel, which is completely submerged in water, houses the core, the control rods, the once-through steam generator, the four primary circulating pumps, and the primary water. The containment vessel, approximately 19 ft in diameter and 38 ft high, encapsulates the reactor vessel, the containment heat exchangers, the condensing tanks, and approximately 390,000 lb of water (see Fig. VII-3).

The reactor is self-pressurized by means of a steam space at the top of the pressure vessel. Net boiling is allowed in the core, although the power removed from the core is transported to the peripheral heat exchangers in sensible heat only. The control system is designed to maintain constant coolant outlet temperature from the core, and hence constant reactor pressure, by matching the reactor power to the load. The control system consists of a central regulating rod, six shim rods, and a soluble poison (boric acid) system. The central rod is positioned automatically by a pressure control system, whereas the other rods and poison system are controlled manually. The shims are used primarily for xenon, and the boric acid is used to compensate the effects of fuel burnup and for cold shutdown.

The reactor vessel, approximately 10 ft in diameter and 27 ft high, is 3 in. thick and is insulated from the external water by an 8-in. layer of lead that is also used for gamma shielding. The relatively poor thermal insulation afforded by the lead is chosen purposely to make possible shutdown cooling by conduction through the pressure vessel to the surrounding water. The vessel will normally operate at an internal pressure of 800 psig with a temperature of 520°F. The core is near the bottom of the vessel, and flow is upward. Water leaving the core flows up through a central riser that contains the control-rod extensions. At the top of the riser, the water spills radially out toward the vessel wall where it makes another 90° turn and then flows downward through the shell side of the once-through steam generator. Steam is generated at 402 psia and is heated to a throttle temperature of 515°F. Primary water discharged from the steam generator enters the four circulating pumps that are located outside the reactor vessel. These pumps discharge to a common plenum at the core inlet.

The reactor core, hexagonal in cross section (see Fig. VII-4), has an effective diameter of 49 in. and an effective height of 42 in. Thirty-seven hexagonal fuel assemblies comprise the core, which is divided radially into three zones for radial power flattening.

There are two different types of fuel assemblies, one with 108 fuel pins and the other with 121 fuel pins. The Zircaloy-2-clad fuel is UO_2 with the following enrichments:

Zone	UO_2, wt.%
Center	1.6
Middle	2.1
Outer	3.1

The UNIMOD plant described in Ref. 10 is a compact, demand-controlled closed-cycle nuclear steam supply system for a 30,000-shp ship propulsion plant (Fig. VII-5). The reactor vessel contains the steam generators, the reactor core, and, in fact, nearly all the primary loop. The reactor vessel with its surrounding shielding is completely encapsulated by the containment vessel, which is 16 ft in diameter and 34 ft high. The total assembled dry weight of the plant is 364 tons, whereas the wet weight

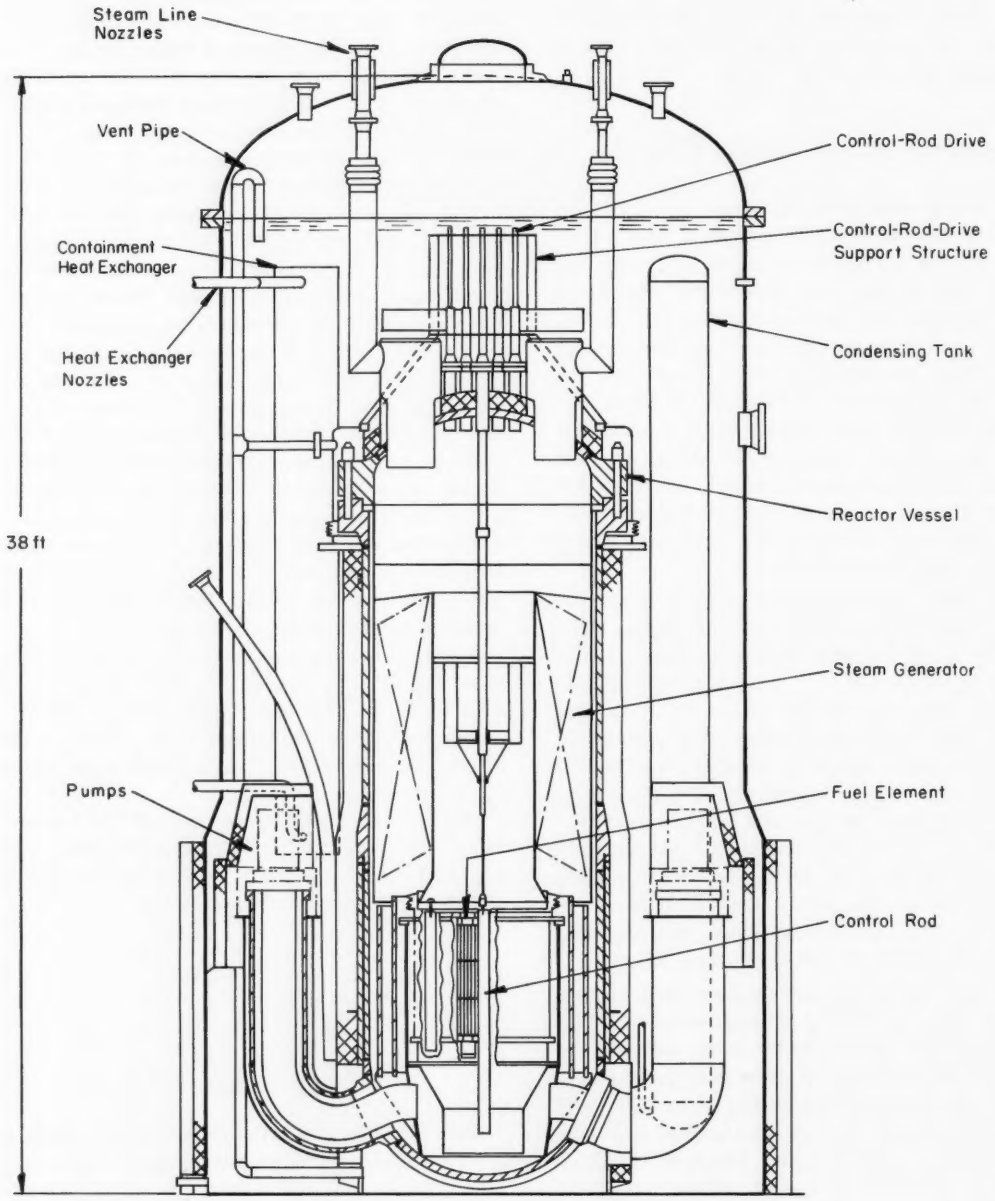

Fig. VII-3 Elevation of the Consolidated Nuclear Steam Generator reactor.[9]

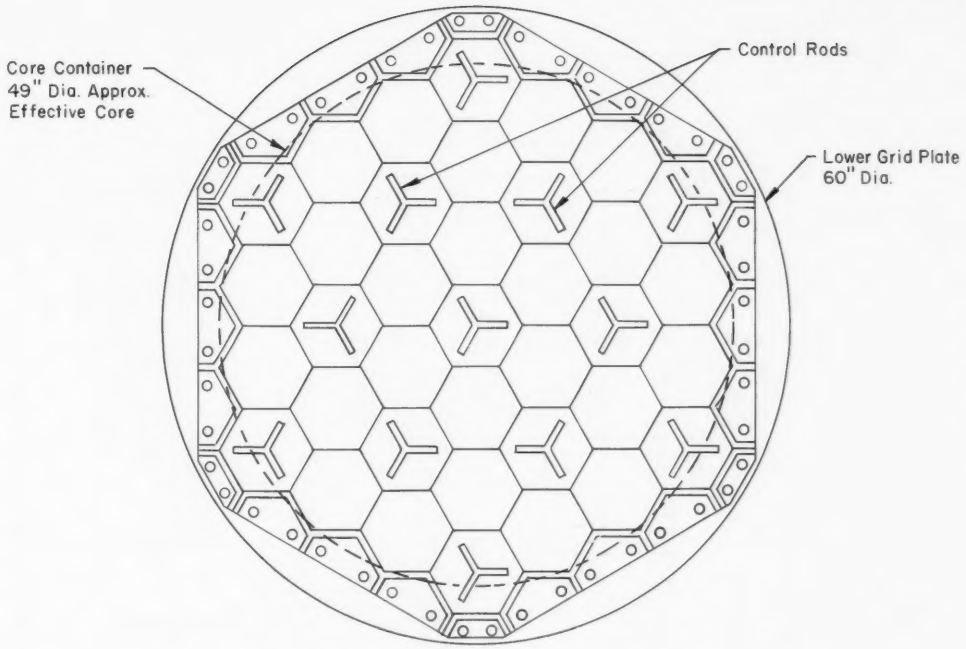

Fig. VII-4 Core cross section of the Consolidated Nuclear Steam Generator.[9]

of the plant is 481 tons. It can be installed in the ship as a unit or, alternatively, it can be loaded as four preassembled and factory-tested modules, each weighing less than 112 tons.

The reactor vessel is 71 in. in inside diameter and is approximately 22 ft high. The once-through heat exchanger, composed of six independent circumferential segments, any five of which will provide full steam flow, is arranged along the inside of the reactor vessel. The total heat-exchanger height is approximately 17 ft. The core can be refueled without removal of the heat exchangers. In the unlikely event of a major heat-exchanger failure, the inoperative segment can be isolated on the secondary side by valves external to the containment vessel. If necessary, the failed segment can be removed and replaced at the next scheduled ship servicing without removal of the core or any other heat-exchanger segments.

The reactor vessel is thermally insulated. Watertight canning extends around the vessel, circulating pumps, and cold shutdown mechanisms. The space between the canned reactor assembly and the containment-vessel wall is filled with borated water to a level over the reactor vessel head. This water provides a reservoir for vapor suppression for the major accident situation and also provides part of the shielding. The principal radiation shielding is provided by iron and water with lead added in local areas for additional gamma attenuation.

Primary water leaving the core flows upward to the steam dome and radially into the six heat-exchanger segments, where it makes a downward pass followed by an upward pass over the total length of the exchanger. It then flows into three downcomers located between pairs of heat-exchanger segments, out through the three pumps, back into the reactor vessel, and down to the core inlet.

The fuel rods are stainless-steel fuel-supported tubes that contain low-enrichment UO_2 and are spaced on a triangular pitch to form the hexagonal clusters. Twelve of the clusters are movable. Each movable fuel cluster is surmounted by a hollow water-filled neutron-absorbing section to form a cold shutdown assembly that can be moved vertically within a Zircaloy guide tube. All these absorber sections are out of the core during operation. There are two coolant passes through the active core, divided as shown in Fig. VII-6. Of the 61 fuel clusters in the core, 36 are in the first

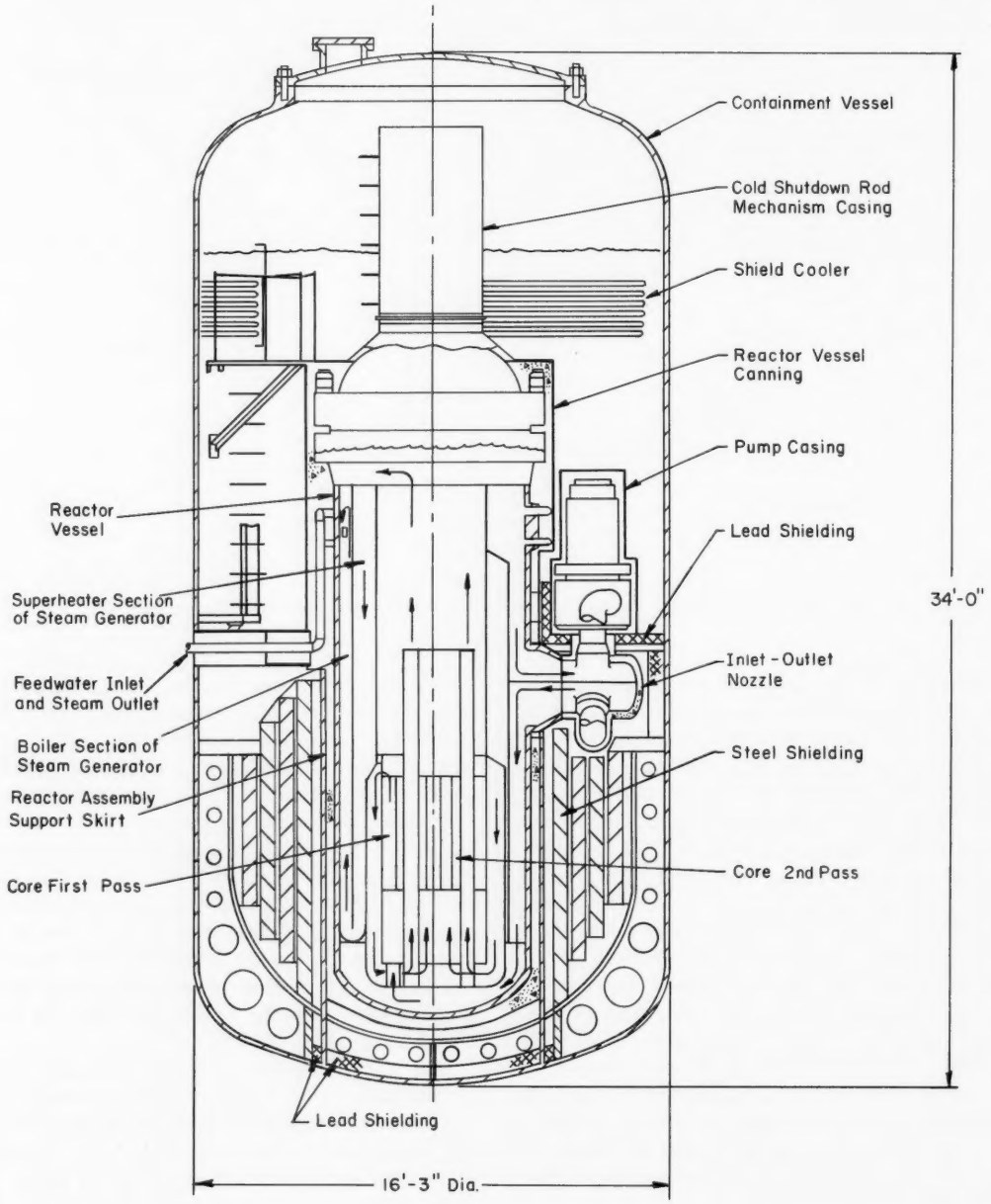

Fig. VII-5 Elevation of the Unified Modular plant.[10]

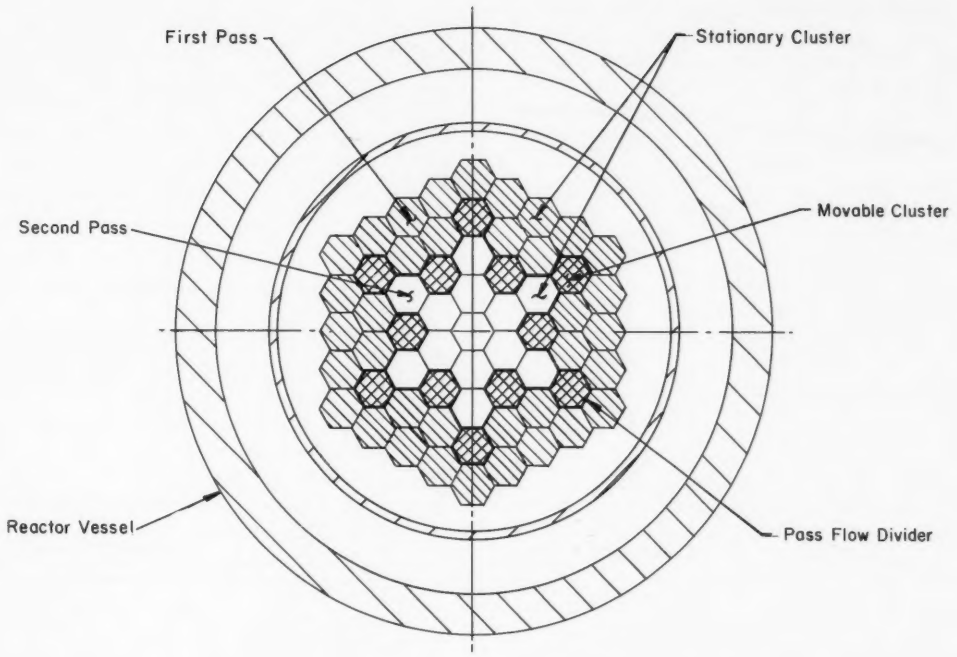

Fig. VII-6 Core cross section of the Unified Modular plant.[10]

(peripheral) pass and 25 in the second (inner) pass. Flow is upward in both passes, the coolant returning between passes to the bottom of the core through the reflector region. Radial power flattening in the core is achieved by the use of two enrichment zones, and burnable poison is used to minimize the lifetime reactivity variation.

The reactor is self-pressurized by a steam dome at the top of the reactor vessel. Net boiling to the extent of 3 to 4% exit quality occurs in the hottest coolant channels, but the effect of the slightly subcooled discharge from the cooler channels, as well as the 5% bypass flow through nonfuel channels in the core, is to reduce the mixed-mean exit temperature to the saturation point under steady-state conditions.

The cold excess reactivity of 13% is held down, under shutdown conditions, by the 12 water-filled absorber control rods. On startup the reactor temperature and pressure are increased to the point that the reactor is just critical with the control rods completely withdrawn. In this condition the control-rod positions are occupied by the fuel-assembly followers, and thereafter, during operation, the reactor is allowed to control itself by means of its rather strong negative temperature coefficient of reactivity.

If the steam flow to the turbine is increased, the initial effect will be to reduce the temperature of the primary water, and the resulting reactivity increase will cause the reactor power to rise until a new equilibrium state is reached in which the reactor power output is just equal to the demand. Reference 10 states that analog-computer studies have shown these changes to occur without power overshoots because the rapidly acting Doppler effect and the negative power coefficient due to the limited amount of boiling in the core come into action during the time-lag interval associated with the heat transport from the primary to the secondary system. Figure VII-7 shows the predicted variation of the coolant temperature and reactor pressure with steady-state power level. It is to be noted that, although the average coolant temperature decreases slightly with power, in order to make up the slight loss of reactivity due to the increased Doppler effect, the outlet temperature, and hence the reactor pressure, actually increases as more power is extracted from the reactor. Figure VII-8 shows the predicted variation in excess reactivity and equilibrium re-

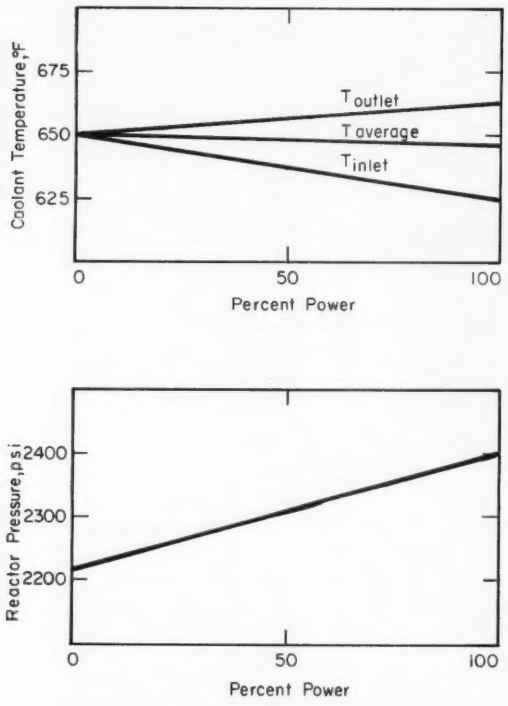

Fig. VII-7 Reactor load characteristics.[10]

actor pressure over the core lifetime. The reactivity change over the interval 1 to 2 (Fig. VII-8), corresponding to the heating up of the reactor, is controlled by the rods. Thereafter the rods remain out, and reactivity changes are compensated by reactor temperature and pressure.

The ability of the pressurized-water reactor to match its output to the load demand is well known, and it is rather common practice to operate such reactors under load-demand control over small ranges of reactivity variation. The departure that is made in the UNIMOD design is to utilize this method of control to compensate all reactivity changes that may occur in the operating core. This is done by designing for a rather large temperature coefficient of reactivity and by holding other reactivity variations to a relatively small range through the use of burnable poisons and a relatively high loading of U^{235}.

It appears from the two design studies discussed above that large improvements in the power-to-weight ratio of pressurized-water propulsion reactors may be possible through the use of the close-coupled concept in combination with the water-filled containment vessel. Although the concept appears to be a straightforward one, there are some questions that apparently have not been entirely resolved. One of these concerns the behavior of the containment vessel in the event of a major rupture of the primary system. Although the equilib-

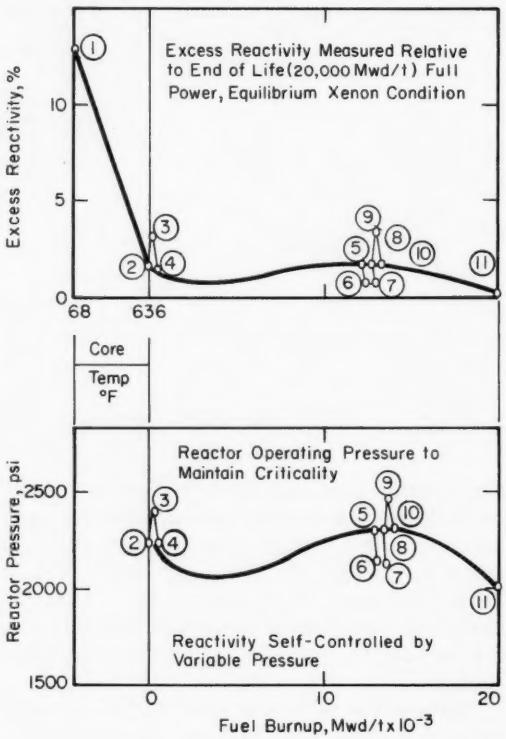

Key for Lifetime Operating Conditions

Point	Conditions			
	Temp	Xenon	Power	Burnup, Mwd/t
1	Cold	Clean	Zero	0
2	Hot			
3			Full	
4		Equilibrium		
5				13,000
6			Zero	
7		Maximum Override		
8		None		
9			Full	
10		Equilibrium		
11				20,000

Fig. VII-8 Lifetime operating conditions.[10]

rium condition can easily be calculated, the possibility of a pressure surge as the result of a major primary-system break apparently needs more attention. Reference 9 notes that the results to date of research on this question are encouraging and that the concept appears practical. Another area involves the question of radioactivity that may enter the containment water from leaks in the primary system. The design concepts minimize this probability through such stratagems as the use of canned-motor pumps. However, it is noted in the CNSG study that there is an accumulation of radioactive materials, which are normally vented through the stack. Apparently these played an important role in determining the size and shielding requirement of the containment vessel as the result of a ground rule which assumed that such venting might not always be permissible.

References

1. George G. Sharp, Inc., Summary Report, The Role of Nuclear Power in the Merchant Marine, VII. A Proposed New System, Maritime Administration Report N-6022, Mar. 15, 1963.
2. High-Speed Nuclear Ships Economic Now, Study Finds, *Nucleonics*, 21(6): 26 (June 1963).
3. General Electric Company, Flight Propulsion Laboratory Department, 630A Maritime Nuclear Steam Generator Scoping Study, USAEC Report GEMP-108, Dec. 15, 1961.
4. General Electric Company, Flight Propulsion Laboratory Department, 630A Maritime Nuclear Steam Generator Progress Report No. 1, USAEC Report GEMP-130, July 31, 1962.
5. General Electric Company, Flight Propulsion Laboratory Department, 630A Maritime Nuclear Steam Generator Progress Report No. 2, USAEC Report GEMP-144, Sept. 28, 1962.
6. General Electric Company, Flight Propulsion Laboratory Department, 630A Maritime Nuclear Steam Generator Progress Report No. 3, USAEC Report GEMP-160, Nov. 30, 1962.
7. General Electric Company, Flight Propulsion Laboratory Department, 630A Maritime Nuclear Steam Generator Progress Report No. 4, USAEC Report GEMP-175, Jan. 31, 1963.
8. *Nucleonics Week*, 3(48): (Nov. 29, 1962).
9. Babcock & Wilcox Co., Consolidated Nuclear Steam Generator for Merchant Ship Application, A Conceptual Design, USAEC Report BAW-1243, August 1962.
10. P. C. Zmola, W. S. Flinn, R. J. Rickert, G. V. Notari, and R. H. Young, The Unified Modular Plant, A Compact Nuclear Steam Generator for Marine Application, USAEC Report CEND-169, Combustion Engineering, Inc., December 1962.

Index

Power Reactor Technology

Volumes 4-6

Included in this issue is a cumulative index for Volumes 4 to 6 of *Power Reactor Technology*. An index for this quarterly is prepared annually and appears in the final (Number 4) issue. In this index the bold numbers denote volumes, the numbers in parentheses denote issues, and the other numbers denote pages.

A

A-nickel alloy, corrosion by carbon monoxide, carbon monoxide–carbon dioxide systems, and carbon monoxide–hydrogen systems, **4**(3): 43-4
  fuel-element applications, **5**(1): 82
A1W Reactor
  See Reactors (A1W)
Accidents, Los Alamos Scientific Laboratory, criticality accident, August 1945, **4**(2): 29
  loss-of-coolant, **4**(1): 38-9
  Oak Ridge National Laboratory criticality accident, May 1954, **4**(2): 29
  Y-12 Plant criticality accident, June 1958, **4**(2): 29
Acetone, reactions with uranium carbides, **4**(1): 47
Acids, reactions with uranium carbides, **4**(1): 47
Activated charcoal
  See Charcoal (activated)
Activation, in boiling-water reactors, **6**(4): 94-6
ADONIS computer code, shields, duct design, **5**(3): 29
Advanced Gas-Cooled Reactor
  See Reactors (Advanced Gas-Cooled) (UK)
Advanced Organic-Moderated Reactor
  See Reactors (Advanced Organic-Moderated)
Advanced Sodium Graphite Reactor
  See Reactors (Advanced Sodium Graphite)
AEC report to the President, **6**(2): 1-4
Age-diffusion kernels, **6**(2): 10
AGN-201 M Reactor
  See Reactors (AGN-201)
AGR Reactor (UK)
  See Reactors (Advanced Gas-Cooled) (UK)
AHFR
  See Reactors (Argonne High-Flux) (AHFR)
Air, reactions with uranium carbides, **4**(1): 46-7
  swirl flow, **6**(1): 21-2
Air-water systems, flow, **5**(3): 19-20
AISI 406 alloy, nuclear superheater applications, **5**(4): 38
Alco Products Critical Facility
  See Reactors (Alco Products Critical Facility)
Alkalies, reactions with uranium carbides, **4**(1): 47
Allis-Chalmers Manufacturing Company, nuclear superheater research, **4**(3): 82
Alpha radiation
  See Radiation (alpha)
ALPR
  See Reactors (SL-1)
Aluminum, compatibility with steel, **4**(1): 1-2
  corrosion, **4**(1): 2; **4**(3): 5-6; **5**(3): 32-3; **5**(4): 40
  criticality effects of tubes, **4**(2): 11
  reactions with uranium carbides, **4**(1): 45
Aluminum alloys, corrosion, **4**(1): 2; **5**(3): 33; **6**(2): 53; **6**(4): 95
  radiation effects, **5**(1): 70
Aluminum-iron alloys, corrosion, **5**(3): 33
  physical properties, **6**(1): 40-1
Aluminum–lithium-6 alloys, reactivity worth, **4**(4): 40
Aluminum-molybdenum-uranium alloys
  See Uranium-molybdenum-aluminum alloys
Aluminum-nickel alloys, corrosion, **5**(3): 33
Aluminum oxide, compatibility with gaseous coolants, **5**(3): 61
Aluminum-plutonium alloys
  See Plutonium-aluminum alloys
Aluminum-silicon systems, corrosion, **5**(3): 33
Aluminum-titanium alloys, corrosion, **5**(3): 33
Aluminum-uranium alloys
  See Uranium-aluminum alloys
Ammonia, hydrazine synthesis from, **4**(3): 1-2
  reactions with uranium carbides, **4**(1): 47
Ammonium citrate process, corrosion of reactor materials, **4**(3): 45
Analytical methods, reactor kinetics, **4**(2): 28-30
Annuli
  See also Tubes
  burnout, **4**(3): 21-4; **5**(2): 16, 18
  cooling with solid-gas systems, **4**(3): 16-17
  forced-convection heat transfer, **4**(2): 13-15
Annuli (eccentric), heat transfer, **6**(2): 18-19
ANP Reactors
  See Reactors (ANP)
ANPP Code Development Program
  See Army Nuclear Power Program Code Development Program
Antimony, shielding applications, **4**(20): 34
APDA Fast-Breeder Reactor
  See Reactors (Enrico Fermi Fast-Breeder)
APPR
  See Reactors (SM-1)
Approach-to-critical experiments, NRU Reactor, **4**(2): 11
APS-1 Reactor (USSR)
  See Reactors (APS-1) (USSR)
Aqueous Homogeneous Suspension Reactor
  See Reactors (HR-2)
Argonne High-Flux Reactor
  See Reactors (Argonne High-Flux) (AHFR)
Argonne Low-Power Reactor
  See Reactors (SL-1)
Argonne National Laboratory, nuclear superheater research, **4**(3): 82-3
Army Nuclear Power Program Code Development Program, **6**(3): 83
Army Package Power Reactor
  See Reactors (SM-1)
ASME Boiler and Pressure Vessel Codes
  See Boiler Codes
ASTM boiler codes
  See Boiler codes
Atomic power
  See Nuclear power
Atomic power plants
  See Power plants (nuclear)
Atomics International, Division of North American Aviation, Inc., nuclear superheater research, **4**(3): 83
Autoradiography, nondestructive testing techniques, **5**(1): 71
AVR Reactor (West Germany)
  See Reactors (AVR) (West Germany)

B

Barytes concretes, shielding properties, **5**(3): 27-8
Benzene, pool boiling, **6**(1): 19-20
  reactions with uranium carbides, **4**(1): 47
Benzene-biphenyl systems, pool boiling, **6**(1): 19-20
BEPO Reactor
  See Reactors (BEPO)
Berkeley Reactors (UK)
  See Reactors (Berkeley) (UK)
Beryllium, corrosion, **5**(2): 48-9; **5**(4): 40; **6**(2): 53
  differential scattering cross sections, **6**(2): 11
  fabrication difficulties, **5**(2): 48, 49-50
  moderating properties, **5**(1): 7-8; **5**(2): 4
  neutron age, **5**(1): 7

Beryllium (Continued)
neutron reflection, 4(3): 10
radiation effects, 4(1): 65; 5(2): 49
reactions with uranium carbides, 4(1): 46
reactor applications, 5(2): 48-50
structural applications, 6(1): 40
Beryllium alloys, development, 6(1): 40
Beryllium-moderated reactors
See Reactors (beryllium-moderated)
Beryllium oxide, compatibility with gaseous coolants, 5(3): 61
differential scattering cross sections, 6(2): 11
moderating properties, 5(1): 7-8; 5(2): 4
neutron age, 5(1): 6-7
neutron-reflecting properties, 5(2): 4
radiation effects, 6(1): 38-40
Beryllium oxide–uranium oxide systems
See Uranium dioxide–beryllium oxide systems
Beryllium-uranium alloys
See Uranium-beryllium alloys
Bibliographies, fissile materials, handling, storage, and safety, 5(3): 8
nuclear superheater materials, 5(4): 38
pressure drop, 5(4): 24
shielding, 5(4): 28
Big Rock Point Power Reactor
See Reactors (Big Rock Point Power)
Biphenyl, chemical structure, 6(1): 64
moderating properties, 5(1): 7-8
pool boiling, 6(1): 19-20
stability under reactor conditions, 6(3): 70-2
Biphenyl-benzene systems
See Benzene-biphenyl systems
Biphenyl, isopropyl, stability under reactor conditions, 6(3): 70-2
Biphenyl-uranium lattices
See Uranium-biphenyl lattices
Bismuth, reactions with uranium carbides, 4(1): 46
Blankets
See Breeding blankets
Blast protection, 6(3): 1-3
Blast-resistant structures
See Structures (blast-resistant)
BN-50 Reactor (USSR)
See Reactors (BN-50) (USSR)
Bohunice Reactor (Czechoslovakia)
See Reactors (Bohunice) (Czechoslovakia)
Boiler codes, ASME boiler and pressure vessel codes and specifications, 4(2): 44-8; 6(3): 41-3
ASTM specifications for reactor pressure vessels, 4(4): 50-1
British specifications for reactor pressure vessels, 4(4): 51-4
Boilers
See Steam generators
Boiling
See also Bubbles
bubble formation, 4(2): 26; 5(4): 25
bubble growth, 5(3): 13-15
Boiling, burnout, 4(3): 21-4; 4(4): 25-8; 5(1): 17-21; 5(2): 10-12, 15-19; 5(3): 15-18; 6(1): 16-18; 6(2): 20-24; 6(4): 58-60
convection, 6(4): 58
fluid flow, 6(4): 55-60
heat transfer, 4(2): 15-18; 4(3): 24-6; 5(1): 12-17; 5(4): 24-26; 6(2): 19-25; 6(4): 55-60
from fuel elements (plates), 5(1): 24-30
songs, in rectangular channels, 4(1): 29
stability, 5(4): 26
transient experiments, 4(2): 26-7
void fractions, 5(4): 24-6
Boiling (bulk), heat transfer with terphenyl, 4(4): 82
Boiling (film), 6(2): 25
Boiling (local), heat transfer, 5(2): 11-12
Boiling (nucleate), departure from, 4(1): 27-9; 4(3): 24-5; 5(1): 13-14, 18; 5(2): 15-17; 6(1): 19-20; 6(4): 86
heat transfer, 4(1): 27-9; 5(2): 11
with terphenyl, 4(4): 82
hydrodynamic factors, 4(3): 25
in spray cooling, 4(4): 22
subcooled, in forced convection, 6(1): 15-16
Boiling (pool), 5(3): 13-15; 5(4): 26; 6(1): 19-21
Boiling (transient), 5(3): 18
Boiling heavy-water reactors
See Reactors (boiling heavy-water)
Boiling Reactor Experiments
See Reactors (BORAX)
Boiling songs, in rectangular channels, 4(1): 29
Boiling-water reactors
See Reactors (boiling-water)
BONUS Reactor
See Reactors (BONUS)
Boral, evaluation for control applications, 6(3): 82
shielding properties, 4(2): 36
BORAX Reactors
See Reactors (BORAX)
Borides
See also specific borides
corrosion, 4(4): 42-3, 44
radiation effects, 4(4): 42-3, 44
Boron, corrosion-inhibition effects, 5(4): 40
corrosion by steam, 4(4): 44
radiation effects, 4(4): 44
reactivity-worth burnup, 4(4): 41
solubility in boiling water, 4(4): 43
Boron-10, evaluation for reactor control, 6(2): 48-9
Boron carbide–dysprosium oxide systems, evaluation for control applications, 6(3): 82
Boron carbide–nickel systems, evaluation for reactor control, 6(2): 49
Boron carbides, control rods, lifetime, 5(3): 34
corrosion by steam, 4(4): 44
radiation effects, 4(4): 44
reactivity worth, 4(4): 40, 41
solubility in boiling water, 4(4): 43
Boron carbides (B_4C), evaluation for control applications, 6(3): 82
Boron glass, reactivity worth, 4(4): 40
Boron nitrides, corrosion by steam, 4(4): 44
solubility in boiling water, 4(4): 43
Boron oxides (B_2O_3), evaluation for control applications, 6(3): 82
Boron–stainless-steel systems
See also stainless steel (boron)
failure in control rods, 4(4): 43, 45-6
poisoning properties, 4(2): 10
Boron steel
See Steel (boron)
Boundary layer, heat-transfer effects, 4(2): 16-17
BR-2 Reactor
See Reactors (BR-2) (Belgium)
BR-3 Reactor
See Reactors (BR-3) (Belgium)
BR-5 Fast Reactor
See Reactors (BR-5) (USSR)
BR-5 Reactor (USSR)
See Reactors (BR-5) (USSR)
Bradwell Reactors (UK)
See Reactors (Bradwell) (UK)
BREACH computer code, 5(1): 20
Breeder reactors
See Reactors (breeder)
Breeding, 4(1): 5-9
factors in U^{238}-Pu^{239} systems, 4(4): 91-4
in nuclear superheaters, 4(3): 83
uranium carbides, ratios, 4(1): 51-2
uranium-molybdenum alloys, 4(1): 51-2
Breeding blankets, analysis of irradiated, 5(1): 1
Experimental Breeder Reactor I, 5(2): 25-6
plutonium buildup, 5(4): 67
Breeding-blanket elements (rods), radiation-effects studies, 5(4): 18-19
Bromine, reactions with uranium carbides, 4(1): 47
Bubbles
See also Boiling
formation, 4(3): 24; 5(4): 25
in boiling in SPERT reactors, 5(1): 24-30
by nucleation, 4(2): 26
growth, 5(3): 13-15
Bulk Shielding Reactors
See Reactors (Bulk Shielding Facility)
Burners, for high-boiling fractions from Piqua Power Reactor, 4(2): 83-4
Burnout, 4(3): 17-24; 4(4): 25-8; 5(1): 17-20; 5(3): 15-18; 6(2): 20-4; 6(3): 5
boiling effects, 6(1): 16-18
boiling water, 5(2): 10-12, 15-19; 6(4): 58-60
BORAX-I Reactor, 4(1): 38
correlation of factors, 6(1): 18-19
effect of flow and pressure drop, 4(2): 18
free convection conditions, 4(2): 17-18
in two-phase flow, 6(3): 10
metals (liquid), 6(4): 54-5
pressurized-water reactors, 5(1): 11-12
SPERT-I Reactor, 4(1): 38
TREAT Reactor, 4(1): 40-1
Burnup, plutonium-thorium fuels, 5(1): 2
Butterfly valves
See Valves (butterfly)
Byeloyarsk Reactor (USSR)
See Reactors (Byeloyarsk) (USSR)

C

Cables (coaxial)
See Coaxial cables
Cadmium, corrosion by water, 6(2): 53
evaluation for control applications, 6(3): 82
flux hardening effects, 4(1): 11-12
neutron absorption, 5(1): 4
reactivity-worth burnup, 4(4): 41-2
Cadmium-covered gold foils
See Foils (gold, cadmium-covered)
Cadmium-indium-silver alloys, control-rod applications, 4(3): 48-50
reactivity-worth burnup, 4(4): 42
Cadmium-indium-silver alloys (silver-plated), corrosion in Yankee Power Reactor, 6(4): 82
Cadmium ratios, 5(2): 2
Cadmium-silver alloys, evaluation for control applications, 6(3): 82
reactivity worth, 4(4): 40
Cadmium tantalates ($Cd_2Ta_2O_7$), evaluation for reactor control, 6(2): 49
Calandria, sodium graphite reactors, 4(3): 88, 89-91
Calcium boride (CaB_6), corrosion by steam, 4(4): 44
radiation effects, 4(4): 44
solubility in boiling water, 4(4): 43
Calcium oxide–uranium dioxide–zirconium oxide systems
See Uranium oxide–calcium oxide–zirconium oxide systems (UO_2-CaO-ZrO_2)
Calder Hall Reactors (UK)
See Reactors (Calder Hall) (UK)
Canada, coal reserves, 4(2): 1-2
CANDU Reactor (Canada)
See Reactors (CANDU) (Canada)
Canned moderators
See Moderators (canned)
Carbon, compatibility with gaseous coolants, 5(3): 61
criticality effects, 5(2): 1
moderating properties, 5(1): 7-8
removal from sodium (liquid), 5(4): 74
Carbon oxide–hydrogen systems (CO-H_2), corrosion of A-nickel, chromium-molybdenum steel, copper, Inconel, Inconel 702, Inconel X, molybdenum, Monel, niobium, niobium-titanium alloys, niobium-zirconium alloys, and stainless steel, 4(3): 43-4

Carbon oxide–hydrogen systems ($CO-H_2$) (Continued)
corrosion inhibition applications, 4(3): 44-6
Carbon oxides (CO), compatibility with ceramic fuel elements, 5(3): 61
corrosion, of A-nickel, chromium-molybdenum steel, copper, Inconel, Inconel 702, Inconel X, molybdenum, Monel, niobium, niobium-titanium alloys, niobium-zirconium alloys, and stainless steel, 4(3): 43-4
of iron alloys, 4(3): 43
of nickel alloys, 4(3): 43
removal from helium, 5(4): 78
Carbon oxides (CO_2), corrosion, of beryllium, 5(2): 48-9
of iron alloys, 4(3): 43
of nickel alloys, 4(3): 43
reactions with uranium carbides, 4(1): 47
Carbon oxides (CO_2) (supercritical), heat transfer, 5(3): 20
Carbon oxides ($CO-CO_2$ systems), corrosion of A-nickel, chromium-molybdenum steel, copper, Inconel, Inconel 702, Inconel X, molybdenum, Monel, niobium, niobium-titanium alloys, niobium-zirconium alloys, and stainless steel, 4(3): 43-4
Carbon steel
See Steel (carbon)
Carbon tetrachloride, reactions with uranium carbides, 4(1): 47
Carbon-uranium systems
See Uranium-graphite systems
Carbonic acid, corrosion of aluminum, 4(3): 46
Carborundum
See Silicon carbide
Carolinas-Virginia Reactor
See Reactors (Parr Shoals Power) (CVTR)
Carrier Vessel Reactor
See Reactors (A1W)
Centrifugal pumps
See Pumps (centrifugal)
Ceramic fuel elements
See Ceramic materials; Fuel elements (ceramic)
Ceramic materials
See also Fuel elements (ceramic); specific materials, e.g., Uranium oxides (UO_2)
emittance, 5(4): 26
uranium oxide–calcium oxide–zirconium oxide systems (UO_2-CaO-ZrO_2), 5(1): 67
Cesium chloride–lithium chloride–rubidium chloride–sodium chloride systems, fuel cell applications, 4(3): 2
CETR
See Reactors (Indian Point Power) (CETR)
Channels
See also Tubes
void static distribution in boiling, 4(2): 28
Channels (circular), hydrodynamic characteristics, 4(1): 59
superheated-steam heat transfer, 4(2): 20
Channels (fuel), spacing measurement methods, 4(1): 32
temperature determination methods, 4(1): 30
Channels (rectangular), boiling songs, 4(1): 29
burnout, 4(3): 17-21
flow distribution determination, steady state, 4(1): 32
friction factors, 6(2): 18-19
heat transfer, 4(2): 19-20; 5(1): 11
Channels (square), hydrodynamic characteristics, 4(1): 59
Chapelcross Reactors
See Reactors (Chapelcross) (UK)
Charcoal (activated), iodine adsorption, 6(3): 20-1
Chemonuclear reactors
See Reactors (chemonuclear)
Chlorine, inhibition of graphite oxidation, 5(3): 66
reactions with uranium carbides, 4(1): 47
Chromium, cooling with mercury, 4(3): 15
Chromium-molybdenum steel
See Steel (chromium-molybdenum)
CHRONOS computer code, 5(1): 7
Circular fuel channels
See Channels (circular)
Circulation systems, Experimental Organic-Cooled Reactor, 5(1): 90-1
CNSG
See Reactors (Consolidated Nuclear Steam Generator) (CNSG)
Coal, Canadian reserves, 4(2): 1-2
European reserves, 4(2): 1-2
U. S. reserves, 4(2): 1-3
Coal-fired power plants
See Power plants (conventional)
Coaxial cables, 4(4): 36
COD (S-4) process, corrosion of reactor materials, 4(3): 45
reactor decontamination, effectiveness, 4(3): 45
Coextrusion, stainless steel with Zircaloy, 6(2): 51-3
Columbium
See Niobium
Combustion Engineering–General Nuclear Engineering Corp., nuclear superheater research, 4(3): 76-82
Commonwealth Edison Reactor
See Reactors (Dresden Power)
Compaction, fuel elements, 5(1): 63
Computer codes, ADONIS, 5(3): 29
BREACH, 5(1): 20
CHRONOS, 5(1): 7
CORN PONE, 5(1): 7
DSN, 6(4): 47
EXCEL, 6(4): 40
FORTRAN, 5(4): 19; 6(4): 47
FUGUE, 5(1): 20
HERESY-I, 6(2): 9
IDIOT, 5(3): 7
LEAP, 6(4): 47
MAC, 6(3): 84
MELEAGER CHAIN, 5(4): 9
MUFT, 5(1): 1; 5(2): 2, 4, 6
PIXMIX, 6(4): 47
PIXSE, 6(4): 47
SNG, 6(4): 40, 47
SOFOCATE, 5(1): 1; 5(2): 2, 4, 6
SPAN-3, 5(4): 28
SWAKRAUM, 6(4): 40
THERMOS, 5(4): 16; 6(4): 40
Concrete
See also specific types of concrete, e.g., Limonite, etc.
shielding applications, 5(3): 27-8
shielding properties, at elevated temperatures, 4(2): 34-5
water loss effects on, 4(2): 35
Concrete (prestressed), pressure-vessel design, 5(4): 78-80
Condensation, steam, 5(3): 18-19
Conduction (thermal)
See Thermal conductivity
Conferences, Fifth National Heat Transfer Conference and Exhibit, Houston, Tex., Aug. 5–8, 1962, 6(1): 15-25
IAEA Symposium on Power Reactor Experiments, Vienna, Oct. 1961, 5(4): 87-92
International Heat Transfer Conference, University of Colorado, Boulder, Aug. 28–Sept. 1, 1961, 5(3): 12-26
Reactor Kinetics Conference, Sun Valley, Idaho, Oct. 12–14, 1960, 4(2): 22-30
Symposium on Sodium Reactors Technology, Lincoln, Nebr., May 24–25, 1961, 6(1): 60
Consolidated Edison reactors
See Reactors (Indian Point Power) (CETR); Reactors (Ravenswood Power)
Consolidated Edison Thorium Reactor
See Reactors (Indian Point Power) (CETR)
Consolidated Nuclear Steam Generator
See Reactors (Consolidated Nuclear Steam Generator) (CNSG)
Construction practices, 4(2): 44-51
Consumers Power Reactor
See Reactors (Big Rock Point Power)
Containment, 4(2): 31-3; 5(1): 33-6; 5(2): 51-5
Dresden Power Reactor, 4(4): 66-7
Elk River Power Reactor, 5(2): 44-6
heat transfer after cooling-system rupture, 4(2): 31-2
Indian Point Power Reactor, 6(3): 39
iodine removal from building, 5(4): 29-33
N. S. *Savannah* Reactor, 6(1): 54
Parr Shoals Power Reactor, 6(4): 79-81
Piqua Power Reactor, 5(4): 59-60
Peach Bottom Power Reactor, 5(3): 62-3
pressure suppression, 4(2): 32-3
Ravenswood Power Reactor. 6(3): 21-6
SPERT-III Reactor, 5(3): 85
Yankee Power Reactor, 4(3): 55
Control
See also Control rods
Dresden Power Reactor, 4(4): 61, 62-3, 67
Hallam Power Reactor, 5(3): 50-1
Indian Point Power Reactor, 6(3): 32, 33, 34, 39-40
sodium graphite reactors, 4(3): 92-3
Yankee Power Reactor, 4(3): 53-4, 55
Control materials, 4(4): 39-46; 6(2): 48-9; 6(3): 15-16
evaluation, 6(3): 82
Control-rod drives
Indian Point Power Reactor, 6(3): 35-6
N. S. *Savannah* Reactor, 6(1): 50-2
Control rods, boiling-water reactors, 4(3): 87
cadmium, 5(1): 4
cadmium-indium-silver alloys, 4(3): 48-51
design, for Dresden Power Reactor, 4(4): 46, 59; 5(3): 34
for Nuclear Steam Generator 630A, 6(4): 109
for Parr Shoals Power Reactor, 6(4): 66, 81
Elk River Power Reactor, 5(2): 35, 38
failure, of boron–stainless-steel systems, 4(4): 45-6
in experimental Boiling-Water Reactor, 4(4): 45-6
gadolinium oxide–samarium oxide, 5(3): 42-3
Hallam Power Reactor, design, 5(3): 42-3
Indian Point Power Reactor, 6(3): 68
lifetime, 5(3): 34
N. S. *Savannah* Reactor, 6(1): 47
nuclear superheaters, 4(3): 79, 82
Organic-Moderated Reactor Experiment, 4(4): 45
Pathfinder Power Reactor, 5(2): 46-7
Piqua Power Reactor, 5(4): 52-4
PM-1 Reactor, 6(3): 46
Shippingport Pressurized-Water Reactor, 4(4): 45
sodium graphite reactors, 5(4): 74-5
Sodium Modular Reactor, 4(3): 93, 95
Spectral Shift Control Reactor, 5(4): 84
Vallecitos Boiling-Water Reactor, 4(4): 45
Yankee Power Reactor, 4(3): 48-50; 6(4): 82
Control systems, Elk River Power Reactor, 5(2): 40-1, 46
Convection (forced), in annuli, 4(2): 13-15
burnout, 4(3): 24
coefficients in superheated steam, 4(2): 19
heat transfer, 5(3): 22; 5(4): 25-6; 6(2): 18-19
in spray cooling, 4(4): 22
subcooled nucleate boiling, 6(1): 15-16
under boiling conditions, 6(4): 58
Convection (free), 5(3): 24-5
boiling heat transfer, 4(2): 17
burnout, 4(2): 17-18; 4(3): 17-21
Conventional power plants
See Power plants (conventional)

Coolant flow
See also Fluid flow; Gas flow; Liquid flow; Slurry flow; Steam flow
boiling-water reactors, 5(2): 14-15
BONUS Reactor, 4(3): 72-82
Experimental Breeder Reactor I, 5(2): 25-6
organic-cooled and -moderated reactors, 4(1): 59
Pathfinder Power Reactor, 4(3): 82
Piqua Power Reactor, 5(4): 55
Shippingport Pressurized-Water Reactor, 6(3): 49-50
sodium graphite reactors, 4(3): 90
Sodium Modular Reactor, 4(3): 93, 94
SPERT reactors, 5(1): 28-30; 5(2): 24
supercritical water reactors, 4(2): 79-80
Coolant purification, 4(3): 44-6
Elk River Power Reactor, 5(2): 43
Piqua Power Reactor, 5(4): 56-7
sodium (liquid), 5(3): 48
Coolant radioactivity, control in Shippingport Pressurized-Water Reactor, 5(4): 69-70
Experimental Boiling-Water Reactor, 4(3): 65-9
Sodium Reactor Experiment, 5(4): 73
Coolants, contamination, 5(3): 62-3; 5(4): 30
radioactivity induction, 5(4): 43-6
sodium (liquid), 5(3): 46, 48; 5(4): 73-5
Coolants (gaseous), compatibility with ceramic fuel elements, 5(3): 61
helium, 4(1): 63; 5(3): 67-8; 5(4): 76-8
nitrogen, 5(4): 26
temperature measurement, 5(3): 65-6
Coolants (organic), 6(1): 62-73
decomposition in Organic-Moderated Reactor Experiment, 4(4): 76, 80
pool boiling, 6(1): 19-20
purification, 4(2): 82-3; 6(3): 70
in reactors, 6(2): 57-9
Santowax OM, 5(3): 57
Santowax OMP, 5(1): 88; 5(3): 57
Santowax R, 5(1): 88; 5(3): 52-6, 57
stability under reactor conditions, 4(4): 76, 79, 82; 5(3): 52-6, 57; 6(3): 70-2
terphenyls, 5(3): 57
Cooling (spray)
See Cooling systems (spray)
Cooling systems
See also under specific reactors
deposits, radioactive, 5(4): 43-6
design modifications in Sodium Reactor Experiment service cooling system, 4(4): 73
Dresden Power Reactor, 4(4): 61-2, 63-6
Elk River Power Reactor, 5(2): 39, 41-3, 44
gas-circulating equipment, 6(1): 79-80
Hallam Power Reactor, 5(3): 39, 44-6, 48
Indian Point Power Reactor, 6(3): 37-8
N. S. *Savannah* Reactor, 6(1): 52
Parr Shoals Power Reactor, 6(4): 75-8
Peach Bottom Power Reactor, 5(3): 62-3
Piqua Power Reactor, 5(4): 55-6
SPERT-III Reactor, 5(3): 85-6
Variable-Moderated Reactor, 5(3): 89
Yankee Power Reactor, 4(3): 50-2, 54
Cooling systems (spray), 4(4): 20-5
heat transfer, 5(1): 12
heat transfer during rupture of pressurized water, 4(2): 31-2
Copper, cooling with mercury, 4(3): 15
corrosion by carbon monoxide, carbon monoxide–carbon dioxide systems, and carbon monoxide–hydrogen systems, 4(3): 43-4
neutron absorption cross section, 4(1): 19
Copper (chrome-plated), cooling with mercury, 4(3): 15
Copper–europium hexaboride systems
See Europium hexaboride–copper systems
CORN PONE computer code, 5(1): 7
Corrosion
See also as subheading under specific corrodants and materials
effects of water on common reactor materials, 6(2): 53
graphite, 5(1): 80-1
stainless steel (304), 5(1): 76-7
stainless steel (304L), 5(1): 76-7
stress, in stainless steels, 6(2): 50-1
Zircaloy-2 alloy, 5(1): 69; 6(3): 16-17
Corrosion inhibitors, hydrogen peroxide–carbonate solutions, 4(3): 44-6
Corrosion products
See also Crud
radioactivity, 5(4): 43-6
Coupled reactors
See Reactors (coupled)
CPC Reactor
See Reactors (Big Rock Point Power)
Critical assemblies
See Reactors (name of critical assembly)
Critical experiments, 4(3): 4-12; 4(4): 11-13; 5(4): 15-18; 6(1): 3-4; 6(2): 12-16; 6(3): 80-3
BR-3 Reactor, 4(1): 22
High-Temperature Test Facility, 4(1): 23-4
plutonium-graphite systems, 4(1): 23
plutonium-Plexiglas systems, 4(1): 23
Thorium Uranium Physics Experimental Program, 4(1): 22-3
uranium-zirconium alloys (zirconium-clad), 4(1): 23-4
uranyl nitrate–water systems, 4(1): 23
in Yankee Power Reactor, 4(1): 21-2
Criticality
See also as subheading under specific reactor, alloys, etc.
calculations in heterogeneous reactors, 6(2): 8-9
Criticality studies, 5(2): 1-3; 5(3): 6-8
Hallam Power Reactor, 5(1): 5-6
Spectral Shift Control Reactor, 5(1): 5
U^{235}, 5(1): 6
uranium dioxide (enriched), 5(1): 4-5
uranium-molybdenum alloys, 5(1): 5-6
Crud
See also Corrosion products
control with lithium hydroxide, 6(2): 47-8
deposits in Experimental Boiling-Water Reactor, 6(4): 95
deposits in Yankee Power Reactor, 6(4): 82-3

D

Dana Plant, design, 5(4): 1-5
Dancoff integral, 4(1): 16
Decontamination, carbon steel, 4(2): 49
cooling systems, 5(4): 45-6
helium, 5(4): 76-8
water in pressurized-water reactors, 4(3): 44-6
Degassing, Piqua Power Reactor, 5(4): 56-7
Departure from nucleate boiling, 4(3): 24; 5(1): 13-14, 18
burnout correlation, 6(1): 19-20
heat transfer from horizontal tubes, 4(1): 27-9
Shippingport Pressurized-Water Reactor, 5(2): 15-17
Yankee Power Reactor, 6(4): 86
Destructive testing, fuel-element cladding materials, 5(1): 69-70
Deuterium oxide
See Heavy water
DIDO Reactor
See Reactors (DIDO)
DIMPLE pile oscillator
See Reactors (DIMPLE)
Diphenyl
See Biphenyl
DNB
See Departure from nucleate boiling
Doppler effect, in thermal reactors, 4(4): 14-17
Doppler temperature coefficients, 4(1): 12-14
Dounreay Fast-Breeder Reactor (UK)
See Reactors (Dounreay Fast-Breeder) (UK)
Dowex 1 resin, radiation effects, 5(4): 48
Dowex 50W resin, radiation effects, 5(4): 48
Dowtherm A, thermal-neutron diffusion, 4(1): 16-17
Dragon Reactor
See Reactors (Dragon) (UK)
Dresden Power Reactor
See Reactors (Dresden Power)
DSN computer code, neutron cross-section calculations, 6(4): 47
Ducts, design for gas-cooled reactors, 4(1): 65-7
neutron transmission, 6(3): 86-7
in shields, 5(3): 29
Dungeness Reactors (UK)
See Reactors (Dungeness) (UK)
Duolite C-10 resin, radiation effects, 5(4): 48
Dysprosium, reactivity-worth burnup, 4(4): 42
Dysprosium compounds, evaluation for reactor control applications, 6(3): 15
Dysprosium oxide, evaluation for control applications, 6(3): 82
reactivity worth, 4(4): 41
Dysprosium oxide–boron carbide systems
See Boron carbide–dysprosium oxide systems

E

EBOR
See Reactors (Experimental Beryllium Oxide) (EBOR)
EBR
See Reactors (Experimental Breeder) (EBR)
EBWR
See Reactors (Experimental Boiling-Water)
Economics of nuclear power, 4(4): 1-10; 5(4): 1-7; 6(1): 1-2; 6(2): 1-4; 6(3): 1-3
See also specific power reactors
breeding and conversion of nuclear fuels, 6(4): 1-4
Enrico Fermi Fast-Breeder Reactor fuel-fabrication costs, 4(4): 93
heavy-water reactors, 4(2): 62-4, 67, 68, 69-73
Plutonium-Fuel Fast-Breeder Reactor, 4(4): 94
Plutonium-Fuel Fast-Breeder Reactor fuel-fabrication costs, 4(4): 93
plutonium-thorium fuel cycle, 5(1): 1-3
remote power stations, 4(2): 4-9
seed-blanket reactors, 4(3): 38-41
sodium graphite reactors, 4(3): 92
EDF Reactors (France)
See Reactors (EDF) (France)
EFOR
See Reactors (Experimental Fast Oxide) (EFOR)
EGCR
See Reactors (Experimental Gas-Cooled) (EGCR)
EL-4 Reactor
See Reactors (EL-4)
Electromagnetism, nondestructive testing applications, 5(1): 72-3
Electron microscopy, nondestructive testing applications, 5(1): 72
Electron radiography, nondestructive testing applications, 5(1): 71
Elk River Power Reactor
See Reactors (Elk River Power)
ELTHR
See Reactors (Experimental Low-Temperature Process-Heat)
Energy, available from coal, 4(2): 2-3
available from uranium, 4(2): 2-3
Engineering Test Reactor
See Reactors (Engineering Test) (ETR)
Enriched uranium
See Uranium (enriched); Uranium (highly enriched)
Enriched uranium dioxide
See Uranium oxides (enriched)

Enrico Fermi Fast-Breeder Reactor
See Reactors (Enrico Fermi Fast-Breeder)
EOCR
See Reactors (Experimental Organic-Cooled) (EOCR)
Epoline-n (boron carbide-impregnated), moderating properties, 4(3): 5
Erbium, reactivity-worth burnup, 4(4): 42
Erbium compounds, evaluation for reactor control applications, 6(3): 15
Erbium oxide, reactivity worth, 4(4): 40
ESADA Reactor
See Reactors (Vallecitos Experimental Superheat) (VESR)
Ethanol, reactions with uranium carbides, 4(1): 47
Ethylene glycol, reactions with uranium carbides, 4(1): 47
swirl flow, 6(1): 21-2
synthesis from methanol, 4(3): 1
ETR
See Reactors (Engineering Test)
European coal reserves, 4(2): 1-2
Europium, reactivity-worth burnup, 4(4): 42
Europium boride (EuB_6), corrosion by steam, 4(4): 44
radiation effects, 4(4): 44
solubility in boiling water, 4(4): 43
Europium boride–copper systems (EuB_6-Cu), reactivity worth, 4(4): 39, 40
Europium compounds, evaluation for reactor control applications, 6(3): 15
Europium titanate, control-rod applications, 6(3): 46
EXCEL computer code, neutron-flux calculations, 6(4): 40
Experimental Beryllium Oxide Reactor
See Reactors (Experimental Beryllium Oxide) (EBOR)
Experimental Boiling-Water Reactor
See Reactors (Experimental Boiling-Water)
Experimental Breeder Reactors
See Reactors (Experimental Breeder) (EBR)
Experimental Fast Oxide Reactor
See Reactors (Experimental Fast Oxide) (EFOR)
Experimental Gas-Cooled Reactor
See Reactors (Experimental Gas-Cooled) (EGCR)
Experimental Low-Temperature Process-Heat Reactor
See Reactors (Experimental Low-Temperature Process-Heat)
Experimental Organic-Cooled Reactor
See Reactors (Experimental Organic-Cooled) (EOCR)
Exponential experiments, 4(4): 11-13; 5(2): 1-3; 5(3): 6-8; 5(4): 15-18; 6(1): 3-4; 6(2): 12-16; 6(3): 80-3
Physical Constants Testing Reactor, 5(1): 4
Spectral Shift Control Reactor, 5(1): 5
uranium dioxide lattices, 5(1): 4-5
Extrusion
See also Coextrusion
fuel elements, 5(1): 62-3

F

Failed-Element Detection and Location System, Shippingport Pressurized-Water Reactor, 6(3): 49
Fast-breeder reactors
See Reactors (fast-breeder)
Fast reactors
See Reactors (fast)
FBGR
See Reactors (Fuel-Bearing Graphite) (FBGR)
FEDAL System
See Failed-Element Detection and Location System
Federal regulations, radiation-protection standards, 4(1): 43-4
Fermi Fast-Breeder Reactor
See Reactors (Enrico Fermi Fast-Breeder)
Ferrophosphorus concrete, shielding properties, 4(2): 34
at elevated temperatures, 4(2): 35
Ferrous alloys
See Iron alloys; Stainless steel; Steel; specific iron alloys
Filters, iodine adsorption, 6(3): 20-1
Finned fuel elements
See Fuel elements (finned)
First Atomic Power Station Reactor
See Reactors (First Atomic Power Station) (USSR)
Fissile materials, bibliographies on handling, storage, and safety, 5(3): 8
Fission-gas release, BORAX-IV Reactor, 4(1): 54
Experimental Boiling-Water Reactor, 4(1): 52-3
Shippingport Pressurized-Water Reactor, 4(1): 54
temperature effects on rates, 4(1): 54
from uranium, 4(1): 54-5
uranium oxide fuel elements, 4(1): 65
uranium oxide–thorium oxide systems, 4(1): 52-3
Vallecitos Boiling-Water Reactor, 4(1): 54
Fission products, contamination of Peach Bottom Power Reactor cooling system, 5(3): 62-3
decay heating, 5(3): 28
entrainment in water, 5(4): 30
Flanges, leaks in Calder Hall Reactors, 4(3): 69-70
Florida Power Reactor
See Reactors (Florida Power)
Fluid flow, 4(1): 27-33; 4(3): 13-28; 4(4): 19-30; 5(2): 9-21; 6(2): 24-5; 6(4): 54-62
See also Coolant flow; Gas flow; Liquid flow; Slurry flow; Steam flow
effect of rate of burnout, 4(2): 18; 5(1): 17-18, 19; 5(3): 17
heat-transfer effects on stability, 4(2): 17
hydrodynamic instability, 4(2): 27-8
swirl, 6(1): 21-2
in tubes, 5(1): 13
Fluid flow (turbulent), boiling-heat transfer, 4(2): 15-18
Fluid flow (two-phase), 4(4): 28-9, 31; 6(4): 57-60
air-water systems, 5(3): 19-20
boiling heat transfer, 4(2): 15-18
burnout, 5(3): 15-18; 6(3): 10
gas-liquid systems, 5(1): 13
hydrodynamics, 6(3): 5-10
pressure drop, 5(2): 19
slip-velocity determination, 4(2): 26
stability with boiling, 5(2): 12-14
steam-water systems, 5(1): 13
transients, 4(3): 24
Fluid-fuel reactors
See Reactors (fluid-fuel)
Fluidized-bed reactors
See Reactors (fluidized-bed)
Fluids (supercritical), heat transfer, 5(3): 20
Fluorine, reactions with uranium carbides, 4(1): 47
Fluoroscopy, nondestructive testing applications, 5(1): 71
Foils (gold), neutron-attenuation measurements, 4(2): 34
Foils (gold, cadmium-covered), neutron-attenuation measurements, 4(2): 34
Foils (sulfur), neutron-attenuation measurements, 4(2): 34
Forced convection
See Convection (forced)
FORTRAN computer code, 5(4): 19; 6(4): 47
Free convection
See Convection (free)
Freeze seals, Hallam Power Reactor, 4(2): 60; 4(4): 55
Friction factors, rectangular channels, 6(2): 18-19
Fuel alloys
See also fuels
corrosion by water, 6(2): 53
plutonium-thorium alloys, 5(1): 1-3
Fuel assemblies
See also Fuel elements
Elk River Power Reactor, 5(2): 34-5, 38
Hallam Power Reactor, 5(3): 41-2
hydrodynamic characteristics, 5(3): 20-2; 5(4): 24
Indian Point Power Reactor, 6(3): 29-32, 66-8
Parr Shoals Power Reactor, 6(4): 63-6
Piqua Power Reactor, 5(4): 51-2
PM-1 Reactor, 6(3): 44-6
SPERT-III Reactor, 5(3): 85
Fuel-Bearing Graphite Reactor
See Reactors (Fuel-Bearing Graphite) (FBGR)
Fuel blankets
See Breeding blankets
Fuel canals, coating in Shippingport Pressurized-Water Reactor, 6(3): 51
Fuel cells, cesium chloride–lithium chloride–rubidium chloride–sodium chloride systems, 4(3): 2
in combination with reactors, 4(3): 2-3
lithium hydride, 4(3): 2-3
Fuel channels
See Channels (fuel)
Fuel conversion ratio, 4(1): 5-9
Fuel cycles, 4(1): 3-10; 4(3): 38-41; 4(4): 37-8; 5(1): 1-3; 5(3): 1-5; 5(4): 8-14; 6(4): 1-37
Fuel development, 4(2): 38-43
Fuel elements, 5(1): 54-67
See also Fuel assemblies
Advanced Organic-Moderated Reactor, 4(1): 61-2
burnup, 4(1): 61-2
CANDU Reactor, 4(2): 65-6, 74
comparison of various dispersions, 4(1): 61
criticality of Puerto Rico Nuclear Center Research Reactor, 4(3): 7
damage in Sodium Reactor Experiment, 5(1): 84-7
design for fast-breeder reactors, 4(4): 84-96
development, 4(1): 45-56
Enrico Fermi Fast-Breeder Reactor, 4(1): 51-2
Experimental Gas-Cooled Reactor, 4(1): 63-5
Experimental Organic-Cooled Reactor, 5(1): 88-9
exponential experiments in uranium, 4(2): 10
fabrication costs, 5(3): 3
fabrication by powder metallurgy, 6(1): 26-37
Gas-Cooled Reactor Experiment II, 5(1): 81-2
Hallam Power Reactor, 4(1): 51
Indian Point Power Reactor, 6(3): 38-9
melting in fast reactors, 5(2): 29-31
NPD-2 Reactor, 4(2): 65
nuclear superheaters, 4(3): 76-80
organic-moderated and -cooled reactors, 4(1): 58-62
Peach Bottom Power Reactor, 5(3): 63-4
Piqua Power Reactor, 4(1): 58
rupture detection, 5(4): 47, 49, 56
sodium graphite reactors, 4(3): 88
spray-cooled reactors, 4(1): 75-6
temperature-determination methods, 4(1): 30
thermal conductivity of uranium dioxide, 4(2): 38-43
uranium-aluminum alloys, 4(1): 61
uranium-beryllium alloys, 4(1): 61-2
uranium carbide–plutonium carbide systems, 4(1): 51
uranium carbides, economic factors, 4(1): 52

Fuel elements (Continued)
uranium-graphite systems, 4(1): 61-2
uranium-magnesium alloys, 4(1): 61
uranium-molybdenum-aluminum alloy (aluminum-clad, finned), 4(1): 60
uranium-niobium alloys, 4(1): 61-2
uranium oxide, 4(1): 75-8
uranium oxide–thorium oxide systems, radiation effects, 4(1): 52-4
uranium-zirconium alloys, 4(1): 61-2
Variable-Moderator Reactor, 4(1): 77-8
Fuel elements (balls)
See also fuel elements (pellets)
development for Pebble-Bed Reactor Experiment, 6(3): 64
heat transfer, 5(3): 23
Fuel elements (ceramic), compatibility with gases, 5(3): 61
defective, operation of BORAX-IV Reactor with, 6(4): 95-6
uranium oxide–calcium oxide–zirconium oxide systems (UO_2-CaO-ZrO_2), 5(1): 67
Fuel elements (compacted-powder), performance, 6(2): 28-42
Fuel elements (finned), fabrication, 4(1): 60
heat transfer in organic reactors, 4(1): 58
Piqua Power Reactor, 5(4): 51-2
thermal analysis, 6(2): 25
Fuel elements (pellets)
See also Fuel elements (balls)
criticality, 6(3): 80
design for Indian Point Power Reactor, 6(3): 66
sintering of uranium oxide, 6(2): 42-3
thermal conductivity, 5(4): 23
Fuel elements (pins), application in Plutonium-Fuel Fast-Breeder Reactor, 4(4): 94
criticality studies on uranium-molybdenum alloy, 5(1): 5-6
melting in Experimental Breeder Reactor II, 5(2): 30-1
radiation effects, 4(4): 84-5
Fuel elements (plates), application in Plutonium-Fuel Fast-Breeder Reactor, 4(4): 94
buckling measurements on uranium, 4(2): 11-12
burnout, 4(1): 38
development of uranium oxide for, 6(2): 44-5
heat transfer, 4(4): 19-20; 5(1): 24-30
surface-boiling effects of, 5(1): 24
uranium-molybdenum alloys, 4(1): 58
Fuel elements (plates) (enriched) (stainless-steel-clad), reactivity, 5(2): 2
Fuel elements (plutonium), reactivity, 5(2): 6
Fuel elements (ribbed), heat transfer, 5(1): 11-12
Fuel elements (rod-in-tube), buckling measurements, 5(2): 1
Fuel elements (rods), assemblies for Hallam Power Reactor, 5(3): 41-2
boiling burnout, 6(1): 16-18
boiling-water reactors, 4(3): 86-7
bowing in Sodium Reactor Experiment, 6(1): 57-60
buckling measurements on uranium, 4(2): 11-12
buckling measurements on uranium dioxide, 4(2): 11
burnout, 5(1): 18
criticality of plutonium-aluminum alloys, Zircaloy-2-clad, 4(3): 6
criticality studies, 5(4): 16, 17; 6(3): 80
criticality of uranium oxide in heavy water, 6(3): 82
design for consolidated Nuclear Steam Generator, 6(4): 113-14
design for N. S. *Savannah* Reactor, 6(1): 43-7
design of rods and assemblies for Dresden Power Reactor, 4(4): 56-9
Doppler effect, 4(4): 14
Elk River Power Reactor, 5(2): 33-5
failure in Shippingport Pressurized-Water Reactor, 6(3): 55
fast-fission factors, 4(3): 4-5
flux hardening effects, 4(1): 11-12
heat transfer, 4(2): 20; 5(3): 20-2; 5(4): 24
heat transfer by gas, 4(1): 29-30
Indian Point Power Reactor, 6(3): 28-32
neutron resonance, temperature-distribution effects, 5(3): 9
nuclear measurements, 4(3): 5
Sodium Reactor Experiment, 4(4): 73-4; 5(1): 84-7
thermal conductivity, 5(4): 22-3
Fuel elements (rods) (enriched), exponential studies, 5(2): 3
Fuel elements (rods) (enriched) (stainless-steel-clad), reactivity, 5(2): 2-3
thermal conductivity, 5(4): 22-3
Fuel elements (rods) (ThO_2), age to indium resonance in water–heavy-water mixtures, 6(1): 5-6
Fuel elements (rods) ($U^{235}O_2$-ThO_2), exponential experiments, 5(3): 7
Fuel elements (rods) (UO_2), operating transients, 5(2): 22-4
Fuel elements (rods) (UO_2) (Zircaloy-2-clad), buckling, 5(3): 6-7
Fuel elements (rods) (Zircaloy-2-clad), buckling, 5(3): 6-7
radiation effects, 5(4): 41
Fuel elements (slugs), neutron spectra, 5(3): 9-10
Fuel elements (spheres)
See Fuel elements (balls)
Fuel elements (thimbles), sodium graphite reactors, 4(3): 88-9
Sodium Modular Reactor, 4(3): 93-4
Fuel elements (tubes), buckling measurements in hollow, 5(2): 1
burnout, 5(1): 18
criticality studies, 5(4): 17
criticality of uranium oxide, aluminum-clad, 4(3): 4
design for Nuclear Steam Generator 630A, 6(4): 107-9
design for PM-1 Reactor, 6(3): 44
exponential experiments on aluminum-clad, 5(1): 4
Heavy-Water Components Test Reactor, 4(2): 65
nondestructive testing, 6(2): 53
NPD-2 Reactor, 4(2): 64
uranium, aluminum-clad, 5(1): 4
uranium oxide (Zircaloy-2-clad), 4(2): 67-70
uranium-zirconium alloys (Zircaloy-clad), 4(2): 65
Yankee Power Reactor, 4(3): 47-8
Fuel elements (tubes) (UO_2) (Zircaloy-2-clad), buckling studies, 5(2): 3
Fuel elements (uranium), radiation effects, 5(3): 31
Fuel elements (uranium) (enriched), criticality, 5(3): 7
Fuel elements [uranium carbide (UC)], development, 6(2): 43-4
Fuel elements (uranium-molybdenum alloy) (stainless-steel-clad), assemblies for Hallam Power Reactor, 5(3): 41-2
Fuel elements (uranium-molybdenum-aluminum alloy) (aluminum, finned clad), Piqua Power Reactor, 5(4): 51-2
Fuel elements (UO_2), thermal analysis, 6(2): 25
Fuel elements (UO_2) (irradiated), reactivity, 5(2): 6
Fuel elements (UO_2) (stainless-steel-clad), thermal analysis, 5(3): 60-1
Fuel elements (Zircaloy-clad), autoclave testing, 4(2): 49
Fuel handling, Dresden Power Reactor, 4(4): 65-6
Parr Shoals Power Reactor, 6(4): 78-9
Yankee Power Reactor, 4(3): 54-5
Fuel-handling systems, Elk River Power Reactor, 5(2): 43-4
Hallam Power Reactor, 5(3): 49-50
Peach Bottom Power Reactor, 5(3): 64-5
Fuel pins
See Fuel elements (pins)
Fuel plates
See Fuel elements (plates)
Fuel-reprocessing plants, nuclear safety, 4(4): 14
Fuel resources, 4(2): 1-3
Fuel rods
See Fuel elements (rods)
Fuel thimbles
See Fuel elements (thimbles)
Fuel tubes
See Fuel elements (tubes)
Fuel-washing systems, design modifications in Sodium Reactor Experiment, 4(4): 74
Fuels
See also Fuel alloys; Fuel assemblies; Fuel elements
efficient utilization, 6(4): 1-37
FUGUE computer code, 5(1): 20
Furfural, moderating properties, 4(3): 4
Furfuryl alcohol, moderating properties, 4(3): 4

G

G2 Reactor
See Reactors (G2) (France)
G3 Reactor
See Reactors (G3) (France)
Gadolinium, flux hardening effects, 4(1): 11-12
Gadolinium compounds, evaluation for reactor control applications, 6(3): 15
Gadolinium oxide, evaluation for reactor control applications, 6(3): 15-16
thermal conductivity, 6(3): 15-16
Gadolinium oxide–samarium oxide systems, control rods for Hallam Power Reactor, 5(3): 42-3
evaluation for reactor control applications, 6(3): 15-16
thermal conductivity, 6(3): 15-16
Gamma counting, nondestructive testing applications, 5(1): 72
Gamma radiation
See Radiation (gamma)
Gamma spectrometry, nondestructive testing applications, 5(1): 72
Gas-cooled heavy-water reactors
See Reactors (gas-cooled heavy-water-moderated)
Gas-Cooled Reactor Experiments
See Reactors (Gas-Cooled, Experiment) (GCRE)
Gas-cooled reactors
See Reactors (gas-cooled)
Gas disposal, 4(2): 87-8
Gas flow, determination methods, 4(1): 29
duct design, 4(1): 65-7
nitrogen, 5(4): 26
Gas-liquid systems, flow, 5(1): 13
Gaseous diffusion plants, cost factors, 4(1): 3-5
production costs, 5(4): 6
Gases
See also Coolants (gaseous); specific gases
heat transfer, 5(2): 10-12
Gaskets, leaks, 5(3): 37-8
Gas removal, from Piqua Power Reactor, 4(2): 84-8
Gas-solid systems
See Solid-gas systems
GBSR
See Reactors (Graphite-Moderated Boiling and Superheating) (GBSR)
GCRE
See Reactors (Gas-Cooled, Experiment)
General Electric Company, nuclear superheater research, 4(3): 72-5
General Electric 630A Nuclear Steam Generator
See Reactors (Nuclear Steam Generator 630A)

General Electric Test Reactor
See Reactors (General Electric Test)
General Nuclear Engineering Corp.–Combustion Engineering
See Combustion Engineering–General Nuclear Engineering Corp.
Generators (steam)
See Steam generators
Glands, leaks in Calder Hall Reactors, **4**(3): 69-70
Glass (boron)
See Boron glass
Glass beads, thermal conductivity, **5**(3): 22-3
GLEEP Reactor
See Reactors (GLEEP)
Godiva Critical Facility
See Reactors (Godiva Critical Facility)
Godiva Reactors
See Reactors (Godiva)
Gold, foils, **4**(2): 34
neutron-absorption cross section, **4**(1): 19
reactivity worth, **4**(4): 39, 40
Gold-197, resonance integrals, **6**(1): 5
Graphite, corrosion by carbon dioxide, **5**(1): 80-1
dimensional stability, **5**(4): 39
emittance, **5**(4): 26
moderating properties, **4**(3): 6-7; **5**(1): 5-6
moderator assembly for Hallam Power Reactor, **5**(3): 39-41
neutron-absorption cross sections, **4**(1): 19-20
oxidation in gas-cooled reactors, **5**(3): 66-7
radiation effects, **5**(1): 80-1; **5**(4): 39-40
rethermalization properties, **5**(2): 3-4, 5
thermal conductivity, **5**(4): 39-40
thermal expansion, **5**(4): 40
Graphite (pyrolytic), fabrication, **6**(3): 18
Graphite-Moderated Boiling and Superheating Reactor
See Reactors (Graphite-Moderated Boiling and Superheating) (GBSR)
Graphite-moderated reactors
See Reactors (graphite-moderated)
Graphite-plutonium systems
See Plutonium-graphite systems
Graphite systems, nondestructive testing, **5**(1): 71
Graphite-thorium systems
See Thorium-graphite systems
Graphite-uranium systems
See Uranium-graphite systems

H

Hafnium, corrosion by water, **6**(2): 53
evaluation for reactor control, **6**(2): 49
radiation effects, **6**(3): 16
resonance integrals, **6**(2): 7
Hafnium borides (HfB_2), corrosion by steam, **4**(4): 44
radiation effects, **4**(4): 44
solubility in boiling water, **4**(4): 43
Half-fast reactors
See Reactors (coupled)
Hallam Power Reactor
See Reactors (Hallam Power)
Hanford Production Reactors
See Reactors (Hanford Production)
Hanford Test Reactor
See Reactors (Hanford Test)
Hastelloy N alloy, nuclear superheater applications, **5**(4): 38
Hastelloy X alloy, nuclear superheater applications, **5**(4): 38
Hazards
See Safety
Heat exchangers, failure of stainless-steel, **5**(1): 76-7
Hallam Power Reactor, **5**(3): 44-5, 46, 47
Heat exchangers (gas-liquid), once-through, design, **5**(3): 13
Heat transfer, **4**(1): 27-33; **4**(2): 13-21; **4**(3): 13-28; **4**(4): 19-30; **5**(1): 10-21; **5**(2): 9-21; **5**(3): 12-26; **5**(4): 22-7; **6**(1): 15-25; **6**(2): 17-27; **6**(3): 4-11; **6**(4): 54-62
fuel elements (plates), **5**(1): 24-30
mathematical analysis, **4**(3): 26-7
N. S. *Savannah* Reactor, **6**(1): 50
SPERT reactors, **5**(1): 24-30
Heat-Transfer Reactor Experiment 1
See Reactors (Heat-Transfer, Experiment 1) (HTRE-1)
Heaters, feedwater, failure in Shippingport Pressurized-Water Reactor, **5**(4): 69
Heavy free-gas approximation (generalized), **6**(4): 41-5
Heavy water, lattices, resonance absorption of uranium in, **6**(3): 79-80
losses in reactors, **6**(1): 55-6
moderating properties, **5**(1): 7
production costs, **5**(4): 1-5
production-plant design, **5**(4): 1-5
radiolysis in boiling heavy-water reactors, **6**(4): 92-4
recovery in Experimental Boiling-Water Reactor, **4**(2): 59
Heavy-water boiling reactors
See Reactors (heavy-water boiling)
Heavy-Water Components Test Reactor
See Reactors (Heavy-Water Components Test) (HWCTR)
Heavy-water-cooled organic-moderated reactors
See Reactors (organic-cooled heavy-water-moderated)
Heavy-water-moderated reactors
See Reactors (heavy-water-moderated)
Heavy-water–uranium lattices
See Uranium–heavy-water lattices
Heavy-water–uranium oxide lattices
See Uranium oxides (UO_2)–heavy-water lattices
Heavy-water–uranyl nitrate systems
See Uranyl nitrate–heavy-water systems
Heavy-water–water systems, effects on age to indium resonance of thorium oxide rods, **6**(1): 5-6
moderating properties, **5**(1): 5, 7-9
Helium, beryllium corrosion, **5**(2): 48-9
compatibility with ceramic fuel elements, **5**(3): 61
corrosion problems caused by impurities, **4**(3): 43-4
Peach Bottom Power Reactor cooling, **5**(3): 62-3
Prandtl numbers from 270–680°K, **5**(3): 24
purification, **5**(3): 67-8
reactor cooling, **4**(1): 63
technology, **5**(4): 76-8
thermal conductivity, **5**(3): 69
HERESY-I computer code, criticality calculations, **6**(2): 9
Heterogeneous reactors
See Reactors (heterogeneous)
HFIR
See Reactors (High-Flux Isotope) (HFIR)
High-Flux Isotope Reactor
See Reactors (High-Flux Isotope) (HFIR)
High-Temperature Gas-Cooled Reactor
See Reactors (Dragon)
High-Temperature Test Facility
See Reactors (High-Temperature Test Facility)
Hinkley Point Reactors (UK)
See Reactors (Hinkley Point) (UK)
HIPPO
See Reactors (HIPPO) (Canada)
HNPF
See Reactors (Hallam Power)
Homogeneous Reactor Experiments
See Reactors (Homogeneous, Experiment)
Homogeneous reactors
See Reactors (homogeneous)
Horizontal tubes
See Tubes (horizontal)
Hot-channel factors, **4**(1): 30-2
HR-2 Reactor
See Reactors (HR-2)
HTGCR
See Reactors (dragon)
HTGR
See Reactors (Peach Bottom Power)
HTRE
See Reactors (Heat-Transfer, Experiment) (HTRE)
HTTF
See Reactors (High-Temperature Test Facility)
Humboldt Bay Power Reactor
See Reactors (Humboldt Bay Power)
Hunterston Reactors (UK)
See Reactors (Hunterston) (UK)
HWCTR
See Reactors (Heavy-Water Components Test) (HWCTR)
Hydraulic effects, **4**(2): 26-8
Hydrazine, synthesis from ammonia, **4**(3): 1-2
Hydrogen, compatibility with ceramic fuel elements, **5**(3): 61
corrosion, of iron alloys, **4**(3): 43
of nickel alloys, **4**(3): 43-4
moderating properties, **5**(1): 7
reactions with uranium carbides, **4**(1): 47
removal from helium, **5**(4): 78
Hydrogen–carbon monoxide systems
See Carbon oxide–hydrogen systems ($CO-H_2$)
Hydrogen peroxide–carbonate solutions, corrosion inhibition applications, **4**(3): 44-6
Hydrogen sulfide, reactions with uranium carbides, **4**(1): 47
Hydrogen sulfide dual-temperature process, plant design, **5**(4): 1-5

I

IBSHR
See Reactors (Integral Boiling and Superheating) (IBSHR)
IDIOT computer code, **5**(3): 7
IN-102 alloy, nuclear superheater applications, **5**(4): 38
Incoloy alloy, nuclear superheater applications, **5**(4): 38
Inconel alloy, corrosion by carbon monoxide, carbon monoxide–carbon dioxide systems, and carbon monoxide–hydrogen systems, **4**(3): 43-4
corrosion by water, **6**(2): 53
nuclear superheater applications, **5**(4): 38
Inconel 702 alloy, corrosion by carbon monoxide, carbon monoxide–carbon dioxide systems, and carbon monoxide–hydrogen systems, **4**(3): 43-4
Inconel X alloy, corrosion by ammonium citrate process solutions, **4**(3): 45
corrosion by carbon monoxide, carbon monoxide–carbon dioxide systems, and carbon monoxide–hydrogen systems, **4**(3): 43-4
corrosion by sodium bisulfate process solutions, **4**(3): 44
Indian Point Power Reactor
See Reactors (Indian Point Power) (CETR)
Indium, flux hardening effects, **4**(1): 11-12
resonance to neutron age, **5**(1): 8-9
Indium-115, resonance integrals, **6**(1): 5
Indium-cadmium-silver alloys
See Cadmium-indium-silver alloys
Instrumentation, **4**(4): 34-6; **5**(1): 37-53; **5**(2): 61-73
air supply for Hallam Power Reactor, **5**(3): 48
Elk River Power Reactor, **5**(2): 40-1
Hallam Power Reactor, **5**(3): 50-1
Indian Point Power Reactor, **6**(3): 34-5
N. S. *Savannah* Reactor, **6**(1): 52
Parr Shoals Power Reactor, **6**(4): 73-5

Instrumentation (Continued)
Piqua Power Reactor, 5(4): 56
radiation gauges, 5(1): 71
Shippingport Pressurized-Water Reactor, 4(2): 52, 56
Yankee Power Reactor, 4(3): 53-4; 6(4): 83-6
Insulation
See Thermal insulation
Integral Boiling and Superheating Reactor
See Reactors (Integral Boiling and Superheating) (IBSHR)
Integral Nuclear Superheater Reactor
See Reactors (Integral Nuclear Superheater) (ISR)
Iodine, adsorption on filters, 6(3): 20-1
entrainment in water, 5(4): 30
reactions with uranium carbides, 4(1): 47
removal, 5(4): 29-33
Ion-exchange resins, radiation effects, 5(4): 47, 48
Iron, shielding properties, 4(2): 35
Iron alloys, corrosion by carbon oxides, 4(3): 43
corrosion by hydrogen, 4(3): 43
iodine adsorption, 6(3): 20-1
Iron-aluminum alloys
See Aluminum-iron alloys
Iron-nickel-zirconium alloys, corrosion, 5(3): 32
Isopropyl biphenyl, stability under reactor conditions, 6(3): 70-2
ISR
See Reactors (Integral Nuclear Superheater) (ISR)

J

JAPC Reactor (Japan)
See Reactors (JAPC) (Japan)
Jezebel Plutonium Critical Facility
See Reactors (Jezebel Plutonium Criticality Facility)
JPDR Reactor (Japan)
See Reactors (JPDR) (Japan)

K

K-Monel alloy, fuel-element applications, 5(1): 82
Kahl Reactor (West Germany)
See Reactors (Kahl) (West Germany)
KEMA Suspension Test Reactor
See Reactors (KEMA Suspension Test) (KSTR)
Kernels, theoretical scattering laws, 6(4): 49-51
Kerosene, reactions with uranium carbides, 4(1): 47
KEWB
See Reactors (Kinetic Experiment on Water Boilers) (KEWB)
Kinetic Experiment on Water Boilers
See Reactors (Kinetic Experiment on Water Boilers) (KEWB)
Krypton, entrainment in water, 5(4): 30
removal from helium, 5(4): 76

L

Latina Reactor (Italy)
See Reactors (Latina) (Italy)
Lattices, buckling, 6(1): 4
structure in Indian Point Power Reactor, 6(3): 32-3
Laundries, radioactive contamination, 5(4): 49
Lead, reactions with uranium carbides, 4(1): 46
Leak testing, nondestructive testing applications, 5(1): 73
Leaks, Calder Hall Reactors, 4(3): 69-70
Experimental Boiling-Water Reactor, 4(3): 56
LEAP computer code, neutron cross-section calculations, 6(4): 47
Limonite concrete, shielding properties at elevated temperatures, 4(2): 34-5
Liquid-gas systems
See Gas-liquid systems
Liquid-metal-cooled reactors
See Reactors (liquid-metal-cooled)
Liquid-metal pumps
See Pumps (liquid-metal)
Liquid metals
See Metals (liquid)
Lithium-aluminum alloys
See Aluminum-lithium alloys
Lithium chloride–cesium chloride–rubidium chloride–sodium chloride systems
See Cesium chloride–lithium chloride–rubidium chloride–sodium chloride systems
Lithium hydride, fuel cell applications, 4(3): 2-3
Lithium hydroxide, effectiveness in crud control, 6(2): 47-8
Lithium-6–magnesium alloys, reactivity worth, 4(4): 40
Loops, instabilities in boiling pentane, 4(3): 27
Los Alamos Scientific Laboratory, criticality accident, August 1945, 4(2): 29
Loss of coolant, experiments in ZEEP, 4(2): 11
Loss-of-coolant accidents, 4(1): 38-9
Loss of flow, Shippingport Pressurized-Water Reactor, 6(3): 50
Lutetium, flux hardening effects, 4(1): 11-12
reactivity-worth burnup, 4(4): 42

M

MAC computer code, 6(3): 84
Magnesium, corrosion by water, 6(2): 53
Magnesium-lithium alloys
See Lithium-magnesium alloys
Magnesium oxide, compatibility with gaseous coolants, 5(3): 61
Magnesium-uranium alloys
See Uranium-magnesium alloys
Magnetite concrete, shielding properties at elevated temperatures, 4(2): 34
Magnetite limonite concrete, shielding properties at elevated temperatures, 4(2): 34-5
Marine reactors
See Reactors (marine)
Maritime Gas-Cooled Reactor
See Reactors (Maritime Gas-Cooled) (MGCR)
Mass flow
See also Fluid flow
effect on burnout, 5(3): 17
Materials
See specific materials; Reactor materials
Materials Testing Reactor
See Reactors (Materials Testing) (MTR)
McMurdo Sound Reactor
See Reactors (McMurdo Sound)
MELEAGER CHAIN computer code, 5(4): 9
Merchant ships
See Ships
Merchant-vessel reactors
See Reactors (marine)
Mercury, heat transfer, 4(3): 15-17
Metal-water reactions, rates, 4(1): 39-40
Metals (liquid)
See also specific metals and alloys
flow, 6(4): 54-5
flow partitioning with variable orifices, 4(4): 19
heat transfer, 4(3): 15-17; 6(4): 54-5
pumping, 4(2): 59-61
Methane, removal from helium, 5(4): 78
Methanol, ethylene glycol synthesis from, 4(3): 1
MGCR
See Reactors (Maritime Gas-Cooled) (MGCR)
Microradiography, nondestructive testing applications, 5(1): 71
MIT Research Reactor
See Reactors (MIT Research) (MITR)
Mixed-Spectrum Superheater Reactor
See Reactors (Mixed-Spectrum Superheater) (MSSR)
ML-1 Reactor
See Reactors (ML-1)
MLSR
See Reactors (Modified Lynchburg Source) (MLSR)
Moderator tanks, design for Parr Shoals Power Reactor, 6(3): 69-70
Moderators, beryllium, 5(1): 7-8
beryllium oxide, 5(1): 7-8
biphenyl, 5(1): 7-8
carbon, 5(1): 7-8
design for Nuclear Steam Generator 630A, 6(4): 109
experimental power determination, 6(4): 44-5
Hallam Power Reactor, design, 5(3): 39-41
heavy-water, 5(1): 7
heavy-water–water systems, 5(1): 5, 7-9
hydrogen, 5(1): 7
oils, 5(1): 7-8
organic-moderated reactors, power absorption, 5(3): 58
oxygen, 5(1): 7
power calculations, 6(4): 41-5
Spectral Shift Control Reactor, 5(4): 81-2
water, 5(1): 7
Moderators (canned), sodium graphite reactors, 4(3): 89
Sodium Modular Reactor, 4(3): 93, 95
Modified Lynchburg Source Reactor
See Reactors (Modified Lynchburg Source) (MLSR)
Molten-Salt Reactor Experiment
See Reactors (Molten-Salt, Experiment) (MSRE)
Molybdenum, corrosion by carbon oxides, 4(3): 43-4
corrosion by carbon monoxide–hydrogen systems, 4(3): 43-4
reactions with rare earths, 6(3): 15
reactions with uranium carbides, 4(1): 46
Molybdenum-aluminum-uranium alloys
See Uranium-molybdenum-aluminum alloys
Molybdenum-silicon-uranium systems
See Uranium-molybdenum-silicon systems
Molybdenum-uranium alloys
See Uranium-molybdenum alloys
Molybdenum-zirconium alloys, reactions with water, 4(1): 40-1
Monel alloys, corrosion by ammonium citrate process solutions, 4(3): 45
corrosion by carbon dioxide–carbon monoxide systems, carbon monoxide, and carbon monoxide–hydrogen systems, 4(3): 43-4
MSRE
See Reactors (Molten-Salt, Experiment) (MSRE)
MSSR
See Reactors (Mixed-Spectrum Superheater) (MSSR)
MTR
See Reactors (Materials Testing) (MTR)
MUFT computer code, 5(2): 2, 4, 6
blanket-element composition determination, 5(1): 1
Multiregional Reactor Lattice Studies Program, 5(1): 4-5; 5(2): 2

N

NaK
See Sodium-potassium alloys (liquid)
Natural convection
See Convection (free)
Neptunium-239, neutron cross sections, **5**(2): 7
Neuglobsow Reactor (East Germany)
See Reactors (Neuglobsow) (East Germany)
Neutron absorption
See Control; Poisoning
Neutron activation distribution measurements, High-Temperature Test Facility, **4**(1): 23-4
uranium-zirconium alloys (zirconium-clad), **4**(1): 23-4
Neutron age, beryllium, **5**(1): 7
beryllium oxide, **5**(1): 6-7
indium resonance to, **5**(1): 8-9
tables, **5**(1): 7
Neutron cross sections, **5**(2): 4, 6-7
computer codes for calculating, **6**(4): 47
differential scattering, **6**(2): 11-12
formulation of scattering law, **6**(4): 48-9
Neutron economy, in heavy-water reactors, **4**(2): 64
Neutron radiation
See Radiation (neutron)
Neutron rethermalization cross sections, **5**(2): 3-4, 5
Neutron-scattering law, experiments and theory, **6**(1): 6-10
Neutron spectrum, application of scattering law to calculations, **6**(1): 9-10
measurements, **6**(1): 10-13
Neutron thermalization experiments, **6**(1): 6-14
Neutrons, absorption, theory, **6**(2): 5-7
attenuation in zirconium, **4**(4): 36
background source in new reactors, **4**(1): 17-19
penetration through iron slabs, **4**(2): 35
production per fission of U^{235} in U^{233}, average, **4**(1): 19
reflection by beryllium, **4**(3): 10
scattering-law formulation, **6**(4): 48-9
spectra in uranium-graphite lattices, **5**(3): 9-10
spectrum hardening by absorption, **6**(4): 46
transport equation, **6**(4): 39-41
Neutrons (fast), transmission in ducts, **6**(3): 86-7
Neutrons (thermal), calculation, beyond reactor core, **6**(3): 83-4
capture spectra, **4**(2): 34
comparison of spectrum calculations with experiment, **6**(4): 47-8
diffusion, in Dowtherm A, **4**(1): 16-17
in water, **4**(1): 16-17
flux-spectrum calculations in polyethylene, **6**(4): 50-1
penetration through boral, **4**(2): 36
transmission in ducts, **6**(3): 86-7
New Production Reactor
See Reactors (New Production)
Nichrome V alloy, reactions with uranium carbides, **4**(1): 46
Nickel, coatings, nondestructive testing of, **5**(1): 71
cooling with mercury, **4**(3): 15
Nickel (chrome-plated), cooling with mercury, **4**(3): 15
Nickel alloys
See also specific nickel alloys
corrosion, by carbon oxides, **4**(3): 43
by hydrogen, **4**(3): 43
Nickel-aluminum alloys
See Aluminum-nickel alloys
Nickel–boron carbide systems
See Boron carbide–nickel systems
Nickel-iron-zirconium alloys, corrosion, **5**(3): 32
Niobium, corrosion, **4**(3): 43-4; **6**(2): 53
reactions with uranium carbides, **4**(1): 46
Niobium alloys, corrosion, **5**(3): 31-2
Niobium oxides (Nb_2O_5), compatibility with gaseous coolants, **5**(3): 61
Niobium-titanium alloys, corrosion by carbon oxides and carbon oxide–hydrogen systems, **4**(3): 43-4
reactions with uranium carbides, **4**(1): 46
Niobium-uranium alloys
See Uranium-niobium alloys
Niobium-vanadium alloys, corrosion, **5**(3): 32
Niobium-zirconium, corrosion by carbon oxides and carbon oxide–hydrogen systems, **4**(3): 43-4
Nionel alloy, nuclear superheater applications, **5**(4): 38
Nitric acid process, corrosion of reactor materials, **4**(3): 45
Nitrogen, heat transfer, **5**(4): 26
reactions with uranium carbides, **4**(1): 46-7
Nondestructive testing, **5**(1): 71-3
fuel-element cladding materials, **5**(1): 69
Zircaloy tubing, **6**(2): 53
NPD Reactors
See Reactors (NPD) (Canada)
NRU Reactor
See Reactors (NRU) (Canada)
NRX Reactor
See Reactors (NRX) (Canada)
N. S. *Savannah* Reactor
See Reactors (N. S. *Savannah*)
Nuclear defense, blast protection for power plants, **6**(3): 1-3
Nuclear power, economics, **4**(2): 4-9
Nuclear safety
See Safety
Nuclear safety guide, **4**(4): 13-14
Nuclear superheat
See Superheat (nuclear)
Nucleate boiling
See Boiling (nucleate)

O

Oak Ridge National Laboratory, criticality accident, **4**(2): 29
Oak Ridge Research Reactor
See Reactors (Oak Ridge Research) (ORR)
OCDRE
See Reactors (Organic-Cooled Deuterium, Experiment) (OCDRE)
Oils, moderating properties, **5**(1): 7-8
OMR
See Reactors (Organic-Moderated) (OMR)
OMRE
See Reactors (Organic-Moderated, Experiment) (OMRE)
Once-Through Superheater Reactor
See Reactors (Once-Through Superheater) (OTSR)
Oralloy
See Uranium (highly enriched)
Organic coolants
See Coolants (organic)
Organic-Cooled Deuterium Reactor Experiment
See Reactors (Organic-Cooled Deuterium, Experiment) (OCDRE)
Organic-cooled and -moderated reactors
See Reactors (organic-cooled and -moderated)
Organic materials
See specific organic materials; Coolants (organic)
Organic-Moderated Reactor
See Reactors (Organic-Moderated) (OMR)
Organic-Moderated Reactor Experiment
See Reactors (Organic-Moderated, Experiment) (OMRE)
ORNL Critical-Experiments Facility
See Reactors (ORNL Critical Experiments Facility)
ORR
See Reactors (Oak Ridge Research)
OTSR
See Reactors (Once-Through Superheater) (OTSR)
Oxalic acid process, corrosion of reactor materials, **4**(3): 45
Oxygen, moderating properties, **5**(1): 7
reactions with uranium carbides, **4**(1): 46-7
removal from helium, **5**(4): 78

P

Pajarito Critical-Assemblies Facility
See Reactors (Pajarito Critical-Assemblies Facility)
Paraffin, neutron cross sections, **6**(1): 5
Parr Shoals Power Reactor
See Reactors (Parr Shoals Power) (CVTR)
Pathfinder Power Reactor
See Reactors (Pathfinder Power)
PBRE
See Reactors (Pebble-Bed, Experiment) (PBRE)
PCTR
See Reactors (Physical Constants Testing)
Peach Bottom Power Reactor
See Reactors (Peach Bottom Power) (HTGR)
Pebble-Bed Reactor Experiment
See Reactors (Pebble-Bed, Experiment) (PBRE)
Pebble-bed reactors
See Reactors (pebble-bed)
Pentane, instabilities in boiling loops, **4**(3): 27
Permanganate solutions, corrosion film oxidation, **4**(3): 44
Permutit SK resin, radiation effects, **5**(4): 48
PFFBR
See Reactors (Plutonium-Fuel Fast-Breeder) (PFFBR)
Phenanthrenes, alkyl-, evaluation as reactor coolants, **4**(4): 79
radiation effects, **4**(4): 79
Phosphoric acid process, corrosion of reactor materials, **4**(3): 45
Physical Constants Testing Reactor
See Reactors (Physical Constants Testing) (PCTR)
Pins (fuel)
See Fuel elements (pins)
Pipes, steam-line corrosion, **4**(3): 65-6
Piping, Hallam Power Reactor, **5**(3): 45-6
Parr Shoals Power Reactor, **6**(4): 71, 72, 77
Piqua City Power Reactor
See Reactors (Piqua Power)
PIXMIX code, neutron cross-section calculation, **6**(4): 47
PIXSE code, neutron cross-section calculation, **6**(4): 47
PL-2 Reactor
See Reactors (PL-2)
Plexiglas, moderating properties, **4**(3): 5
Plexiglas-plutonium systems
See Plutonium-Plexiglas systems
PLUTO Reactor
See Reactors (PLUTO)
Plutonium, analysis, **5**(1): 71
buildup in breeding blankets, **5**(4): 67
corrosion by water, **6**(2): 53
criticality, **4**(3): 8, 9
fuel elements, fabrication costs, **5**(3): 3
neutron-multiplication measurements, **4**(3): 5
production from U^{238}, **6**(4): 1-4
reactivity, **5**(2): 6
recycle, **5**(4): 8-14
Plutonium-239, alpha activities, specific, **4**(1): 19
breeding ratios, **4**(1): 9
criticality, **6**(1): 4
flux hardening effects, **4**(1): 11-12
neutron cross sections, **5**(2): 6, 7
radiation effects, **4**(4): 86
resonance fission integrals, **4**(4): 13

Plutonium-240, alpha activities, specific, 4(1): 19
  criticality, 6(1): 3, 4
  neutron cross sections, 5(2): 7; 6(1): 5
Plutonium-241, criticality, 6(1): 4
  flux hardening effects, 4(1): 11-12
  neutron cross sections, 5(2): 6, 7
  resonance fission integrals, 4(4): 13
Plutonium-242, neutron cross sections, 5(2): 7
Plutonium-aluminum alloys, fuel-element applications in organic reactors, 4(1): 58
Plutonium-aluminum alloys (Zircaloy-2-clad), criticality, 4(3): 6
Plutonium carbide–uranium carbide systems
  See Uranium carbide–plutonium carbide systems
Plutonium carbide–uranium systems
  See Uranium–plutonium carbide systems
Plutonium carbides, physical properties, 4(1): 48
Plutonium-Fuel Fast-Breeder Reactor
  See Reactors (Plutonium-Fuel Fast-Breeder) (PFFBR)
Plutonium-fuel reactors
  See Reactors (plutonium-fuel)
Plutonium-graphite systems, criticality measurements, 4(1): 23
Plutonium oxide–uranium oxide systems
  See Uranium oxide–plutonium oxide systems
Plutonium oxides (PuO_2), burnup, 5(3): 2-5
Plutonium-Plexiglas systems, criticality measurements, 4(1): 23
Plutonium recycle reactors
  See Reactors (plutonium recycle)
Plutonium Recycle Test Reactor
  See Reactors (Plutonium Recycle Test) (PRTR)
Plutonium-thorium alloys, fuel cycles, 5(1): 1-3
Plutonium-uranium alloys
  See Uranium-plutonium alloys
PM-1 Reactor
  See Reactors (PM-1)
PM-2A Reactor
  See Reactors (PM-2A)
PNPF
  See Reactors (Piqua Power)
Poisoning, stainless-steel, effects, 5(1): 5-6
Polyethylene plastic, neutron cross sections, 6(1): 5
  thermal-neutron flux spectrum calculations in, 6(4): 50-1
Polyphenyls
  See also Terphenyl
  purification, 4(2): 82-8
Pool boiling
  See Boiling (pool)
POPR
  See Reactors (Prototype Organic Power) (POPR)
Popsy Critical Assembly
  See Reactor (Popsy Critical Assembly)
Potassium-sodium alloys (liquid)
  See Sodium-potassium alloys (liquid)
Powder metallurgy, 6(1): 26-37
Power excursions, research, 4(2): 22-5
Power plants, N. S. *Savannah*, 6(1): 53-4
  blast protection of coal fired, 6(3): 1-3
Power plants (remote), 4(2): 4-9
  cooling with mercury, 4(3): 15-16
Power reactors
  See Reactors (power)
Prandtl numbers, for helium, 270–680°K, 5(3): 24
PRDC Reactor
  See Reactors (Enrico Fermi Fast-Breeder)
Preamplifiers, 4(4): 36
Pressure drop, 5(4): 24
  calculation, 5(1): 20
  effect on burnout, 4(2): 18
  steam-water flow, 5(2): 19
Pressure suppression, Humboldt Bay Power Reactor, 6(3): 27
  iodine containment, 5(4): 29-33
Pressure-tube reactors
  See Reactors (pressure-tube)
Pressure-Tube Superheater Reactor
  See Reactors (Pressure-Tube Superheater) (PTSR)
Pressure tubes, design for Parr Shoals Power Reactor, 6(4): 67-8
  Zircaloy-2, 5(2): 50
  evaluation after irradiation, 6(2): 67
Pressure vessels, ASME codes for design and construction, 4(2): 44-8; 4(4): 50-1
  British specifications for reactor, 4(4): 51-4
  concrete, prestressed, 5(4): 78-80
  design, for British reactors, 4(4): 52, 54
  for Dresden Power Reactor, 4(4): 62
  for Elk River Power Reactor, 5(2): 39-40
  for Hallam Power Reactor, 5(3): 43-4
  for Indian Point Power Reactor, 6(3): 34
  for Latina Reactor, 4(4): 52, 54
  for nuclear superheaters, 4(3): 79
  for Piqua Power Reactor, 5(4): 55
  for sodium graphite reactors, 4(3): 90
  for Yankee Power Reactor, 4(3): 52-3
  design theory, 6(3): 40-3
  fatigue, 5(1): 74-5
  radiation effects, 4(2): 46
  stress relief, 6(1): 41
Pressure waves, propagation in steam-water systems, 4(4): 31
Pressurized Critical Assembly
  See Reactors (Pressurized Critical Assembly)
Pressurized water
  See Water (pressurized)
Pressurized-water reactors
  See Reactors (pressurized-water)
Prestressed concrete
  See Concrete (prestressed)
PRO Reactor
  See Reactors (PRO) (Italy)
Process Development Pile
  See Reactors (Process Development Pile)
Process-heat reactors
  See Reactors (process-heat)
Protactinium-231, neutron cross sections, 6(1): 5
Prototype Organic Power Reactor
  See Reactors (Prototype Organic Power) (POPR)
PRTR
  See Reactors (Plutonium Recycle Test) (PRTR)
PTSR
  See Reactors (Pressure-Tube Superheater) (PTSR)
Puerto Rico Nuclear Center Research Reactor
  See Reactors (Puerto Rico Nuclear Center Research)
Puerto Rico Reactor
  See Reactors (BONUS)
Pumps, cost studies, 5(3): 35-7
  Dresden Power Reactor, 4(4): 64-5
  failure in Shippingport Pressurized-Water Reactor, 5(4): 69
  leakage in heavy-water reactors, 4(4): 70-3
  leaks, 5(3): 35-7
  Parr Shoals Power Reactor, 6(4): 77
  replacement of radioactive, 5(4): 46-7
  SL-1 Reactor, 4(1): 69
Pumps (centrifugal), for liquid metal, 4(2): 59-61
Pumps (liquid-metal), Hallam Power Reactor, 4(2): 59-61
  sodium graphite reactors, 4(3): 90
PWR
  See Reactors (Shippingport Pressurized-Water)
Pyrolytic-Capsule Fouling Test, 6(2): 58-9
Pyrolytic graphite
  See Graphite (pyrolytic)

R

R-3 Adam Reactor
  See Reactors (R-3/Adam)
RA-330 alloy, nuclear superheater applications, 5(4): 38
Radiation (alpha), specific activities in plutonium, 4(1): 19
Radiation (gamma), materials for shielding, 4(3): 36
  penetration through iron slabs, 4(2): 35
  shielding, calculation by MAC code, 6(3): 84
  from U^{233} decay at 74 kev, 4(1): 16
Radiation (neutron), penetration through iron slabs, 4(2): 35
Radiation (thermal)
  See Thermal radiation
Radiation (X), nondestructive testing applications, 5(1): 71
Radiation chemistry, ethylene glycol synthesis from methanol, 4(3): 1
  hydrazine synthesis from ammonia, 4(3): 1
Radiation effects, alkylphenanthrenes, 4(4): 79
  aluminum alloys, 5(1): 70
  beryllium, 4(1): 65; 5(2): 49
  beryllium oxide, 6(1): 38-40
  borides, 4(4): 42-3, 44
  boron, 4(4): 44
  boron carbide, 4(4): 44
  boron stainless steel, 5(3): 33
  breeding-blanket elements, 5(4): 18-19
  compacted-powder fuel elements, 6(2): 28-42
  fuel elements, 4(4): 84-5; 5(1): 84-7; 5(3): 31; 5(4): 23, 41
  graphite, 5(1): 80-1; 5(4): 39-40
  hafnium, 6(3): 16
  hafnium borides, 4(4): 44
  heavy water in boiling heavy-water reactors, 6(4): 92-4
  ion-exchange resins, 5(4): 47, 48
  organic coolants, 4(4): 76, 79, 82; 5(3): 52-6, 57; 6(3): 70-2
  Organic-Moderated Reactor Experiment coolant, 4(4): 82
  pressure vessels, 4(2): 46
  Pu^{239}, 4(4): 86
  rare-earth compounds, 6(3): 15-16
  Santowax OM, 5(3): 57
  Santowax OMP, 5(3): 57
  Santowax R, 5(3): 52-6, 57
  stainless steel, 5(1): 70; 5(3): 33; 5(4): 35-6
  state-of-the-art survey, 6(2): 53
  steels, 4(2): 46; 5(3): 33; 5(4): 34-6
  terphenyls, 5(3): 57
  thorium, 5(4): 18-19
  uranium, 4(1): 54-5; 5(3): 31; 5(4): 40-1
  uranium (tantalum-clad), 5(4): 41
  uranium (stainless-steel-clad), 5(4): 41
  uranium (Zircaloy-2-clad), 5(4): 41
  U^{235}, 4(4): 86
  U^{239}, 4(4): 84-5
  uranium alloys, 4(1): 60; 4(4): 84-5; 5(3): 31
  uranium carbides, 4(1): 48-50
  uranium oxide–thorium oxide systems, 4(1): 52-4
  uranium oxides (UO_2), 5(1): 56-62, 66-7
  water, in boiling-water reactors, 6(4): 92-4
  welds, stainless-steel, 5(1): 70
  Zircaloy-2 alloy, 4(3): 42-3; 5(1): 70; 5(4): 40; 6(2): 67
  zirconium, 5(1): 70
Radiation gauges, nondestructive testing applications, 5(1): 71
Radiation protection, regulations, 4(1): 43-4
Radiation surveys, N. S. *Savannah*, 6(3): 84-5
Radiation techniques, nondestructive testing applications, 5(1): 71-2

Radioactive maintenance, Vallecitos Boiling-Water Reactor, 5(4): 46-7
Radioactivity monitoring, environmental, Shippingport Pressurized-Water Reactor, 5(4): 70
Radioactivity problems, 5(4): 43-50
Radio-induced heating, 5(3): 28
in Hallam Power Reactor shield, 5(3): 29
Radioisotopes, nuclear properties, 4(4): 32-3
Rapsodie Reactor (France)
See Reactors (Rapsodie) (France)
Ravenswood Power Reactor
See Reactors (Ravenswood Power)
Reactivity, characteristic in Yankee Power Reactor, 6(4): 86-91
Reactivity excursions, 4(1): 37-8
Reactivity factors, fast-breeder reactors, 4(4): 86-96
Reactor constants, 6(1): 4-6
Reactor containment
See Containment
Reactor control
See Control
Reactor control materials
See Control materials
Reactor control-rod drives
See Control-rod drives
Reactor core design
See also specific reactors
Dresden Power Reactor, 4(4): 59-60
Reactor cores, design in N. S. *Savannah* Reactor, 6(1): 47-50
support structure in Parr Shoals Power Reactor, 6(4): 69, 70-1
thermal analysis of multipass, 6(1): 23-4
Reactor design, 4(2): 44-51; 4(4): 50-68; 5(1): 74-5; 5(2): 33-47
Reactor dynamics, 4(1): 34-6; 4(3): 29-35; 5(1): 22-32; 5(2): 22-32
Reactor fuel alloys
See Fuel alloys
Reactor fuel breeding blankets
See Breeding blankets
Reactor fuel elements
See Fuel elements
Reactor hazards
See Safety
Reactor instrumentation
See Instrumentation
Reactor kinetics, 4(2): 22-30
Reactor maintenance, N. S. *Savannah* Reactor, 6(1): 53
Reactor materials, 4(2): 42-6; 5(1): 69-70; 5(2): 48-50; 5(3): 31-4; 5(4): 34-42; 6(1): 38-42; 6(2): 47-54; 6(3): 12-19
Reactor moderators
See Moderators
Reactor operation, 4(3): 56-70; 5(1): 76-7; 5(2): 56-60
Reactor physics, 4(1): 11-26; 4(2): 10-12; 4(3): 4-12; 4(4): 11-18; 5(1): 4-9; 5(2): 1-8; 5(3): 6-11; 5(4): 15-21; 6(1): 3-14; 6(2): 5-15; 6(3): 79-88; 6(4): 39-53
Reactor refueling, N. S. *Savannah* Reactor, 6(1): 53
Reactor safety, 5(2): 22-32
See Safety
Reactor shielding
See Shielding
Reactor theory, control, 6(2): 5-7
Reactor transfer functions, 4(2): 25-6
Reactor vessels
See Pressure vessels
Reactors, in combination with fuel cells, 4(3): 2-3
core instrumentation, 4(4): 34-6
decontamination by COD(S-4) process, 4(3): 45
design, 4(2): 44-51; 4(4): 50-68
dynamics, 4(1): 34-6; 4(3): 29-35
evaluation, 4(1): 1-2
hazards, 4(1): 37-42
kinetics, 4(2): 22-30
operating experience, 4(4): 69-75
shutdown cooling with steam, 5(4): 26
specifications for pressure vessels, 4(2): 44-8; 4(4): 50-4
spray cooling, 4(4): 20-5
Reactors (A1W), carbon-steel applications, 4(2): 49
Reactors (Advanced Gas-Cooled) (UK), pressure-vessel design, 4(4): 52, 54
steam-cycle efficiency, 4(4): 48
Reactors (Advanced Organic-Moderated), fuel-element development, 4(1): 61-2
Reactors (Advanced Sodium Graphite), design, 4(3): 91-3
Reactors (AGN-201), radiation chemistry applications, 4(3): 2
Reactors (AGR) (UK)
See Reactors (Advanced Gas-Cooled) (UK)
Reactors (Alco Products Critical Facility), critical experiments, 4(3): 7-8
Reactors (ANP), 6(3): 57
Reactors (APS-1) (USSR), steam-cycle efficiency, 4(4): 48
Reactors (Argonne High-Flux) (AHFR), core physics, 5(2): 2
Reactors (Argonne Low-Power)
See Reactors (SL-1)
Reactors (AVR) (West Germany), steam-cycle efficiency, 4(4): 48
Reactors (BEPO), coolant degradation, 5(3): 53
graphite corrosion in, 5(1): 80-1
Reactors (Berkeley) (UK), pressure-vessel design, 4(4): 52, 54
steam-cycle efficiency, 4(4): 48
Reactors (beryllium-moderated), breeding ratios, 4(1): 8
Reactors (Big Rock Point Power), economics, 4(4): 3, 4, 5
hydrodynamic characteristics, 6(3): 9
instrumentation, 5(2): 67, 73
steam-cycle efficiency, 4(4): 48
Reactors (BN-50) (USSR), steam-cycle efficiency, 4(4): 48
Reactors (Bohunice) (Czechoslovakia), steam-cycle efficiency, 4(4): 48
Reactors (boiling heavy-water), critical experiments, 5(4): 17
heavy-water radiolysis in boiling reactors, 6(4): 92-4
Reactors (boiling-water), 4(1): 68-70
See also Reactors (BONUS); Reactors (BORAX); Reactors (Byeloyarsk) (USSR); Reactors (Dresden Power); Reactors (Elk River Power); Reactors (Experimental Boiling-Water); Reactors (Humboldt Bay Power); Reactors (JPDR) (Japan); Reactors (Kahl) (West Germany); Reactors (Kinetic Experiment on Water Boilers); Reactors (Pathfinder Power); Reactors (PL-2); Reactors (SENN) (Italy); Reactors (SL-1); Reactors (Vallecitos Boiling-Water); Reactors (Variable-Moderator)
applications for remote power stations, 4(2): 4-9
control rods, 4(3): 87
coolant flow, 5(2): 14-15
dynamics, 4(3): 29-33
economics, 4(4): 8, 9; 6(1): 1-2
fuel utilization, 5(3): 2-5
heat transfer, 5(2): 14-15
marine applications, 4(3): 86-7
plutonium recycle, 5(4): 9, 10, 12, 13
stability, 4(1): 34-5
steam separation, 6(2): 69-74
water chemistry, 6(4): 92-6
Reactors (BONUS), bibliographies, 4(1): 57
containment, 5(1): 34-5; 5(2): 53, 54-5
design, 5(3): 82-3
development, 4(3): 76-82
economics, 4(4): 3, 4, 5
instrumentation, 5(2): 68, 73
nuclear superheaters, 6(2): 75-80
steam-cycle efficiency, 4(4): 48
Reactors (BORAX), BORAX-IV, operation, 5(2): 59-60
coolant radioactivity problems, 6(4): 95
design of BORAX-V, 5(3): 82-3; 5(4): 89, 90
fission-gas release in BORAX-IV, 4(1): 54
nuclear superheater in BORAX-V, 6(2): 77
operation with defective fuel plates in BORAX-IV, 6(4): 95-6
reactivity excursion in BORAX-I, 4(1): 38
stability, 4(1): 34
step tests on BORAX-IV, 4(2): 25
superheated-steam heat transfer in BORAX-V, 4(2): 19-20
superheater design for BORAX-V, 4(1): 71-3; 4(3): 82-3
water analysis in BORAX-IV, 4(3): 63
water chemistry, 6(4): 93-4
Reactors (BR-2) (Belgium), design and status, 5(4): 87
Reactors (BR-3) (Belgium), critical experiments, 4(1): 22
steam-cycle efficiency, 4(4): 48
Reactors (BR-5) (USSR), design and status, 5(4): 88, 90
fuel materials, 4(4): 85
Reactors (Bradwell) (UK), pressure-vessel design, 4(4): 52, 54
steam-cycle efficiency, 4(4): 48
Reactors (breeder)
See also Reactors (fast-breeder); Reactors (power breeder); Reactors (thermal breeder)
fuel utilization, 5(2): 2-5
Reactors (Bulk Shielding Facility), criticality experiments, 4(3): 7
$1/\beta$ measurements, 4(2): 25
Reactors (Byeloyarsk) (USSR), steam-cycle efficiency, 4(4): 48
Reactors (Calder Hall) (UK), cooling-water treatment, 5(1): 77
duct design, 4(1): 66-7
leak testing, 4(3): 70
pressure-vessel design, 4(4): 52, 54
resonance integrals, 4(1): 15
shield design, 5(3): 28-9
Reactors (CANDU) (Canada), design, 4(4): 65
economics, 4(4): 3, 4
fuel utilization, 6(4): 15
steam-cycle efficiency, 4(4): 48
Reactors (Carolinas-Virginia Power)
See Reactors (Parr Shoals Power) (CVTR)
Reactors (Chapelcross) (UK), cooling-water treatment, 5(1): 77
pressure-vessel design, 4(4): 54
Reactors (chemonuclear), 4(3): 1-2
Reactors (Commonwealth Edison)
See Reactors (Dresden Power)
Reactors (Consolidated Edison)
See Reactors (Indian Point Power) (CETR); Reactors (Ravenswood Power)
Reactors (Consolidated Nuclear Steam Generator) (CNSG), design, 6(4): 107, 111-13
Reactors (couples), 4(2): 29
Reactors (DIDO), iodine containment, 5(4): 29
Reactors (DIMPLE), Doppler temperature coefficients, measurement on, 4(1): 12-13
resonance integrals, 4(1): 19
Reactors (Dounreay Fast-Breeder) (UK), cooling-water treatment, 5(1): 77
design and status, 5(4): 88, 90
steam-cycle efficiency, 4(4): 49
Reactors (Dragon) (UK), design and status, 5(4): 87, 88; 6(1): 74-80
helium purification, 5(4): 76-8
pressure-vessel design, 4(4): 52
Reactors (Dresden Power), control, 4(4): 61, 62-3, 67
control-rod composition, 4(4): 46; 5(3): 34
control-rod failure, 4(4): 43, 45-6
coolant radioactivity problems, 6(4): 95
core instrumentation, 4(4): 35
corrosion problems, 6(4): 95
design details, 4(4): 56-68
fuel fabrication costs, 4(4): 5
instrumentation, 5(1): 46, 51, 52

Reactors (Dresden Power) (Continued)
operation, 5(2): 56-9; 6(2): 60-4
spatial power distribution stability, 4(2): 26
steam-cycle efficiency, 4(4): 48
waste disposal, 5(4): 49-50
Reactors (Dungeness) (UK), steam-cycle efficiency, 4(4): 48
Reactors (EDF) (France), pressure vessel, prestressed concrete for EDF-3, 5(4): 79
steam-cycle efficiency, 4(4): 48
Reactors (EL-4), 4(2): 74
Reactors (Elk River Power), bibliographies, 4(1): 57
design, 5(2): 33-46
economics, 4(4): 3, 4, 5
instrumentation, 5(1): 47, 51
steam-cycle efficiency, 4(4): 48
Reactors (Engineering Test) (ETR), control-rod experience, 4(4): 45
heat transfer, 5(4): 24
Reactors (Enrico Fermi Fast-Breeder), bibliographies, 4(1): 57
Doppler effect, 4(4): 16-17
economics, 4(4): 3, 4, 5
fuel-element melting, 5(2): 30-1
fuel elements, 4(1): 51-2
fuel fabrication costs, 4(4): 93
fuel materials, 4(4): 85
instrumentation, 5(1): 50, 51
steam-cycle efficiency, 4(4): 49
Reactors (ESSOR) (Italy), status, 6(1): 63
Reactors (Experimental Beryllium Oxide) (EBOR), design and status, 5(4): 87, 88
Reactors (Experimental Boiling-Water) (EBWR), control-rod failure, 4(4): 43, 45-6
coolant radioactivity problems, 6(4): 9
core instrumentation, 4(4): 35
corrosion problems, 6(4): 94-6
criticality studies, 5(4): 16
dynamics, 4(3): 29-33
economics, 4(4): 3
fission-gas release, 4(1): 53-4
fuel elements, radiation effects, 4(1): 32-4
heavy-water recovery, 4(2): 59
inspection after operation, 4(3): 56-69
instrumentation, 5(1): 44, 51, 52
operating experience, 4(3): 65-69
stability, 4(1): 34
steam contamination, 4(1): 54
steam-cycle efficiency, 4(4): 48
steam-void measurement, 5(2): 19
step tests, 4(2): 25
superheater experiments, 4(3): 82-3
test report list, 4(3): 62-3
turbine-shaft seals, 5(3): 37
vapor recovery system testing, 4(2): 59
water chemistry, 6(4): 93-4
Reactors (Experimental Breeder) (EBR), core design of EBR-I, 4(1): 35
dynamics of EBR-I, 5(2): 24-9
economics of EBR-II, 4(4): 3, 5
fuel-element melting in EBR-II, 5(2): 30-1
fuel elements, radiation effects, 5(3): 31
instrumentation in EBR-II, 5(2): 72, 73
radiation effects on fuel pins in EBR-II, 4(4): 84-5
shield design, EBR-II, 6(3): 85-6
steam-cycle efficiency of EBR-II, 4(4): 49
Reactors (Experimental Breeder II) (EBR-II), fuel-element melting, 5(2): 30-1
Reactors (Experimental Fast Oxide) (EFOR), design and status, 5(4): 88, 99
Reactors (Experimental Gas-Cooled) (EGCR), 4(1): 63-5
coolant temperature measurement, 5(3): 65-6
cooling system, 4(1): 29-30
core instrumentation, 4(4): 35
economics, 4(4): 3, 5
fuel-element critical experiments, 4(3): 6
fuel elements, thermal analysis, 5(3): 60-1
heat transfer, 5(3): 21-2
lattice-parameter measurements, 4(1): 23
seals, 5(1): 82-3
steam-cycle efficiency, 4(4): 48
temperature coefficient of reactivity, 4(1): 15
test loops, 4(3): 6
Reactors (Experimental Low-Temperature Process-Heat), design, 4(1): 1-2
Reactors (Experimental Organic-Cooled) (EOCR), design, 4(4): 76; 5(1): 88-91
status, 6(1): 63
Reactors (fast), fuel-element melting, 5(2): 29-31
fuel utilization, 5(3): 2-5
oxide fuel (dilute) reactivity, 5(2): 1
Reactors (fast-breeder), 4(4): 84-96
See also Reactors (BN-50) (USSR); Reactors (BR-5) (USSR); Reactors (Dounreay Fast-Breeder) (UK); Reactors (Enrico Fermi Fast-Breeder); Reactors (Experimental Breeder); Reactors (Plutonium-Fuel Fast-Breeder); Reactors (Rapsodie) (France); Reactors (Zebra) (UK); Reactors (ZPR-III)
applications for remote power stations, 4(2): 4
economics, 4(4): 8, 9; 6(1): 1-2; 6(3): 1-3
fuel utilization, 6(4): 24-7
Reactors (First Atomic Power Station) (USSR), design and status, 5(4): 90-1
Reactors (Florida Power), bibliographies, 4(1): 57
design, 4(2): 73-6
economics, 4(4): 3, 4, 5
steam-cycle efficiency, 4(4): 48
Reactors (fluid-fuel)
See also Reactors (homogeneous); Reactors (Homogeneous, Experimental); Reactors (Molten-Salt, Experiment) (MSRE)
applications for remote power stations, 4(2): 4
Reactors (fluidized-bed), heat transfer, heat transfer, 5(3): 22-4
Reactors (Fuel-Bearing Graphite) (FBGR), design, 6(3): 74-6
Reactors (G2) (France), pressure vessel, prestressed concrete, 5(4): 79
Reactors (G3) (France), pressure vessel, prestressed concrete, 5(4): 79
Reactors (gas-cooled), 4(1): 63-7; 5(1): 80-3; 5(3): 60-70; 5(4): 76-80; 6(3): 57-65
See also Reactors (Advanced Gas-Cooled) (UK); Reactors (AVR) (West Germany); Reactors (Berkeley) (UK); Reactors (Bohunice) (Czechoslovakia); Reactors (Bradwell) (UK); Reactors (Calder Hall) (UK); Reactors (Chapelcross) (UK); Reactors (Dragon) (UK); Reactors (Dungeness) (UK); Reactors (EDF) (France); Reactors (Experimental Gas-Cooled) (EGCR); Reactors (Gas-Cooled, Experiment) (GCRE); Reactors (GLEEP) (UK); Reactors (Hanford Test); Reactors (Hinkley Point) (UK); Reactors (Hunterston) (UK); Reactors (JAPC) (Japan); Reactors (Latina) (Italy); Reactors (ML-1); Reactors (Maritime Gas-Cooled); Reactors (Neuglobsow) (East Germany); Reactors (Sizewell) (UK); Reactors (Trawsfynydd) (UK); Reactors (TREAT)
applications for remote power stations, 4(2): 4
cooling systems, 4(1): 29-32
design, 6(1): 74-80
economics, 6(3): 1-3
fuel utilization, 6(4): 21-2
heat transfer, 5(3): 20-2
merchant-ship propulsion applications, 6(4): 106-11
plutonium recycle, 5(4): 9, 10, 12
shield design, 5(3): 28-9
Reactors (Gas-Cooled, Experiment) (GCRE), 6(3): 57
core instrumentation of GCRE-I, 4(4): 35
fuel-element design for GCRE-II, 5(1): 81-2
seals for GCRE-I, 5(1): 82-3
Reactors (gas-cooled heavy-water-moderated) *See* Reactors (EL-4) (France); Reactors (Florida Power)
Reactors (General Electric Test) (GETR), control-rod failure, 4(4): 43, 45-6
superheater tests, 4(3): 72
Reactors (GLEEP), neutron absorption cross-section measurements, 4(1): 20
thorium irradiation studies, 5(4): 18-19
Reactors (Godiva), power excursion in Godiva I, 4(2): 24, 29
Reactors (Godiva Critical Facility), 4(3): 8-9
Reactors (graphite-moderated)
See also Reactors (Sodium graphite); Reactors (Advanced Gas-Cooled) (UK); Reactors (APS-1) (USSR); Reactors (AVR) (West Germany); Reactors (Berkeley) (UK); Reactors (Bohunice) (Czechoslovakia); Reactors (Bradwell) (UK); Reactors (Calder Hall) (UK); Reactors (Chapelcross) (UK); Reactors (Dragon) (UK); Reactors (Dungeness) (UK); Reactors (EDF); Reactors (Experimental Gas-Cooled) (EGCR); Reactors (Gas-Cooled, Experiment) (GCRE); Reactors (GLEEP) (UK); Reactors (Hanford Test); Reactors (Hinkley Point) (UK); Reactors (Hunterston) (UK); Reactors (JAPC) (Japan); Reactors (Latina) (Italy); Reactors (Neuglobsow) (East Germany); Reactors (New Production); Reactors (Physical Constants Testing); Reactors (Sizewell) (UK); Reactors (Thermal Test); Reactors (Trawsfynydd) (UK); Reactors (TREAT)
breeding ratios, 4(1): 8
Reactors (Graphite-Moderated Boiling and Superheating) (GBSR), design, 5(3): 71-4, 79-83
Reactors (Hallam Power), bibliographies, 4(1): 57
boiling, 5(4): 26
component fabrication, 6(2): 81-2
core II, 4(3): 91
criticality studies, 5(1): 5-6
design, 5(3): 39-51
economics, 4(4): 3, 4, 5
flow orifices, 4(4): 19
fuel elements, 4(1): 51
fuel enrichment, 5(2): 3
fuel utilization, 6(4): 21
instrumentation, 5(2): 71, 73
pumps, 4(2): 59-61
seals, 4(2): 60-1; 4(4): 55
shielding, radio-induced heating in, 5(3): 29
steam-cycle efficiency, 4(4): 49
valve design, 4(4): 54-6
waste disposal, 5(4): 49-50
Reactors (Hanford Production), core instrumentation, 4(4): 35
Reactors (Hanford Test), neutron absorption cross-section measurements, 4(1): 19-20
Reactors (Heat-Transfer, Experiment 1) (HTRE-1), modification for marine applications, 6(4): 106
Reactors (heavy-water)
See also Reactors (CANDU) (Canada); Reactors (DIMPLE) (UK); Reactors (EDF) (France); Reactors (Florida Power); Reactors (Heavy-Water Components Test); Reactors (HIPPO) (Canada); Reactors (NPD) (Canada); Reactors (NRU) (Canada); Reactors (Parr Shoals); Reactors (Plutonium Recycle Test) (PRTR); Reactors (Process Development Pile); Reactors (Spectral Shift Control) (SSCR); Reactors (ZEEP) (Canada); Reactors (Zoé) (France)
applications for remote power stations, 4(2): 4
heavy-water losses, 6(1): 55-6
physics, 4(2): 11
plutonium recycle, 5(4): 9, 10, 12, 13
pump leakage, 4(4): 70-3; 5(3): 35
supercritical water reactors, 4(2): 78-81
valve leakage, 4(4): 70-3

Reactors (heavy-water boiling, design, 4(2): 65-6
Reactors (Heavy-Water Components Test) (HWCTR), burnout, 4(3): 21
carbon-steel applications, 4(2): 49
containment, 5(2): 51-4
design, 4(2): 74
fuel elements, 4(2): 65
pump seals, 5(3): 36-7
Reactors (heavy-water-moderated)
See also Reactors (EL-4) (France); Reactors (Florida Power)
breeding ratios, 4(1): 8
thermal converters, fuel utilization, 6(4): 13-16
Reactors (heavy-water-moderated organic-cooled)
See Reactors (organic-cooled heavy-water-moderated)
Reactors (heterogeneous)
See also specific reactors
flux hardening effects, 4(1): 11-12
physics calculations, 6(2): 7-11
Reactors (High-Flux Isotope) (HFIR), burnout, 4(3): 17
criticality studies on mockup, 4(3): 7
fuel-element corrosion, 5(3): 32-3
heat transfer, 5(1): 10-11
Reactors (High-Temperature Test Facility), criticality measurements, 4(1): 23-4
neutron-activation distribution measurements, 4(1): 23-4
Reactors (Hinkley Point) (UK), steam-cycle efficiency, 4(4): 48
Reactors (HIPPO) (Canada), temperature coefficient of reactivity, 4(2): 11
Reactors (homogeneous)
See also Reactors (Gas-Cooled, Experiment) (GCRE); Reactors (Homogeneous, Experiment) (HRE); Reactors (TREAT)
critical experiments, 4(3): 7
fuel utilization, 6(4): 21
Reactors (Homogeneous, Experiment) (HRE), fuel instability in HRE-II, 4(2): 26
Reactors (HR-2), design and status, 5(4): 88, 90
Reactors (Humboldt Bay Power), containment, 5(1): 33-4
economics, 4(4): 3, 4, 5
instrumentation, 5(2): 66, 73
pressure suppression, 4(2): 32-3; 5(4): 29; 6(3): 27
steam-cycle efficiency, 4(4): 48
Reactors (Hunterston) (UK), pressure-vessel design, 4(4): 52, 54
steam-cycle efficiency, 4(4): 48
Reactors (hydride-moderated)
See Reactors (Maritime Gas-Cooled); Reactors (SNAP Experiment)
Reactors (Indian Point Power) (CETR), critical experiments, 4(1): 22-3
design, 6(3): 28-41, 66-8
economics, 4(4): 3, 4
instrumentation, 4(4): 35; 5(1): 41, 51
steam-cycle efficiency, 4(4): 48
Reactors (Integral Boiling and Superheating) (IBSHR), design, 5(3): 71-4, 74-5, 79-83
Reactors (Integral Nuclear Superheater) (ISR), design, 5(3): 71-4, 75, 76, 79-83
Reactors (JAPC) (Japan), steam-cycle efficiency, 4(4): 48
Reactors (Jezebel Plutonium Critical Facility), 4(3): 8
Reactors (JPDR) (Japan), steam-cycle efficiency, 4(4): 48
Reactors (Kahl) (West Germany), steam-cycle efficiency, 4(4): 48
Reactors (KEMA Suspension Test) (KSTR), design and status, 5(4): 88
Reactors (Kinetic Experiment on Water Boilers) (KEWB), power excursions, 4(2): 23-4
transfer-function measurements, 4(3): 33
Reactors (Latina) (Italy), pressure-vessel design, 4(4): 52, 54
steam-cycle efficiency, 4(4): 48
Reactors (liquid-metal-cooled)
See also Reactors (sodium graphite); Reactors (BN-50) (USSR); Reactors (BR-5) (USSR); Reactors (Dounreay Fast-Breeder) (UK); Reactors (Enrico Fermi Fast-Breeder); Reactors (Experimental Fast-Breeder); Reactors (Plutonium-Fuel Fast-Breeder); Reactors (Rapsodie) (France); Reactors (SNAP Experimental); Reactors (ZEBRA) (UK); Reactors (ZPR-III)
conferences, 6(1): 60
economics, 4(4): 8, 9
Reactors (Lynchburg Pool) (LPR), nuclear constants studies, 6(1): 5-6
Reactors (marine), 6(1): 81-4; 6(4): 106-17
See also Reactors (Maritime Gas-Cooled); Reactors (N. S. *Savannah*)
boiling-water reactors, 4(3): 86-7
Reactors (Maritime Gas-Cooled) (MGCR), corrosion problems, 4(3): 43-4
seals, 5(1): 82-3
Reactors (Materials Testing) (MTR), fuel-element costs, 5(3): 3
fuel elements, radiation effects, 5(3): 31
heat transfer, 5(4): 24
scattering-law experiments, 6(1): 6-14
Reactors (McMurdo Sound), fuel-fabrication costs, 4(4): 5
steam-cycle efficiency, 4(4): 48
Reactors (merchant vessel)
See Reactors (Marine)
Reactors (MIT Research) (MITR), critical experiments, 5(4): 16
Reactors (Mixed-Spectrum Superheater) (MSSR), design, 5(3): 71-4, 75-7, 79-83
Reactors (ML-1), criticality experiments on ML-1-1B, 4(4): 12
design, 6(3): 59-60
design parameters, 4(2): 7
Reactors (Modified Lynchburg Source) (MLSR), critical experiments, 5(2): 14
Reactors (Molten-Salt, Experiment) (MSRE), design and status, 5(4): 88, 90
Reactors (Neuglobsow) (East Germany), steam-cycle efficiency, 4(4): 48
Reactors (New Production), carbon-steel applications, 4(2): 49
Reactors (NPD) (Canada), buckling measurements on fuel rods of NPD-1, 4(2): 11
containment of NPD-2, 5(1): 33
design of NPD-2, 4(2): 64-5, 74
iodine removal in NPD-2, 5(4): 31-2
steam-cycle efficiency of NPD-2, 4(4): 48
Reactors (NRU) (Canada), approach-to-critical experiments, 4(2): 11
scattering-law experiments, 6(1): 6-8
temperature coefficient of reactivity, 4(2): 11
Reactors (NRX) (Canada), thorium irradiation studies, 5(4): 18
Reactors (N. S. *Savannah*), design, 6(1): 43-54
instrumentation, 4(4): 35; 5(1): 40, 51
neutron-flux distribution, 5(3): 7
shielding, 4(3): 36; 6(3): 84-5
Reactors (Nuclear Steam Generator 630A), design, 6(4): 106-11
Reactors (nuclear superheat), 6(4): 97-105
See also Reactors (BONUS); Reactors (Pathfinder Power); Superheaters (nuclear)
Reactors (Oak Ridge Research) (ORR)
burnout studies for High-Flux Isotope Reactor, 4(3): 17
Reactors (Once-Through Superheater) (OTSR), design, 5(3): 71-4, 77, 79-83
Reactors (Organic-Cooled Deuterium, Experiment) (OCDRE), design, 4(2): 76
Reactors (organic-cooled heavy-water-moderated)
See also Reactors (Organic-Cooled Deuterium, Experiment) (OCDRE)
design, 4(4): 76
design and status, 5(4): 89
status, 6(1): 63
Reactors (organic-cooled and -moderated), 4(1): 58-62; 4(4): 76-83; 5(3): 52-9; 6(1): 62-73; 6(3): 70-2
See also Reactors (organic-cooled heavy-water-moderated); Reactors (Advanced Organic-Moderated); Reactors (Experimental Organic-Cooled) (EOCR); Reactors (Organic-Moderated, Experiment) (OMRE); Reactors (Piqua Power)
applications for remote power stations, 4(2): 4, 6
coolant energy absorption, 6(1): 67-70
coolant purification, 6(2): 57-9
economics, 4(4): 8, 9; 6(1): 1-2
fuel utilization, 6(4): 20-1
plutonium recycle, 5(4): 9, 10, 12
Reactors (Organic-Moderated) (OMR), coolant costs, 5(3): 58-9
criticality experiments in USSR, 4(1): 23
Reactors (Organic-Moderated, Experiment) (OMRE), control-rod experience, 4(4): 45
coolant degradation, 5(3): 52-6
coolant properties, 6(1): 62-3
coolant purification, 6(2): 57-9
coolant stability, 6(3): 72
design, 4(1): 58; 4(4): 76-83; 5(3): 56, 58-9; 6(1): 69
status, 6(1): 63
instrumentation, 4(4): 35; 5(1): 48, 51, 52
Reactors (ORNL Critical Experiments Facility), critical experiments on highly enriched uranium, 4(3): 7
Reactors (Pajarito Critical Assemblies Facility), 4(3): 9-10
Reactors (Parr Shoals Power) (CVTR), bibliographies, 4(1): 57
design, 4(2): 73, 74; 6(4): 63-81
economics, 4(4): 3, 4, 5
fuel elements, 5(1): 62
instrumentation, 5(2): 62, 73
steam-cycle efficiency, 4(4): 48
Reactors (Pathfinder Power), bibliographies, 4(1): 57
control rods, 5(2): 46-7
design, 5(3): 82-3
economics, 4(4): 3, 4, 5
instrumentation, 5(2): 69, 73
nuclear superheater, 6(2): 75-80
shield analysis, 6(3): 84
steam-cycle efficiency, 4(4): 48
superheater development, 4(3): 82
Reactors (Peach Bottom Power) (HTGR), 5(3): 61-5; 6(3): 64
comparison with Dragon Reactor, 6(1): 75
control-rod evaluation, 6(2): 49
economics, 4(4): 3, 4, 5
steam-cycle efficiency, 4(4): 48
Reactors (pebble-bed), design and status, 5(4): 87, 88
heat transfer, 5(3): 23-4
Reactors (Pebble-Bed, Experiment) (PBRE), fuel development, 6(3): 64
Reactors (Physical Constants Testing) (PCTR), critical experiments, 5(2): 1; 5(4): 15; 6(1): 4
Experimental Gas-Cooled-Reactor fuel-element testing, 4(3): 6
exponential experiments, 5(1): 4; 6(1): 4
graphite-moderating properties measurement, 4(3): 6-7
neutron-absorption cross-section measurements, 4(1): 19-20
neutron rethermalization studies, 5(2): 3-4, 5
temperature coefficient of reactivity, 4(1): 15
Reactors (Piqua Power), auxiliary systems, 4(2): 82-8
bibliographies, 4(1): 57
coolant costs, 5(3): 58
design, 4(4): 76; 5(4): 51-60; 6(1): 69
economics, 4(4): 3, 4, 5
fuel-element development, 4(1): 58, 60-1

Reactors (Piqua Power) (Continued)
instrumentation, 4(4): 35; 5(2): 70, 73
moderator, power absorption, 5(3): 58
status, 6(1): 63
steam-cycle efficiency, 4(4): 49
Reactors (PL-2), critical experiments, 6(2): 13-14
design parameters, 4(2): 7
economics at remote locations, 4(2): 6-8
Reactors (PLUTO), iodine containment, 5(4): 29, 30-1
Reactors (plutonium-fuel)
See also Reactors (BN-50) (USSR); Reactors (BR-5) (USSR); Reactors (Jezebel Plutonium Critical Facility); Reactors (Plutonium-Fuel Fast-Breeder); Reactors (Plutonium Recycle Test); Reactors (Rapsodie) (France)
breeding ratios, 4(1): 7-8
reactivity factors, 4(4): 86-96
Reactors (Plutonium-Fuel Fast-Breeder) (PFFBR), fuel elements, 4(4): 93, 94
Reactors (plutonium recycle), fuel utilization, 6(4): 16-20
Reactors (Plutonium Recycle Test) (PRTR), cooling with transverse flow of air, 6(4): 61
core instrumentation, 4(4): 35
critical experiments, 6(2): 13-14
heavy-water losses, 6(1): 55-6
design, 4(2): 73-4; 5(4): 89
fuel-element costs, 5(3): 3
pump design, 4(4): 71-3
Reactors (PM-1), critical experiments, 5(4): 15-16, 17-18
design, 4(2): 7; 6(3): 43-6
instrumentation, 4(4): 35; 5(2): 64, 73
Reactors (PM-2A), design, 4(2): 7
instrumentation, 5(1): 43, 51
Reactors (Popsy Critical Assembly), 4(3): 8
Reactors (power)
See also specific power reactors
breeding ratios, 4(1): 5-9
experiments, 5(4): 87-92
evaluation of U. S. programs, 6(2): 1-4
heat transfer, 4(2): 20
radiation from, 4(4): 33
Reactors (pressure tube), 4(2): 65-7
See also Reactors (Byeloyarsk) (USSR); Reactors (CANDU) (Canada); Reactors (New Production) (NPR); Reactors (Parr Shoals Power) (CVTR)
Reactors (Pressure-Tube Superheater) (PTSR), design, 5(3): 71-4, 77-8, 79-83
Reactors (Pressurized Critical Assembly), criticality studies, 4(2): 10
Reactors (pressurized-water)
See also Reactors (A1W); Reactors (APS-1) (USSR); Reactors (BR-3) (Belgium); Reactors (Experimental Low-Temperature Process-Heat); Reactors (High-Temperature Test Facility); Reactors (Indian Point Power); Reactors (McMurdo Sound); Reactors (N. S. *Savannah*); Reactors (PM); Reactors (Pressurized Critical Assembly); Reactors (Saxton Power); Reactors (SELNI) (Italy); Reactors (Shippingport Pressurized-Water); Reactors (SM); Reactors (Spectral Shift Control); Reactors (SPERT); Reactors (Ulyanovsk) (USSR); Reactors (Veronezh) (USSR); Reactors (Yankee Power)
applications for remote power stations, 4(2): 4-9
economics, 4(4): 8, 9; 6(1): 1-2; 6(3): 1-3
heat transfer, 4(2): 31-2; 5(4): 24
merchant-ship propulsion applications, 6(1): 83; 6(4): 109-17
operation without coolant purification, 6(2): 55-7
plutonium recycle, 5(4): 9-14
pressurization, 5(1): 78-9
thermal analysis, 4(1): 32
water decontamination, 4(3): 44-6
Reactors (PRO) (Italy), status, 6(1): 63
Reactors (Process Development Pile), buckling measurements, 4(2): 11-12; 5(2): 3
critical experiments, 5(4): 17
thermal-neutron-distribution measurements, 4(2): 10-11
Reactors (process-heat)
See also Reactors (Low-Temperature Process-Heat)
evaluation, 4(1): 1-2
Reactors (Prototype Organic Power) (POPR), 5(3): 58
Reactors (Puerto Rico)
See Reactors (BONUS)
Reactors (Puerto Rico Nuclear Center Research), fuel-element criticality, 4(3): 7
Reactors (R-3/Adam), fuel-element buckling studies, 5(2): 3; 5(3): 6-7
Reactors (Rapsodie) (France), design and status, 5(4): 88, 90
fuel materials, 4(4): 85
Reactors (Ravenswood Power), containment, 6(3): 21-6
Reactors (Savannah River Production), fuel-element-rupture detection, 5(4): 47, 49
heat-exchanger failure, 5(1): 76-7
step tests, 4(2): 25
Reactors (Saxton Power), bibliographies, 4(1): 57
design and status, 5(4): 89
fuel-fabrication costs, 4(4): 5
steam-cycle efficiency, 4(4): 48
Reactors (seed-blanket), economic potentials, 4(3): 38-41
Reactors (SELNI) (Italy), economics, 4(4): 3, 4
steam-cycle efficiency, 4(4): 48
Reactors (SENN) (Italy), economics, 4(4): 3, 4, 5
steam-cycle efficiency, 4(4): 48
Reactors (Separate Superheater) (SSR), design, 5(3): 71-4, 79-83
Reactors (Shippingport Pressurized-Water) (PWR), control-rod experience, 4(4): 45
core design, 4(2): 52-3
core modifications, 4(2): 58
departure from nucleate boiling, 5(2): 15-17
economics, 4(4): 3, 5
fission-gas release, 4(1): 54
fuel-burnup analysis in core I, 5(1): 1
fuel cycle, 4(3): 38-41
fuel-element thermal conductivity, 4(2): 41
fuel elements, 5(1): 54-6, 66-7
instrumentation, 4(2): 52, 56; 4(4): 35; 5(1): 37-8, 51, 52
boiling burnout, 6(1): 16-18
operating experience, 5(4): 61-72; 6(2): 64-7; 6(3): 49-55
operation without coolant purification, 6(2): 55-7
refueling, 4(2): 52-8
steam-cycle efficiency, 4(4): 48
step tests, 4(2): 25
waste disposal, 5(4): 49, 50
Reactors (Sizewell) (UK), steam-cycle efficiency, 4(4): 48
Reactors (SL-1), 4(1): 68-70
coolant radioactivity problems, 6(4): 95
instrumentation, 5(1): 45, 51
water chemistry, 6(4): 93-4
Reactors (SM-1), control-rod failure, 4(4): 43, 45-6
economics, 4(4): 3
instrumentation, 5(1): 42, 51
nuclear measurements, 4(3): 8
steam-cycle efficiency, 4(4): 48
pressure suppression during cooling-system rupture, 4(2): 33
Reactors (SM-1A), instrumentation, 5(2): 63, 73
Reactors (SM-2), critical experiments, 4(3): 7-8
economics at remote locations, 4(2): 6-8
Reactors (small power)
See also Reactors (AVR) (West Germany); Reactors (BONUS); Reactors (Dounreay Fast-Breeder) (UK); Reactors (Experimental Boiling-Water) (EBWR); Reactors (Experimental Breeder); Reactors (Kahl) (West Germany); Reactors (McMurdo Sound); Reactors (ML-1); Reactors (Piqua Power); Reactors (PM); Reactors (Saxton Power); Reactors (SL-1); Reactors (SM); Reactors (Sodium, Experiment) (SRE); Reactors (Vallecitos Boiling-Water)
critical measurements, 4(3): 4
Reactors (SNAP Developmental) (SDR), critical experiments, 6(3): 81-2
Reactors (SNAP Experimental) (SER), critical experiments, 4(4): 12; 6(3): 81-2
Reactors (sodium-cooled), 5(4): 73-5
See also Reactors (liquid-metal cooled)
Reactors (Sodium, Experiment) (SRE), boiling, 5(4): 26
carbon removal from coolant, 5(4): 74
control-rod experience, 4(4): 45
corrosion, 5(4): 73
design, 4(4): 73-4; 5(4): 89
economics, 4(4): 3, 5
fuel-element damage, 5(1): 84-7
fuel elements, radiation effects, 5(3): 31
fuel-rod bowing, 6(1): 57-60
instrumentation, 4(4): 35; 5(1): 49, 51
thermal analysis, 6(2): 25
oscillation measurements, 4(3): 33-4
steam-cycle efficiency, 4(4): 49
waste disposal, 5(4): 49-50
Reactors (sodium graphite), 4(3): 89-96
See also Reactors (Advanced Sodium Graphite); Reactors (Hallam Power)
applications for remote power stations, 4(2): 4
control rods, 5(4): 74-5
economics, 4(3): 92; 4(4): 8, 9; 6(1): 1-2; 6(3): 1-3
pressure vessels, 4(3): 90
Reactors (Sodium Modular), 4(3): 93-6
Reactors (Spectral Shift Control) (SSCR), criticality experiments, 4(4): 12; 5(1): 5; 5(3): 7; 5(4): 16-17; 6(2): 13-14; 6(3): 80-1
fuel utilization, 6(4): 21, 23
design, 5(4): 81-6
reactor constants, 6(1): 5-6
Reactors (SPERT), criticality studies, 5(2): 2
design of SPERT-III, 5(3): 85-7
dynamics, 5(2): 24
Hydrodynamic instabilities in SPERT-IA, 4(2): 27-8
operating transients, 5(2): 22-4
oscillator program in SPERT-I, 4(2): 25
power excursions in SPERT-I, 4(2): 22-3
reactivity excursions in SPERT-I, 4(1): 38
reactor dynamics, 5(1): 22-32
stability, 4(1): 34
steam voids in SPERT-IA, 4(2): 27
Reactors (spray-cooled), 4(1): 74-7
Reactors (steam-cooled), 5(3): 71-84
Reactors (Steam-Cooled Fast-Breeder) (SCFBR), design, 5(3): 71-4, 76, 78-9, 79-83
Reactors (Steam-Cooled Heavy-Water-Moderated) (SCDMR), design, 5(3): 71-4, 76, 78, 79, 79-83
Reactors (Supercritical Once-Through Tube) (SCOTT-R), design, 6(3): 74-8
Reactors (Supercritical Pressure Power) (SPPR), design, 6(3): 73-8
Reactors (supercritical water), 4(2): 78-81; 6(3): 73-8
Reactors (superheat), design, 5(1): 14
heat transfer, 5(1): 13-14
Reactors (superheater)
See Superheaters (nuclear); Reactors (BONUS); Reactors (Byeloyarsk) (USSR); Reactors (Elk River Power); Reactors (Pathfinder); Reactors (Separate Superheater) (SSR)

Reactors (thermal), Doppler effect, 4(4): 14-17
Reactors (thermal breeder), 6(4): 27-8
Reactors (thermal converter), fuel utilization, 6(4): 7-24
Reactors (Thermal Test), neutron multiplication and exponential experiments, 4(3): 6
Reactors (thorium-cycle), fuel utilization, 6(4): 22-4
Reactors (Topsy Critical Facility), 4(3): 8
Reactors (Trawsfynydd) (UK), steam-cycle efficiency, 4(4): 48
Reactors (TREAT), burnout, 4(1): 40-1
  fuel-element melting, 5(2): 29-31
  kinetics, 4(3): 34
  power excursions, 4(2): 24-5
Reactors (Ulyanovsk) (USSR), steam-cycle efficiency, 4(4): 48, 49
Reactors (Unified Modular) (UNIMOD), design, 6(4): 107, 111, 114-17
Reactors (Vallecitos Boiling-Water) (VBWR), control-rod experience, 4(4): 45
  coolant radioactivity problems, 6(4): 95
  design and status, 5(4): 90
  fission-gas release, 4(1): 54
  fuel-fabrication costs, 4(4): 5
  hydrodynamic characteristics, 6(3): 9-10
  instrumentation, 5(2): 65, 73
  maintenance procedures, 5(4): 46-7
  SADE loop superheater experiments, 4(3): 74-5
  stability, 4(1): 34
  steam-cycle efficiency, 4(4): 48
  water chemistry, 6(4): 93-4
Reactors (Vallecitos Experimental Superheat) (VESR), design and status, 5(4): 89, 90
Reactors (Variable-Moderator), 4(1): 77-8
  critical assemblies, 4(3): 4
  design, 5(3): 88-9
Reactors (Veronezh) (USSR), steam-cycle efficiency, 4(4): 48
Reactors (VULCAIN), design and status, 5(4): 89
Reactors (water-cooled)
  See Reactors (water-cooled and -moderated); Reactors (ML-1); Reactors (New Production); Reactors (Thermal Test)
Reactors (water-cooled and -moderated)
  See also Reactors (boiling-water; Reactors (pressurized-water); Reactors (Alco Products Critical Facility); Reactors (Bulk Shielding); Reactors (Engineering Test); Reactors (General Electric Test) (GETR); Reactors (Homogeneous, Experiment) (HRE); Reactors (ORNL Critical Experiments Facility)
  breeding ratios, 4(1): 6-8
  metal-water reaction studies, 4(1): 37
  power distributions, 4(1): 17
  thermal converters, fuel utilization, 6(4): 9-13
Reactors (Whiteshell No. 1) (WR-1), status, 6(1): 63
Reactors (Yankee Power), 4(3): 47-55
  bibliographies, 4(1): 57
  core evaluation after operation, 6(3): 55-6
  corrosion problems, 6(4): 82-3
  critical experiments, 4(1): 21-2
  instrumentation, 4(4): 35; 5(1): 39, 51
  nuclear constants measurements, 4(1): 21
  operating experience, 4(4): 69-70; 6(4): 82-91
  power distributions in critical experiments, 4(1): 17
  pump leakage, 5(3): 35
  reactivity characteristics, 6(4): 86-91
  steam-cycle efficiency, 4(4): 48
Reactors (ZEBRA) (UK), buckling measurements, 4(2): 11
Reactors (ZEEP) (Canada), critical experiments, 4(2): 11
  reactivity, 4(2): 11
  temperature coefficient of reactivity, 4(2): 11
Reactors (Zoé) (France), neutron-absorption cross-section measurements, 4(1): 20
Reactors (ZPR-III), criticality studies, 5(2): 1-2; 5(3): 6-7; 6(3): 80
  step tests, 4(2): 25
Reactors (ZPR-VII), critical experiments, 5(4): 16
Rectangular channels
  See Channels (rectangular)
Refueling, Piqua Power Reactor, 5(4): 59
  Shippingport Pressurized-Water Reactor, 4(2): 52-8
  Sodium Modular Reactor, 4(3): 94
Remote power plants
  See Power plants (remote)
Resonance absorption, 6(3): 79-80
Resonance integrals, measurement, 5(4): 19-20
Rods
  See also Control rods; Fuel elements (rods)
  boiling burnout, 6(1): 16-18
  cooling with mercury, 4(3): 15-16
Rubidium chloride–cesium chloride–lithium chloride–sodium chloride systems
  See Cesium chloride–lithium chloride–rubidium chloride–sodium chloride systems

S

SADE
  See Superheater Advance Demonstration Experiment (SADE)
Safety, 5(2): 22-32
  containment for Indian Point Power Reactor, 6(3): 39
  criticality hazards, 4(4): 13-14; 5(1): 6
  Experimental Boiling-Water Reactor, 4(3): 59
  Failed-Element Detection and Location System, 6(3): 49
  guide, 4(4): 13-14
  metal-water reactions, 4(1): 37-42
  overpower protection system in Shippingport Pressurized-Water Reactor, 6(2): 66
  pressure suppression, 6(3): 27
  radiation from power reactors, 4(1): 43
  Ravenswood Power Reactor containment, 6(3): 21-6
  Yankee Power Reactor, 4(3): 47
Saline water conversion, reactor application, 4(1): 2
Samarium, flux hardening effects, 4(1): 11
  reactivity-worth burnup, 4(4): 42
Samarium compounds, evaluation for reactor control applications, 6(3): 15
Samarium hexaboride, 4(4): 44
Samarium oxide–gadolinium oxide systems
  See Gadolinium oxide–samarium oxide systems
Santowax OM coolant, 6(1): 65
Santowax OM-2 coolant, 6(1): 65
  radiation effects, 5(3): 57
Santowax OMB coolant
  See also Polyphenyls
  gas removal, 4(2): 84-8
  purification, 4(2): 82-3
Santowax OMP coolant, 6(1): 65
  radiation effects, 5(3): 57
  reactor cooling, 5(1): 88
  stability under reactor conditions, 6(3): 71-2
Santowax R
  See also Terphenyl coolant
  pyrolysis, 5(3): 52
  radiation effects, 5(3): 52-6, 57
  reactor cooling, 5(1): 88
  stability under reactor conditions, 6(3): 70-2
Santowax R–uranium lattices
  See Uranium–Santowax R lattices
Savannah Reactor
  See Reactors (N. S. *Savannah*)
Savannah River Plant, design, 5(4): 1-5
Savannah River Production Reactors
  See Reactors (Savannah River Production)
Saxton Power Reactor
  See Reactors (Saxton Power)
SCDMR
  See Reactors (Steam-Cooled Heavy-Water-Moderated (SCDMR)
SCFBR
  See Reactors (Steam-Cooled Fast-Breeder Reactor) (SCFBR)
SCOTT-R
  See Reactors (Supercritical Once-Through Tube) (SCOTT-R)
SDR
  See Reactors (SNAP Developmental) (SDR)
Seals, BORAX-V superheater, 4(3): 83
  Experimental Gas-Cooled Reactor, 5(1): 82-3
  Gas-Cooled Reactor Experiment I, 5(1): 82-3
  Hallam Power Reactor, 4(2): 60-1; 4(4): 55
  leakage in Calder Hall Reactors, 4(3): 69-70
  Maritime Gas-Cooled Reactor, 5(1): 82-3
  pump, 5(3): 35-7
  turbine shaft, 5(3): 37
Seals (freeze), Hallam Power Reactor, 4(2): 60; 4(4): 55
Seed-blanket reactors
  See Reactors (seed-blanket)
Seed-blankets, analysis, 4(3): 38-41
SELNI (Italy) Power Reactor
  See Reactors [SELNI (Italy) Power]
SENN (Italy) Power Reactor
  See Reactors [SENN (Italy) Power]
Separate Superheater Reactor
  See Reactors (Separate Superheater) (SSR)
SER
  See Reactors (SNAP Experimental) (SER)
17-4 CuMo alloy, nuclear superheater applications, 5(4): 38
SGR
  See Reactors (Hallam Power)
Shielding, 4(2): 34-7; 4(3): 36-7; 4(4): 32-3; 5(3): 27-30; 5(4): 28
  calculations, 6(3): 83-4
  Dresden Power Reactor, 4(4): 67-8
  effectiveness of N. S. *Savannah* Reactor, 6(3): 84-5
  Elk River Power Reactor, 5(2): 46
  Experimental Breeder Reactor II, 6(3): 85-6
  Indian Point Power Reactor, 6(3): 40
  N. S. *Savannah* Reactor, 6(1): 53
  Parr Shoals Power Reactor, 6(4): 81
  Pathfinder Power Reactor, 6(3): 84
  SL-1 Reactor, 4(1): 68
  Yankee Power Reactor, 4(3): 54
Ship propulsion reactors
  See Reactors (marine)
Shippingport Pressurized-Water Reactor
  See Reactors (Shippingport Pressurized-Water)
Ships, nuclear propulsion studies, 6(1): 81-4; 6(4): 106-17
Shock-resistant structures
  See Structures (blast-resistant)
Silicon, reactions with uranium carbides, 4(1): 46
Silicon-aluminum systems
  See Aluminum-silicon systems
Silicon carbide, compatibility with gaseous coolants, 5(3): 61
Silicon-molybdenum-uranium systems
  See Uranium-molybdenum-silicon systems
Silver, corrosion in Yankee Power Reactor, 6(4): 82
  evaluation for control applications, 6(3): 82
Silver alloys, corrosion by water, 6(2): 53
Silver-cadmium alloys
  See Cadmium-silver alloys
Silver-cadmium-indium alloys
  See Cadmium-indium-silver alloys
Sintering, fuel elements, 5(1): 67
Sioux Falls Reactor
  See Reactors (Pathfinder Power)
Sizewell Reactors (UK)
  See Reactors (Sizewell) (UK)
SL-1 Reactor
  See Reactors (SL-1)
Slip velocity, determination, 4(2): 26

SM-1 Reactor
See Reactors (SM-1)
SM-1A Reactor
See Reactors (SM-1A)
SM-2 Reactor
See Reactors (SM-2)
Small power reactors
See Reactors (small power)
SNAP Critical Assembly
See Reactors (SNAP Critical Assembly)
SNAP Developmental Reactor
See Reactors (SNAP Developmental) (SDR)
SNAP Experimental Reactor
See Reactors (SNAP Experimental) (SER)
SNG code, neutron cross-section calculation, **6**(4): 47
neutron-flux calculation, **6**(4): 40
Sodium (liquid), boiling, **5**(4): 26
carbon, removal from, **5**(4): 74
pool boiling, **6**(1): 20-1
reactions with uranium carbides, **4**(1): 46
service system for Hallam Power Reactor, **5**(3): 46, 48
stainless-steel corrosion, **5**(4): 73
valve design for containing, **4**(4): 54-6
zirconium corrosion, **5**(4): 73
Sodium bisulfate process, corrosion of reactor materials, **4**(3): 44
Sodium chloride–cesium chloride–lithium chloride–rubidium chloride systems
See Cesium chloride–lithium chloride–rubidium chloride–sodium chloride systems
Sodium-cooled reactors
See Reactors (sodium-cooled)
Sodium Graphite Reactor
See Reactors (Hallam Power); Reactors (Sodium, Experiment) (SRE)
Sodium graphite reactors
See Reactors (sodium graphite)
Sodium iodide, entrainment in water, **5**(4): 30
Sodium Modular Reactor
See Reactors (Sodium Modular)
Sodium-potassium alloys (liquid), reactions with uranium carbides, **4**(1): 46
Sodium Reactor Experiment
See Reactors (Sodium, Experiment) (SRE)
SOFOCATE computer code, **5**(2): 2, 4, 6
Solid-gas systems, heat transfer, **4**(3): 16-17; **6**(1): 22-3
SPAN-3 computer code, **5**(4): 28
Special Power Excursion Reactor Test
See Reactors (SPERT)
Spectral Shift Control Reactor
See Reactors (Spectral Shift Control) (SSCR)
SPERT reactors
See Reactors (SPERT)
Spheres, heat transfer, **5**(3): 22-4
hydrodynamic characteristics, **5**(3): 22-4
SPPR
See Reactors (Supercritical Pressure Power) (SPPR)
Spray-cooled reactors
See Reactors (spray-cooled)
Spray cooling
See Cooling systems (spray)
Square fuel channels
See Channels (square)
SRE
See Reactors (Sodium, Experiment) (SRE)
SSCR
See Reactors (Spectral Shift Control) (SSCR)
SSR
See Reactors (Separate Superheater) (SSR)
Stainless steel, application in supercritical water reactors, **4**(2): 81
coextrusion with Zircaloy, **6**(2): 51-3
corrosion, by ammonium citrate process solutions, **4**(3): 45
by carbon oxides, **4**(3): 43-4
by carbon monoxide–hydrogen systems, **4**(3): 43-4
by oxalic acid process solutions, **4**(3): 45
by phosphoric acid process solutions, **4**(3): 45
by sodium (liquid), **5**(4): 73
by sodium bisulfate process solutions, **4**(3): 44
by water, **6**(2): 53
nuclear superheater applications, **5**(4): 36-8
neutron absorption, **5**(1): 5-6
physical properties, **6**(3): 17-18
radiation effects, **5**(1): 70; **5**(3): 33; **5**(4): 35-6
reactions, with rare earths, **6**(3): 15
with uranium carbides, **4**(1): 46
stress corrosion, **6**(2): 50-1
Stainless steel (304), failure in heat exchangers, **5**(1): 76-7
radiation effects, **5**(1): 70
Stainless steel (304L), failure in heat exchangers, **5**(1): 76-7
Stainless steel (308), radiation effects, **5**(1): 70
Stainless steel (boron), radiation effects, **5**(3): 33
Stainless-steel–boron systems
See Boron–stainless-steel systems
Stainless-steel–uranium oxides (UO_2) cermets
See Uranium oxides (UO_2)–stainless-steel cermets
Stationary Low-Power Plant No. 1
See Reactors (SL-1)
Steam, aluminum corrosion, **5**(4): 40
beryllium corrosion, **5**(4): 40
condensation, **5**(3): 18-19
contamination in Experimental Boiling-Water Reactor, **4**(1): 54
cooling properties, **5**(4): 26
corrosion, of borides, **4**(4): 43, 44
of boron, **4**(4): 44
of boron carbide, **4**(4): 44
of boron nitride, **4**(4): 43, 44
of pipes, **4**(3): 65-6
corrosive effects in nuclear superheaters, **4**(3): 72-4
heat transfer in superheated, **4**(2): 19-20
niobium-vanadium alloy corrosion, **5**(3): 32
reactions, with uranium carbides, **4**(1): 47
with uranium carbide–zirconium carbide systems, **4**(1): 52
with zirconium, **4**(1): 38-9
separation from water, **4**(3): 81, 82; **6**(2): 69-74
superheater cooling, **4**(3): 13-15
Zircaloy-2 corrosion, **5**(3): 31-2; **5**(4): 40
Zircaloy-4 corrosion, **5**(3): 32
zirconium corrosion, **5**(4): 40
zirconium-iron-nickel alloy corrosion, **5**(3): 32
Steam (saturated), heat transfer, **5**(2): 18-19
Steam (superheated), heat transfer, **4**(2): 19-20; **5**(1): 12; **5**(3): 20
thermal conductivity, **4**(2): 19
viscosity, **4**(2): 19
Steam-Cooled Fast-Breeder Reactor
See Reactors (Steam-Cooled Fast-Breeder) (SCFBR)
Steam-Cooled Heavy-Water-Moderated Reactor
See Reactors (Steam-Cooled Heavy-Water-Moderated) (SCDMR)
Steam-cooled reactors
See Reactors (steam-cooled)
Steam cycles, efficiency, **4**(4): 47-9
Steam flow, tubes, **5**(1): 13
Steam generators, circulation, **5**(1): 13
corrosion in Shippingport Pressurized-Water Reactor, **5**(4): 69
Elk River Power Reactor, **5**(2): 44
Hallam Power Reactor, **5**(3): 45, 47
once-through design, **5**(3): 13
Parr Shoals Power Reactor, **6**(4): 77
temperature distribution, **5**(1): 13
Steam plants, Dresden Power Reactor, **4**(4): 66
Steam separators, **6**(2): 69-74
Steam void, measurement, **5**(2): 19
Steam-water systems, burnout characteristics, **5**(3): 15-18
flow, **4**(4): 28-9, 31
flow characteristics, **6**(2): 24-5
flow stability, boiling effects, **5**(2): 12-14
heat transfer, **5**(1): 15-17
pressure drop in flow, **5**(2): 19
pressure-wave propagation, **4**(4): 31
Steel, coatings, nondestructive testing, **5**(1): 71
compatibility with aluminum, **4**(1): 1-2
corrosion by water, **4**(1): 2
radiation effects, **4**(2): 46; **5**(3): 33; **5**(4): 34-6
reactions with uranium carbides, **4**(1): 46
Steel (boron), impact tests, **4**(4): 46
Steel (carbon), corrosion, by ammonium citrate process solutions, **4**(3): 45
by COD (S-4) process solutions, **4**(3): 45
by nitric acid process solutions, **4**(3): 45
by oxalic acid process solutions, **4**(3): 45
by phosphoric acid process solutions, **4**(3): 45
by sodium bisulfate process solutions, **4**(3): 44
corrosion rates, **4**(2): 49-50
decontamination, **4**(2): 49-50
reactor applications, **4**(2): 49-50
Steel (chromium-molybdenum), corrosion by carbon monoxide, carbon monoxide–carbon dioxide systems, and carbon monoxide–hydrogen systems, **4**(3): 43-4
Steel (mild), corrosion by water, **6**(2): 53
Steel (stainless)
See Stainless steel
Steel spheres, heat transfer, **5**(3): 23
hydrodynamic characteristics, **5**(3): 23
Stellite alloy, corrosion by nitric acid process solutions, **4**(3): 45
Structures (blast-resistant), reactor containment, **5**(1): 35-6
Subcritical assemblies
See Reactors (name of subcritical assembly)
blanket-element composition determination, **5**(1): 1
Sulfur foils
See Foils (sulfur)
Supercritical carbon dioxide
See Carbon oxides (CO_2) (supercritical)
Supercritical fluids
See Fluids (supercritical)
Supercritical Once-Through Tube Reactor
See Reactors (Supercritical Once-Through Tube) (SCOTT-R)
Supercritical Pressure Power Reactor
See Reactors (Supercritical Pressure Power) (SPPR)
Supercritical water
See Water (supercritical)
Supercritical water reactors
See Reactors (supercritical water)
Superheat reactors
See Reactors (superheat)
Superheated steam
See Steam (superheated)
Superheater Advance Demonstration Experiment (SADE), materials, **5**(4): 37-8
superheater studies, **4**(3): 74-5
Superheaters, Hallam Power Reactor, **5**(3): 46
shutdown, **4**(3): 13-15
Superheaters (nuclear), **4**(1): 71-3; **4**(2): 19-20; **4**(3): 71-85; **6**(2): 75-80; **6**(4): 97-105
See also Reactors (BONUS); Reactors (Byeloyarsk) (USSR); Reactors (Elk River Power); Reactors (Pathfinder Power)
critical experiments, **6**(2): 12-16
design, **6**(4): 97-105
materials, **5**(4): 36-9
spray-cooled reactors, **4**(1): 75-6; **4**(4): 24-5
Surface testing, nondestructive testing applications, **5**(1): 73
Swaging, fuel elements, **5**(1): 63

SWAKRAUM code, neutron-flux calculations, 6(4): 40

T

Tables, neutron age, 5(1): 7
Tankers, nuclear propulsion, 4(3): 87
Tanks
See Moderator tanks
Tantalum, reactions with uranium carbides, 4(1): 46
Terbium oxide, reactivity worth, 4(4): 40
Terphenyls
See also Coolants (organic)
boiling heat transfer, 4(4): 82
chemical structure, 6(1): 64
properties, 4(4): 77-8
radiation effects, 5(3): 57
reactions with uranium carbides, 4(1): 47
stability under reactor conditions, 6(3): 70-2
Thermal breeder reactors
See Reactors (thermal breeder)
Thermal conductivity, 5(1): 10; 5(2): 9-10; 6(2): 17-18
calculations, 5(4): 22-3
fuel elements, 4(2): 41; 5(4): 22-3
gadolinium oxide, 6(3): 15-16
gadolinium oxide–samarium oxide systems, 6(3): 15-16
glass beads, 5(3): 22-3
graphite, 5(4): 39-40
helium, 5(3): 69
mathematical analysis, 4(2): 13
perforated solids, 4(4): 19-20
superheated steam, 4(2): 19
thorium carbide, 4(1): 48
thorium oxide, 4(1): 53
uranium-aluminum alloys, 4(1): 61
uranium carbides, 4(1): 50
uranium-graphite systems, 4(1): 61-2
uranium-magnesium alloys, 4(1): 61
uranium oxide (UO_2), 4(1): 50; 4(2): 38-43; 4(4): 22-3; 5(2): 9-10; 5(4): 22-3; 6(2): 17-18; 6(3): 4-5, 12-15
uranium oxide (UO_2)–calcium oxide–zirconium oxide systems, 5(1): 67
uranium oxide (UO_2) (stainless-steel-clad), 5(4): 22-3
Thermal converter reactors
See Reactors (thermal converter)
Thermal effects, 4(2): 26-8
Thermal expansion, graphite, 5(4): 40
uranium carbides, 4(1): 50
uranium dioxide, 4(1): 50
Thermal insulation, gas-cooled reactors, 5(3): 68-9
Thermal-neutron diffusion parameters, 4(1): 16-17
Thermal neutrons
See Neutrons (thermal)
Thermal radiation, 5(1): 10
heat transfer, 4(2): 20
Thermal reactors
See Reactors (thermal); specific reactors
Thermal Test Reactor
See Reactors (Thermal Test)
Thermal testing, nondestructive testing techniques, 5(1): 73
THERMOS computer code, 5(4): 16
neutron-flux calculations, 6(4): 40
Thinbles (fuel)
See Fuel elements (thimbles)
Thorium, corrosion by water, 6(2): 53
Doppler coefficients, 4(1): 12-14; 4(4): 15-16
radiation effects, 5(4): 18-19
resonance integrals, 5(4): 20
Thorium-232, conversion to U^{233}, 6(4): 1-4
neutron cross sections, 5(2): 7
resonance integrals, 6(1): 5
Thorium (irradiated), radioactivity, 4(4): 37
reactivity, 4(4): 37-8; 5(4): 18-19
Thorium carbides, physical properties, 4(1): 48
Thorium-cycle reactors
See Reactors (thorium-cycle)
Thorium-graphite systems, resonance absorption, 6(3): 79-80
Thorium oxide, age to indium resonance in water–heavy-water mixtures, 6(1): 5-6
Doppler coefficients, 4(4): 15-16
thermal conductivity, 4(1): 53
Thorium oxide–uranium oxide (UO_2) systems
See Uranium oxide (UO_2)–thorium oxide systems
Thorium oxide–uranium oxide (UO_2)–heavy-water lattices
See Uranium oxide (UO_2)–thorium oxide–heavy-water lattices
Thorium oxide–uranium oxide (UO_2)–water lattices
See Uranium oxide (UO_2)–thorium oxide–water lattices
Thorium oxide–uranium systems
See Uranium–thorium oxide systems
Thorium-plutonium alloys
See Plutonium-thorium alloys
Thorium-uranium alloys
See Uranium-thorium alloys
Thorium Uranium Physical Experimental Program, critical experiments, 4(1): 22-3
THUD program, critical experiments, 5(4): 16
Tin, shielding applications, 4(2): 34
Tin (liquid), reactions with uranium carbides, 4(1): 46
Tin-zirconium alloys
See Zirconium-tin alloys
Titanium, corrosion by water, 6(2): 53
reactions with uranium carbides, 4(1): 46
Titanium-aluminum alloys
See Aluminum-titanium alloys
Titanium boride (TiB_2), corrosion by steam, 4(4): 44
radiation effects, 4(4): 44
solubility in boiling water, 4(4): 43
Titanium-niobium alloys
See Niobium-titanium alloys
Topsy Critical Facility
See Reactors (Topsy Critical Facility)
Transient analysis, 4(2): 28-30
Transient boiling
See Boiling (transient)
Transient Reactor Test Facility
See Reactors (TREAT)
Transport equation, 6(4): 39-41
Trawsfynydd Reactors (UK)
See Reactors (Trawsfynydd) (UK)
TREAT Reactors
See Reactors (TREAT)
Tubes
See also Channels; Fuel elements (tubes); Pressure tubes
burnout, 4(3): 21-4; 4(4): 28; 5(1): 19-20; 5(3): 16-17
burnout flow conditions, 5(2): 18
cooling with mercury, 4(3): 15-16
criticality effects of aluminum, 4(2): 11
criticality effects of Zircaloy-2, 4(2): 11
fabrication of Zircaloy-2, 4(3): 42
fluid flow, 5(1): 12, 13
heat transfer, 5(1): 13; 5(3): 21
nondestructive testing of Zircaloy, 6(2): 53
subcooled nucleate boiling in forced convection, 6(1): 15-16
Tubes (horizontal), heat transfer, 4(1): 27-9
Tungsten, reactions with rare earths, 6(3): 15
Tungsten alloys, neutron reflection, 4(3): 10
TUPE
See Thorium Uranium Physical Experimental Program
Turbines, failure in Shippingport Pressurized-Water Reactor, 5(4): 69
design of gas, 6(1): 79
inspection of Experimental Boiling-Water Reactor, 4(3): 56-7
shaft seals, 5(3): 37
SL-1 Reactor, 4(1): 69
Yankee Power Reactor, 4(3): 55
Two-phase flow
See Fluid flow (two-phase); Gas-liquid systems; Slurry flow; Steam-water systems

U

Ultrasonics, nondestructive testing techniques, 5(1): 72
Unified Modular Reactors
See Reactors (Unified Modular) (UNIMOD)
UNIMOD
See Reactors (Unified Modular) (UNIMOD)
United States coal reserves, 4(2): 1-3
Ulyanovsk Reactor (USSR)
See Reactors (Ulyanovsk) (USSR)
Uranium, analysis, 5(1): 71
background neutron source in new reactors, 4(1): 17-19
buckling measurements, 4(2): 11-12
Canadian reserves, 4(2): 1-2
corrosion by water, 6(2): 53
criticality studies on beryllium oxide-moderated, 4(2): 10
Doppler coefficients, 4(1): 12-14; 4(4): 14-15
European reserves, 4(2): 1-2
fission-gas release, 4(1): 54-5
fuel-element applications in organic reactors, 4(1): 58
fuel elements (tubes), aluminum-clad, 5(1): 4
neutron reflection, 4(3): 10
prices, official AEC, 4(4): 1-2
radiation effects, 4(1): 54-5; 5(3): 31; 5(4): 40-1
reactions with water, 4(1): 40-1
resonance absorption in heavy-water lattices, 6(3): 79-80
resonance integrals, 4(1): 16; 5(4): 19-20
thermal-neutron distribution in heavy-water-moderated, 4(2): 10-11
U. S. reserves, 4(2): 1-3
Uranium (aluminum-clad), buckling measurements on tubes, 5(2): 1
criticality studies, 5(4): 16, 17
exponential experiments, 5(3): 8
Uranium carbides (UC), development for fuel elements, 6(2): 43-4
Uranium (depleted), neutron reflection, 4(3): 9-10
prices, 5(4): 5-7
Uranium (enriched), background neutron source in Zircaloy-2-clad, 4(1): 17-19
cost factors, 4(1): 3-5
criticality, 4(3): 9; 5(3): 7
neutron reflection, 4(3): 10
prices, official AEC, 4(4): 1-2; 5(4): 5-7
Uranium (highly enriched), criticality, 4(3): 7
Uranium (irradiated), analysis of breeding blankets, 5(1): 1
Uranium (Lucite-clad), buckling measurements, 4(3): 5
Uranium (Magnox-clad), heat transfer, 5(3): 12-13
Uranium (niobium-clad), melting in fast reactors, 5(2): 31
Uranium (stainless-steel-clad), melting in fast reactors, 5(2): 30-1
radiation effects, 5(4): 41
Uranium (tantalum-clad), melting in fast reactors, 5(2): 31
Uranium (Zircaloy-2-clad), heat transfer, 4(4): 19-20
radiation effects, 5(4): 41
Uranium-233, breeding ratio, 4(1): 7-8
neutron age to indium resonance measurements in water, isoamyl alcohol, cyclohexanone, benzyl alcohol, toluene, formic

Uranium-233 (Continued)
acid, and a mixture of organic compounds, 4(1): 20-1
neutron cross sections, 5(2): 6, 7
production from Th^{232}, 6(4): 1-4
Uranium-234, neutron cross sections, 5(2): 7
Uranium-235, criticality, 5(1): 6; 6(1): 4; 6(2): 14-15
fission ratio to U^{238}, 5(2): 2
flux hardening effects, 4(1): 11-12
neutron cross sections, 5(2): 6, 7
neutron production per fission in U^{238}, average, 4(1): 19
nuclear properties, 4(3): 4
radiation effects, 4(4): 86
resonance fission integrals, 4(4): 13
resonance to thermal capture ratio, 5(2): 2
Uranium-236, neutron cross sections, 5(2). 7
Uranium-238, cadmium ratios of wire, 4(2): 11
conversion to plutonium, 6(4): 1-4
conversion ratio, 5(2): 2
fission ratio to U^{235}, 5(2): 2
neutron production per fission of U^{235} atom, average, 4(1): 19
nuclear properties, 4(3): 4
resonance capture integrals, 4(1): 16; 4(4): 13; 6(1): 5
resonance to thermal capture ratio, 5(2): 2
Uranium-239, gamma activity from decay at 74 kev, 4(1): 16
breeding ratios, 4(4): 91-4
Uranium alloys, fabrication costs, 4(4): 5
radiation effects, 4(4): 84-5
Uranium-238–plutonium-239 systems, breeding ratios, 4(4): 91-4
Uranium-aluminum alloys, radiation effects, 4(4): 84-5
physical properties, 4(1): 61
Uranium-aluminum alloys (aluminum-clad), burnout, 4(1): 38
Uranium-beryllium alloys, physical properties, 4(1): 61-2
Uranium-biphenyl lattices, exponential lattices, 5(3): 8
Uranium carbide, breeding ratios, 4(1): 51-2
chemical reactions, 4(1): 45-7
criticality studies, 4(1): 51
development for reactor fuels, 4(1): 45-56
fabrication, 4(1): 50-1
Hallam Power Reactor fuel elements, 4(3): 91
mechanical properties, 4(1): 48
physical properties, 4(1): 48
preparation, 4(1): 50-1
radiation effects, 4(1): 48-50
thermal conductivity, 4(1): 50
thermal expansion, 4(1): 50
Uranium carbide (UC) (enriched), reactivity, 5(2): 1-2
Uranium carbide–plutonium carbide systems, fuel-element applications, 5(1): 51
heat-transfer characteristics, 4(1): 51
Uranium carbide–zirconium carbide systems, reactions with water and steam, 4(1): 52
Uranium chlorides, reactions with kerosene, 4(1): 47
Uranium-graphite systems, buckling measurements, 4(3): 5
critical experiments, 5(4): 15
exponential measurements, 5(3): 8
mechanical properties, 4(1): 48
neutron spectra, 5(3): 9-10
nondestructive testing, 5(1): 71
physical properties, 4(1): 61-2
Uranium–heavy-water lattices, critical experiments, 5(4): 16, 17
exponential experiments, 5(3): 7-8
Uranium-magnesium alloys, physical properties, 4(1): 61
Uranium-molybdenum alloys, application in Plutonium-Fuel Fast-Breeder Reactor, 4(4): 94
breeding ratios, 4(1): 51-2
criticality studies, 5(1): 5-6, 51
exponential studies, 5(2): 3
fuel-element applications in organic reactors, 4(1): 58
fuel elements for Hallam Power Reactor, 5(3): 41-2
heat-transfer characteristics, 4(1): 51
radiation effects, 4(1): 60; 5(3): 31
reactions with water, 4(1): 40-1
sodium graphite reactor fuel elements, 4(3): 90
Uranium-molybdenum alloys (stainless-steel-clad), melting in fast reactors, 5(2): 30-1
Uranium-molybdenum-aluminum alloys, fuel elements for Piqua Power Reactor, 5(4): 51-2
radiation effects, 4(1): 60
Uranium-molybdenum-aluminum alloys (aluminum-clad), fabrication, 4(1): 60
Uranium-molybdenum-silicon systems, radiation effects, 4(1): 60
Uranium-niobium alloys, physical properties, 4(1): 61-2
Uranium oxide (UO_2), application as fuel in BR-5 Reactor (USSR), 4(4): 85
application as fuel in Rapsodie Reactor (France), 4(4): 85
breeding ratio, 4(1): 7
buckling measurements, 4(2): 11
burnup, 5(3): 2-5
compatibility with gaseous coolants, 5(3): 61
criticality constants of cylinders in water lattices, 4(4): 11-12
criticality in heavy water, 6(3): 82
development for fuel plates, flat, 6(2): 44-5
differential scattering cross sections, 6(2): 11
Doppler coefficients, 4(4): 15-16
fission-gas release, 4(1): 65
fuel elements, 4(1): 75-8; 4(3): 47-8; 4(4): 85; 5(1): 54-67
fuel elements, fabrication costs, 4(4): 5; 5(3): 3
operating transients in fuel rods, 5(2): 22-4
powder compaction, 6(1): 26-37
radiation effects, 4(1): 65; 4(2): 41; 5(1): 56-62, 66-7
removal from cooling systems, 5(4): 45-6
resonance integrals, 4(1): 16; 5(4): 19-20
sintering, 6(2): 42-3
thermal conductivity, 4(1): 50; 4(2): 38-43; 4(4): 22-3; 5(1): 58, 63-5; 5(2): 9-10; 5(4): 22-3; 6(2): 17-18; 6(3): 4-5, 12-15
thermal expansion, 4(1): 50
Uranium oxide (UO_2) (aluminum-clad), criticality, 4(3): 4
Uranium oxide (UO_2) (enriched), criticality studies, 5(1): 4-5
temperature coefficient of reactivity for seven-rod cluster, 4(1): 15
Uranium oxide (UO_2) (enriched) (stainless-steel-clad), reactivity, 5(2): 2-3
Uranium oxide (UO_2) (irradiated); reactivity, 5(2): 6
Uranium oxide (UO_2) (stainless-steel-clad), criticality, 4(2): 10; 4(3): 5
thermal conductivity, 5(4): 22-3
Uranium oxide (UO_2) (Zircaloy-2-clad), buckling studies, 5(2): 3; 5(3): 6-7
fabrication, 4(2): 67-70
NPD-2 Reactor fuel elements, 4(2): 65
Uranium oxide–beryllium oxide systems (UO_2-BeO) (Hastelloy-X-clad), criticality 4(4): 12
Uranium oxide–calcium oxide–zirconium oxide systems (UO_2-CaO-ZrO_2), fuel elements, 5(1): 67
Uranium oxide (UO_2)–heavy-water lattices, buckling measurements, 5(3): 6, 7
criticality measurements, 5(3): 7
Uranium oxide (UO_2)–heavy-water–water lattices, criticality studies, 5(4): 17
Uranium oxide–stainless-steel cermets (UO_2-S.S.), application as fuel in Enrico Fermi Fast-Breeder Reactor, 4(4): 85
criticality studies, 5(4): 15-17
thermal conductivity, 5(4): 22-3
Uranium oxide–thorium oxide–heavy-water lattices (UO_2-ThO_2-D_2O), critical experiments, 5(4): 16
Uranium oxide–thorium oxide–heavy-water–water lattices (UO_2-ThO_2-D_2O-H_2O), critical experiments, 5(4): 17
Uranium oxide (UO_2)–thorium oxide systems (UO_2-ThO_2), criticality studies, 4(3): 7
fission-gas release, 4(1): 52-3
fuel elements in Elk River Power Reactor, 5(2): 33-5
radiation effects, 4(1): 52-3
Uranium oxide–thorium oxide systems ($U^{235}O_2$-ThO_2), exponential experiments, 5(3): 7
Uranium oxide–thorium oxide–water lattices (UO_2-ThO_2-H_2O), critical experiments, 5(4): 16
Uranium oxide–uranyl nitrate systems [UO_3-$UO_2(NO_3)_2$], critical experiments, 5(4): 15
Uranium oxide–water lattices (UO_3-H_2O), critical experiments, 5(4): 15
Uranium-plutonium alloys, criticality experiments, 4(4): 12-13
Uranium-plutonium systems (U^{238}-Pu^{239}), breeding effects, 4(4): 91-4
Uranium–plutonium carbide systems, application in Plutonium-Fuel Fast-Breeder Reactor, 4(4): 94
Uranium–Santowax R lattices, exponential lattices, 5(3): 8
Uranium–stainless-steel alloys, application in Plutonium-Fuel Fast-Breeder Reactor, 4(4): 94
Uranium-thorium alloys, radiation effects, 3(3): 31
Uranium–thorium oxide systems, fabrication costs, 4(4): 5
Uranium-water lattices, buckling measurements, 5(3): 7
heat transfer, 4(4): 19-20
Uranium-zirconium alloys, physical properties, 4(1): 61-2
radiation effects, 5(3): 31
Uranium-zirconium alloys (Zircaloy-clad), Heavy-Water Components Test Reactor fuel elements, 4(2): 65
Uranium-zirconium alloys (zirconium-clad), burnout, 4(1): 38
criticality measurements, 4(1): 23-4
neutron activation distribution measurements, 4(1): 23-4
Uranyl nitrate–heavy-water systems, criticality, 4(3): 7
Uranyl nitrate–uranium oxide systems
See Uranium oxide–uranyl nitrate systems [UO_3-$UO_2(NO_3)_2$]
Uranyl nitrate–water systems, criticality measurements, 4(1): 23
USSR, criticality experiments on organic-moderated reactors, 4(1): 23

V

Vallecitos Boiling-Water Reactor
See Reactors (Vallecitos Boiling-Water) (VBWR)
Vallecitos Experimental Superheat Reactor
See Reactors (Vallecitos Experimental Superheat) (VESR)
Valves, design for Hallam Power Reactor, 4(4): 54-6; 5(3): 45
leakage in Calder Hall Reactors, 4(3): 69-70
leakage in heavy-water reactors, 4(4): 70-3
stem leakage, 5(3): 37-8
Valves (butterfly), gas-cooled reactor applications, 4(1): 66-7

Vanadium diboride, corrosion by steam, 4(4): 44
solubility in boiling water, 4(4): 43
Vanadium-niobium alloys
See Niobium-vanadium alloys
Vapor recovery systems, Experimental Boiling-Water Reactor, 4(2): 59
Variable-Moderator Reactor
See Reactors (Variable-Moderator) (VMR)
VBWR
See Reactors (Vallecitos Boiling-Water) (VBWR)
Vena contracta, effect on heat-transfer coefficient, 4(2): 20
Veronezh Reactor (USSR)
See Reactors (Veronezh) (USSR)
Vessels (pressure)
See Pressure vessels
Vibration compaction
See Compaction
VMR
See Reactors (Variable-Moderator) (VMR)
Voids, distribution calculation, 5(1): 20
VULCAIN
See Reactors (VULCAIN)

W

Waste disposal, 5(4): 49-50
Piqua Power Reactor, 5(4): 56-9
Shippingport Pressurized-Water Reactor, 5(4): 70
Waste-disposal systems, Dresden Power Reactor, 6(2): 62
Water, aluminum alloy corrosion, 5(3): 33
aluminum corrosion, 5(3): 32-3
beryllium corrosion, 5(2): 48
contamination in Shippingport Pressurized-Water Reactor, 6(3): 51-5
corrosive effects, 6(2): 53
criticality effects, 5(2): 1
decontamination in pressurized-water reactors, 4(3): 44-6
fission-product entrainment, 5(4): 39
heat transfer, 5(2): 10-12
moderating properties, 4(3): 4; 5(1): 7
purification, 4(4): 65; 5(1): 77; 5(2): 43; 6(1): 52-3; 6(3): 38, 51-5
radiolysis in boiling-water reactors, 6(4): 92-4
reactions, with uranium, 4(1): 40-1
with uranium carbide–zirconium carbide systems, 4(1): 52
with Zircaloy, 4(1): 37; 5(3): 31-2
removal from helium, 5(4): 78
rethermalization properties, 5(2): 3-4, 5
separation from steam, 4(3): 81, 82
swirl flow, 6(1): 21-2
thermal-neutron diffusion, 4(1): 16-17
Water (pressurized), heat transfer, 5(1): 10-12; 5(4): 24
Water (supercritical), heat transfer, 5(3): 20
technology, 4(2): 80-1
Water-air systems
See Air-water systems
Water-cooled and -moderated reactors
See Reactors (Water-cooled and-moderated)
Water–heavy-water systems
See Heavy-water–water systems
Water-purification systems, Dresden Power Reactor, 4(4): 65
Indian Point Power Reactor, 6(3): 38
N. S. *Savannah* Reactor, 6(1): 52-3
Shippingport Pressurized-Water Reactor, 6(3): 51-5
Water-steam systems
See Steam-water systems
Water-uranium lattices
See Uranium-water lattices
Water vapor
See Steam
Welds, radiation effects on stainless-steel, 5(1): 70
Wet steam
See Steam (saturated)
Wolfram
See Tungsten

X

X-ray fluorescence, nondestructive testing applications, 5(1): 71
X rays
See Radiation (X)
Xenon, entrainment in water, 5(4): 30
removal from helium, 5(4): 76
Xylene, reactions with uranium carbides, 4(1): 47

Y

Y-12 Plant, criticality accident, June 1958, 4(2): 29
Yankee Power Reactor
See Reactors (Yankee Power)
Yttrium boride (YB_5), corrosion by steam, 4(4): 44
radiation effects, 4(4): 44
Yttrium boride (YB_6), corrosion by steam, 4(4): 44
radiation effects, 4(4): 44
solubility in boiling water, 4(4): 43

Z

ZEBRA
See Reactors (ZEBRA) (UK)
ZEEP Reactor
See Reactors (ZEEP) (Canada)
Zero Power Reactor VII
See Reactors (ZPR-VII)
Zero Power Reactor III
See Reactors (ZPR-III)
Zinc (liquid), reactions with uranium carbides, 4(1): 46
Zinc sulfide, entrainment in water, 5(4): 30
Zircaloy alloy, coatings, nondestructive testing, 5(1): 71
coextrusion with stainless steel, 6(2): 51-3
corrosion by organic coolants, 6(1): 71
evaluation for reactor use, 6(2): 47-8
reactions, with steam, 4(1): 38-9
with water, 4(1): 37
tubing, nondestructive testing, 6(2): 53
Zircaloy-2 alloy, autoclave testing, 4(2): 48-9
cladding for uranium dioxide fuel elements, 5(1): 57, 66-7
corrosion, 4(3): 44-5; 5(1): 69; 5(3): 31-2; 5(4): 40; 6(3): 16-17
criticality effects of tubes, 4(2): 11
evaluation for fuel-element cladding, 5(1): 69-70
fabrication into tubing, 4(3): 42; 5(2): 50
fuel-element applications, 5(1): 82
heat transfer, 4(4): 19-20
mechanical properties, 5(1): 69-70
physical properties, 6(3): 16-17
radiation effects, 4(3): 42-3; 5(1): 70; 5(4): 40; 6(2): 67
reactions, with uranium carbides, 4(1): 46
with water, 4(1): 40-1
Zircaloy-2 alloy (irradiated), corrosion, 5(3): 32
evaluation of pressure tubes, 6(2): 67
Zircaloy-4 alloy, corrosion, 5(3): 32
evaluation for fuel-element cladding, 5(1): 69-70
Zirconium, corrosion, 4(3): 45; 5(4): 40, 73
data manual, 6(2): 47
evaluation for reactor use, 6(2): 47-8
fuel-element applications, 5(1): 82
radiation effects, 5(1): 70
reactions, with steam, 4(1): 38-9
with uranium carbides, 4(1): 46
shielding properties, 4(2): 36
Zirconium alloys, corrosion, 5(3): 31-2; 6(2): 53
Zirconium carbide, compatibility with gaseous coolants, 5(3): 61
Zirconium carbide–uranium carbide systems
See Uranium carbide–zirconium carbide systems
Zirconium boride (ZrB_2), corrosion by steam, 4(4): 44
radiation effects, 4(4): 44
solubility in boiling water, 4(4): 43
Zirconium hydride, moderator for nuclear superheaters, 4(3): 83
Zirconium-iron-nickel alloys, corrosion, 5(3): 32
Zirconium-niobium alloys
See Niobium-zirconium alloys
Zirconium oxide, compatibility with gaseous coolants, 5(3): 61
Zirconium oxide–calcium oxide–uranium dioxide systems
See Uranium oxide–calcium oxide–zirconium oxide systems (UO_2-CaO-ZrO_2)
Zirconium-tin alloys
See also Zircaloy
radiation effects, 5(1): 70
Zirconium-uranium alloys
See Uranium-zirconium alloys
Zoé Reactor
See Reactors (Zoé)
ZPR-III
See Reactors (ZPR-III)
Zyglo solution, reactions with uranium carbides, 4(1): 47

LEGAL NOTICE

This document was prepared under the sponsorship of the U. S. Atomic Energy Commission. Neither the United States, nor the Commission, nor any person acting on behalf of the Commission:

A. Makes any warranty or representation, expressed or implied, with respect to the accuracy, completeness, or usefulness of the information contained in this report, or that the use of any information, apparatus, method, or process disclosed in this report may not infringe privately owned rights; or

B. Assumes any liabilities with respect to the use of, or for damages resulting from the use of any information, apparatus, method, or process disclosed in this report.

As used in the above, "person acting on behalf of the Commission" includes any employee or contractor of the Commission, or employee of such contractor, to the extent that such employee or contractor of the Commission, or employee of such contractor prepares, disseminates, or provides access to, any information pursuant to his employment or contract with the Commission, or his employment with such contractor.

NUCLEAR SCIENCE ABSTRACTS

The U. S. Atomic Energy Commission, Division of Technical Information, publishes *Nuclear Science Abstracts (NSA)*, a semimonthly journal containing abstracts of the literature of nuclear science and engineering.

NSA covers (1) research reports of the U. S. Atomic Energy Commission and its contractors; (2) research reports of government agencies, universities, and industrial research organizations on a world-wide basis; and (3) translations, patents, books, and articles appearing in technical and scientific journals.

Complete indexes covering subject, author, source, and report number are included in each issue. These are cumulated quarterly, semiannually, and annually providing a detailed and convenient key to the literature.

Availability of *NSA*

SALE *NSA* is available on subscription from the Superintendent of Documents, U. S. Government Printing Office, Washington 25, D. C., at $22.00 per year for the semimonthly abstract issues and $15.00 per year for the four cumulated-index issues. Subscriptions are postpaid within the United States, Canada, Mexico, and all Central and South American countries, except Argentina, Brazil, British and French Guiana, Surinam, and British Honduras. Subscribers in these Central and South American countries, and in all other countries throughout the world, should remit $27.50 per year for subscriptions to semimonthly abstract issues and $17.50 per year for the four cumulated-index issues.

EXCHANGE *NSA* is also available on an exchange basis to universities, research institutions, industrial firms, and publishers of scientific information. Inquiries should be directed to the Division of Technical Information Extension, U. S. Atomic Energy Commission, P. O. Box 62, Oak Ridge, Tennessee.

TECHNICAL PROGRESS REVIEWS may be purchased from Superintendent of Documents, U. S. Government Printing Office, Washington 25, D. C. for $2.00 per year for each subscription or for $0.55 per issue. The use of the coupon below will facilitate the handling of your order.

POSTAGE AND REMITTANCE: Postpaid within the United States, Canada, Mexico, and all Central and South American countries except as hereinafter noted. Add $0.50 per year, or $0.15 per single issue, for postage to all other countries, including Argentina, Brazil, British and French Guiana, Surinam, and British Honduras. Payment should be by check, money order, or document coupons, and MUST accompany order. Remittances from foreign countries should be made by international money order, or draft on an American bank, payable to the Superintendent of Documents, or by UNESCO book coupons.

order form

SUPERINTENDENT OF DOCUMENTS
U. S. GOVERNMENT PRINTING OFFICE
WASHINGTON 25, D. C.

Enclosed:
document coupons ☐ check ☐ money order ☐

Charge to Superintendent of Documents No._____

Please send a one-year subscription to

☐ ISOTOPES AND RADIATION TECHNOLOGY
☐ NUCLEAR SAFETY
☐ POWER REACTOR TECHNOLOGY
☐ REACTOR FUEL PROCESSING
☐ REACTOR MATERIALS

(Each subscription $2.00 a year; $0.55 per issue.)

SUPERINTENDENT OF DOCUMENTS
U. S. GOVERNMENT PRINTING OFFICE
WASHINGTON 25, D. C.

(Print clearly)

Name _____

Street _____

City _____ Zone ____ State _____